

**The human 7-transmembrane orphan receptor family
MRGPRX: native expression and identification,
development and pharmacological characterization of
agonists and antagonists**

Dissertation

zur

Erlangung des Doktorgrades (Dr. rer. nat.)

der

Mathematisch-Naturwissenschaftlichen Fakultät

der

Rheinischen Friedrich-Wilhelms-Universität Bonn

vorgelegt von

Mohamad Wessam Alnouri

aus

Damaskus (Syrien)

Bonn 2016

Angefertigt mit Genehmigung der Mathematisch-Naturwissenschaftlichen
Fakultät der Rheinischen Friedrich-Wilhelms-Universität Bonn

1. Gutachter: Prof. Dr. Christa E. Müller

2. Gutachter: PD Dr. Anke C. Schiedel

Tag der Promotion: 02.09.2016

Erscheinungsjahr: 2016

Die vorliegende Arbeit wurde in der Zeit von Januar 2012 bis November 2015 am pharmazeutischen Institut der Rheinischen Friedrich-Wilhelms-Universität Bonn unter der Leitung von Frau Prof. Dr. Christa E. Müller durchgeführt.

**Nurcan, Yasir
and my parents**

“we have to remember that what we observe is not nature in itself, but nature exposed to our method of questioning”

Werner Heisenberg (1901-1976)

Table of Contents

1. Introduction	1
1.1 7-Transmembrane receptors.....	1
1.2 Neuropathic pain.....	2
1.3 MAS-related gene receptors	4
Excursus: Bovine adrenal medulla-22 and opioid system	13
1.3.1 MRGPRX1 receptor.....	15
Excursus: Cortistatin-14	20
1.3.2 MRGPRX2 receptor.....	22
1.3.3 MRGPRX3 receptor.....	28
1.3.4 MRGPRX4 receptor.....	29
1.4 Aim of the thesis.....	29
2. Results and Discussion	31
2.1 MRGPRX1 receptor.....	31
2.1.1 Screening of compound libraries in search for MRGPRX1 antagonists.....	31
2.1.2 Discussion.....	36
2.2 MRGPRX2 receptor.....	39
2.2.2 Screening of compound libraries in search for MRGPRX2 antagonists.....	39
2.2.3 <i>In vitro</i> pharmacokinetic data of selected MRGPRX2 antagonists	54
2.2.4 Mechanism of the mode of antagonism	55
2.2.5 Investigation of some reported agonists.....	57
2.2.6 MRGPRB2 receptor	58
2.2.7 Discussion.....	59
2.3 MRGPRX3 receptor.....	63
2.3.1 Cloning of MRGPRX3 β -arrestin cell line	63
2.3.2 Screening of compound libraries in search for agonists.....	64
2.3.3 Discussion.....	67
2.4 MRGPRX4 receptor.....	69
2.4.1 MRGPRX4 receptor: the human adenine receptor?.....	69
2.4.2 Screening of compound libraries in search for agonists: a challenging search	71
2.4.3 The second deorphanization approach: cerebrospinal fluid.....	71
2.4.4 Soybean trypsin inhibitor	77
2.4.5 Interleukin-1 β and its N-terminal cleavage products: The third deorphanization approach and an elusive entity	80
2.4.6 Discussion I.....	86
2.4.7 Screening further compound libraries: a breakthrough.....	91
2.4.8 MSX-3 and its related compounds as agonists at MRGPRX4.....	92

2.4.9 Determination of the G-protein coupling of MRGPRX4 receptor	96
2.4.10 Structure-activity relationships of MRGPRX4 receptor agonists.....	97
2.4.11 Adenosine monophosphate: final deorphanization approach.....	103
2.4.12 A search for a native cell line expressing MRGPRX4 receptor.....	107
2.4.13 Screening of compound libraries in search for antagonists at MRGPRX4 receptor	118
2.4.14 Discussion II	119
3. Summary and Outlook.....	129
4. Experimental part.....	133
4.1 General.....	133
4.1.1 Chemicals	133
4.1.2 Instruments and Software.....	135
4.1.3 Buffers	137
4.2 Cell culture	139
4.2.1 Cells and Media	139
4.2.2 Membrane preparation.....	141
4.2.3 Reagents for protein determination (Lowry)	141
4.3 Molecular biology.....	142
4.3.1 Kits, enzymes and reagents	142
4.3.2 PCR DNA amplification	143
4.3.3 β -arrestin vectors	145
4.3.4 Subcloning of the cDNA.....	146
4.3.5 Ligation	146
4.3.6 Agarose gel electrophoresis	147
4.3.7 LB medium.....	147
4.3.8 Preparation of competent bacteria.....	147
4.3.9 Transformation of competent bacteria	148
4.3.10 Bacterial cultures.....	148
4.3.11 Sequencing	148
4.3.12 Glycerol Stocks	148
4.4 Cell counting.....	149
4.5 Transfection.....	149
4.5.1 Lipofection.....	149
4.6 Immunofluorescence experiments	150
4.7 Competition radioligand binding assays.....	150
4.8 Pharmacological assays	151
4.8.1 β -Arrestin assay	151
4.8.2 cAMP assay.....	153
4.8.3 Calcium mobilization assay.....	153

4.9 Digestion of IL-1 β	155
4.10 Compound libraries	156
5. Abbreviations	157
6. Literature.....	161

1. Introduction

1.1 7-Transmembrane receptors

Since the description of the first 7-transmembrane receptor (7TMR) in 1983,¹ the importance of this class of receptors, in drug research and development, has constantly increased and could not be overestimated. Fredriksson et al. identified 802 human 7TMR (also termed G protein-coupled receptors or GPCR) genes and divided them into five families based on phylogenetic criteria. The families were termed *Glutamate*, *Rhodopsin*, *Adhesion*, *Frizzled/Taste2* and *Secretin* (this classification is shortened to GRAFS).² These proteins share two features; first they all have 7 stretches of 25-35 amino acids with high degree of hydrophobicity, which enables them to span the cell membrane. The second feature is their ability to interact with heterotrimeric G proteins.^{2,3} The *Secretin* receptor family consists of 15 members. All deorphanized members of this family bind peptide hormones. The *Adhesion* receptor family consists of 33 members and can be divided into eight subgroups. The members of this family have diverse and long N-termini with a proteolytic site and several functional domains. Only three members of this class have been deorphanized so far. The *Glutamate* receptor family consists of 22 7TMRs, 8 metabotropic glutamate receptors, 2 GABA receptors, one calcium-sensing receptor as well as 7 orphan receptors. The ligand-binding was compared to a Venus flytrap mechanism, in which the two lobes of the extracellular region form a cavity where glutamate binds and thereby activates the receptor. The *Frizzled/Taste2* receptor family consists of 36 members. The *Frizzled* receptors bind the family of Wnt glycoproteins and control cell fate, proliferation and polarity. With 672 members, the *Rhodopsin* receptor family is by far the biggest 7TMR receptor family. This family has been further divided into α , β , γ and δ branches. The α branch contains many important drug targets like histamine, dopamine, and serotonin receptors. The β branch includes mainly peptide-binding receptors like endothelin and oxytocin receptors. The γ branch has several members that are of interest for drug development like angiotensin, opioid and somatostatin receptors. The δ branch contains a variety of receptors, activated by nucleotides, lipids

Introduction

or peptides, e.g. P2Y receptors, protease activated receptors (PAR), leukotriene as well as the olfactory and many orphan receptors.^{2,4}

The importance of the 7TMRs could be evident by their ability to bind to a broad range of ligands, including inorganic ions, small organic compounds, lipid metabolites, peptides and even proteins and translate the binding into intracellular information. This class of proteins has its origins in the early evolution of eukaryotes. During evolution 7TMRs underwent substantial expansion and pseudogenization. This made some 7TMRs essential for eukaryotic life and enabled many organisms to readily adapt to new sensory functions, which may represent an evolutionary advantage.^{5,6} Not only is the physiological role of this protein family outstanding but also its current share in the druggable human genome. Approximately 30% of the marketed drugs target a 7TMR, which makes it the most successfully addressed protein family of drug targets.^{7,8} Nevertheless, the assumption that 7TMRs have achieved their full potential as drug targets cannot be more misleading. Taking into consideration that the pharmacology of 7TMRs is complex and that the currently available drugs exert their effect via only few receptors of this large family (e.g. less than 30% of non-olfactory 7TMRs are targeted with aminergic receptors being heavily drugged), there is still a huge untapped potential for this class of proteins in the development of novel drugs.^{9,10}

1.2 Neuropathic pain

Neuropathic pain, according to the international association for the study of pain (IASP), is defined as “pain caused by a lesion or disease of the somatosensory nervous system”. Neuropathic pain affects up to 10% of the population according to community-based surveys and causes substantial disability, but current treatment is inadequate. It is associated with sensory abnormalities, including ongoing pain and paraesthesia (an abnormal sensation of tingling, prickling or burning of the skin without apparent physical effect), and altered stimulus–response function, including allodynia (such that low threshold stimuli, e.g. brushing of the skin, can evoke pain), hyperalgesia (increased sensitivity to noxious stimuli), and loss of sensation in some areas.¹¹⁻¹³ The most common etiologies of neuropathic pain in humans are metabolic diseases (diabetes), viral diseases (herpes zoster), immunological

Introduction

mechanisms (multiple sclerosis), spinal cord injuries and alcoholism.¹⁴ Itch (pruritus) is another unpleasant sensation, which was given a still-valid definition more than 340 years ago by Samuel Hafenreffer as “unpleasant sensation that elicits the desire or reflex to scratch”. Clinical relevance is obviously highest in chronic itch conditions that last longer than 3 months. In many cases such as dry skin, atopic eczema, psoriasis, urticaria, scabies and other inflammatory skin diseases, chronic itch comprises more complex skin-associated symptoms than are seen in, for example, acute insect bite reactions (see table 1).¹⁵

Table 1: Clinical classification of itch

Clinical classification	Mediators and mechanisms	Diagnosis	Therapy
Itch caused by skin disorders	Histamine, interleukins, prostaglandin and proteases	Inflammatory dermatoses (atopic dermatitis, psoriasis, drug reactions, mites and urticaria) and dry skin	Antihistamines, anti-inflammatory, immunomodulatory topical and systemic therapy (cyclosporine A, pimecrolimus, tacrolimus and corticosteroids)
Itch caused by systemic disorders	Opiates, interleukins?	Chronic liver disease and chronic renal failure	Naltrexone, κ -opioid receptor agonists and gabapentin
Neuropathic itch	Damage to nerve fibres, neuropeptides (such as substance P) and proteases	Postherpetic pruritus, notalgia paresthetica and brachioradial pruritus	Gabapentin, pregabalin and capsaicin
Psychogenic itch	Serotonin, noradrenaline	Delusions of parasitosis, stress and depression	Olanzapine, pimozide and SSRI antidepressants

Although pain and itch are universal sensations, elucidating the molecular underpinnings of these processes is far from being complete. Itch can be reduced by painful stimuli; analgesia can reduce this inhibition and so enhance itch. This phenomenon is particularly relevant to spinally administered μ -opioid receptor agonists, which induce segmental analgesia that is often combined with segmental pruritus. Given that μ -opioids can induce itch, it is not surprising that μ -opioid receptor antagonists have antipruritic effects in experimental itch studies. Interestingly, buprenorphine, a drug combining μ -opioid antagonistic and κ -opioid agonistic effects, has been used therapeutically to fight intractable itch.¹⁵ Intriguingly, an accumulating evidence suggests that itch-specific neurons constitute a subset of TRPV1-positive (transient receptor potential V1) neurons, which were initially presumed to be all nociceptors.¹⁶ In recent years several proteins involved in sensory functions like purinergic receptors,

Introduction

tetrodotoxin (TTX) insensitive sodium channels consolidated our understanding of nociception and itch, but the discovery of mas-related gene receptors in 2001 opened new avenues in the elucidation of neuropathic pain as well as itch. It also represents a novel possibility to develop powerful pharmacological tools and drugs for several clinical cases.¹⁷

1.3 MAS-related gene receptors

Mas-related gene receptors (MRGs) belong to the 7 transmembrane receptors (7TMRs). These receptors are in the δ branch of the *Rhodopsin* receptor family together with purine, glycoprotein and olfactory receptors.² This receptor family was discovered independently by two groups. Dong et al. exploited the fact that mouse embryos lacking the transcription factor neurogenin1 fail to develop sensory neurons. By subtracting the cDNA from neonatal wild-type and deficient mice, signaling molecules involved in nociception emerged. In their first paper they reported 31 murine and 8 human intact coding sequences belonging to 7TMR, which they designated mas-related gene receptors (MRGs) due to their relatedness to the mas oncogene.¹⁷ Lembo et al. discovered the same 7TMR family during search in the RNA isolated from a primary culture of rat dorsal root ganglia (DRG). Due to their unique expression in small nociceptive sensory neurons, they were named sensory neuron-specific receptors (SNSRs).¹⁸ In order to avoid any confusion, the HUGO Gene Nomenclature Committee refers to these proteins as MAS-related G protein-coupled receptors (MRGPR). This abbreviation will be adopted from now on in this thesis and capital letter abbreviation (MRGPR) will be used for proteins and small letter one (mrgpr) would be used to refer to the gene or mRNA. MRGPRs represent the nonodorant 7TMR family with the largest number of members known so far as shown in figure 1.¹⁹ The MRGPR family consists of 38 members (see table 2) that are grouped into nine distinct subfamilies (MRGPRA to -H and -X) and belongs to the δ branch of the *Rhodopsin* receptor family. According to our current knowledge, the mrgprA subfamily consists of one member in the rat and 18 protein-coding genes in the mouse as well as many pseudogenes. The mrgprB subfamily comprises 7 in the rat, 9 in the mouse and several pseudogenes in both species.

Introduction

The mrgprC subfamily has one protein-coding member in the rat and one in the mouse, in addition to 13 pseudogenes in the mouse. The mrgprD-G subfamilies comprise only one member each in mouse, rat and human. The mrgprH subfamily has again one member in the mouse and the rat but it is not found in human. The rat mrgprF gene was actually first reported in 1990 and named rat thoracic aorta (RTA) gene. The related mas1L gene was reported in 1991. The last subfamily is called mrgprX and it is primate-specific and comprises only 4 members mrgprX1-4 while the other reported sequences are polymorphisms of these 4 members. All the members are still considered orphan by the International Union of Basic and Clinical Pharmacology (IUPHAR)^{19,20} It was also possible to clone members of the mrgprX subfamily from other primates like crab-eating macaque (*Macaca fascicularis*) and rhesus monkey. This enables development of animal models for this primate-specific subfamily.^{22,23}

Subfamilies A, B, C and H are rodent-specific, subfamily X is primate-specific and subfamilies D-G are conserved in rodents and primates (see table 2). The evolution of mrgpr genes indicate that mrgprD-G are old genes but since no mrgpr member was found outside Tetrapoda, it is tempting to conclude that this family of genes has emerged after the divergence of bony fish from the line leading to Tetrapoda. MrgprH is the oldest gene since it includes a frog and two chicken members. Interestingly, all genes for mrgpr other than mas, mas1L, and mrgprH are located on a single chromosome in human (chromosome 11), rat (chromosome 1), and mouse (chromosome 7) as shown in figure 2.²⁰ In addition, an evolutionary analysis on the mrgpr gene subfamilies in human and mouse was performed. A pairwise comparison of the members within each subfamily was conducted and the Ka/Ks ratios were calculated (the ratio between nonsynonymous and synonymous substitution rates). Interestingly, the results showed a robust positive selection in the extracellular regions, whereas the intracellular loops as well as 7 transmembrane helices were under negative selection. Since the extracellular loops are responsible for ligand binding, this suggests that these receptors could couple to non-related ligands. This was especially the case for the human MRGPRX

Introduction

subfamily, which showed an excess of radical amino acid replacements that usually influence the function of the protein.²¹

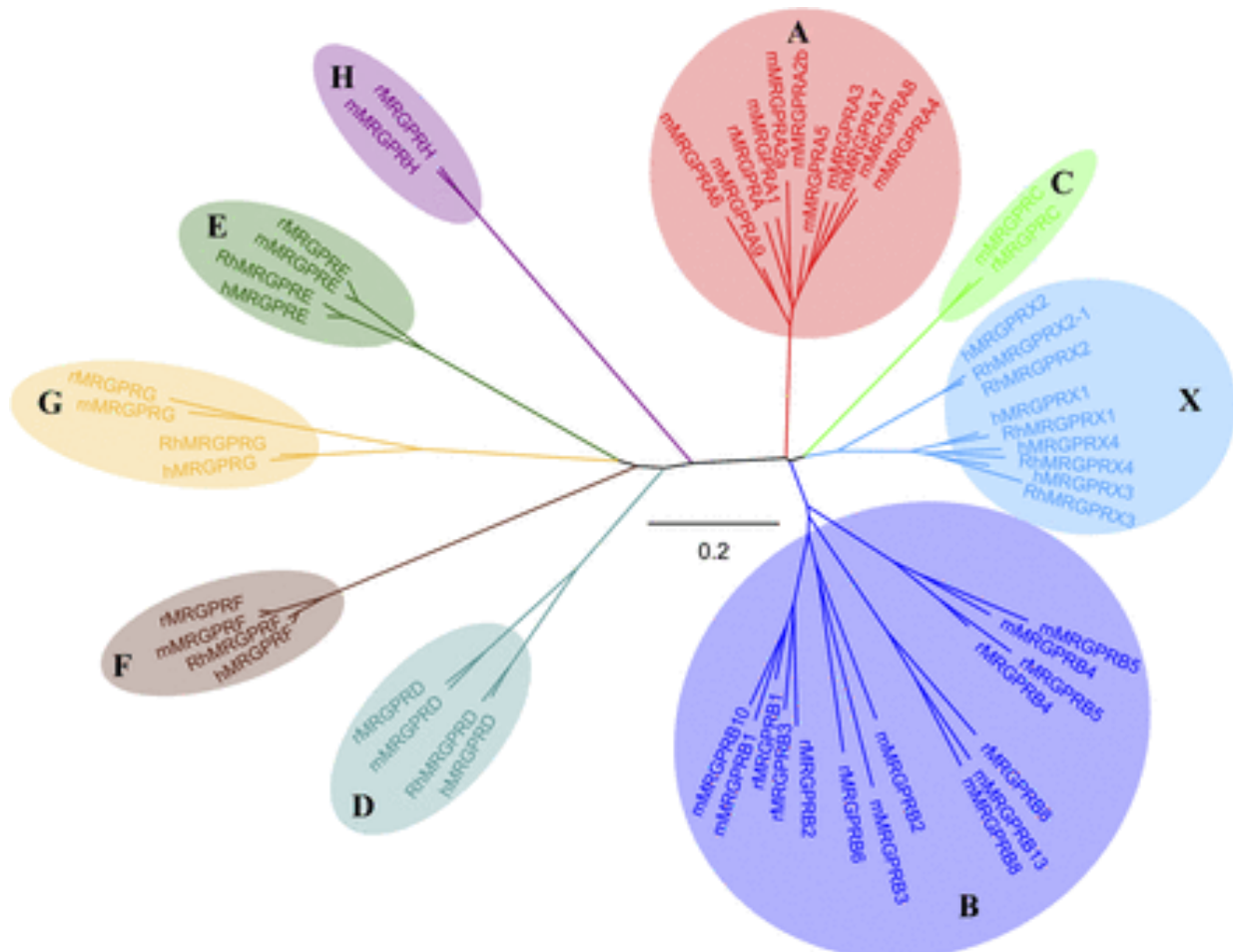


Figure 1: Phylogeny of mas-related seven transmembrane receptors. A phylogenetic tree of all 38 mrgpr members from the nine mrgpr subfamilies (A–H, X) of mice (m), rat (r), human (h), and rhesus monkey (Rh).¹⁹

Table 2: The different subfamilies of mas-related protein-coding genes and their number in mouse, rat and human

Subfamily	Number of genes		
	Mouse	Rat	human
mrgprA*	18	1	n.a
mrgprB**	9	7	n.a
mrgprC*	1	1	n.a
mrgprD	1	1	1
mrgprE	1	1	1
mrgprF	1	1	1
mrgprG	1	1	1
mrgprH	1	1	n.a
mrgprX	n.a	n.a	4

n.a: not available

*: several pseudogenes in the mouse

** : several pseudogenes in both rat and mouse

Introduction

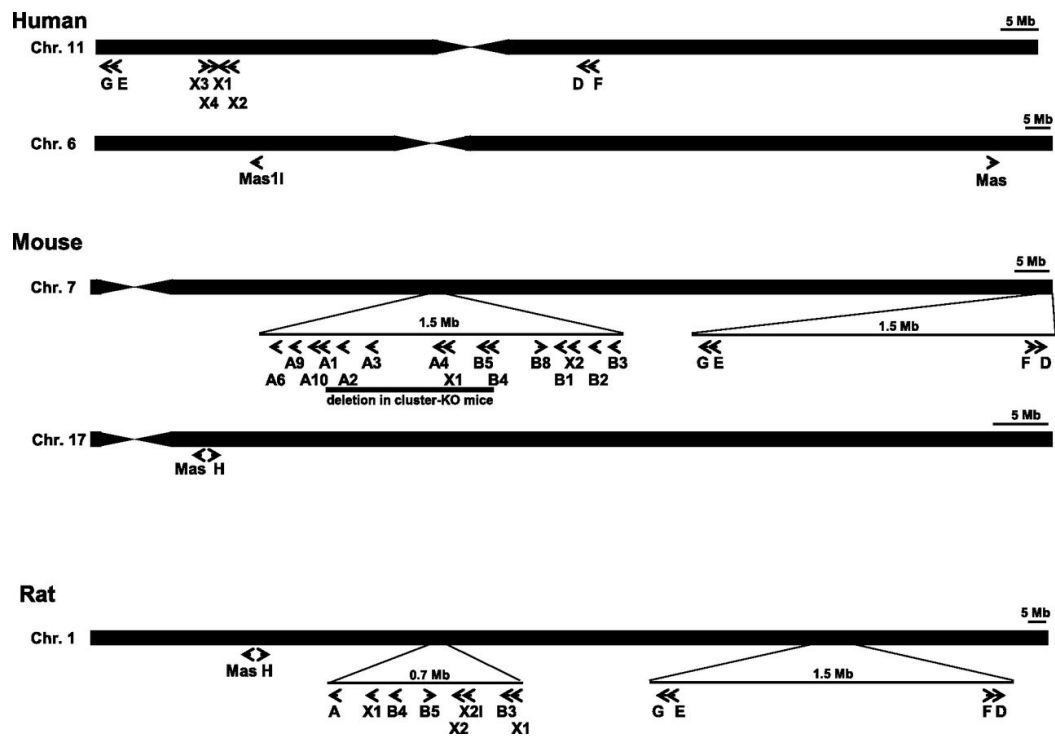


Figure 2: Chromosomal (Chr.) localizations of mrgpr genes in human, rat, and mouse. The genes are shown as arrows in their direction of transcription.²⁰

Since the mouse has more than 20 mrgprA and 14 mrgprC genes and pseudogenes (rat has only one from each subfamily), the big expansion of the mrgpr family in mouse has also been investigated. The suggested model was that mrgprA and mrgprC had a common ancestor gene whereas mrgprB originated from a different ancestor. Of note, according to the model mrgprX receptors should have had the same ancestor as mrgprA and mrgprC. The expansion in mice took place after rat-mouse speciation due to retrotransposon-mediated crossover events. The findings suggest that the diversity of mrgpr in rodents could be reduced to a core set of 4 different genes approximating the limited mrgpr diversity in humans.²⁴ Unfortunately, despite the probable redundancy in rodents, the later investigations revealed that it is not accurate to oversimplify the diversity of mrgpr in rodents as discussed below.

The expression of different MRGPR subfamilies and receptors was a major point of interest since the very discovery of these receptors. The restricted expression in dorsal root ganglia (DRG) is an indication of involvement in nociception. In more details, two main populations of sensory neurons of the DRG emerge in the adulthood. The first population is called peptidergic neurons. These

Introduction

neurons are regulated by nerve growth factor (NGF) and its trk A receptor. NGF enhances the expression of peptides like substance P and calcitonin gene-related peptide (CGRP). The second population is non-peptidergic neurons. These neurons are regulated by glial cell line-derived neurotrophic factor (GDNF) and its ret receptor. These neurons do not contain substance P or CGRP but they express P2X3 receptors. Most importantly, the non-peptidergic neurons bind the isolectin-B4 (IB4+).^{25,26} Interestingly, IB4+ neurons respond preferentially to non-noxious inputs, which are a main characteristic of neuropathic pain as well as an indication of the involvement in establishing chronic pain states.^{27,28} This suggests that selectively targeting a biochemical molecule in IB4+ neurons may be an approach to deal with neuropathic pain. Dong et al. found a distinct expression profile of mouse MRGPRA2-8 receptor subtypes in different subpopulations of IB4+ neurons with some overlapping in the expression at least at birth. Moreover, it was discovered that there is ca. 15% overlapping between MRGPRA subtypes and MRGPRD receptor at birth. Nevertheless, in adulthood the expression will be segregated.¹⁷ Most interestingly, MRGPRD+ and MRGPRB4+ neurons in adult mice innervate distinct peripheral targets, skin epidermis and the hairy skin, respectively.^{29,30} The reason behind this compartmentalized expression seems to be the runt domain transcription factor Runx1. It turned out that MRGPRA/B/C expression persists only in Runx1 negative, whereas the MRGPRD compartment is Runx1 positive as illustrated in figure 3.³¹

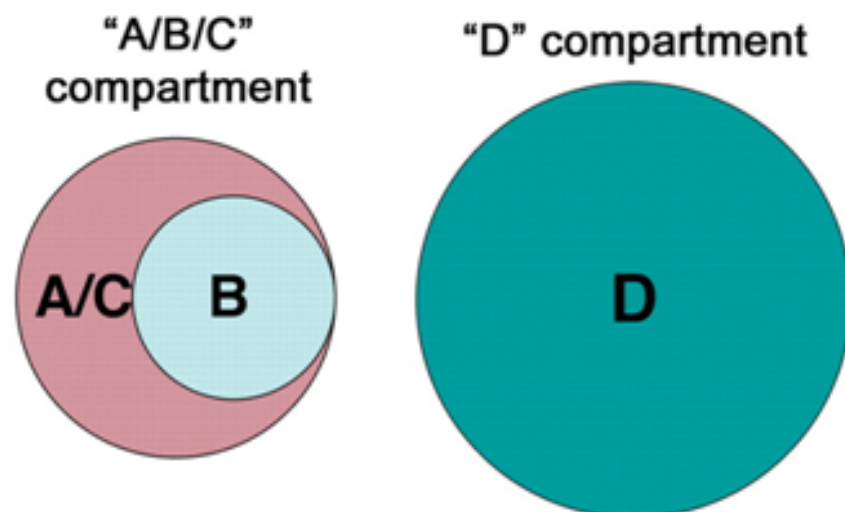


Figure 3: Schematics of two MRGPR compartments. The "A/B/C" compartment expresses MRGPRA3/A4, MRGPRB4, and MRGPC11 in a partially overlapping manner, and the "D" compartment expresses MRGPRD.³¹

Introduction

In an approach to overcome the apparent complexity and potential gene redundancy, Liu et al. generated deficient mice with a deleted 845-kilo base region (instead of knocking out individual genes) in chromosome 7, which comprises 30 mrgpr genes and pseudogenes as shown in figure 2. More precisely, this region comprises 12 intact open reading frames (mrgprA1-A4, A10, A12, A14, A16, A19, B4, B5 and C11). The deficient mice did not show any difference compared to wt mice regarding acute noxious heat, cold mechanical and chemical stimulation. The L5 spinal nerve ligation model of neuropathic pain and histamine-induced itch induced the same responses in wt and deficient mice. Interestingly, the deficient mice, in contrast to wt mice, showed a significantly reduced itch response to the pruritogenic anti-malaria drug chloroquine. Further investigations of the individual knocked out genes revealed that only MRGPRA3 responded to chloroquine with an EC₅₀ of 27 μ M. This indicated that MRGPRA3+ neurons could be histamine-independent itch-specific neurons and revealed its potential molecular mechanism for the first time.³² Wilson et al. tried to further investigate the itch mechanism, in which it was found that chloroquine and BAM8-22, the agonists at murine MRGPRA3 and MRGPRC11, respectively, depend on transient receptor potential A1 (TRPA1) for their itch transduction. Although TRPA1 is expressed in a subset of TRPV1-positive neurons, it was suggested that TRPV1 is not required for BAM8-22 and chloroquine-dependent itch. In contrast, TRPV1 is necessary for histamine-related itch. Hence, selective TRPA1, MRGPRA3 or MRGPRC11 antagonists could inhibit itch transduction.³³

In an interesting paper, it was described that MRGPRA3+ neurons in DRG could be labeled and it was demonstrated that they exclusively innervate the epidermis of the skin and confirmed that only MRGPRA3+ neurons respond to chloroquine. It was also demonstrated that MRGPRA3+ neurons represent a compartment within the pain-related TRPV1+ neurons. Most strikingly, it was shown that capsaicin would induce only pain in wild-type mice but the same dosage of capsaicin would induce only itch if the TRPV1 was knocked out from all neurons except the MRGPRA3+ neurons as shown in figure 4. Thus, it was proven that MRGPRA3+ neurons are itch-specific neurons and the relatedness between pain, itch and compartmentalization of MRGPR receptors was elegantly demonstrated.³⁴

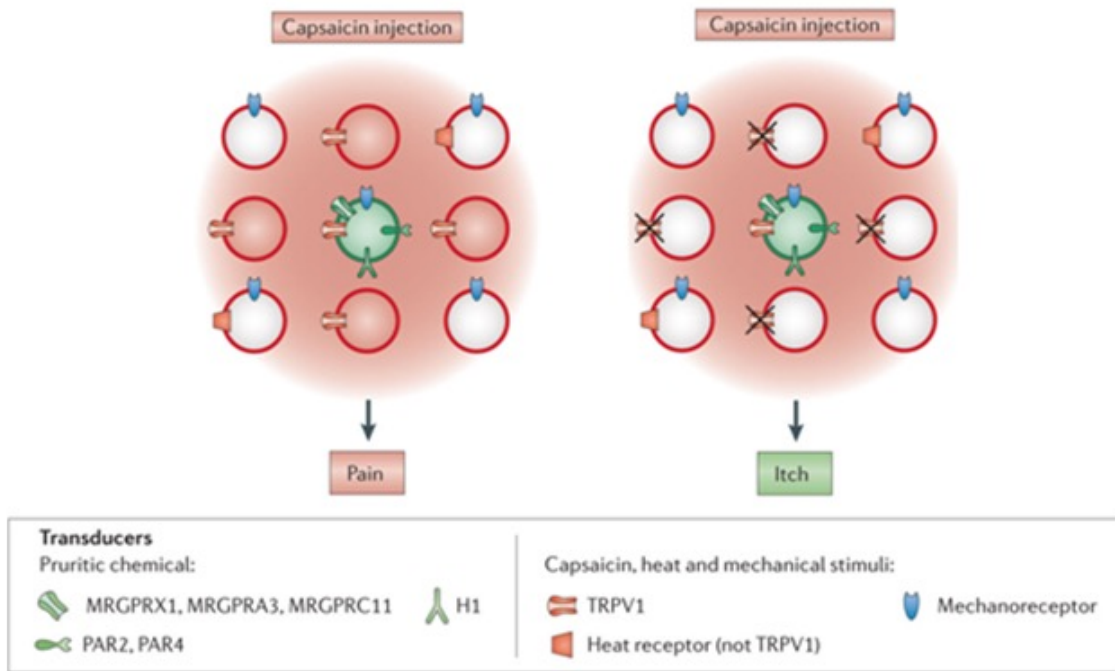


Figure 4: Both pruriceptive (green circles) and non-pruriceptive (red circles) neurons respond to capsaicin. The response is pain if the both types of neurons are activated and itch if only pruriceptive neurons are activated, modified from.³⁵

Unfortunately, the expression pattern of the human MRGPRX receptors has not been investigated in detail. Only Lembo et al. investigated the mRNA expression of *mrgrprX1* and *mrgrprX4* receptors in the DRG and trigeminal ganglia. It has been found that only 7 % of *mrgrprX*-positive cells expressed substance P or CGRP, whereas most of the *mrgrprX*-positive-neurons bind IB4 (76%) and many express TRPV1 (56%) indicating that *mrgrprX* receptors are associated preferentially with the IB4 class of nociceptors.¹⁸

In this thesis the main interest is the human MRGPRX subfamily. Hence, the ligands, signaling pathways as well as physiologic functions of the members of this family will be discussed in detail (see below). Nevertheless, the knowledge about other human MRGPR subfamilies and rodent-specific subfamilies could provide insights into the functions of MRGPRX subfamily. Therefore, the current knowledge will be briefly mentioned.

The MRGPRD subfamily consists of only one member, which is conserved among rodents and humans. Four pairings have been suggested for this receptor, the first with β -alanine and the second with alamandine (Ala-angiotensin-1-7).^{36,37} Two other ligands have also been suggested (GABA and β -aminoisobutyric acid). This member is both G_q - and G_i -coupled and suggested to have a high

Introduction

constitutive activity. As mentioned above MRGPRD has its own compartment in DRG and the activation of MRGPRD+ neurons induced itch and pain. MRGPRD is also expressed in the heart and was shown to have vasodilatory effects, which makes this receptor the only member of MRGPR till now that is not only phylogenetically but also functionally related to the MAS gene receptor.^{19,20} The human MRGPRD is the best characterized human MRGPR member after MAS itself.

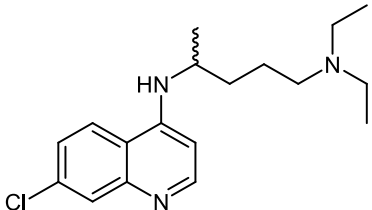
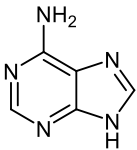
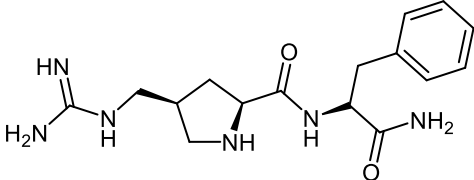
MRGPRE/F/G subfamilies consist of only one member each and do not have any reported ligands till now. This is also the case for the rodent-specific MRGPRH subfamily. The rat MRGPRD was shown to form multi-heterodimers with MRGPRE in HEK293 cells. MRGPRE and MRGPRF seem to be linked as well since mrgprE KO mice have a strong reduction in the expression of MRGPRF receptors.^{20,38}

The MRGPR receptors in the rodents have been studied in more detail and many ligands have been identified till now. Bender et al. reported the nucleobase adenine as the physiological ligand for the only member of the rat MRGPRA subfamily with a K_i value of 18 nM in binding assays.³⁹ The murine MRGPRA9 and A10 were also found to be activated by adenine in the nanomolar range but testing adenine at the human MRGPRX subfamily members did not show any signal. In addition, a hamster receptor was found to be activated by adenine.^{40,41,23} Dong et al. described RF-amide peptides as potential physiological neuropeptides for activating murine MRGPRA1 and MRGPRA4 receptors. MRGPRA1 was activated most by FLRFamide peptide with an EC_{50} of 20 nM, whereas MRGPRA4 was activated by NPFAFamide with an EC_{50} of 60 nM in calcium mobilization assay. Both receptors responded similarly to adrenocorticotropin (ACTH).¹⁷ The search for ligands confirmed that distinct RF(Y)G and/or RF(Y) amide-peptides could activate MRGPC11 as well as MRGPRA1. MRGPC11 was found to be activated most potently by proopiomelanocortin (POMC) products γ 1- and γ 2-MSH (melanocyte stimulating hormone), dynorphine-14 and BAM22 (bovine adrenal medulla) with EC_{50} values in the low nanomolar range.⁴² The rat MRGPC receptor was also activated by the same RF-amide peptides and it turned out that the active moiety is the 7-C-terminal amino acids of γ 2-MSH.⁴³ The nature of these agonists led Lee et al. to propose that the native ligands to some MRGPR

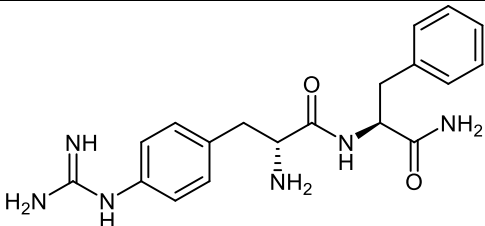
Introduction

receptors are mediators of mast cell-sensory nerve interactions. Therefore, mMRGPC11-expressing HEK cells were activated both by the supernatant of IgE-sensitized RBL-2H3 mast cells and by coculture of both cells after IgE-sensitization and therefore gave support to this hypothesis.⁴⁴ Hin et al. developed recently small molecules as peptidomimetic agonists at MRGPC receptor in both rat and mouse. They synthesized short Arg-Phe-NH₂ derivatives in which the arginine residue is substituted by an arginine mimetic. Interestingly, there were species differences within the rodents since some active derivatives in the mouse were inactive in the rat and vice versa as shown for compound 1 and 2.⁴⁵ This means there are interspecies differences on the medicinal chemistry level in addition to the lack of clear orthologs between humans and rodents. Hence, the extrapolation of the data from rodents to the humans should be conducted with great caution when it comes to physiological functions and ligand affinities of MRGPC receptors. Table 3 shows the structures of the agonists at the rodent receptors.

Table 3: The structure of the most potent agonistic compounds at the rodent MRGPC receptors

Name	Structure	Receptor	EC ₅₀ value
Chloroquine		mMRGPRA3	27 μM ³²
Adenine		mMRGPRA9/A10 rMRGPRA	8/9.8 nM ^{40,41} 2.9 nM ³⁹
FLRFamide	FLRFa	mMRGPRA1	20 nM ¹⁷
NPAFamide	AGEGLNSQFWSLAAPQRFa	mMRGPRA4	60 nM ¹⁷
ACTH	SYSMEHFRWGKPVGKKRRPVKVYPNGAEDSAEAFPLEF	mMRGPRA1/A4	60/200 nM ¹⁷
γ2-MSH	YVMGHFRWDRFG	mMRGPC11 rMRGPC	11 nM ⁴² 37 nM ⁴³
Dynorphin-14	IRPKLKWDNQKRYG	mMRGPC11	22 nM ⁴²
Compound 1		mMRGPC11	794 nM ⁴⁵

Introduction

Compound 2		mMRGPC11 rMRGPC	1,260 nM ⁴⁵ 630 nM ⁴⁵
------------	---	--------------------	--

Excursus: Bovine adrenal medulla-22 and opioid system

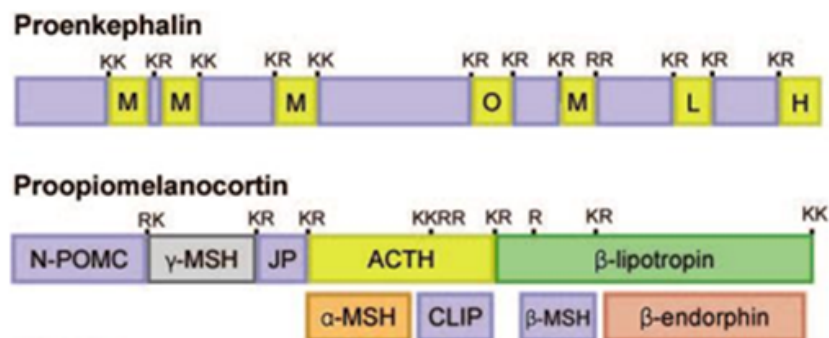
According to IUPHAR, the suggested putative ligands for MRGPRX1 and MRGPRX2, bovine adrenal medulla-22 (BAM22) and cortistatin-14, respectively, are neuropeptides. Hence, it is important to address these ligands in some detail before delving into both receptors. Cortistatin-14 will be discussed in detail later (see below). It is important to keep in mind that BAM22 is a neuropeptide and neuropeptides are derived from larger proteins known as proneuropeptides or prohormones. These precursors undergo proteolytic processing to generate the smaller active neuropeptides.⁴⁶ The proteolytic processing occurs usually at dibasic residues that flank the N- and C-termini of neuropeptides within their precursors. The dibasic residues Lys-Arg (KR) most often flank the neuropeptides but also KK, RR and RK occur. Processing at nonbasic residues occurs occasionally. This means proteolysis and tissue-specific processing of the proneuropeptides depend on the proteases available in a specific tissue in the first place.⁴⁷

Since the discovery of the enkephalins in 1975, many other opioids have been described. BAM20 as well as BAM22 were isolated from bovine adrenal medulla and were designated “big” Met-enkephalins at first. It is now clear that the opioid peptides belong to three peptide families, proenkephalin (also proenkephalin A), prodynorphin (also proenkephalin B) and proopioidmelanocortin (POMC). Proenkephalin A is processed to 4 copies of Met-enkephalin, one copy of Leu-enkephalin, one copy of the heptapeptide Met-enkephalin-Arg-Phe, one copy of the octapeptide Met-enkephalin-Arg-Gly-Leu, in addition to peptide E and its fragments as shown in figure 5.^{48,49} Peptide E is a 25 amino acid (aa) peptide with Met-enkephalin at its N-terminus and Leu-enkephalin at its C-terminus. Its fragments are BAM22, BAM20 and BAM12. These neuropeptides have been shown to be released from adrenal medulla along with catecholamine. All of these

Introduction

peptides were physiologically more active than Met-enkephalin on the contractility of canine small intestine. BAM22 was able to activate all three opioid receptor subtypes.⁵⁰ Further investigations revealed that of Proenkephalin processing in chromaffin cells plays a role in immunomodulation in addition to nociception. Using MALDI-TOF mass spectrometrical analysis, it was feasible to unravel 16 novel cleavage sites and 30 cleavage products. The role of these peptides was not clear and the possibility that these novel entities were due to the extraction procedure could not be excluded.^{51,52} Nevertheless, this study shows that there could be many peptides still to be characterized. It was also found that BAM22 is significantly elevated in the plasma of rats in a model of induced acute cholestasis. This could have a biological relevance since in liver cholestasis there are abnormalities in immune function, adrenal steroidogenesis and glucose homeostasis. BAM22, as a potent opioid, could well be involved in these abnormalities (including itch).⁵³

A



B

*MARFLTLCTWLLLLGPGLLATVRAECSQDCATCSYRLVRPADINFLACVMECEGKLPSLKIWETCKELLQLSKPELPQDGTSTLRE
NSKPEESHLLAKRYGGFMKRYGGFMKKMDELYPMEPEEEANGSEILAKRYGGFMKKDAEEDDSLANSDDLKELLETGDNRRR
SHHQDGSNDNEEVSKRYGGFMRGLKRSPQLEDEAKELQKRYGGFMRRVGRPEWWMDYQKRYGGFLKRFAEALPSDEEGESY
SKEVPEMEKRYGGFMRF*

_____ (Peptide E)
 _____ (BAM22)
 _____ (BAM20)
 _____ (BAM12)

Figure 5: **A:** Schematic representation of proenkephalin and the dibasic amino acids flanking Met-enkephalin (M), Leu-enkephalin (L), octapeptide Met-enkephalin-Arg-Gly-Leu (O), heptapeptide Met-enkephalin-Arg-Phe (H). Proopiomelanocortin (POMC) and its active smaller neuropeptides are also flanked by dibasic amino acids. **B:** The primary sequence of preproenkephalin. The first 28 amino acids (in italics) are a cleavable signal peptide. The dibasic amino acids are in red in case of Met-enkephalin, green in case of Leu-enkephalin, blue in case of the octapeptide Met-enkephalin-Arg-Gly-Leu and last seven amino acids represent the heptapeptide Met-enkephalin-Arg-Phe. Peptide E (underlined sequence) and its fragments are also represented. Figure 5 is modified from ref.47.

1.3.1 MRGPRX1 receptor

MRGPRX1 (accession number: NM147199) is till now the best characterized human receptor in the MRGPRX subfamily. Although MRGPRX1 is officially an orphan receptor, BAM22 has been described as a putative agonist. Interestingly, the classical opioid YGGFM motif in BAM22 was not required to activate MRGPRX1. Hence, BAM8-22 was a potent full agonist and its effect was not antagonized by naloxone.¹⁸ The coupling of MRGPRX1 was reported to be via G_q in all relevant publications, but some reported an additional G_i coupling as well.^{18,23} Although the brain has the required machinery to process BAM8-22, it is not clear if this peptide could be produced in the vicinity of DRG. Hence, it is not clear if BAM8-22 could be an endogenous ligand for MRGPRX1.¹⁹ It was also found that rMRGPC and mMRGPC11 could be activated by BAM22. Thus, it was supposed that the rodent MRGPC and the human MRGPRX1 are functional orthologs. In addition, it turned out that MRGPC but not MRGPRX1 could be more potently activated by γ 2-MSH, a POMC cleavage product (see figure 5 and table 2). As with BAM22, the active moiety of γ 2-MSH was found to be in the C-terminal part. γ 2-MSH6-12 was the active form at MRGPC.^{42,43}

These interspecies differences should always be taken into account and this is especially the case when it comes to MRGPR receptors. Two other findings demonstrate this point. First, Solinski et al. showed that MRGPRX1 receptor expressed in HEK293, COS, F11 and ND-C cells does not undergo agonist induced endocytosis upon activation via BAM22. In contrary, both rMRGPC and mMRGPC underwent endocytosis upon activation. Since endocytosis could have important pharmacodynamical ramifications like the correlation between tolerance and opioid receptor endocytosis, using results of animal experiments should only be conducted with great caution.⁵⁴ Of note, Kunapuli et al. reported contradictory data about MRGPRX1, in which they showed BAM8-22-induced endocytosis in U2OS cells.⁵⁵ This contradiction could be due to the U2OS cell line. Second, Liu et al. investigated the relationship between protease activated receptor 2 (PAR2) and mMRGPC11, which are both expressed in the same neurons in the DRG. PAR2 is activated by trypsin, tryptase or the synthetic ligand SLIGRL, which is derived from its tethered ligand sequence. Since SLIGRL induces histamine-

Introduction

independent itch, it was assumed that this effect is PAR2-dependent. However, PAR2^{-/-} mice did scratch more significantly than wild-type mice after SLIGRL-subcutaneous administration. This proved that this peptide targeted other receptors than PAR2 in order to induce itch. Upon further investigation, it was found that SLIGRL activated exclusively mMRGPC11 with an EC₅₀ of 10.1 μM. In accordance, the previously mentioned mrgpr KO-mice³² showed a reduced itch response to the peptide. Most interestingly, the human corresponding peptide SLIGKV was not able to activate the functional ortholog MRGPRX1 but MRGPRX2, revealing the complexity of the interspecies relationships between MRGPR members.⁵⁶ Despite these differences, it remains important to go through the known information about MRGPC receptor, which could offer insights into MRGPRX1 and other human MRGPR members. It should be mentioned that the effect of BAM8-22 on nociception was a matter of controversy with some publications attributing analgesic effects and other algesic effects to BAM8-22.

The effect of BAM22 on *c-fos*-like immunoreactivity (an indication of nociceptive input from primary afferents) was investigated in the rat dorsal horn after thermal noxious stimulus. BAM22 could inhibit the immunoreactivity in both opioid-dependent and opioid-independent manner.⁵⁷ Intrathecal (i.t) administration of BAM22 potently and persistently increased the tail withdrawal latency. This effect was only partially inhibited by naloxone.⁵⁸ The expression of BAM22 itself was also investigated in an inflammation model using complete Freund's adjuvant (CFA). BAM22 was upregulated in the spinal cord and the DRG small to medium size sensory neurons. Inhibitory anti-BAM22 antibodies reduced the mechanical threshold in the inflammation model but not in the naïve rats.⁵⁹ BAM8-22 was not able to prevent morphine tolerance and hyperalgesia in rat when administered with morphine on a daily basis but it could significantly reduce morphine tolerance and hyperalgesia when administered every other day (intermittently). These findings could be explained by the desensitization of rMRGPC receptor after daily BAM8-22 administration.⁶⁰ In order to explain the analgesic effects of BAM8-22, it was suggested that BAM8-22 can modulate NMDA-mediated activation of spinal dorsal horn neurons.⁶¹ Guan et al. exploited the mouse line deficient in the 12

Introduction

mrgpr genes³² (see also figure 2) by comparing its response to formalin injection (nociceptor activation as well as tissue inflammation) with the response of wt-mice. KO-mice showed a greater increase in *c-fos*-expressing neurons, which means a more pronounced inflammatory pain response. Hence, at least one of the 12 MRGPRs seems to be involved in limiting the excitability of neurons. Upon i.t administration of BAM8-22 there was a significant decrease in both thermal hyperalgesia and mechanical allodynia in the wt-mice whereas the KO-mice were unaffected.⁶² The same group further investigated both BAM8-22 and the selective MRGPRC agonist, compound 2 (see table 2), and found out that MRGPRC agonism at spinal but not peripheral sites contributed to the inhibition of hyperalgesia and neuropathic pain.⁶³ These data suggest that agonists rather antagonists are relevant as drugs at MRGPRC and its human ortholog MRGPRX1.

On the other hand, Grazzini et al. found that the selective rMRGPRC agonist γ 2-MSH6-12 induced hyperalgesia and allodynia after intradermal injection and hyperalgesia after central application.⁴³ BAM22 was also found to increase noxious heat-induced calcitonin gene-related peptide (CGRP) release as an indication of activation of a large nociceptor population.⁶⁴ In another study, γ 2-MSH6-12 was also found to induce hyperalgesia and allodynia in the rat upon intradermal application. siRNA was designed to knock out the *mrgprC* gene both *in vivo* and *in vitro*. This knockout was adequate to completely terminate the responses to the agonist.⁶⁵ Heterologous expression of MRGPRX1 in rat neurons showed that MRGPRX1 can inhibit M-type potassium channels, which could increase the excitability.⁶⁶ In order to investigate downstream signaling of MRGPRX, the receptor was expressed in the dorsal root ganglia-like F11 cell line. BAM8-22 could activate MRGPRX1 resulting in protein kinase C (PKC)-dependent sensitization of TRPV1 to heat and protons. MRGPRX1 could also activate TRPV1 in PKC-independent manner, via diacylglycerol (DAG) and phosphatidylinositol-4,5-bisphosphate (PIP₂) after phospholipase C activation.⁶⁷ The same group investigated the previously mentioned hypothesis that the biochemical communication between mast cells and sensory neurons could provide insights into MRGPR receptor.⁴⁴ In their interesting study they demonstrated that MRGPRX1 can up-regulate chemokine receptor 2 (CCR2). BAM8-22 could induce the expression of

Introduction

CCR2, which has been linked to neuropathic pain, in both HEK and dorsal root ganglia cells. Since MRGPRX1 is also expressed in the immune system, BAM8-22 was investigated at LAD-2 mast cells. Interestingly, BAM8-22 induced the release of the chemokine CCL2, the native agonist at CCR2 receptor. This shows that BAM8-22 exerts its effect on the immune and peripheral nervous system.⁶⁸ These data imply that MRGPRX1 antagonists could represent a novel approach to tackle neuropathic pain.

It is difficult to reconcile all the previous data. The fact that MRGPR receptor induce itch via activation of the neurons and simultaneously inhibit neuropathic pain could not be easily explained. It is also noticeably that the analgesic and algescic effects of BAM22 and BAM8-22 were observed in the same animal models.^{43,60,65,66} These contradictions could be, at least partially, explained by different BAM8-22 effects at the periphery vs. central terminals. Alternatively, BAM8-22 could modulate cellular activities differently at cell bodies as compared to central termini. Differences could also occur as a result of disparate distribution and compartmentalization of MRGPR receptors, different signaling machinery (G_q vs. G_i) and unique modulation of ion channels.⁶² In a seminal study on 15 healthy human volunteers, BAM8-22 applied via cowhage spicules induced significant itch, which was occasionally accompanied by hyperalgesia but no wheal or neurogenic flare (histaminergic symptoms). Thus, the only investigation in humans so far indicates that BAM8-22 mediates itch via MRGPRX1.⁶⁹

The medicinal chemistry of MRGPRX1 is the most developed among the MRGPRX subfamily members with potent agonistic and antagonistic compounds described. Wroblowski et al. discovered by calcium mobilization assay in a high throughput context a series of pyridazinones as active compounds at the MRGPRX1 receptor. Modeling study of the receptor with the most active compound (see figure 7) was also conducted based on the crystal structure of bovine rhodopsin. The proposed key interactions were with the following amino acids: Tyr 99, Tyr 106, Glu 157, Asp 177, Phe 232, Phe 236 and His 254.⁷⁰ In another work and in order to synthesize agonists for MRGPRX1,

Introduction

Malik et al. adopted a solid-phase approach and synthesized a class of small molecules belonging to tetracyclic benzimidazoles, which demonstrated a high affinity for both MRGPRX1 and MRGPRX2 receptors as shown in figure 7.⁷¹ It was also shown that chloroquine could activate MRGPRX1 in addition to mMRGPRA3 (see above), which means that MRGPRX1 could also be considered as related to both mMRGPRA3 and mMRGPC11. Nevertheless the affinity was 10-fold lower at the human receptor with an EC₅₀ value of 297 μM.³² Kunapuli et al. developed the first antagonists at MRGPRX1. The scaffold was 2,3-disubstituted azabicyclo-octanes.⁵⁵ Interestingly, this class of compounds was found to antagonize MRGPC receptors as well.⁶³ The most active compound is shown in figure 7. Bayrakdarian et al. developed 2,4-diaminopyrimidine derivatives as potent antagonists after finding an initial hit with a quinazoline core.⁷² Potent and selective positive allosteric modulators (PAMs) have been recently developed for the MRGPRX1 receptor based on 2-(cyclopropanesulfonamido)-*N*-(2-ethoxyphenyl)benzamide. These PAMs were human-specific with no activity at MRGPC receptors.⁷³ Figure 6 shows the most potent ligands developed so far.

There are still two important unrelated findings about MRGPRX1 receptor in the literature. The first was the formation of heterodimers between MRGPRX1 and the delta opioid receptor when both receptors are overexpressed. When both are coactivated by BAM22, MRGPRX1 dominates over delta opioid receptor and inhibits its signal. It is not known if this interaction is physiologically relevant but it could have implications for pain and morphine tolerance if proven in native tissues.⁷⁴ The second finding was the extensive copy number variation in the *mrgprX1* gene. Using a novel PCR technique to determine the absolute copy number of a gene, it was found that some individuals could have up to 6 copies of *mrgprX1*. This could be an explanation for the great variation between individuals regarding the itch sensation.^{38,75}

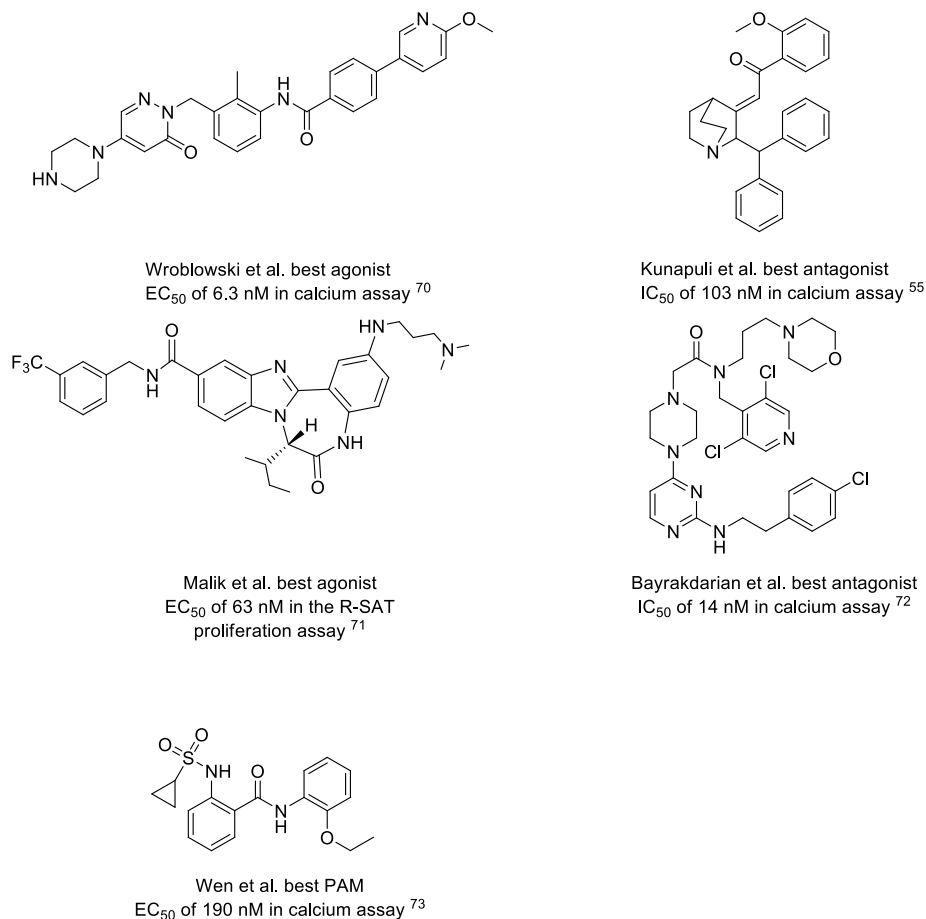


Figure 6: Structures of the most potent ligands developed at MRGPRX1 receptor with the reported potency and type of the assay used in the corresponding publications.

Excursus: Cortistatin-14

In 1996 a new mRNA in the rat brain was discovered, corresponding to a 112 amino acid protein with a secretion-signal sequence and two cleavage sites for mature peptides. The protein showed in its C-terminus a remarkable similarity to somatostatin. Further investigations found that this protein is expressed mainly in the cerebral cortex and hippocampus and more precisely in the GABAergic interneurons. The novel neuropeptide reduced dramatically the electrical activity of the cerebral cortex. Taking this inhibitory property and the marked expression in the cortex into consideration, the protein was named precortistatin and the mature neuropeptides were named cortistatin-14 (CST-14) and cortistatin-29 (CST-29).⁷⁶ Tostivint et al. have published in the same year the CST of the frog but they figured out that it is a second variant of somatostatin in the tetrapods and named it somatostatin-2.⁷⁷ In 1997, the human peer of the rat precortistatin was cloned. The human

Introduction

neuropeptides were named CST-17 and CST-29 and showed a similar expression profile in the brain as in the rat. CST has shown an impressive affinity to all 5 somatostatin (SST) receptor subtypes. The IC_{50} values in the cAMP assays as well as K_i values in the binding assays of CST at SST receptors showed affinities in the low nanomolar to the sub-nanomolar range. This affinity was comparable to that of SST itself.⁷⁶⁻⁷⁸ This high affinity led to the assumption that CST and SST activate solely the same receptors. Nevertheless, some observed effect of CST could not be induced by SST. Mendez-Diaz et al. found for example that CST could induce analgesia in rat but not SST. Intracerebroventricular administration of CST reduced pain perception using the Hot Plate test.⁷⁹ Such findings could be explained by the binding of CST to its own receptor. Several years later, two targets have been identified to bind CST-14, namely the MRGPRX2 receptor and ghrelin receptor (also known as GHS-R or growth hormone secretagogue receptor). CST-14 binds to these receptors with less potency than to SST receptors. The IC_{50} and K_D values described were two-digit figures in the nanomolar range.^{80,81} The previous findings could explain that 1) CST and SST are encoded by different genes, 2) CNS neural populations expressing these neuropeptides do not fully overlap, 3) SST increased cortical excitability, whereas this is depressed by CST, 4) if coexpressed in the same neurons, CST and SST are regulated by different signals.⁸²

Table 4: Names and sequences of the 3 neuropeptides, whose receptors could be addressed by cortistatin-14.

Name	Sequence	Modification
Cortistatin-14	PCKNFFWKTFSSCK	Disulfide bridge between 2 - 13
Somatostatin-14	AGCKNFFWKTFSTSC	Disulfide bridge between 3 - 14
Ghrelin	GSSFLSPEHQRVQQRKESKKPPAKLQPR	Ser-3 = Ser(n-octanoyl)

The fact that CST is expressed not only in the cerebral cortex but in other peripheral tissues like the immune system and gastrointestinal tract as well as its ability to bind to more than one 7TMR, promoted the search for a unique physiological role of this neuropeptide. CST was proposed to take the role of a connecting link between different tissues (brain-gut communication for instance) and was investigated more rigorously in the immunology and endocrinology (both physiologically and malignant pathologically) fields. It should be noted that the role of CST in the immune system is suggested to take place through any of the three receptors, whereas its endocrinological importance

Introduction

is due to SST and ghrelin receptors.⁸³⁻⁸⁷ Capuano et al. have demonstrated that CST does not modify the basal release of calcitonin gene-related peptide (CGRP), a main neuropeptide mediator of pain transmission, but it significantly reduces CGRP after its stimulation with different secretagogues. The inhibition of CGRP release could have been shown both in primary cultures of rat trigeminal neurons and rat brainstem explants. This could be of importance for chronic pain, migraine or post-herpetic neuralgia.⁸⁹ In a murine trinitrobenzene sulfonic acid (TNBS) induced model of Crohn's disease (CD), CST-29 could significantly reverse the manifestations of CD. Interestingly, CST-29 reversed the lost body weight and was found to inhibit the inflammatory cascade via inhibition of tumor necrosis factor alpha (TNF- α), interleukin 1 beta (IL-1 β), interleukin-6 (IL-6) and NO as well as the induction of the anti-inflammatory interleukin-10 (IL-10). These effects could not be fully induced by SST.⁹⁰ Due to its modulation of the immune response, CST was further investigated in various murine models of endotoxemia. CST-29 could attenuate the production of the inflammatory mediators of activated macrophages.⁹¹ In a recent interesting study CST KO-mice were generated. The lack of CST significantly exacerbated pain in acetic acid induced visceral pain, CFA-induced chronic inflammatory pain, paw incision-induced allodynia and thermal hyperalgesia as well as arthritis-induced bilateral allodynia models. CST was found to be highly expressed in dorsal root ganglia, especially in the small to medium diameter neurons. At the molecular level, it was demonstrated that the kinases ERK and Akt were inhibited by CST which caused decreases in substance P, CGRP and expression of TRPV1 in the DRG. CST was also expressed in GABAergic interneurons and in the spinal cord.⁹²

The aforementioned publications, especially the ones based on *in vivo* models in the rat and mouse, indicate an interesting potential of CST in the therapy of several diseases. Nevertheless, it should always be kept in mind that the differences between humans and rodents are very big. The extrapolation of such data on CST to humans should be carried out very cautiously.

1.3.2 MRGPRX2 receptor

MRGPRX2, (accession number: NM-054030), is the second member of MRGPRX subfamily, which was discovered in 2001 and was thought to be exclusively expressed in the small diameter sensory

Introduction

neurons of the DRG and play a role in nociception.^{17,18} Like other human MRGPRX receptors, MRGPRX2 does not have a direct ortholog in rodents but orthologs have been found in macaque and rhesus monkeys.^{22,23} This member is less characterized than MRGPRX1 regarding both physiological functions and medicinal chemistry. Nonetheless, it is far better understood than MRGPRX3 and MRGPRX4. Although all MRGPRX members are still officially orphans, the first putative ligand for MRGPRX2, CST-14, was put forward by Robas et al. in 2003. CST-14 showed an EC₅₀ value of 25 nM in calcium assay in HEK cells, whereas SST-14 showed an EC₅₀ of 780 nM. In addition, it was found that the receptor has a sole G_q coupling.^{19,81} Kamohara et al. demonstrated that MRGPRX2 can be activated by another physiological ligand, namely, proadrenomedullin N-terminal peptide. The powerful hypotensive proadrenomedullin N-terminal 20 peptide (PAMP-20) and its truncated form PAMP-9-20/PAMP-12 activated MRGPRX2 in calcium assays with an EC₅₀ value like that of CST-14. It has also been shown that MRGPRX2 is also expressed in the adrenal chromaffin cells besides DRG. In that paper it was reported that MRGPRX2 expressed in CHO cells is both G_q and G_i coupled.⁹³ Burstein et al. confirmed MRGPRX2 dual coupling to G_q and G_i both in human and rhesus using an interesting proliferation assay.²³ Akuzawa et al. reported that MRGPRX2 could be activated in calcium assays by morphine (EC₅₀ value 4.5 μM), dextrophan (EC₅₀ 1.4 μM) as well as 3-methoxy-morphinan (EC₅₀ 4.7 μM). It was reported that MRGPRX2 is desensitized and internalized after incubation with 1 μM CST-14 or 100 μM morphine.⁹⁴ In a screening campaign it was possible to identify TAN-67, a potent δ opioid agonist, as an agonist at MRGPRX2 receptor with an EC₅₀ value of ca. 1 μM in both β-arrestin and calcium mobilization assays.⁹⁵ A recent paper described the natural product complanadine A as a selective MRGPRX2 agonist after screening it at 165 7TMRs (see figure 7). The EC₅₀ value was 5.5 μM in calcium assays.⁹⁶ The only novel synthetic agonists for MRGPRX2 were proposed by Malik et al. (also for MRGPRX1 as mentioned above). These agonists were not peptidergic but have a tetracyclic benzimidazole scaffold as illustrated in figure 7.⁷¹ These data revealed that MRGPRX2 is the only member of the MRGPRX family (at least for now) to be found outside the DRG and seems to be rather promiscuous regarding the activating ligands. Van Hagen et

Introduction

al. have found that monocytes, macrophages and dendritic cells produce CST and express SST2 receptors but not mrgprX2, whereas thymus expresses SST1, 2, 3 and mrgprX2 receptors on the mRNA level.⁸⁸ In fact immunology turned out to be the field with the most extensive research concerning MRGPRX2 functions and ligands. The only cells in the immune system, which undoubtedly express MRGPRX2 receptors on the protein level, are mast cells.

Mast cells express beta2 adrenergic receptors, adenosine receptors, several chemokine receptors, GPR34, Histamine H4, several nucleotide receptors as well as MRGPRX1 and MRGPRX2. The activation of some of these receptors leads to degranulation of the mast cells, which means a potential to treat diseases like asthma and urticaria. MRGPRX2 is one of these potential target receptors.⁹⁷ Mast cells can release its inflammatory mediators via IgE-dependent and IgE-independent pathway. The IgE-independent pathway involves the activation via basic secretagogues (substance P, mast cell-degranulating peptide, neuropeptide Y, compound 48/80 etc.). Since no receptor for basic secretagogues was found, it was suggested that these mediators interact directly with the G proteins. Tatemoto et al. have found that basic secretagogues could activate MRGPRX2 (but not MRGPRX1) receptor with EC₅₀ values between 10⁻⁴ and 10⁻⁷ M in calcium assays using HEK-293 cells. Thus, MRGPRX2 was proposed to be an atypical 7TMR with various weak endogenous agonists.⁹⁸

It is also noteworthy to mention that the LAD2 mast cell line is a suitable cell line to investigate natively expressed MRGPRX1 and MRGPRX2. Up to date there is no known cell line able to natively express MRGPRX3 or MRGPRX4 receptors.¹⁹

Subramanian et al. have demonstrated that the C5a receptor antagonist PMX-53, a cyclic hexapeptide based on the terminal amino acid sequence of C5a, behaves as an agonist at MRGPRX2 receptor. PMX-53 (see table 5) could induce mast cell degranulation and a calcium signals via MRGPRX2 receptor and this effect could not be detected in a murine cell line due to the lack of MRGPRX2 receptors. The EC₅₀ value of PMX-53 was not determined in this paper.⁹⁹ The same group found also that the C3a agonist, E7, could activate MRGPRX2 receptors in mast cells and induce

Introduction

degranulation, thus behaving as a dual agonist at MRGPRX2 and C3a receptors as well.¹⁰⁰ Another component of the immune system, which was reported to act via MRGPRX2 receptors, is the antimicrobial peptide LL-37 (see table 5). LL-37 was previously reported to induce chemokine production and mast cell degranulation via unknown mechanisms. In this study, it was also suggested that MRGPRX2 is one of the few 7TMRs that are resistant to phosphorylation, desensitization and internalization.¹⁰¹ It is noteworthy to mention that the resistance of MRGPRX2 to phosphorylation means that no β -arrestin recruitment can take place. This is apparently not true since we, in our group, are able to conduct β -arrestin assay using the MRGPRX2 cell line with very clear positive results. In this publication, a cell-based radioactive phosphorylation assay was employed to investigate the phosphorylation. The text in this paper described a resistance to phosphorylation. Intriguingly, in the same paper a figure showed a CST-induced phosphorylation. Although the CST-induced phosphorylation was less pronounced than C3a-induced phosphorylation, it does not mean that MRGPRX2 is phosphorylation resistant since the degree of phosphorylation is 7TMR-dependent.¹⁰² The resistance to desensitization and internalization is contrary to the findings of Akuzawa et al.⁹⁴ The same discrepancy has also been reported regarding the MRGPRX1 receptor (see above). The resistance to desensitization and internalization would make sense as the *mrgpr* genes were conceived to function as “nociceptive sensors”.^{17,18,23} Hence, they are expressed in a permanent manner in the cell membrane to intercept painful stimuli.

Other cationic antimicrobial peptides, human β -defensin 2 and 3 (hBD 2, 3), were found to activate MRGPRX2 and cause mast cell degranulation.¹⁰³ To the best of our knowledge no antagonists at MRGPRX2 receptor have been described yet.

In a recent interesting study, MRGPRX2 receptor expression in skin mast cells of patients with chronic urticaria (CU) was compared with that of a nonatopic control. The study showed that the expression levels of *mrgprX2* mRNA in skin mast cells are much higher than in lung-derived mast cells and that the number of MRGPRX2+ mast cells was significantly greater in skin tissues from CU patients than the in nonatopic control. Hence, the blockade of MRGPRX2 on human skin mast cells might offer a

Introduction

novel approach to the prevention and treatment of severe CU.¹⁰⁴ This study is the first one to investigate MRGPRX2 expression in patients.

Table 5 shows the peptidergic agonists whereas figure 8 shows all non-peptidergic agonists described above. It is clear now that MRGPRX2 is activated by many ligands, which do not have that much in common at first glance. In order to elucidate this agonism, Nothacker et al. have investigated the similarity between the most potent agonists CST-14 and PAMP-12. An active core consisting of 2 aromatic amino acids and a basic amino acid at the C-terminus arranged in a specifically spaced manner seems to be important to activate MRGPRX2 (amino acids in **bold** in table 5).¹⁰⁵ It is also clear from the later reported agonists that aromatic as well as positively charged amino acids are important (see table 5).

Efforts to identify a peer for MRGPRX2 in rodents have also been made. Tatemoto et al. investigated rat MRGPR receptors in mast cells and could detect the mRNA of *mrgprB1*, *mrgprB2*, *mrgprB3*, *mrgprB6*, *mrgprB8* and *mrgprB9*. Nevertheless, only MRGPRB3 was reported to be activated by basic secretagogue in a reporter gene assay and calcium assay.⁹⁸ McNeil et al. suggested that MRGPRB2 is the murine ortholog of MRGPRX2 using pharmacological and expression data. MRGPRB2 was activated by CST-14, PAMP-9-20 as well as compound 48/80 (and other basic secretagogues) and expressed exclusively in connective tissue mast cells (but not mucosal mast cells). Importantly, MRGPRB2 was involved only in IgE-independent histamine release. This led to investigation of drugs which show allergic adverse reactions with low IgE-titre and have structure relatedness to cyclized compound 48/80 (more potent mast cell activator than compound 80/48). At first, peptidergic drugs like icatibant, cetorelix and mastoparan were considered. Secondly, the motif tetrahydroisoquinoline (THIQ) was searched for in approved drugs. This led to the identification of non-steroidal neuromuscular blocking drugs (nicotine receptor antagonists). By expanding the search to dihydroquinolines, the fluoroquinoline antibiotics were identified. Interestingly, the investigated peptidergic drugs, fluoroquinolones and non-steroidal neuromuscular blocking drugs (except succinylcholine) were all able to activate both MRGPRB2 receptor (*in vivo* and *in vitro*) and MRGPRX2

Introduction

receptor (*in vitro*). These findings led to the establishment of a mouse model to investigate MRGPRX2 receptor. Nevertheless, it should be noted that CST-14 and PAMP-9-20 were very weak at MRGPRB2 with EC₅₀ values of 21.3 and 12.4 μM, respectively.¹⁰⁶ These values seem to be too high for physiological neuropeptides.

Table 5: The sequences of the peptides (except compound 48/80) reported to activate MRGPRX2 receptor. All EC₅₀ values were obtained using calcium assay

Name	Sequence	EC ₅₀ value
CST-14	PCKNFFWKTFSCK	25 to 1,585 nM ^{2381,116}
SST-14	AGCKNFFWKTFTSC	780 nM ⁸¹
PAMP-20	ARLDVASE FRKKWNKWALSR-amide	251 nM ⁹³
PAMP-9-20/PAMP-12	FRKKWNKWALSR-amide	57.2 nM ⁹³
Minimal core structure	WxxFxxxK/R	
Substance P	RPKPQQFFGLM	2,470 nM ⁹⁸
Oxytocin	CYIQNCPLG	1,470 nM ⁹⁸
Dynorphin A	YGGFLRRIRPKLWDNQ	1,850 nM ⁹⁸
PMX-53	Ace-Phe-[Orn-Pro-dCha-Trp-Arg]	n.d. ⁹⁹
E7	WWGKKYRASKLGLAR	n.d. ¹⁰⁰
LL-37	LLGDFFRKSKEKIGKEFKRIVQRIKDFLRNLPRTES	n.d. ¹⁰¹
hBD2	GIGDPVTLCKSGAICHVFCPRRYKQIGTCGLPGTKCCKKP	n.d. ¹⁰³
hBD3	GIINTLQKYICRVRGGCAVLSCLPKEEQJGKCSTRGRKCCRKK	n.d. ¹⁰³

n.d.: not determined

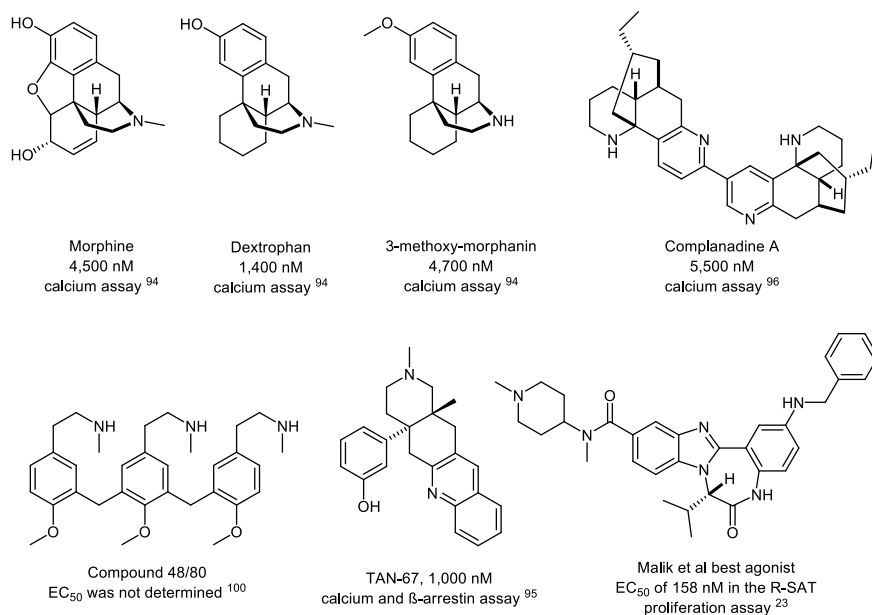


Figure 7: The structures of non-peptidergic ligands reported to activate MRGPRX2 receptor.

It is obvious that the signaling as well as physiological and pathological roles of this receptor still need to be further investigated. Hence, more drug-like pharmacological tools would be of high value. In the case of MRGPRX2, unlike MRGPRX1, antagonists seem to have more therapeutic potential than the agonists. It should be mentioned that it is unusual that many physiological agonists have

Introduction

been described for one receptor. A further issue is that the most potent agonist native (CST-14) has an EC₅₀ value in the lower micromolar range, which is rather unimpressive for a neuropeptide. In addition, the expression of CST is mainly in the cortex, whereas that of MRGPRX2 is in the DRG and mast cells, makes the pairing of the receptor with this ligand even more questionable.

1.3.3 MRGPRX3 receptor

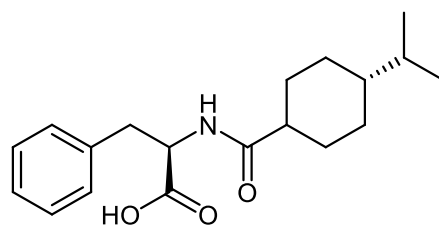
MRGPRX3, (accession number: NM_054031.3), is the third member of MRGPRX subfamily. There is no reported ligand till now. Burstein et al. used a proliferation assay to predict the coupling of the receptor. It was found that MRGPRX3 is only G_q coupled.²³ Nevertheless, a direct agonist should be used to verify this finding. Kaisho et al. overexpressed MRGPRX3 receptor in rats, in which MRGPRX3 gene was put under the control of actin promoter. The rats showed liquification/degeneration and swelling of the lens fiber cells. Focal skin desquamation was also observed in these rats. In both epidermis and lens, an increase in cell proliferation was detected.¹⁰⁷ Another study detected SVA (SINE-VNTR-*Alu*) elements in the 5' untranslated region of *mrgprX3* gene. SVA elements are capable of generating individual variation in gene expression at loci in which they are present and they cause various human diseases like insertional mutagens.¹⁰⁸ SVA belong to the retroelements, which have been suggested to have caused the expansion of the *mrgpr* subfamilies in mice²⁴ (see above). A recent paper has shown the expression of *mrgprX3* on mRNA and protein level in the corneal endothelial cells. This protein was suggested as a molecular marker for this cell type since it was not found in other cell types in the eye.¹⁰⁹ These findings suggest a physiological role of MRGPRX3 in the eye, in addition to nociception. A study in epigenetic changes (methylation) in newborns has revealed that *mrgprX3* gene undergoes increase in methylation with age and with periconceptual environment (micronutrient supplementation). Interestingly, these epigenetic changes were detected only in male newborns, suggesting a potential sexual dimorphism (genetic differentiation between men and women) of *mrgprX3* gene regulation.¹¹⁰ A recent genome-wide association study to analyze the genetic variants related to *hallux valgus* found that a SNP in the 5' flanking of the

Introduction

mrgprX3 gene has a protective effect in women but is associated with a higher risk in men.¹¹¹ These differences between sexes in association with MRGPRX3 still need to be further elucidated.

1.3.4 MRGPRX4 receptor

MRGPRX4 (accession number: NM_054032.3) is the fourth member of the MRGPRX subfamily. There is no reported endogenous ligand till now but recently Kroeze et al. reported nateglinide, a K_{ATP} -channel blocker (see figure 8), as an agonist with an EC_{50} value of 9.1 μ M in a β -arrestin assay.¹¹² Burstein et al. predicted a sole G_q coupling of the receptor.²³ Gylfe et al. have detected MRGPRX4 receptor in colorectal cancer tissue samples and identified this gene as a potential oncogene.¹¹³ Recently two new proteomics data banks, humanproteomemap.org and proteomicsdb.org, were introduced. Both are based on mass spectrometrical techniques.^{114,115} According to the new data, MRGPRX4 is expressed in CD8+ T-lymphocytes. This could simplify the investigation of MRGPRX4 since T-lymphocytes are easier to culture than sensory neurons. In addition, this could reveal a new way of communication between neurons and the immune system via MRGPRX4 receptors. Data^{107,113} indicate that MRGPRX3 and MRGPRX4 could play a role as oncogenes.



Nateglinide

Figure 8: The chemical structure of Nateglinide, an MRGPRX4 agonist. The reported EC_{50} value in β -arrestin assay was 9.1 μ M.

1.4 Aim of the thesis

The aim of the thesis was to characterize the four subtypes of human MRGPRX receptors. The first step was to search for pharmacological tools, taking advantage of the diverse compound libraries available in the pharmaceutical chemistry department. Further optimization of the found ligands was intended to improve both potency and selectivity. Since agonistic synthetic ligands for both

Introduction

MRGPRX1 and MRGPRX2 have already been discovered, our search was focused on antagonists for these two subtypes.

On the contrary, MRGPRX3 and MRGPRX4 had no published pharmacological tools available at the beginning of this thesis. Hence, the aim was to find agonistic tool compounds and then search for antagonistic ones. The initial tools were intended to be further optimized to ideally reach the highest feasible affinity and selectivity.

Having found tools, the goal was to employ them for a pharmacological characterization using several assays like β -arrestin, cAMP, calcium mobilization assay in order to further elucidate the signal transduction of these poorly understood receptors.

It should be noted that MRGPRX4 was of central interest from the very beginning. Therefore, this thesis aimed at deepening the characterization of this particular receptor regarding its physiological and pathological role, searching for cell lines with native expression, in addition to the synthesis of a radioligand as a valuable pharmacological tool.

In essence, we aspired to pave a new way to investigate the MRGPRX receptors. This could open new doors to elucidate these exclusive primate 7TMRs and enable other research group to investigate them in a variety of aspects.

2. Results and Discussion

2.1 MRGPRX1 receptor

The medicinal chemistry of the MRGPRX1 receptor, with several moderately potent agonists and antagonists, is the most advanced one among the four members of the MRGPRX receptor subfamily.^{55,70,71,72} Since the current understanding of the physiological role of this receptor^{54,67,69} indicates a potential role of antagonists as therapeutics for pain and itch, it was decided to carry out screening for antagonists.

2.1.1 Screening of compound libraries in search for MRGPRX1 antagonists

In order to identify potential antagonists, the compound libraries 1-8 were screened (see chapter 4.10). The screening was done using a β -arrestin assay at 10 μ M (n=1). A specific compound was considered as a hit if it showed more than 50% inhibition of the signal induced by the agonist BAM22 at its EC₈₀ concentration (see chapter 4.8.1).

Prior to searching for antagonists at MRGPRX1 receptors, it was required to choose an agonist and perform a concentration-response curve. The β -arrestin cell line used in the assay was commercially available from DiscoverX®. BAM22 was chosen as agonist to perform the assay and it showed an EC₅₀ value of $2.51 \pm 0.49 \mu$ M as shown in figure 9. This value is higher than the reported EC₅₀ values in the nanomolar range,^{18,116} which are reported using calcium assays. This could be due to the frequently observed tendency of β -arrestin assays to give higher EC₅₀ values than calcium assays.¹¹⁷ This finding is also an indication that BAM22 is probably not the physiological ligand since neuropeptides tend to have much lower EC₅₀ values at their receptors.^{82,84}

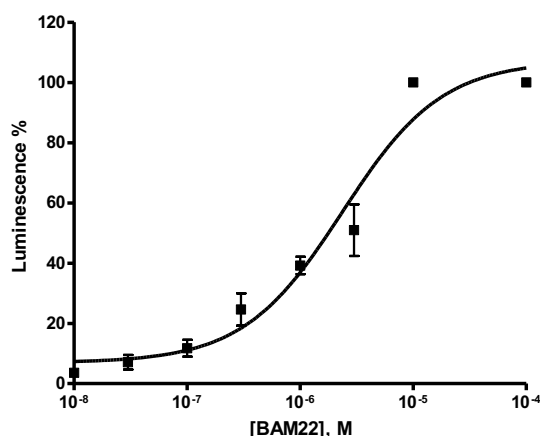


Figure 9: The mean curve of three independent experiments of BAM22 at MRGPRX1 receptor using β -arrestin assay. The determined EC_{50} value was $2.51 \pm 0.49 \mu\text{M}$.

A cheap alternative to BAM22 could be the antimalaria drug chloroquine.³² Unfortunately, it was not possible to conduct β -arrestin assays using chloroquine as an agonist because no signal could be detected upon screening at $100 \mu\text{M}$ (data not shown). The described EC_{50} value of $297 \mu\text{M}$ in calcium assays is extremely high and could explain the lack of signal in the less sensitive β -arrestin assay. It should also be noted that BAM8-22 could be used as an alternative agonist at MRGPRX1 since it has no opioid activity like BAM22, but it is more expensive.

Having ensured the suitability of the assay and determined the EC_{50} value of BAM22, it was possible to initiate screening for antagonists. This screening was done at the beginning of 2014, and since the compound libraries would always be reviewed and expanded, the reported results concerning MRGPRX1 applies to the status of compound libraries in April 2014.

The screening of compound libraries 3-7 (see chapter 4.10) resulted in no hit (data not shown). It should here be mentioned that the glycoside digitonin from the compound library 7 blocked 80% of the signal at $10 \mu\text{M}$ but this result is probably an artifact due to the detergent properties of the compound.

The screening of compound library 2 resulted in very weak hits. The compounds were so weak that no full curves could be obtained, but it might be interesting for future investigations to keep in mind that xanthine derivatives could be antagonistic at MRGPRX1. The structure of the hits is shown in figure 10.

Results and Discussion

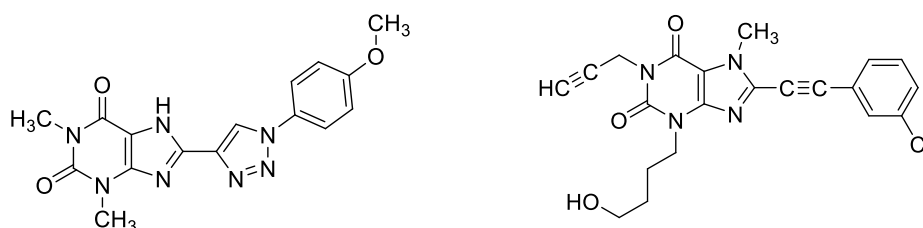


Figure 10: The structures of the weak hits at MRGPRX1 receptor from the compound library 2. Both showed an inhibition of 48% and 49% at 10 μ M in β -arrestin assay.

The most potent hits were identified in the compound library 1. The three hits were MIRA-1, cantharidin and ZM39923, and their structures are shown in table 6. Taking the chemical structure and biological activity into account, it seemed that there could be instability (cyclic acid anhydride) and non-specific activity (kinase inhibition) issues. Therefore, it was decided to further investigate the compounds. The effect of cantharidin on cells was first investigated because it is a toxin.¹¹⁹ Cantharidin turned out to be too toxic since the cells died within 30 minutes of the addition of the compound. Hence, this compound was considered inappropriate to be a pharmacological tool at least in β -arrestin assays due to the 3 hours incubation time.

Table 6: The detected hits (first three compounds) with their previously described biological activity.

Name	Structure	Biological Activity
MIRA-1		Restores wild-type function of mutant p53 and promotes apoptosis in a mutant p53-dependent manner with IC ₅₀ of 10 μ M ¹¹⁸
Cantharidin		Toxin inhibitor of protein phosphatases 1 and 2A with K _i values of 1.7 and 0.16 μ M, respectively ¹¹⁹
ZM39923		Potent inhibitor of Janus tyrosine kinase 3 (JAK3), pIC ₅₀ is 7.1 ¹²⁰
ZM449829		Potent inhibitor of Janus tyrosine kinase 3 (JAK3), pIC ₅₀ is 6.8 ¹²⁰

It is noteworthy that ZM39923 would break down in neutral buffer ($t_{1/2}$ =36 min, pH=7.4) to ZM449829 (see table 5). Owing to the long incubation time in β -arrestin assay, the detected inhibition is probably due mainly to ZM449829. Since this compound could interact with amino acids via Michael addition, the inhibition could be irreversible. Therefore, ZM39923 was also excluded.

Results and Discussion

MIRA-1 was investigated as well. The determined IC_{50} value was $12.1 \pm 0.6 \mu\text{M}$ as shown in figure 11. So far, this seems to be the most promising antagonist to be found at MRGPRX1, especially that it seems to be relatively selective since it was not reported as a hit at other receptors. Nonetheless, it is inferior to the best antagonists mentioned in the literature. MIRA-1 should be further investigated since this compound is an ester, which means it will probably be degraded upon contact with the cells. Since this compound could induce apoptosis, it is important to exclude this effect (cell death or decrease in cell number) as a cause of signal inhibition. This result should be viewed with caution because the inhibition was only noticeable at a high concentration of $10 \mu\text{M}$ as seen in figure 11.

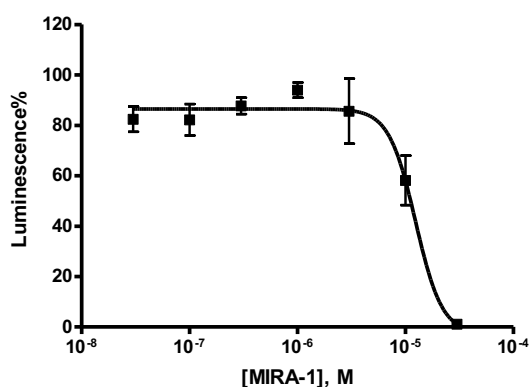


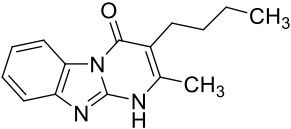
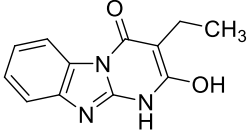
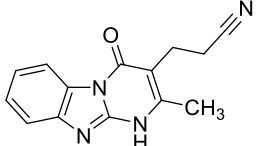
Figure 11: The mean curve of three independent experiments of MIRA-1 at MRGPRX1 receptor using β -arrestin assay.

It should be added that the compound library 9 was screened at $10 \mu\text{M}$ both as agonists and antagonists but no hit could be found (data not shown).

Since MRGPRX1 and MRGPRX2 could both be activated by tetracyclic benzimidazole derivatives⁷¹, it is also plausible that both could also be inhibited by benzimidazole derivatives. Hence, the synthesized compounds for the MRGPRX2 project (till CB39) (see MRGPRX2, chapter 2.2, for all compounds) were screened at MRGPRX1 receptor both as agonists and antagonists. The screening for antagonists led to very weak inhibition or no inhibition at all. The best inhibitors are shown in table 7. The inhibition was unfortunately weak so that no curves could be determined. It was also difficult to deduce SAR for this receptor from these data.

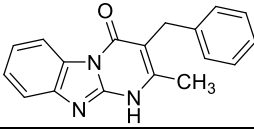
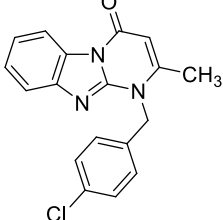
Results and Discussion

Table 7: The compounds with the best inhibition results at MRGPRX1 receptor

Code	Structure	IC ₅₀ ± SEM (μM)	Max. Inhibition at 100 μM (%)
CB18		> 100 μM	48
CB20		> 100 μM	39
CB24		> 100 μM	42

The results of screening for agonists are shown in table 8. Only two hits have been found. CB16 turned out to be a partial agonist. The normalized curves of BAM22 and CB16 are given in figure 13. It could be interesting to test derivatives of CB16 with a substituted benzyl group or a longer side chain than methyl (see figure 12). CB22 was not active. Hence, phenethyl- instead of benzyl-substitution is not tolerated. CB27 was too weak an agonist to carry out a curve.

Table 8: The compounds with the best activation results at MRGPRX1 receptor

Code	Structure	EC ₅₀ ± SEM (μM)*	Max. Activation at 100 μM (%)
CB16		18.1 ± 0.3	40
CB27		> 100 μM	24

*: Results are mean ± SEM of three independent β-arrestin experiments

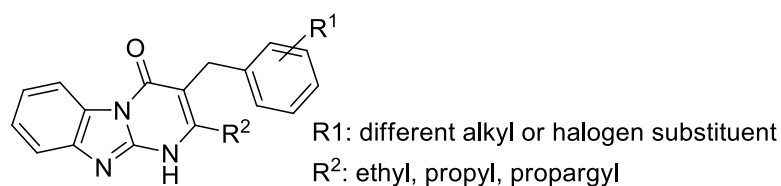


Figure 12: Potential agonists at MRGPRX1 receptor derived from the structure of CB16

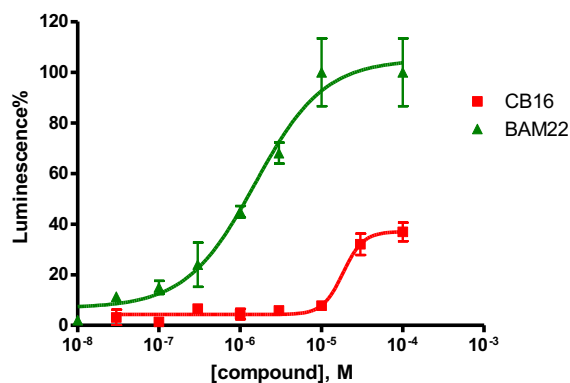


Figure 13: Normalized dose-response curves of BAM-22 and CB16 at MRGPRX1 receptor.

2.1.2 Discussion

It was possible to confirm the activity of BAM22 at the MRGPRX1 receptor and a β -arrestin assay was chosen for further investigations. In addition, a systematic search for antagonists using the then available compound libraries has been done. The results indicate a difficulty in identifying a potent antagonist at MRGPRX1 receptor. This is a general problem with the MRGPRX receptor subfamily.^{121,122} Nevertheless, it was possible to single out one candidate (MIRA-1) as a potential antagonist. MIRA-1 should be further investigated to verify its activity. Calcium mobilization assay could in principle be performed since this receptor is G_q coupled.²³ Due to the fact that calcium mobilization assays are real-time assays and the incubation time is considerably shorter, it could be advantageous to investigate MIRA-1 using this kind of assay to avoid any toxicity due to the long incubation time. It should be mentioned that initial calcium assay experiments in an attached-cell format have been conducted but were not fruitful. This could be due to this kind of assay format. It is advisable to carry out the suspension cell format. In this context it is important to refer to the issue of expression systems. All investigated MRGPRX receptors in this thesis were overexpressed in CHO cells and calcium assays were always difficult to conduct, and when conducted successfully the signal was pretty low. This raised the question about the suitability of the CHO expression system for carrying out an effective calcium assay. This point still needs to be addressed and since MRGPRX receptors are exclusive primate receptors and have restricted expression profiles,^{17,18} other expression systems like astrocytoma cells, COS 7 or HEK 293 cell, could be tried out. The nature of

Results and Discussion

the 7TMRs in β -arrestin assays as a fusion protein could interfere with the G protein coupling as well. In addition, two weakly potent xanthine derivatives have been found. This could be interesting to follow since many such derivatives are available in our department and the compound library 2 is in constant expansion. The MRGPRX2 ligands provided another source of screening for MRGPRX1 receptor. Having screened many derivatives, it was not possible to identify any interesting antagonist. Nonetheless, it was possible to find a weak partial agonist (CB16). Since MRGPRX2 project would likely be further followed, it is recommended to screen the rest of the MRGPRX2 ligands at MRGPRX1 receptor. These findings indicate that more efforts should be done to find new hits at MRGPRX1 receptor like expanding the screening and/or choosing another assay to confirm the detected hits. However, since potent ligands for MRGPRX1 receptor have already been described in the literature, this had lower priority within this study and we focused more on the other MRGPRX receptor subtypes.

2.2 MRGPRX2 receptor

MRGPRX2 receptor is the only member of MRGPRX subfamily that is reported to be expressed outside the DRG. It is expressed in the mast cells, a component of the immune system, and in the adrenal chromaffin cells.^{93,98} The described agonist at this receptor, cortistatin-14, could activate three 7TMRs (somatostatin, ghrelin and MRGPRX2) as mentioned in the introduction. Hence, it could be interesting to develop selective and potent agonists at MRGPRX2 without activating the other two 7TMRs. The MAS-related gene receptors share characteristics like a big expansion in the rodents (especially in the mouse) and the ability to be activated by very heterogeneous ligands ranging from the small adenine to large peptides like BAM22. In addition, it is difficult to define orthologs between species based on the sequence of these genes.^{17,23} However, a recent study suggested that the mouse MRGPRB2 receptor is a functional and pharmacological ortholog of the human MRGPRX2, which could have important implications for elucidating the function of the human receptor.¹⁰⁶

2.2.2 Screening of compound libraries in search for MRGPRX2 antagonists

Our first efforts were to validate the finding that CST-14 is able to activate MRGPRX2 receptor in β -arrestin assay. The used cell line was a commercial cell line from DiscoverX®. Figure 14 shows a clear activation of the receptor with an EC_{50} 252 ± 13 nM value of and a maximal S/N of 18.

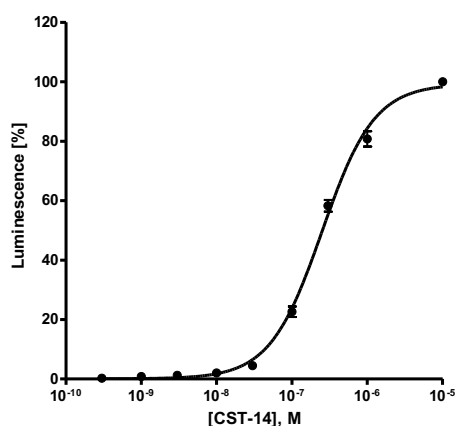


Figure 14: The mean curve of three independent experiments of CST-14 at MRGPRX2 receptor using β -arrestin assay. The determined EC_{50} value was 252 ± 13 nM.

Results and Discussion

It is important to mention that S/N ratio throughout this study was calculated by dividing the maximal signal induced via a compound or a test sample by the basal signal induced by the negative control, which is usually DMSO or buffer.

After establishing the assay, a search for antagonists using our compound libraries has been initiated. The antagonist assay was performed as described in (see chapter 4.8.1) and the compound libraries 1-7 and the compound library 10 have been screened. The screening was done at 10 μ M using β -arrestin assay (n=1). A specific compound was considered as a hit if it showed more than 50% inhibition of the signal induced by CST-14 at its EC₈₀ value (1 μ M).

The first phase (April 2013) was the screening of compound libraries 1 and 7. Several hits have been identified in the initial screening but upon further investigations only menadione (structure in figure 14) from the compound library 7 seemed to demonstrate reproducible results. The IC₅₀ value was determined to be 5.39 ± 1.51 μ M as shown in figure 15.

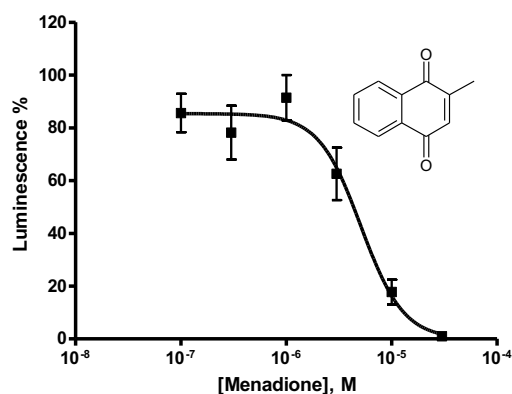


Figure 15: The mean dose-response curve of three independent β -arrestin experiments using menadione as agonist at MRGPRX2 receptor. The determined IC₅₀ value was 5.39 ± 1.51 μ M.

Menadione (2-methyl-1,4-naphthoquinone) is a yellow powder but its stock solution in DMSO is colorless. Due to these results it would be interesting to test other 1,4 naphthoquinone derivatives in order to investigate both toxicity and potency of these derivatives.¹²⁴ Menadione, also known as vitamin K₃, a precursor of vitamins K₁ and K₂, has been used as a therapeutic agent with several applications: for hypothermia, as an anticancer drug, as an anti-inflammatory agent and as a component of multivitamin drugs. Vitamin K₃ presents cytotoxicity towards several types of cells in

Results and Discussion

the human body by inducing oxidative stress through redox-cycle, generating reactive oxygen species (ROS). Oxidative stress in high levels produces oxidative damage in cell structures (lipids, proteins, RNA and DNA) leading to apoptosis or necrosis of the cells. Because of this property menadione has been widely used with cancer chemotherapeutic agents, since it is effective in killing tumor cells. It has also been demonstrated that it kills preferentially fast growing cells. Since tumor cells have this characteristic, its toxicity towards normal cells is much lower. Nowadays menadione is only used as anticancer agent. Its applications on coagulation problems and vitamin deficiency are not advised because of its referred toxicity.¹²⁵⁻¹³¹ One advantage is that menadione could be commercially available and a cheap pharmacological tool.

The second phase of the screening for antagonists (June 2014) encompassed compound libraries 2-6 and the compound library 10. These efforts led to the identification of three hits with reproducible results. The hit from the compound library 5 was termed H351, the one from the compound library 2 was called SL318 and the last hit from the compound library 3 was termed CB8. Figure 15 shows the results of the β -arrestin experiments conducted using these hits as antagonists. The determined IC_{50} values were as follows: **2.42** \pm 0.22 μ M for CB8, **9.80** \pm 1.39 μ M for SL318 and **9.21** \pm 2.28 μ M for H351. These hits were counter-screened at GPR55 and GPR18 and showed no activity at these 7TMRs (data not shown). The hits are from different scaffolds. SL381 is a xanthine derivative; H351 is a pyrimidine derivative, whereas CB8 is tricyclic benzimidazole derivative (see figure 16). SL381 and H351 showed a complete inhibition at their highest concentration, but CB8 showed only 75% inhibition at its highest concentration. CB8 showed the best IC_{50} value and a similar scaffold (tetracyclic benzimidazole) has already been reported to be active at MRGPRX1 and MRGPRX2 but as an agonist⁷¹ (see also figure 8).

Results and Discussion

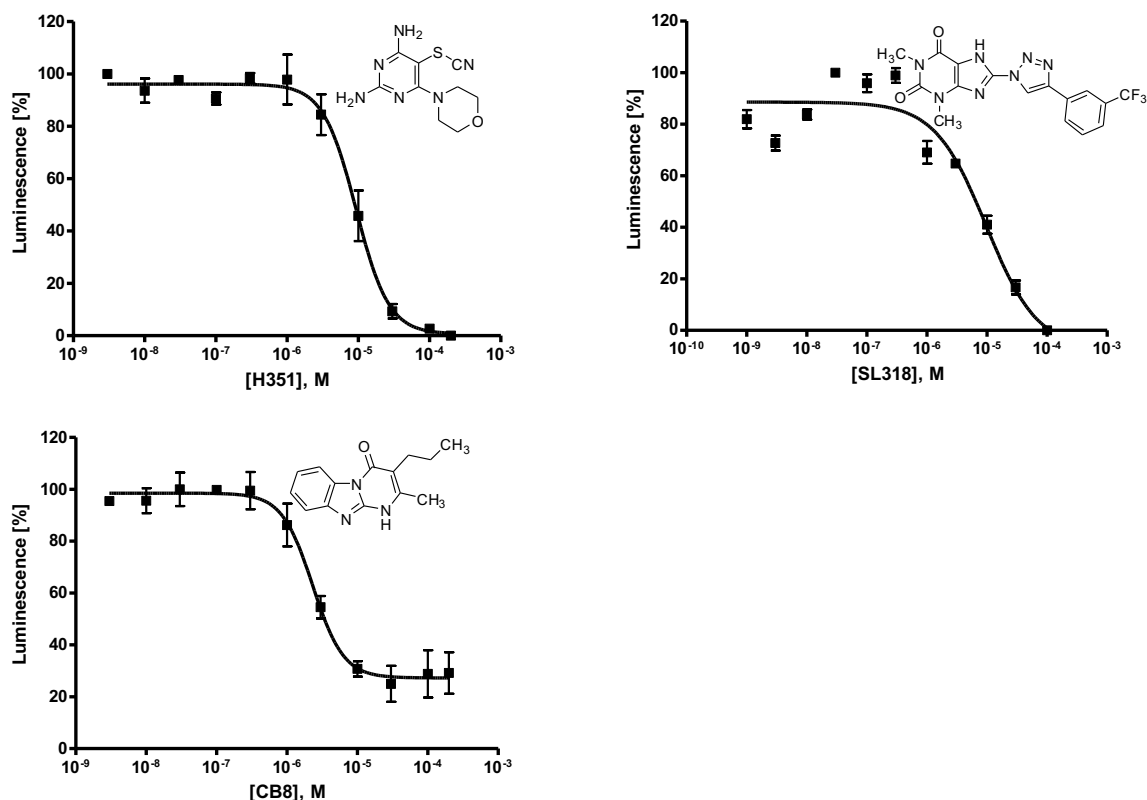


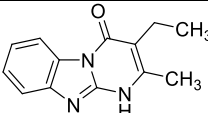
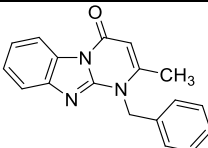
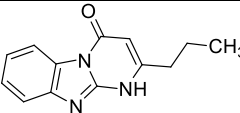
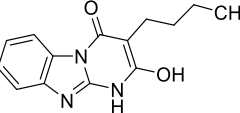
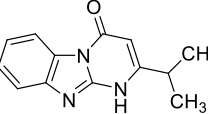
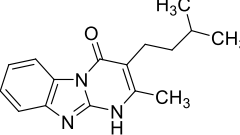
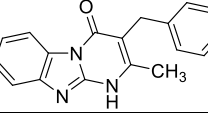
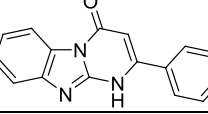
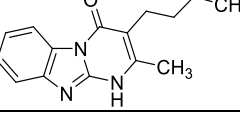
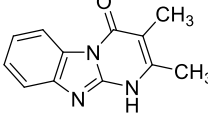
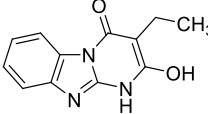
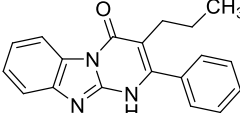
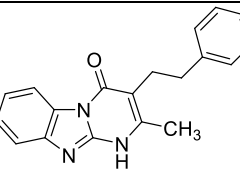
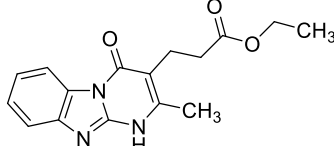
Figure 16: Chemical structure and mean dose-response curve of the three detected hits at MRGPRX2 receptor. The results are mean ± SEM of three independent β-arrestin experiments. The determined IC₅₀ values for H351, SL318 and CB8 were 9.80 ± 1.39, 9.21 ± 2.28 and 2.42 ± 0.22 μM, respectively.

It was decided to take CB8 as a lead compound to develop more potent derivatives. The chemical synthesis was done in collaboration with Professor Herdewijn and his coworkers. In order to establish initial structure-activity relationships (SARs), a total of 19 compounds were screened at MRGPRX2 receptor to determine their IC₅₀ values and maximal inhibitions compared with the parent compound CB8. The results are presented in table 9. The compounds stock solutions CB10, CB12, CB13, CB14, CB16, CB17, CB18, CB19, CB20, CB24, CB25, CB26 and CB28 were soluble at high concentration (10 mM), while 1 mM stock solutions of CB11, CB15, CB21, CB22, CB23 and CB27 in DMSO were prepared. The results are shown in table 9.

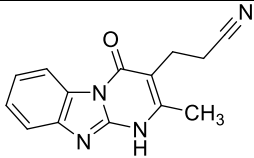
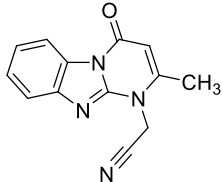
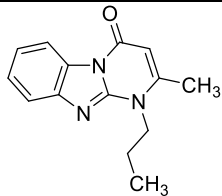
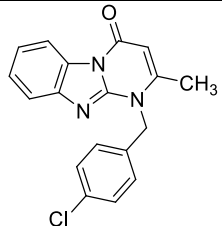
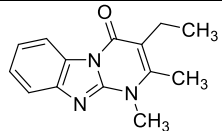
Table 9: Chemical structure and activity of several derivatives of the parent hit CB8 at MRGPRX2 receptor.

Code	Structure	IC ₅₀ ± SEM (μM)*	Max. Inhibition at 10 μM (%)
CB8 (Parent compound)	<chem>CCc1c(C)c2nc3ccccc3n2c1=O</chem>	2.42 ± 0.22	75

Results and Discussion

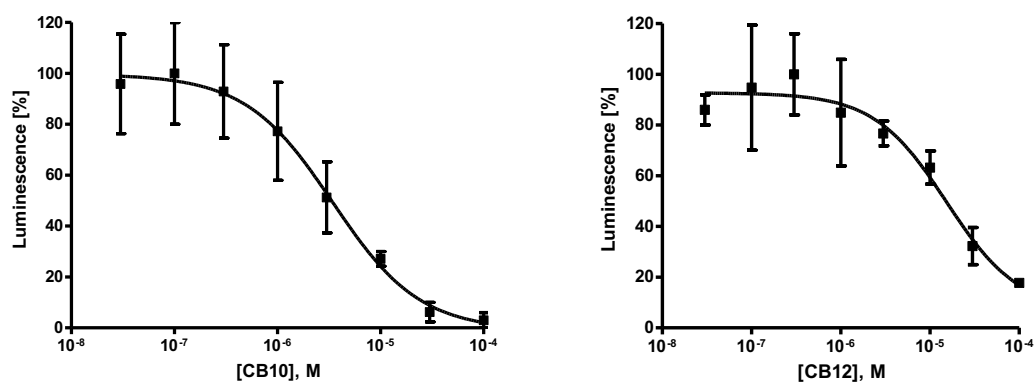
CB10		3.23 ± 0.36	89
CB11		>10	-5
CB12		14.7 ± 1.3	80
CB13		>100	22
CB14		3.22 ± 0.82	86
CB15		>10	-25
CB16		>100	24
CB17		>100	-2
CB18		>100	37
CB19		11.6 ± 3.7	81
CB20		>100	16
CB21		0.583 ± 0.049	62
CB22		>10	19
CB23		1.40 ± 0.88	30

Results and Discussion

CB24		>100	26
CB25		>100	43
CB26		>100	35
CB27		>10	14 ± 16
CB28		>100	2 ± 11

*: Results are mean ± SEM of three independent β -arrestin experiments

Only 6 compounds were found to be active in which CB21 showed the highest antagonistic activity with an IC_{50} of $0.583 \pm 0.049 \mu\text{M}$ but the maximal inhibition was reduced to 63%. CB23 showed a limited maximal inhibition despite the good potency as shown in figure 17. These initial results indicate that the left side of the molecule should not have bulky substituents, while methyl, ethyl, propyl or isopropyl seem to be appropriate.



Results and Discussion

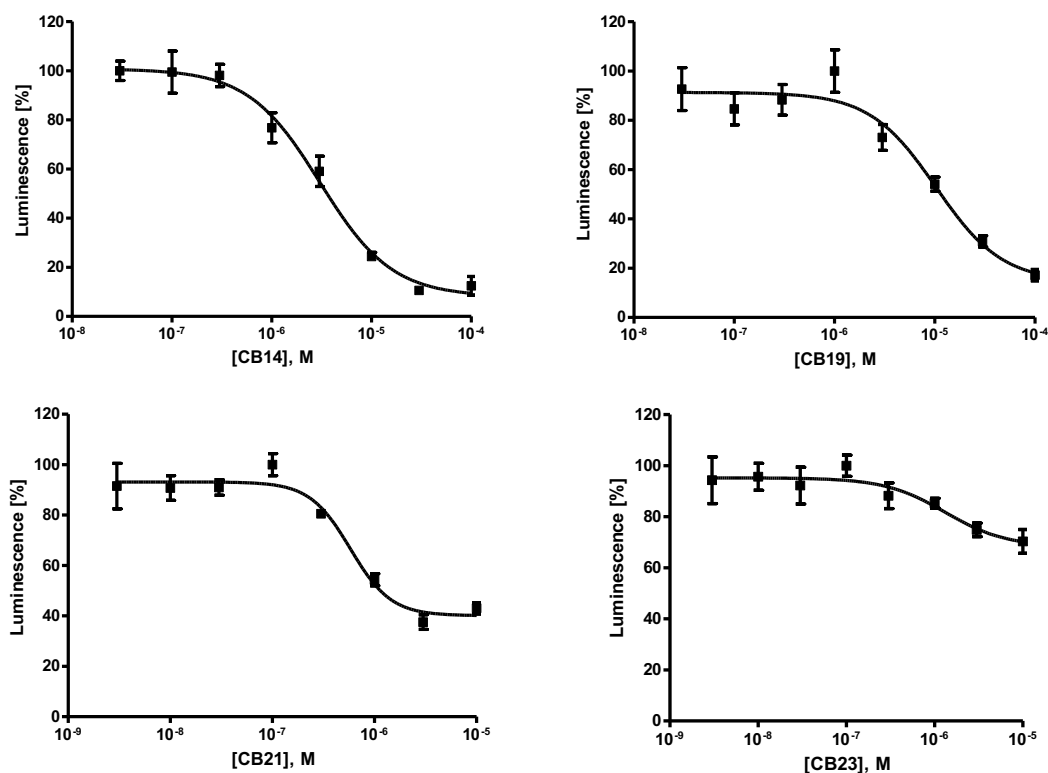
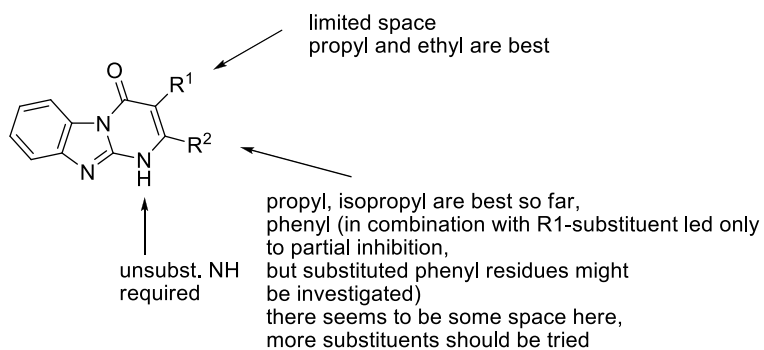


Figure 17: Mean dose-response curve of three independent β -arrestin experiments of the six active antagonists at MRGPRX2 receptor.

From the previous results, it was possible to suggest preliminary structure-activity relationships and make some suggestions for optimization as demonstrated in figure 18.



Predictably active new compounds:

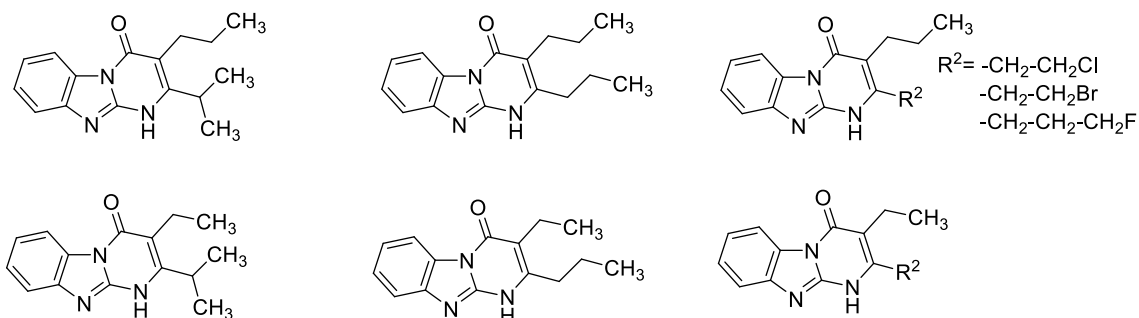
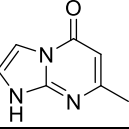
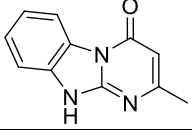
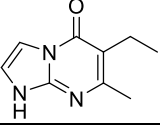
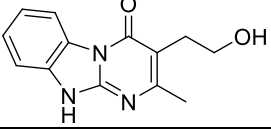
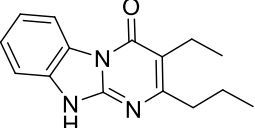
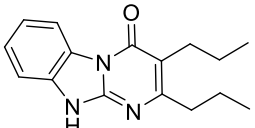
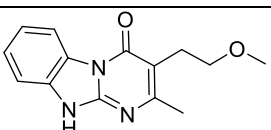
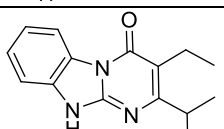
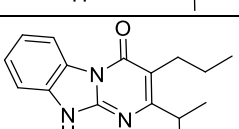
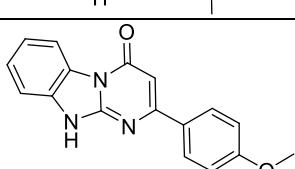
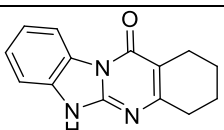


Figure 18: Initial structure activity relationships of the antagonists at MRGPRX2 and some structures predicted to be potent.

Results and Discussion

Another two sets of compounds were synthesized and tested. The results are summarized in table 10.

Table 10: The results of the first and second series of the antagonistic compounds at MRGPRX2 receptor

Code	Structure	IC ₅₀ ± SEM (μM)*	Max. Inhibition at 100 μM (%)
CB29		>100	4
CB30		>100	36
CB31		>100	40
CB32		>100	22
CB33		0.278 ± 0.042	98
CB34		0.214 ± 0.032	97
CB35		>10	20
CB36		0.290 ± 0.098	97
CB37		0.512 ± 0.107	96
CB38		>10	4
CB39		5.66 ± 1.15	68

*: Results are mean ± SEM of three independent β-arrestin experiments

Results and Discussion

These results confirm the suggested initial SAR. CB33 showed approximately 9-fold increase in potency. CB34 demonstrated 11-fold increase in potency compared with CB8. Both compounds showed an almost total inhibition at 10 μ M. The second shipment contained also two important compounds, CB36 and CB37, which showed a considerable increase in potency.

At this point of time there was an optimization of β -arrestin assay protocol was introduced. Hence, in order to have a better comparison and to make a better choice, compounds CB33 and CB34 were tested again according to the new protocol. The results showed a slight difference as given in figure 19 and figure 20. CB33 turned out to be the most potent compound. Therefore, it was decided to consider the right side of the molecule finally optimized and to further modify the benzene residue of CB33 in order to get more potent derivatives.

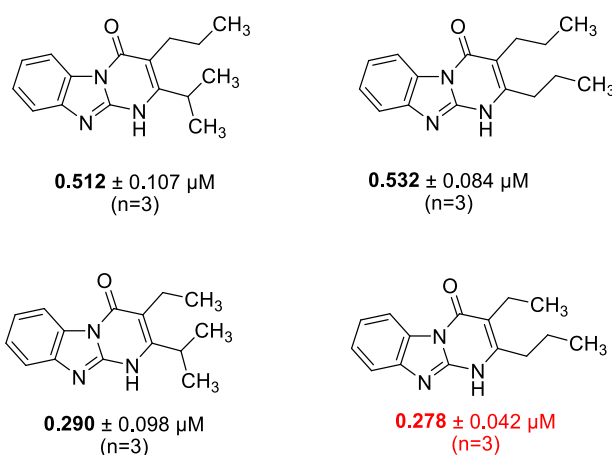
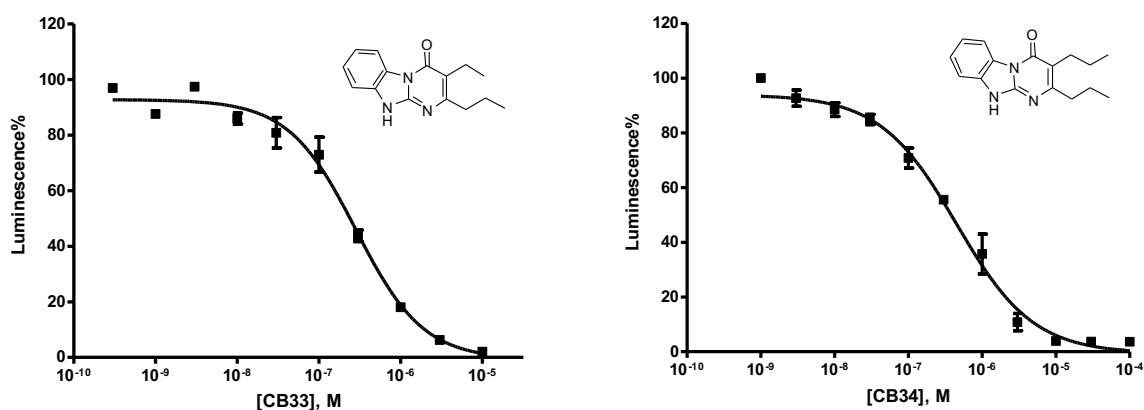


Figure 19: The results of the best four compounds in the first series of derivatives.



Results and Discussion

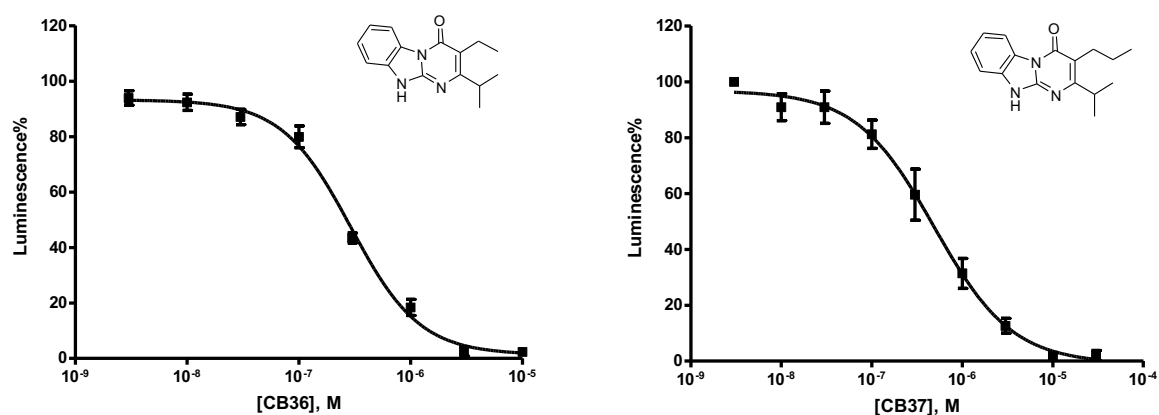


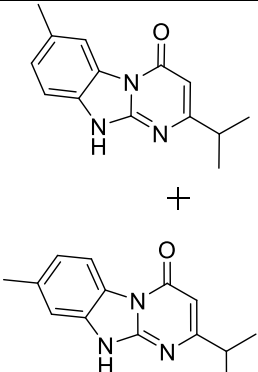
Figure 20: The mean curve of three independent β -arrestin assays of the four best compounds in the first series of the antagonists at MRGPRX2 receptor.

Further series of derivatives were dedicated to modify the benzene residue. Series 3 was tested and the results are shown in table 11. From the results it is clear that only CB44 is of interest in this series. More importantly, CB44 is a mixture of two region-isomers with a ratio of 1:1. CB40 has no modification of the benzene residue but shows a good affinity and interestingly, the bulky *para*-methoxyphenyl substitution is tolerated.

Table 11: The results of the third series of antagonists at the MRGPRX2 receptor

Code	Structure	IC ₅₀ ± SEM (μM)*	Max. Inhibition at 100 μM (%)
CB40 Only n=1		0.548	82
CB41		ca. 100 μM	52
CB42		ca. 100 μM	58
CB43		ca. 100 μM	55

Results and Discussion

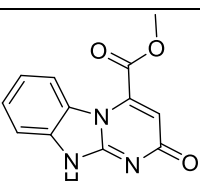
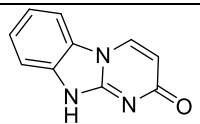
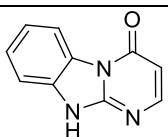
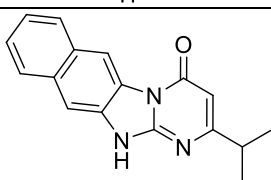
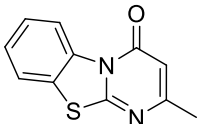
CB44		1.05 ± 0.11	85
------	---	-----------------	----

*: Results are mean \pm SEM of three independent β -arrestin experiments

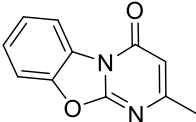
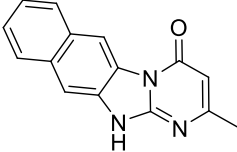
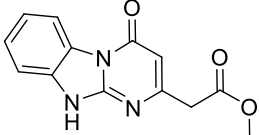
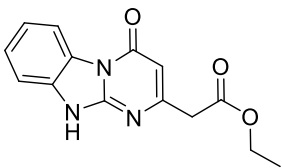
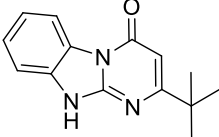
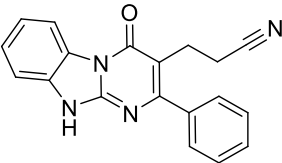
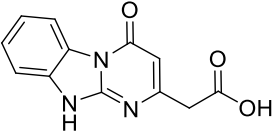
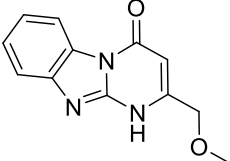
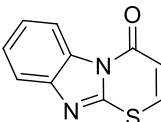
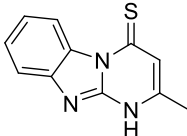
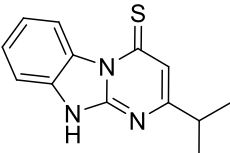
Although CB44 is not a derivative of CB33, CB44 could give an indication of the benefits of substitution of aryl ring since CB44 contains a methylated aryl residue in comparison to CB14. The results show a 3-fold increase in potency of CB44 compared with CB14, which is a good indication of the possibility of developing potent antagonists via an appropriate substitution of the aryl residue.

Two further sets of compounds were tested as shown in table 12 but these derivatives do not possess the required substitution pattern. Therefore, the majority of these compounds were inactive.

Table 12: Results of the fourth and fifth series of the potential antagonists at the MRGPRX2 receptor

Code	Structure	IC ₅₀ \pm SEM (μ M)*	Max. Inhibition at 100 μ M (%)
CB45		ca. 100 μ M	48
CB46		>100 μ M	0
CB47		>100 μ M	18
CB48		>100 μ M	6
CB49		>100 μ M	14

Results and Discussion

CB50		>100 μ M	13
CB51		>100 μ M	18
CB52		ca 100 μ M	4
CB53		>100 μ M	-33
CB54		ca 100 μ M	48
CB55		> 100 μ M	2
CB56		>100 μ M	-18
CB57		>100 μ M	-13
CB58		>100 μ M	-44
CB59		>100 μ M	-4
CB60		0.148 \pm 0.042	99

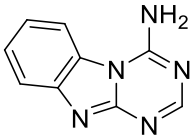
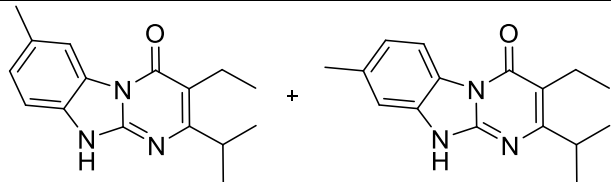
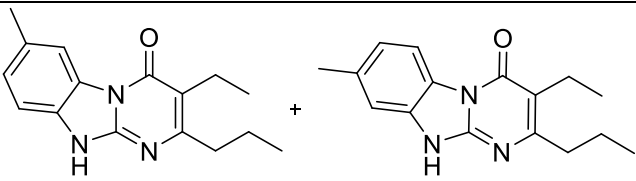
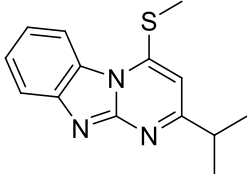
*: Results are mean \pm SEM of three independent assays

Results and Discussion

The only interesting compound in this series was CB60. Its affinity indicates that the substitution of O by S is beneficial since CB60 showed ca. 22-fold increased potency compared to CB14 as well as a complete inhibition of the MRGPRX2 receptor.

The sixth and seventh set of compounds contained potent antagonists as shown in table 13, in particular CB63 and CB64, which are methylated derivatives of CB36 and CB33, respectively. Both compounds were mixtures of regio-isomers and not a single compound. CB63 with an IC₅₀ value of 6.38 nM could be the basis for preparing a radioligand. Unfortunately, this high potency was accompanied by very bad solubility of the compounds. In order to avoid the issue of regio-isomers, methylation of both positions was conducted as demonstrated in CB66 and CB67. The insolubility problem was, unfortunately, evident with CB66 and even more with CB67. The low inhibitory potency of CB67 compared to closely related compounds may be partially due to its bad solubility. The compounds with an isopropyl-substitution had a better solubility than their propyl-substituted counterparts. However, it was clear that the double methylated compounds are not advantageous because of the decreased potency as well as low solubility.

Table 13: The results of the sixth and seventh series of the antagonistic compounds at MRGPRX2 receptor

Code	Structure	IC ₅₀ ± SEM (μM)*	Max. Inhibition at 10μM (%)
CB62		>100	4
CB63		0.00638 ± 0.00189	100
CB64		0.0711 ± 0.0152	98
CB65		>10	2

Results and Discussion

CB66		0.0877 ± 0.0368	99
CB67		$1.40 \pm 0.36^{**}$	98

*: Results are mean \pm SEM of three independent β -arrestin experiments

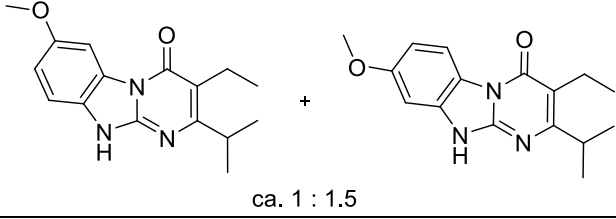
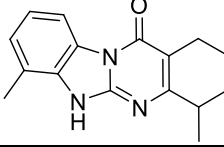
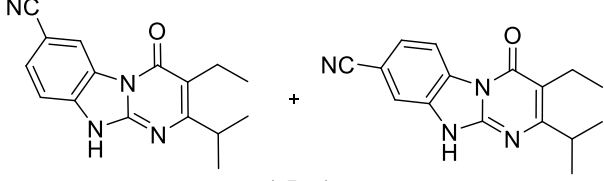
** : Data are extrapolated due to bad solubility of this compound

A last series of compounds was investigated. In this set of compounds, halogens were tried instead of methyl group. CB70 and CB71 with fluorine substitution showed the highest potency. Fluoro derivatives seem to be more suitable than chloro ones. Of note, the di-substitution is better in the case of fluoro compounds than monosubstitution as shown in table 14.

Table 14: The results of the eighth and ninth series of potential antagonists at the MRGPRX2 receptor

Code	Structure	IC ₅₀ \pm SEM (μ M)*	Max. Inhibition at 10 μ M (%)
CB68		0.477 ± 0.087	96
CB69		0.169 ± 0.017	98
CB70		0.0209 ± 0.0054	99
CB71		0.0926 ± 0.0426	99

Results and Discussion

CB72	 ca. 1 : 1.5	0.213 ± 0.079	94
CB73		>10	15
CB74	 1.5 : 1	1.26 ± 0.31	85

*: Results are mean \pm SEM of three independent β -arrestin experiments

These were all the compounds, which have been tested so far within this thesis as antagonists at MRGPRX2 receptor. The curves of the best three synthesized antagonists are presented in figure 21.

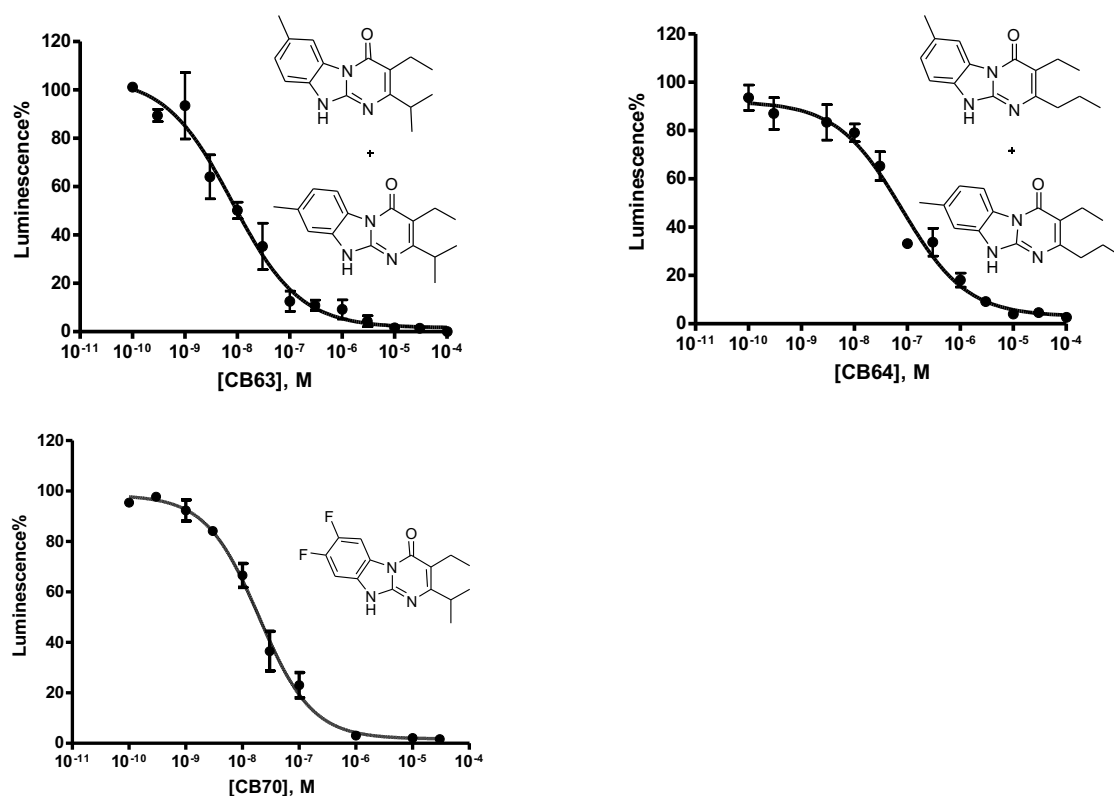
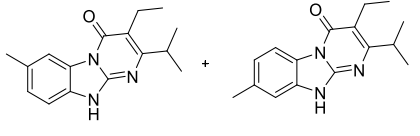
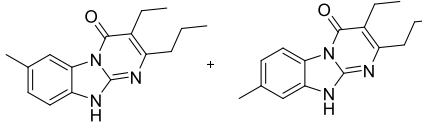
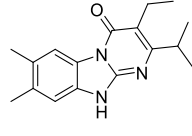


Figure 21: The mean curve of three independent β -arrestin assays of the most potent antagonists at MRGPRX2 receptor. The IC_{50} values of CB63, CB64 and CB70 are 0.00638 ± 0.00189 , 0.0711 ± 0.0152 and 0.0209 ± 0.0054 μ M, respectively.

2.2.3 *In vitro* pharmacokinetic data of selected MRGPRX2 antagonists

The ADME (absorption, distribution, metabolism and excretion) profile is important for *in vivo* studies. Therefore, some of the best antagonists were investigated *in vitro* by Pharmacelsus GmbH, Saarbrücken; a contract research organization specialized in such studies. Three compounds were investigated, namely, CB63, CB64 and CB66 with the IC₅₀ values of 0.00638 ± 0.00189, 0.0711 ± 0.0152 and 0.0877 ± 0.0368 µM, respectively. A summary of the results is given below (see tables 15-18).

Table 15: Blood-brain barrier permeability of the MRGPRX2 antagonists

BBB	CB63	CB64	CB66
Structure			
Flux rate	66.2%	64.5%	4.1%

BBB (blood brain barrier): *in-vitro* test,
Impermeable compound, flux rate < 50%,
Highly permeable compound, flux rate >50%
The test was done at 5 µM for CB63, CB64 and at 10 µM for CB66

The results show that CB63 and CB64 are likely to penetrate into the brain, while CB66 is not able to penetrate. This could be due to the low solubility of CB66.

Table 16: Plasma protein binding of the MRGPRX2 receptor antagonists

PPB	CB63	CB64	CB66
mouse	99.86%	99.41%	99.66%
rat	99.86%	99.81%	99.51%
human	99.72%	99.86%	99.65%

PPB (plasma protein binding): The test was done at 1 µM

The investigated compounds show a relatively high PPB in all investigated species. This is no limitation for further development. The plasma protein-bound fraction may serve as a depot for the drug.

Table 17: The inhibitory IC₅₀ values of the MRGPRX2 receptor antagonists at different cytochrome enzymes

CYP Inhibition (µM)	CB63	CB64	CB66
CYP1A2	2.7	<1	5.2
CYP2B6	>>5	>>5	>>10
CYP2C9	>5	>5	>10
CYP2C19	>5	>5	>10
CYP2D6	>>5	>>5	>>10
CYP3A4	2.6	<1	<1

CYP (Cytochrom P450). Results were extrapolated after screening at 10, 5 and 1 µM

Results and Discussion

The cytochrome enzymes are involved in drug metabolism. Therefore, inhibiting or activating these enzymes is an important source of drug-drug interactions. CB63 shows a moderate inhibition of CYP3A4 (the most relevant enzyme), while CB64 and CB66 show a relevant inhibition. This could mean a potential for interaction with other drugs.

Table 18: The half-life and intrinsic clearance of the MRGPRX2 receptor antagonists

Microsomal Stability Assay	CB63		CB64		CB66	
	t _{1/2} (Min)	CL _{int} (µg/min/mg protein)	t _{1/2} (Min)	CL _{int} (µg/min/mg protein)	t _{1/2} (Min)	CL _{int} (µg/min/mg protein)
mouse	6.5	213.3	5.3	261.6	7.4	187.3
rat	11.9	116.5	9.2	150.7	10.7	129.6
human	7.7	180.0	6.4	216.6	10.6	130.8

t_{1/2} (Half Life), CL_{int} (Intrinsic Clearance)

All investigated compounds show low metabolic stability and a short half-life. This would be a major limitation in drug development. The next step will, therefore, be to develop metabolically more stable derivatives based on a close analysis of the metabolic pathways. The fluoro-substituted compounds, CB70 and CB71, may show improved properties and should, therefore, be subsequently tested for ADME properties.

2.2.4 Mechanism of the mode of antagonism

The observation that the MRGPRX2 agonist, CST-14, is a peptide consisting of 14 amino acids containing two disulfide bridges, while the antagonists are pretty small molecules, prompted us to investigate the mode of action of the synthesized antagonists. The aim was to know if the antagonism is allosteric or orthosteric. To address this question, curves of CST-14 with varying concentrations of the antagonist were plotted and compared with the CST-14 curve without any antagonist. The comparison was in terms of any rightward shift (change of EC₅₀ value) and the depression of the maximal response. During these experiments it turned out that CST-14 could not be used at concentrations higher than 100 µM because it then causes a decrease in signal (data not shown) due to a presumably toxic effect on cells. As mentioned above, all of the best antagonists had shown a full inhibition of the agonist. However, this is not necessarily an indication of an orthosteric mechanism of action.¹³² The first experiments using CB8 did not show clear results (data not shown).

Results and Discussion

After synthesizing CB63, it was decided to repeat the experiment. The first experiment was done in the presence of 10 nM of CB63 and the results showed an orthosteric mode of action since there was a clear rightward shift (from 451 nM to 1570 nM) and there was no depression of the maximal inhibition as shown in figure 22a. A further experiment with more than one concentration (1, 10, 100 and 1000 nM) of CD63 confirmed the rightward shift (EC_{50} values of 0.930, 2.01, 3.04, 6.22 and 27.0 μ M for 0, 1, 10, 100, and 1000 nM of CD63, respectively) and revealed that for 1, 10 and 100 nM of the antagonist there is no depression of the maximal response, whereas for higher concentrations of 1000 nM a full curve could not be obtained due to limitations in CST-14 concentrations (see above) as demonstrated in figure 22b.

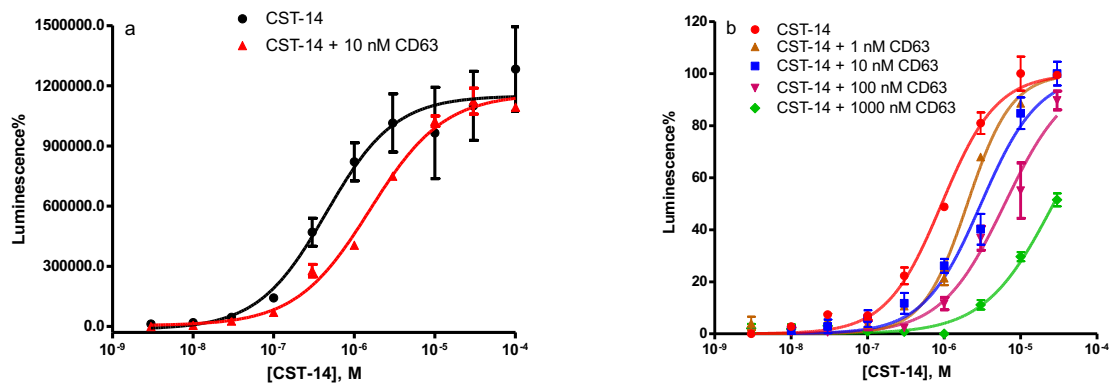


Figure 22: Concentration-response curves of CST-14 in the presence of the antagonist CD63, a: rightward shift of the CST-14 curve in the presence of 10 nM of CB63, b: rightward shift of CST-14 in the presence of several concentrations of CD63. The maximal concentration for CST-14 was 100 μ M due to toxic effects on the cells at higher concentrations.

In figure 21b the curve of CST-14 with 1000 nM did not reach a plateau. The reason for not reaching a maximal response could be an insurmountable antagonist. In order to interpret the point we should keep in mind that the β -arrestin system is a high expression system (high sensitivity) with a receptor reserve. In such systems the depression of the maximal response for insurmountable antagonists (irreversible or allosteric) occurs only at higher concentrations of the antagonists after an initial “pure” rightward shift for the lower concentrations.¹³² Another possibility for not reaching the maximal response is that despite the competitive nature of antagonism, a maximal response could not be reached due to the inability to increase CST-14 concentration (more than 100 μ M) so that CST-14 could displace CD63. In order to interpret these data a Gaddum/Schild EC_{50} shift was conducted to determine the Schild slope, which should be ca. 1 for competitive antagonism and

Results and Discussion

other than one for cooperative antagonism.¹³³ The determined Schild slope for the curve in figure 21a was 1.08, which is a clear indication of the orthosteric nature of the antagonism. Another usual characteristic (but not always) of allosteric modulation can be the shallow SAR,^{134,135} which was not the case for the tricyclic benzimidazole derivatives as shown above. Our findings indicate an orthosteric mode of action for these antagonists, with respect to the peptide agonist CST-14, which has to be further confirmed by structural studies e.g. X-ray crystallography or mutagenesis experiments.

2.2.5 Investigation of some reported agonists

Antagonists were the main focus of this study. However, several interesting agonists have recently been described in the literature as reported in the introduction. Some of these agonists were drugs like morphine,⁹⁴ antibiotics like ciprofloxacin, peptidergic drugs like icatibant, cetrorelix and non-steroidal neuromuscular blocking drugs like suxamethonium.¹⁰⁶ Therefore, we tested the compounds that were available in our laboratory, namely, morphine and ciprofloxacin. Both were confirmed as agonists at the MRGPRX2 receptor. Ciprofloxacin has a very limited solubility and we could not obtain a full curve. The S/N ratio was 3 (i.e. partial agonism) and the absolute increase of the signal was very limited. Morphine, on the other hand, showed a very robust increase in signal and an impressive S/N ratio of 18 (similar to that of CST-14, i.e. a full agonist). The EC₅₀ value for morphine was 25.9 ± 1.3 μ M as shown in figure 23.

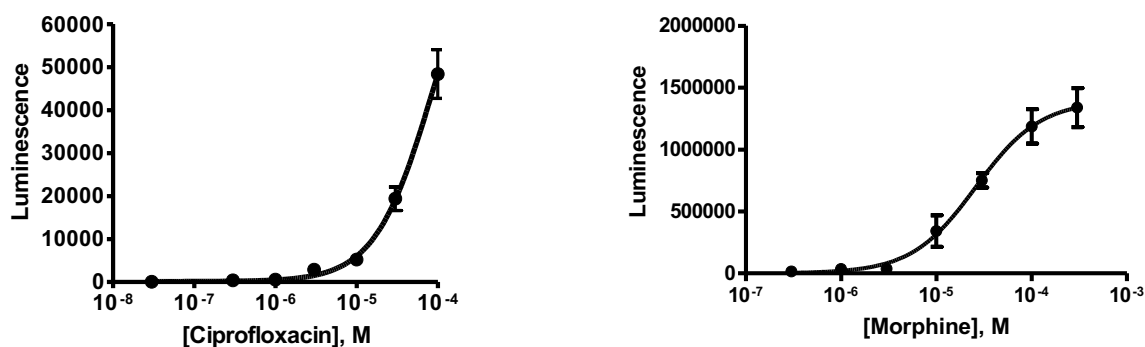


Figure 23: The normalized mean of three curves of ciprofloxacin and morphine as agonists at the MRGPRX2 receptor. Morphine demonstrated an EC₅₀ value of 25.9 ± 1.3 μ M. Results are mean \pm SEM of three independent β -arrestin experiments.

2.2.6 MRGPRB2 receptor

Further attempts in investigating the MRGPRX2 receptor were based on the seminal findings of McNeil et al.¹⁰⁶ in which they suggested the mouse MRGPRB2 (accession number: NM_175531) receptor as a functional ortholog of the human MRGPRX2. Our aim was to investigate if our synthesized antagonists at the human receptor are active at the murine counterpart and to determine their potential affinity. Should there be considerable potency of our antagonist, this would enable us using mouse models to take MRGPRX2 research a step further in pre-clinical studies.

The cDNA of mrgprB2 was provided by OriGene Technologies Inc., USA. The cDNA was sequenced by GATC Biotech AG in Konstanz, Germany, in order to check for any mutations. All sequences were aligned with the reference sequence and no mutation was found. The amplification of the genes and the insertion into the four β -arrestin vectors were done as described in chapter 4.3.4. The Pyrobest™ DNA-Polymerase from TAKARA BIO Inc. was applied to amplify the genes. A sequence analysis was also performed after amplification and insertion into the vector to ensure that no mutation took place during the amplification, and the results were all positive. The lipofectamine transfection was done as described in chapter 4.5.1.

The first step is usually the validation of the agonist and the suitability of the assay. To address this, CST-14 was used as the standard agonist. Unfortunately, it was not possible to detect any signal when using CST-14 up to 100 μ M concentration. The transfection was repeated but the results remained negative for all generated MRGPRB2 constructs in the four β -arrestin vectors. Hence, it is for now not possible to investigate any antagonistic activity of our novel MRGPRX2 ligands at the mouse receptor. It should be mentioned that in reference¹⁰⁶ CST-14 showed an EC₅₀ value of 21.3 μ M, which is unusually high for a neuropeptide. Nevertheless, it would still be possible to perform calcium mobilization assays to circumvent the often less sensitive β -arrestin assay.

2.2.7 Discussion

The MRGPRX2 receptor is a member of the MRGPRX subfamily. It is noteworthy that, in addition to many synthetic drugs (morphine, ciprofloxacin etc.), several physiological agonists (CST-14, PAMP, β -defensin, basic secretagogue and LL-37) have been described as agonists for this receptor.^{81,93,101,103} It is noticeable that these peptides are structurally not very related and the EC₅₀ values are relatively high compared to classical peptide receptors (see figure 8 and table 5). This ability of MRGPRX2 to be activated by several agonists distinguishes this receptor from many 7TMRs and this could be relevant for the physiological function of this receptor if these peptides actually function as agonists under (patho)physiological conditions. One interesting explanation is a kind of similarity of MRGPR receptors to olfactory and taste receptors which are able to detect an extraordinary range of substances from the environment. By the same token, pain and itch demonstrate an outstanding versatility and their receptors could be “tuned” to respond in varying degrees to different stimuli.³⁸ In this thesis we found that this idea applies to antagonists as well (interestingly, no antagonists have been described in the literature so far). Several antagonists have been identified during our screening efforts in contrary to other investigated MRGPRX receptors.

Menadione, from the drug library, was the first detected antagonist with an IC₅₀ value of 5.39 μ M. This could be an interesting and inexpensive pharmacological tool. The ability to modify the molecule could also be an option to increase the potency of this antagonist. In order to verify and substantiate the findings and reduce the toxicity of menadione on the cells during β -arrestin assays, calcium mobilization assays could be performed. Two other antagonists, H351 and SL318 (see figure 15), have been identified in the compound libraries 5 and 2, respectively. Both of them belong to a different chemical scaffold but showed IC₅₀ values of approximately 10 μ M.

The most potent antagonist was detected in the compound library 3 and was termed CB8. The IC₅₀ value was 2.42 μ M and it possessed a tricyclic benzimidazole scaffold. From this parent compound a total of 65 compounds have been synthesized in the group of prof. Herdewijn, Leuven (Belgium).

Solid structure-activity relationships have been established and the current state is summarized in figure 24.

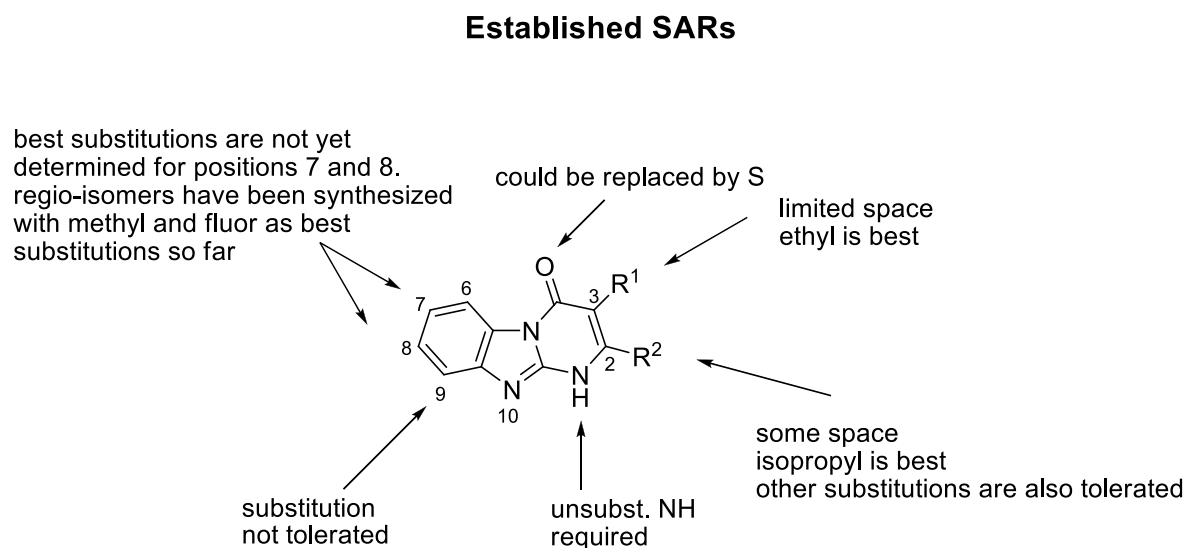


Figure 24: The established structure-activity relationships at the MRGPRX2 receptor after synthesizing a large number of antagonists.

The best antagonist so far, CB63, has an IC_{50} value of 6.38 nM. This potency could be suitable to develop a radioligand, which would be a powerful pharmacological tool for further studies. Hence, developing a radioligand could be a plausible next step in investigating the MRGPRX2 receptor. However, this should take place after further investigation of SARs; especially in positions 7 and 8 of the benzimidazole ring because this could lead to even more potent antagonists. Hence, the first step in the chemical synthesis is to find an approach to get rid of the regio-isomer problem and to get single compounds. The nature of antagonism was also investigated and turned out to be an orthosteric inhibition with regard to the peptide agonist CST-14. The fact that the CST-14 concentration could not be increased over 100 μ M was a barrier during our efforts to investigate the mode of antagonism. This indicates the importance of developing potent agonists as well since other described agonists like morphine or ciprofloxacin are much weaker. The newly developed MRGPRX2 antagonists were also screened at MRGPRX1 and turned out to be selective against MRGPRX1. A further investigation of the selectivity of the new antagonists against MRGPRX4 receptor would be informative as well. Moreover, it would also be of interest to investigate the selectivity at somatostatin and ghrelin receptors since both could be activated by CST-14.

Results and Discussion

Having established SARs for antagonists and developed potent ones, our aim was then directed towards expanding the investigation to a pre-clinical stage through a mouse model. This could be based on the recent finding that the mouse MRGPRB2 receptor could be the functional ortholog of the human MRGPRX2 receptor. As a first step, ADME profiles of the best three antagonists were generated *in vitro*. The obtained results make clear the difficulties throughout stages of developing a drug. The analyzed antagonists, CB63, CB64 and CB66 were all very potent in a cell-based assay. However, the pharmacokinetic data shows a very high plasma protein binding (>99%), in addition to a very short half-life of less than 8 minutes for all investigated antagonists. This would have negative implications for the bioavailability of these antagonists. The CYP-inhibition is also pronounced, which may lead to drug-drug interactions.¹³¹ The CNS accessibility seems to be acceptable (for CB63 and CB64) but the expression profile of MRGPRX2 in mast cells and DRG neurons does not necessarily require BBB penetration depending on the indication pursued. This leads us to further requirements for the next series of antagonists. These requirements, besides getting rid of regio-isomers, are improved water solubility since this seems to be a big problem upon substituting position 7 and 8, in addition to reducing the clearance and abolishing CYP inhibition.

Lastly, the activity of our novel antagonists at human receptors were intended to be also tested at the mouse MRGPRB2 receptor. This could, unfortunately, not be done despite a successful cloning of the respective β -arrestin cell line. The hurdle was the inactivity of the agonist CST-14 at the mouse receptor in the β -arrestin assay. This could be explained by the rather unimpressive EC₅₀ value of CST-14, which was reported in a calcium assay.¹⁰⁶ Therefore, the less sensitive β -arrestin assay would not enable satisfying concentration-response curves to be plotted. Addressing this issue could be via generating another MRGPRB2 cell line and re-testing CST-14 at this cell line. The results of calcium mobilization assays in CHO cells are usually not that satisfying. This could be due to lower levels of G_q protein. Hence, it could be more useful to express the mouse MRGPRB2 receptor in a HEK293 or an astrocytes cell line.

2.3 MRGPRX3 receptor

This member of the MRGPRX subfamily appears to be the most enigmatic one. The expression is thought to be restricted to sensory neurons in the DRG but a new study suggested a role for the receptor in corneal endothelial cells.¹⁰⁹ Since there is no described tool for this receptor, our aim was to find the first agonist.

2.3.1 Cloning of MRGPRX3 β -arrestin cell line

This cell line was cloned since DiscoverX® does not offer this cell line. The reason behind this has not been disclosed. The cDNA of mrgprX3 was provided by OriGene Technologies Inc., USA. The cDNA was sequenced by GATC Biotech AG in Konstanz, Germany, in order to check for any mutations. All sequences were aligned with the reference sequence and no mutation was found. The amplification of the genes and the insertion into the four β -arrestin vectors was done as described below (see chapter 4.3.4). The Pyrobest™ DNA-Polymerase from TAKARA BIO Inc. was applied to amplify the genes. A sequence analysis was also performed after amplification and insertion into the vector to ensure that no mutation took place during the amplification, and the results were all positive.

The lipofectamine transfection was done as described in chapter 4.5.1. To confirm the expression of the cDNA on the protein level and to compare the expression level, immunofluorescent experiments were done as described in chapter 4.6, using the antibody against the ProLink segment. The results showed clearly a higher expression using the ARMS1 and ARMS2 plasmids, while ProLink1 and ProLink2 showed a less pronounced expression. Hence, the MRGPRX3-ARMS2 cell line was used for pharmacological investigations because it showed the highest expression as shown in figure 25.

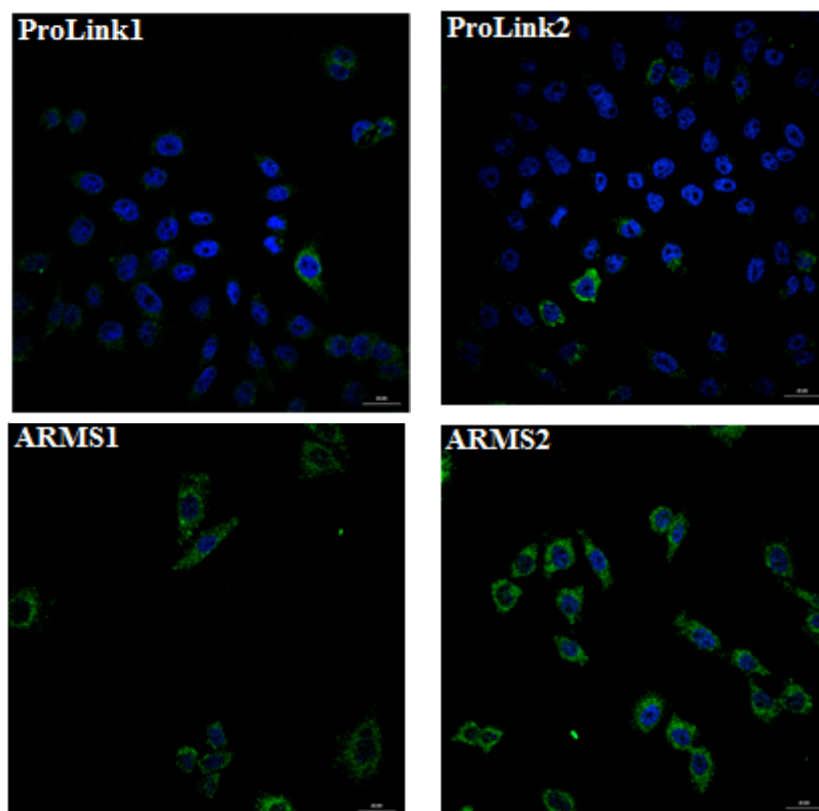


Figure 25: The expression of MRGPRX3 receptor in four different vectors ProLink1, ProLink2, ARMS1 and ARMS2. The expression of the receptor is located in the cell membrane (green fluorescence) and DAPI was used to investigate the cell nuclei. MRGPRX3-ARMS2 construct demonstrated the highest expression.

2.3.2 Screening of compound libraries in search for agonists

In order to search for an agonist a screening of several compound libraries has been conducted. In this search and due to the need for an agonist as indispensable tool for further investigations, the screening was done at 10 μ M and an S/N ratio of as low as 1.3 was considered as a hit. The compound libraries 1-5 and 7-10 were screened (see chapter 4.10). The results of the compound libraries 2 and 4-10 were all negative without any hit (data not shown). Nevertheless, screening of the compound libraries 1 and 3 revealed one hit in compound library 1 with an S/N ratio of 1.6 (BMS 191011: a potent potassium channel opener¹²³) and two in compound library 3 with an S/N ratio of 1.5 and 1.3 (IDs: 6265708 and 6258069, respectively) as shown in figure 26. The screening was repeated three times and could be reproduced. Interestingly, the hits from the compound library 3 share a benzimidazole scaffold like the other CB ligands for the MRGPRX2 receptor. All three hits were also oxadiazole derivatives, nevertheless these are two different isomers. In order to confirm

Results and Discussion

the identity of these hits, an LC-MS measurement was conducted. The results did not demonstrate the expected mass because there was a degradation of all three compounds. An LC-MS was conducted using the mother plates, the results showed no signs of degradation (data not shown). The compounds in the mother plates demonstrated no activity at all, which means that the degradation products in the daughter plates would have been causing the signals.

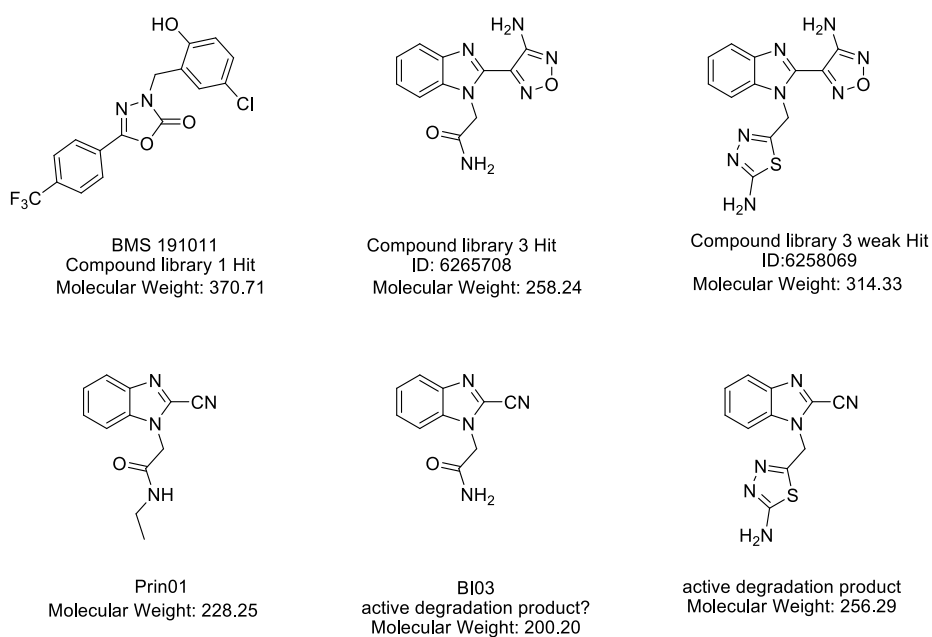


Figure 26: The chemical structures of the detected hits with potential MRGPRX3-agonistic activity and the predicted active degradation products.

In order to make sure that the increase in signal is concentration-dependent a curve was plotted. As shown in figure 27 there was an increase of signal for all three compounds. The absolute increase is not that high compared with that of commercially available MRGPRX receptor cell lines but this could be due to the fact that commercial cell lines of MRGPRX1, 2 and 4 are monoclonal and the MRGPRX3 cell line is a pooled one. These initial results tempted us to trace potential active degradation products.

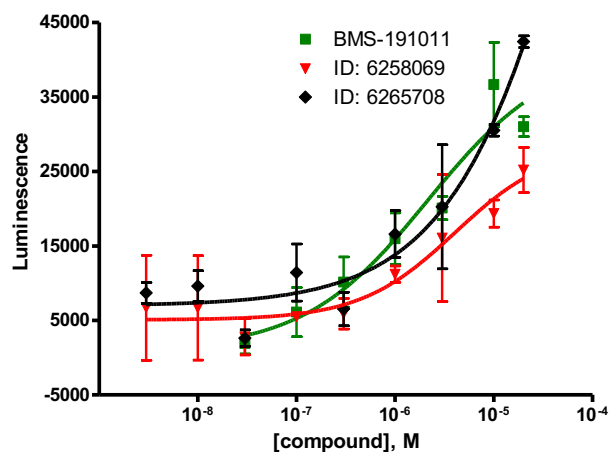


Figure 27: The three curves of the detected hits at MRGPRX3 receptor. All the experiments were done once (n=1) in duplicates.

In order to do this, we analyzed the LC-MS measurements of the active solutions. Unfortunately, for BMS-191011 the remaining stock solution was too little to be analyzed. Hence, it was not possible to have an informed guess. We also tried to heat BMS-191011 to 100°C for 30 minutes but that did not show any increase in activity (data not shown). The measurements of the compounds with the ID: 6265708 and 6258069 showed a molecular weight of 200.2 and 256.29, respectively. This led to the assumption that the oxadiazole ring was degraded and yielded cyano derivatives as shown in figure 26. The proposed degradation products have molecular weights that are in harmony with the detected molecular weights but they were not commercially available according to a search in Scifinder. Yet a similar compound (figure 26) was found and ordered from Princeton BioMolecular Research and designated Prin01. This compound was screened three times but did not show any activity (data not shown). The assumed degradation product of the compound 6265708 was designated BI03, which was synthesized by Younis Baqi. BI03 was also tested at MRGPRX3 and results were unfortunately disappointing. The first step to search for the problem was to compare the LC-MS measurement of BI03 and the 6265708 solutions. Both showed the same spectrum (data not shown). This led to the assumption that the cells could have lost the receptor. New cell aliquots were thawed; one in ARMS1 and the other in ARMS2 plasmid, for the sake of new screening. BI03, Prin01 as well as previously active stock solutions were screened but none of them demonstrated activity.

2.3.3 Discussion

In summary, the cDNA of mrgprX3 was successfully cloned in the four β -arrestin plasmids and four corresponding cell lines have been generated. The expression of the receptor were investigated using an antibody against the ProLink segment and the cell line of MRGPRX3 in the ARMS2 plasmid was chosen for pharmacological assays due to the high expression of the receptor in the cell membrane. The compound libraries 1-5 and 7-10 were screened in search for an agonist at this receptor. The search was done according to the status of the compound libraries in September 2014. The search led to no clear identification of a hit. Three compounds were found to be active but they were degraded compounds. The active moiety remains elusive for now. Interestingly, two of the assumed hits showed a benzimidazole structure. The difficulty in finding an agonist for MRGPRX3 receptor could be due to several reasons.

The first reason could be the unsuitability of the β -arrestin assay. This is difficult to explain but it could be the reason why DiscoverX® does not offer this cell line. The other reason could be the inability to have a stable expression in the cell membrane, which has already been described¹²¹ or a rapid decrease in the expression of the receptor in the cell membrane. In addition to the general difficulty in finding a ligand for the MRGPRX subfamily, which is reflected in the paucity of described ligands so far. To address these issues it is plausible to switch the screening assay to a calcium mobilization assay because MRGPRX3 is G_q coupled and by using FACS techniques it could be possible to pick a monoclonal (e.g. m-Cherry approach) and have a potentially more reliable system. The screening of the compound libraries should be repeated using higher concentration (e.g. 30 or even 100 μ M) because it is important to have even a weak initial tool and then there could be ways to improve the potency. The ligands at MRGPRX2 should be tested at MRGPRX3 as agonists as well. Lastly, it should be kept in mind that the glioblastoma cell line LN229 has shown an expression of mrgprX3 on the mRNA level. Taking into account that the LN229 cell line has shown very encouraging results regarding calcium assays for the MRGPRX4 receptor (more details see chapter 4.8.3), it is very useful to try to detect MRGPRX3 receptor in this cell line on the protein level using either an antibody

Results and Discussion

or (should there be no acceptable antibody) subjecting a membrane preparation sample to proteomics mass spectrometry. If the expression could be confirmed, the LN229 would be very helpful in investigating this receptor via calcium mobilization assay.

2.4 MRGPRX4 receptor

MRGPRX4 is a poorly investigated receptor. No pharmacological tools had been described for this 7TMR at the beginning of this thesis and the physiological role, apart from apparent involvement in nociception, has not been elucidated.^{17,18} MRGPRX4 was reported to be G_q coupled via a novel proliferation assay called Receptor Selection and Amplification Technology (R-SAT™).²³ Recently, the antidiabetic drug nateglinide, a K_{ATP}-channel blocker, was suggested to function as an agonist at this receptor.¹¹²

2.4.1 MRGPRX4 receptor: the human adenine receptor?

The first step in investigating the MRGPRX4 receptor was an approach to find relatedness within the expanded mas-related gene receptors in rodents. Although there are no direct orthologs between human MRGPRX subfamily and the rodents' receptors^{19,20}, the relatedness (sequence identity) could give an indication to a potential shared ligand. From the deorphanized rodents' MAS-related gene receptors, MRGPRA9/A10 (accession number: NM_001288801, JN662396) and rat MRGPRA (also rat MRGPRX3, accession number: NM_145787) and the Chinese hamster adenine receptor (accession number: KC202822.1) showed the highest sequence identity of 66%. Rat MRGPRA and mouse MRGPRA9/10 receptors demonstrated sequence identity of 64%, 63% and 65%, respectively, as shown in table 19. All those receptors are activated by adenine in low nanomolar concentrations (see table 2).

Table 19: Sequence identity of the nucleotides of the cDNA of the corresponding genes using Clustal Omega tool

Nucleotide sequence identity	Rat MRGPRA (rAde)	Mouse MRGPRA9 (mAde2)	Mouse MRGPRA10 (mAde1)	Hamster cAde (cAde)
Human MRGPRX4	64%	63%	65%	66%

Adenine has been already shown to have interesting physiological effects. Yoshimi et al. reported an increase in the number of Purkinje cells in rat primary cerebellar cultures after exposure to high concentrations of adenine (1-2 mM) but this effect was not noticed for astrocytes. The mechanism of

Results and Discussion

this neurotrophic effect remained elusive.¹³⁶ The oldest observation was, nevertheless, that 1-methyladenine acts as a maturation-inducing hormone in starfish oocytes.¹³⁷ The effect of adenine in the dorsal horn was found to be pronociceptive since the spinal administration of adenine in the rat increased the excitability of C-fibres in a concentration dependent manner. The mechanism could also not be readily correlated to mas-related genes since these receptors are not expressed in the dorsal horn but only in the DRG.¹³⁸ Adenine was also found to induce an inhibitory effect on Na⁺-ATPase activity through a G_i protein-coupled receptor inhibition of the adenylyl cyclase/PKA signaling pathway.¹³⁹ Moreover, it was found through binding studies that radioactive adenine could bind with varying affinities at different rat tissues (brain, cerebrum, cerebellum, spinal cord, kidney, testis and heart) and native cell lines (human astrocytoma 1321N1 and murine NG 108-15 cell lines).^{140,141} All the previous data prompted us to investigate MRGPRX4 as a potential human adenine receptor. In fact this was our first deorphanization attempt.

In order to test this deorphanization hypothesis, adenine was tested as an agonist at MRGPRX4 using the β -arrestin assay. The β -arrestin cell line was a commercial one from DiscoverX[®]. The results of the testing showed no increase in signal even when the concentration of adenine was as high as 500 μ M. This is a clear indication that adenine could not activate MRGPRX4 receptor at least in the β -arrestin pathway. Since MRGPRX4 is also G_q coupled, calcium mobilization assay was also tried but the results were negative as well as shown in figure 28.

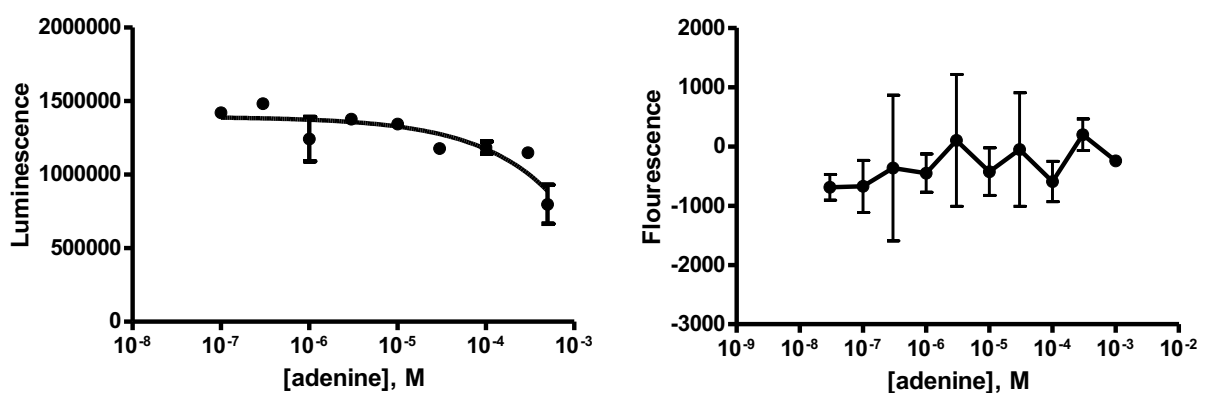


Figure 28: Concentration-response curves of adenine at MRGPRX4 receptor using β -arrestin assay (left) and calcium mobilization assay (right). Both signaling pathways did not show any response to adenine.

In order to further our investigations, binding assays have been conducted to detect a possible binding of [³H]adenine to the receptor. This could be the case if adenine is an antagonist or a modulator of MRGPRX4 receptor. Six separate binding experiments have been done but there was no significant binding of adenine to the MRGPRX4 receptor (data not shown). All these results were enough to conclude that MRGPRX4 is not the human adenine receptor.

2.4.2 Screening of compound libraries in search for agonists: a challenging search

Having proven that adenine is not a ligand for MRGPRX4 receptor, it was necessary to find a tool for investigating this receptor. Screening of the then (August 2012) available compound libraries in our institute was initiated. The high expression of the receptor on the cell membrane was confirmed using an antibody against the ProLink tag of the receptor (data not shown). The compound libraries 1 and 3-6 were screened (see chapter 4.10). Although the screening has been done twice at 10 and at 100 μ M, it was not possible to find any agonist for this receptor.

2.4.3 The second deorphanization approach: cerebrospinal fluid

Since the screening of the available compound libraries and the adenine-based deorphanization approach were not fruitful, it was necessary to find a new approach. The most interesting characteristic of the mas-related genes is their restricted expression in the DRG.^{17,18} One way would be the screening of different tissue extracts of the DRGs (reverse pharmacology approach). The active fractions could then be further fractioned, purified and analyzed (e.g. peptide fraction etc.) till an active metabolite is found. Such an approach has been carried out successfully and led to the deorphanization of several 7TMRs and to the identification of important endogenous neuropeptides. Opioid receptor-like 1 (ORL1) was deorphanized via rat brain extracts and nociceptin was identified as a ligand.^{142,143} The peptides orexin A and B were identified and paired to their receptors in an organ extraction approach and RNA-subtraction approach simultaneously by two different groups.^{144,145} This was followed by the discovery of prolactin-releasing peptide and apelin for GPR10

Results and Discussion

and APJ receptors, respectively.^{146,147} Interestingly, ghrelin was identified in a stomach extract and found to be an endogenous ligand at its 7TMR, which is mainly expressed in the brain.¹⁴⁸ In order to realize such an approach for MRGPRX4 receptor, human or monkey DRGs should be available in relatively big amount since the native ligand is usually found in a very low concentration. This was a main hurdle for this approach. Another way was to investigate the cerebrospinal fluid (CSF). This could be plausible because the DRGs are surrounded by CSF. In addition, CSF has been approached to determine biologically active proteins in pathological conditions.¹⁴⁹ The CSF-based approach would work provided that the native ligand is able to leak from the DRG tissue to CSF in a reasonable amount to be detected. If so, this approach could be advantageous because it reduces the complexity of a tissue extract and circumvents the difficulties of obtaining human DRG tissues.

Professor Ulrich Wüllner from the Neurology Department in the University Clinic in Bonn provided us kindly with 6 samples of CSF. One sample had been taken directly and split into two samples. The first sample was treated with a protease inhibitor (identity not disclosed) and the other was left untreated and both were then frozen. These samples were tested on MRGPRX4 and a weak signal was observed (data not shown). Since the concentration of a potential ligand in the CSF is lower than within the DRG tissue, it was decided to concentrate the CSF by the factor of 10 via lyophilization. The concentrated CSF solutions were then tested in β -arrestin assays. The results are shown in figure 29.

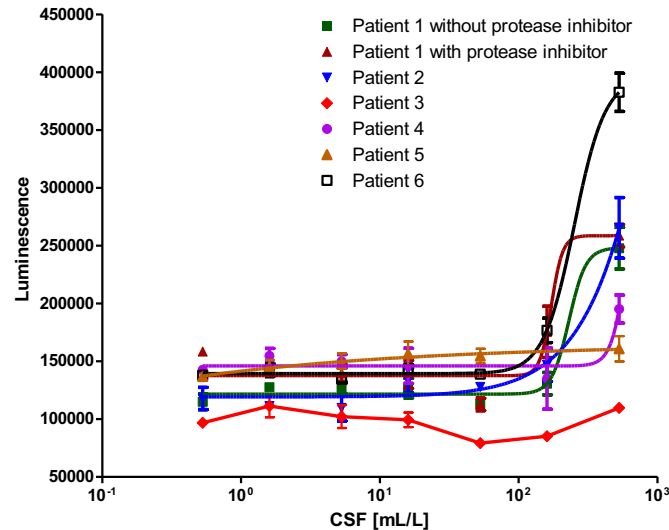


Figure 29: The mean curves of three independent β -arrestin assays of six CSF samples. The induced signals differed considerably between the several samples.

It should first be mentioned that the CSF concentration was given as volume/volume in each well of the 96-well plate. Interestingly, there was a considerable difference in the induced signal between the samples of different origins. While some samples like sample 6 could induce a robust and reproducible signal, sample 3 could not cause any increase in signal. It is not possible to make a confident conclusion out of these data but it is tempting to suggest that there is an agonist of MRGPRX4 in the CSF and this ligand is present at varying concentrations in the different samples. Taken into consideration that MRGPRX receptors are proposed to play a role as pain detectors²³, these varying results could reflect a nociceptive input in the different samples. It could also be noticed that the addition of protease inhibitor did not have any inhibitory effect on the signal. This could mean that the agonist is not a peptide or that it is a relatively small, stable peptide with no cleavage site for a potential protease.

A second set of samples was sent from Prof. Wüllner, but the volumes were too small to be individually investigated. Therefore, it was decided to pool them. This combined CSF sample showed a signal with an S/N ratio of 2 (data not shown).

As a kind of control CSF was tested at GPR55 in the same test system. GPR55 is expressed mainly in the brain and can be activated by cannabinoids and lipids such as lysophosphatidylinositol.¹⁵⁰ CSF activated GPR55, which is not unexpected taken into consideration its expression in the brain and the

Results and Discussion

availability of a potential agonist in CSF. In order to investigate whether the signal is just an artifact or receptor-dependent, it was decided to compare the order of efficiency of the signal via the signal/noise (S/N) ratios produced by the CSF from different samples. The ratios did not show the same order of efficiency as shown in figure 30.

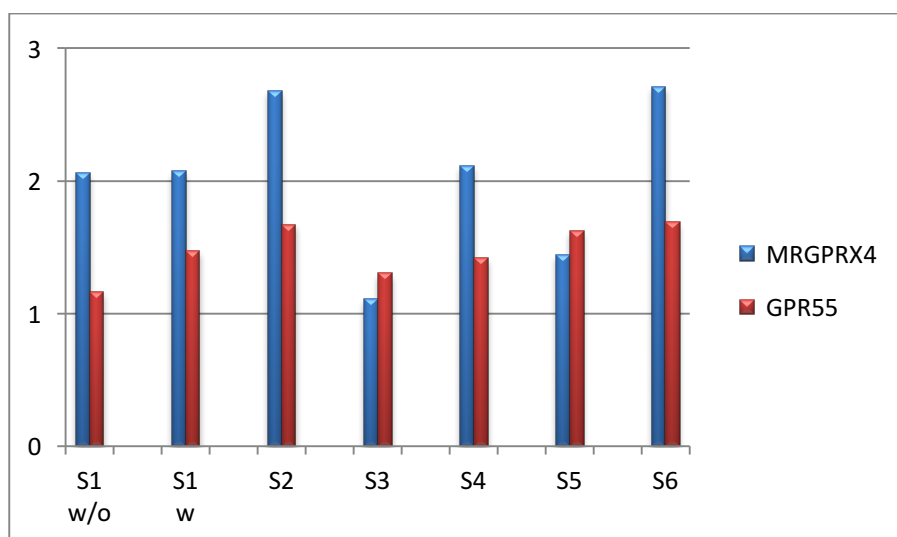


Figure 30: S/N ratios of CSF from different samples at MRGPRX4 and GPR55 receptors. S1 w/o: sample 1 without protease inhibitor, S1 w: sample 1 with protease inhibitor.

The next step was to investigate if the CSF could also induce a signal in the G protein pathways. The coupling according to Burstein et al.²³ should be G_q only, while according to the prediction tool (<http://athina.biol.uoa.gr/bioinformatics/PRED-COUPLE2/>) MRGPRX4 should be G_q and/or G_i -coupled. Therefore, screening of the CSF samples via cAMP and calcium mobilization assays were done. Table 19 shows the results of the calcium mobilization assay. ATP at 100 μ M was used as a positive control in CHO cells because it can activate one or more of P2Y receptors.

Table 20: The results of screening of CSF samples using calcium mobilization assay and the ratio to ATP signal.

Test sample or compound	Fluorescence	Ratio (CSF/ATP)
ATP (100 μ M)	11	1
S1 w/o	40	3.6
S1 w	62	5.6
S2	81	7.3
S3	86	5.6
S4	62	7.8
S5	89	8
S6	63	5.7

Results and Discussion

The results show a different pattern compared to the β -arrestin results. All samples induced a strong calcium signal. Sample 3, for instance, exhibited a robust increase in calcium signal but no β -arrestin signal. These results could be explained by the endogenous expression of different 7TMRs in the CHO cells, which have a G_q coupling and could be activated by CSF. In contrary, β -arrestin assay would ideally give a signal in the case of activating the 7TMR of interest only.

The screening of CSF using the cAMP assay after stimulation of cAMP production with forskolin (10 μ M) did not show any signal (data not shown). It should also be mentioned that heating the CSF to 90 °C for 5 minutes did not change the signal in the β -arrestin assay, which means that the active entity is stable under these condition.

These findings seemed to be encouraging to continue the search for a receptor agonist in the CSF. Since the search should be based on an assumption of the nature of the agonist in order to determine further steps, our assumption was that the agonist could be a peptide. Although MRGPR receptors could be activated by a variety of agonists of different nature that do not have much in common (adenine, β -alanine, CST-14, BAM-22, several RF-peptides)¹²², the reported agonist at human receptors are all peptides. Therefore, it was decided to digest the peptides using a protease and see if the signal would disappear. Trypsin is a serine protease, which cleaves predominantly proteins at the carboxyl side (or "C-terminal side") of the amino acids lysine and arginine except when either is bound to a C-terminal proline.¹⁵¹ Trypsin was chosen as a protease because of its wide specificity and availability. CSF samples were incubated with trypsin for 30 minutes at 37 °C before screening. There was a decrease in the signal of CSF but given that trypsin is used for cell detachment, it was not clear if the decrease in signal is due to a harmful effects of trypsin (e.g. cleaving of the receptor) or due to degradation of an active peptide ligand. The decrease in signal was dependent on the concentration of trypsin as shown in figure 31.

Results and Discussion

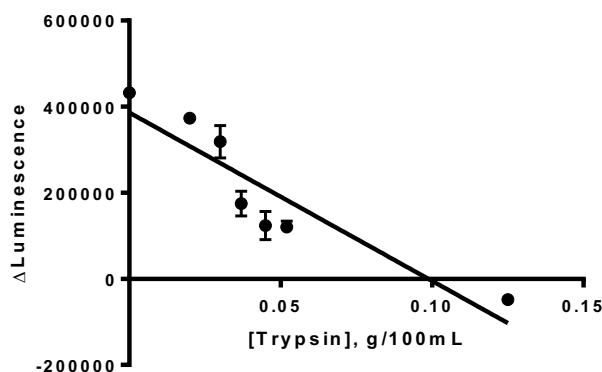


Figure 31: The decrease in β -arrestin signal is dependent on the concentration of trypsin. It should be noted that at higher concentration the basal signal was reduced.

The next plausible step was to fractionate CSF into two fractions using a 3 kDa cutoff Amicon® Ultra, one fraction is more than 3 kDa and the other is less than 3 kDa. Since both BAM22 and CST-14 have a molecular weight of less than 3 kDa, it was expected that only the less than 3 kDa fraction will show an activity. Table 21 shows the results of CSF of two samples after fractionation.

Table 21: The results of testing the two fractions of CSF at MRGPRX4 receptor

	Detected fluorescence			mean \pm SEM	S/N ratio
PBS	93368	109760	106912	103347 \pm 5056	1
Sample M.D. < 3 kDa	159752	181056	193768	178192 \pm 9923	1.72
Sample M.D. > 3 kDa	110680	94744	92440	99288 \pm 5734	0.96
Sample U.P. < 3 kDa	185712	141464	167160	164778 \pm 12828	1.59
Sample U.P. > 3 kDa	92248	93936	93104	93096 \pm 488	0.90

As expected the signal was now only obtained from the fraction of less than 3 kDa. From now on the further testing will only be done with this fraction. Interestingly, screenings at GPR55, MRGPRX2 and GPR35 showed that the less than 3 kDa fraction did not have any agonistic activity (data not shown). Thus, it is clear now that the active entity in CSF is pretty stable at high temperature and it has a molecular weight of less than 3 kDa, but the nature of this entity is still elusive. Therefore, it was decided to add a suitable protease inhibitor to trypsin after digesting CSF so that trypsin would not have any proteolytic effect on the cells.

2.4.4 Soybean trypsin inhibitor

The soybean peptidase inhibitor (STI) can be divided into two types. The most common type (used in this work) is the Kunitz trypsin inhibitor (STI, M_r of about 20 kDa, two disulfide bridges between amino acids 39-86 and amino acids 136-145), which belongs to the clan IC and to the family I3 in the MEROPS database.^{152,153} The inhibitors from this family are tight-binding, reversible inhibitors with β -trefoil structure. The members of this family show inhibition of serine, cysteine and aspartic proteases.¹⁵⁴ STI can be hydrolyzed by trypsin, the cleavage site being situated between Arg63 and Ile64 and the interaction is a one-to-one stoichiometry. This leads to a conversion of the single chain inhibitor to two chains held by a single disulfide bond between residues number 39 and 86. The complex of STI with trypsin has neither tryptic nor inhibitory activity; the cleaved inhibitor has full inhibitory activity.^{155,156}

The active (<3 kDa) fraction was assumed to cause the signal via a peptide. To check this out, incubation with trypsin and then STI each for 30 minutes was done. For this experiment not only PBS should be considered as a negative control but also trypsin/STI and STI alone. The results could not be interpreted because the signal of CSF after treatment with trypsin/STI was considerably higher than for CSF alone. These results were reproducible and Trypsin/STI or STI alone induced approximately the same signal as shown in figure 32. In this case, the CSF-induced signal could not be detected because STI induced a more robust signal with a higher S/N ratio. This fact represented a barrier for further investigations of CSF and shifted the search towards STI and interleukin 1- β (see next two chapters).

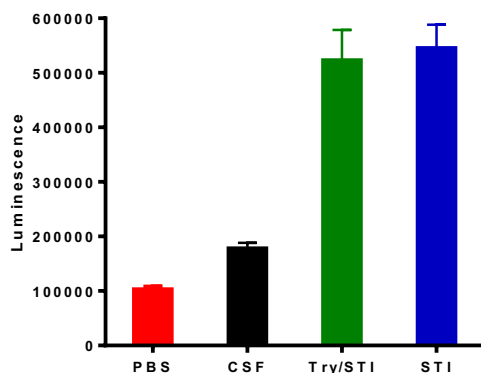


Figure 32: the detected signal in β-arrestin assay

These findings indicate that STI is inducing the robust signal at MRGPRX4 receptor. This was unexpected but due to the high reproducibility of the results it was decided to screen STI at the human MRGPRX2 receptor.

Table 22: The effect of STI on the signal of CST-14 at MRGPRX2 receptor

	Detected fluorescence			mean ± SEM	S/N ratio
PBS	1830176	1692568	1750048	1757597 ± 39902	1
CST-14 (10 μM)	18900952	17086272	18715528	18234250 ± 576479	10
CST-14, Try, STI	2320800	2187640	2336384	2281608 ± 47198	1.2
STI	1975152	2012016	1843080	1943416 ± 51284	1.1

Conducting a two-tailed t test, the difference in signal between PBS and STI was statistically significant (p value of 0.045), the difference between PBS and the CST-14 plus trypsin and STI was also statistically significant (p value of 0.0011). Despite this statistical significance, the increase in signal is minimal compared to the signal induced by CST-14 at MRGPRX2 receptor. It was concluded that trypsin could cleave CST-14 and that STI can be added to inhibit the harmful effect of trypsin on the cells. These results show also that STI does not have an agonistic effect on MRGPRX2. Taking these findings into account, STI was investigated as a potential agonist at MRGPRX4 receptor. STI induced a robust signal as demonstrated in figure 33. However, a plateau could not be reached within the range of tested concentrations.

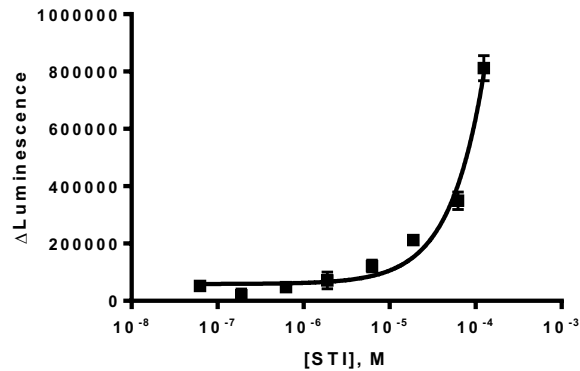


Figure 33: The mean curves of three independent β -arrestin assays with the soybean trypsin inhibitor (STI) at MRGPRX4

Upon further investigating the active fraction using a 3 kDa cutoff Amicon® Ultra, it was shown that the active fraction is, unlike CSF, > 3 kDa (data not shown). This led to the testing of an STI preparation with high purity and the result was identical (data not shown). These results indicate that STI is causing the signal and not a small peptide. Since STI is a plant protein and MRGPRX receptors are human 7TMRs, a search for similarity between STI and human proteins revealed that such a similarity was based on the β -trefoil structure as a common denominator.

β -Trefoil structures have relevance in human proteins and some proteins with high functional versatility share this structure. The proteins with this conserved β -trefoil structure interact selectively with their different targets due to the low sequence homology among them. These targets are divided into the following six groups according to their biological activity (first, hydrolase inhibitors like peptidase inhibitors; second, interleukins belonging to IL-1 family; third, fibroblast growth factors (FGFs); fourth, lectins and carbohydrate-binding modules; fifth, fascin, an actin cross-linking protein; sixth, multi-domain DNA-binding protein LAG-1, which acts as repressor or activator in the Notch signaling pathway).¹⁵⁷ From these six groups only the interleukin-1 family seemed to be interesting due to its role in pain and its expression in DRG (see chapter 2.4.5). This led to a third deorphanization attempt (see chapter 2.4.5). Lastly, it should be stressed that the increase in signal by STI did not reach a plateau even in a concentration up to 200 μ M. This looked like an artifact. Therefore, STI was investigated at 100 μ M using GPR55 and GPR35 cell lines. Both receptors showed a considerable increase in signal. Testing STI at MRGPRX1 receptor resulted in approximately the

same increase as in the MRGPRX4 cell line (data not shown). These observations were enough to consider STI an artifact and stop investigating it further.

2.4.5 Interleukin-1 β and its N-terminal cleavage products: The third deorphanization approach and an elusive entity

The Interleukin 1 (IL-1) subtypes, IL-1 α and IL-1 β , differ markedly in the primary structures but both have the 3D β -trefoil structure. Two distinct IL-1 β receptor binding proteins (IL-1 RI and IL-1 RII), plus a non-binding signaling accessory protein have been identified.^{158,159} Until recently, IL-1 RI was considered a signal transducing receptor, while IL-1 RII was believed to be a dummy receptor. It is now known that IL-1 signaling is not generated by the IL-1 RI molecule, but by an IL-1 RI accessory protein that only interacts with IL-1 RI.^{160,161} The IL-1 β is a potent pleiotropic proinflammatory cytokine, whose concentration in the CSF is commonly monitored in neurological disorders including neuropathic pain and complex regional pain syndrome.¹⁶² In the CNS, endogenous IL-1 β levels increase in neuropathic pain and cause release of excitatory glutamate in the dorsal horn via sphingomyelinase and Src-kinase pathways.^{163,164} A neuropathic pain-induced increase in IL-1 β was also found in the DRG and trigeminal ganglia, both in the neurons as well as in glial cells (satellite cells).^{165,166} In addition to the various indirect activation mechanisms, IL-1 β was suggested to act as a direct sensitizer of nociceptors via augmenting sodium currents.¹⁶⁷ This imminent role of IL-1 β in neuropathic pain led us to investigating it as a potential MRGPRX4 ligand.

Initially, mouse IL-1 α and rat IL-1 β (acquired through Biomedizin Forum of the Uni Bonn) were screened at concentrations from 100 nM till 5 nM but did not show any activity at MRGPRX4 receptor (data not shown). Due to the low sequence identity of murine IL-1 α and rat IL-1 β with their corresponding human counterparts, screening of human IL-1 β seemed necessary. IL-1 β was purchased as a 5 μ g aliquot from InvitrogenTM (manufactured by Sino Biological Inc.). IL-1 β induced concentration-dependently a robust signal in the β -arrestin assay with an EC₅₀ value of 739 \pm 180 nM as demonstrated in figure 34.

Results and Discussion

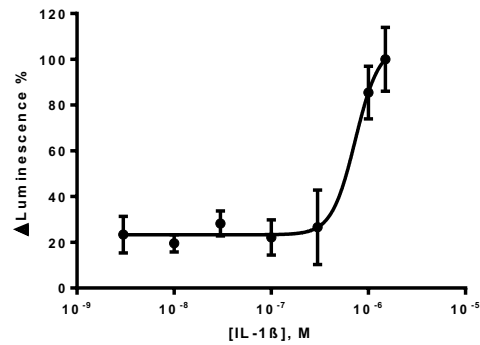


Figure 34: The mean curve of four independent β -arrestin assays of interleukin-1 β (IL-1 β) at MRGPRX4 receptor. The determined EC₅₀ value was 739 \pm 180 nM

This interesting result encouraged us to subsequently test a more pure IL-1 β preparation since the one purchased from InvitrogenTM was only of 85% purity. 5 μ g from R&D systems were ordered but surprisingly no agonism could be detected, but rather a small decrease in the basal activity. For confirmation another 95% pure 5 μ g from InvitrogenTM were tested and once again no agonism could be detected but only a decrease in the signal (data not shown). These findings led us to the assumption that the 15% impurity was causing the increase in signal. The impurities were investigated using SDS-PAGE gel and were found to have a mass of less than 3 kDa. Hence, two fractions (more and less than 3 kDa) of the IL-1 β solution were separated and tested. The result showed that only the less than 3 kDa fraction was active as shown in figure 35.

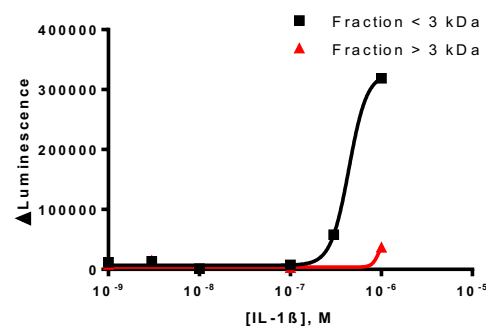


Figure 35: Fractionation of IL-1 β preparation led to the conclusion that only the fraction of less than 3 kDa is the active fraction in β -arrestin assays at MRGPRX4. This experiment was done only once due to the expensive material.

In order to make sense of our findings, a mass spectrometrical approach was necessary for analyzing the active IL-1 β fraction. PD Dr. Anke Schiedel sent IL-1 β as well as a CSF sample to Freiburg for analysis. Both samples were first digested with trypsin and then subjected to MALDI-TOF and electrospray ionization mass spectrometry. The results confirmed the existence of IL-1 β , in addition

Results and Discussion

to other proteins, in both CSF and the active fraction of IL-1 β . The peptides, which could be detected, are listed in table 23 and table 24.

Table 23: The sequences of IL-1 β fragment peptides, their intensities and their masses, which were found in the fraction of less than 3 kDa of CSF after digestion with trypsin. The individual peptides are given in different colors and their location within the mature IL-1 β is shown in the last row of the table.

CSF	Sequence	intensity	mass
	SLNCTLR	80217	862
	SLVMSGPYELK	192730	1222
	DDKPTLQLESVDPK	144380	1583
APVRSLNCTLRDSQQKSLVMSGPYELKALHLQGQDMEQQVVFMSFVQGEESNDKIPVALGLKEKNLYLSCVLKDDKPTLQLESVDPKNYPKKKMEKRFVFNKIEINNKLEFESAQFPNWWYISTSQAENMPVFLGGTKGGQDITDFTMQFVSS			

Table 24: The sequences of IL-1 β fragment peptides, their intensities and their masses, which were found in the fraction of less than 3 kDa of IL-1 β after digestion with trypsin. The individual peptides are given in different colors and their location within the mature IL-1 β is shown in the last row of the table.

IL-1 β	Sequence	intensity	mass
	SLNCTLRDSQQK	9749	1448
	SLVMSGPYELK	782570	1222
	NLYLSCVLK	798420	1108
	NLYLSCVLKDDKPTLQLESVDPK	7085400	2674
	ALHLQGQDMEQQVVFMSFVQGEESNDKIPVALGLK	140660	3971
	DDKPTLQLESVDPK	447050	1583
APVRSLNCTLRDSQQKSLVMSGPYELKALHLQGQDMEQQVVFMSFVQGEESNDKIPVALGLKEKNLYLSCVLKDDKPTLQLESVDPKNYPKKKMEKRFVFNKIEINNKLEFESAQFPNWWYISTSQAENMPVFLGGTKGGQDITDFTMQFVSS			

In order to analyze the sequences, it should be borne in mind that the sequences were detected after digestion with trypsin (i.e. cleavage after basic amino acids R and K) and that the detection limit was ≥ 7 amino acids. The results suggest that the N-terminal sequence could be responsible for the signal and the detection limit of 7 amino acids means that the first 4 amino acids at the N-terminus would not have been detected and it means also that a maximum of 6 amino acids after each R or K would also not have been detected. The overlapping of detected peptides was on the N-terminal side and in the middle of the mature IL-1 β . Since the N-termini of proteins are often reported to have important functions^{168,169}, the fate of IL-1 β could provide an insight into identifying structures with potential activity. Our search found that while the activation of IL-1 β from pro-IL-1 β takes place via several enzymes like caspase-1, trypsin and matrix metalloproteinase 9 (MMP-9) the degradation of mature IL-1 β is not well characterized. Nonetheless, it was demonstrated that MMP-2, MMP-3 and MMP-9

Results and Discussion

can degrade IL-1 β but only MMP-3 could effectively and completely degrade IL-1 β . The primary cleavage site of IL-1 β was, nevertheless, only determined for MMP-2 and turned out to be between Glu²⁵-Leu²⁶^{170,171}. The sequence below is for IL-1 β and the sequence in red is the smaller cleavage product of MMP-2. It consists of 25 amino acids with a molecular weight of 2780.

APVRSLNCTLRDSQQKSLVMSGPYELKALHLQGQDMEQQVVFMSFVQGEESNDKIPVALGLKEKNLYLSCVLKD
DKPTLQLESVDPKNYPKKKMEKRFVFNKIEINNLEFESAQFPNWWYISTSQAENMPVFLGGTKGGQDITDFTMQFV
SS

Since the last sequencing was done using trypsin degradation, the sequences obtained were ending either in arginine or lysine. This corresponds not to the original sequences in the IL-1 β preparation. In order to get a better knowledge of these sequences, the tryptic degradation should not be performed. In order to do this, a new sample of IL-1 β was dissolved in water, and then fractionated into more and less 3 kDa fractions via Amicon® Ultra. Both fractions were investigated by Dr. Marc Sylvester (Prof. Gieselmann group). The fraction of more than 3 kDa could not be analyzed properly without tryptic digestion due to the high molecular weight. The results of the fraction of less than 3 kDa showed pronounced sequences from IL-1 β , especially of the N- and C-terminus as shown in table 25.

Table 25: The sequences of IL-1 β fragment peptides, their confidence levels and their masses, which were found in the fraction of less than 3 kDa of IL-1 β without trypsin digestion. The individual peptides are given in different colors and their location within the mature IL-1 β is shown in the last row of the table.

IL-1 β	Sequence	Confidence level	mass
	APVRSLNCTLRD	high	1433
	PVRSLNCTLRD	high	1273
	APVRSLNCTLRDSQQKSLVMSG	high	2390
	GQDITDFTMQFVSS	high	1575
	TKGGQDITDFTMQFVSS	high	1862
	APVRSLNCTLRDSQQKSLVMS	high	2333
	LESVDPKNYP	medium	1161
	APVRSLNCTLRDSQQKSLVMSGPYELKALHLQGQDMEQQVVFMSFVQGEESNDKIPVALGLKEKNLYLSCVLKD DKPTLQLESVDPKNYPKKKMEKRFVFNKIEINNLEFESAQFPNWWYISTSQAENMPVFLGGTKGGQDITDFTMQFV SS		

These results further supported the potential that an N-terminal fragment of IL-1 β could be the elusive physiological agonist of MRGPRX4 receptor. Similarly, two CSF samples were taken to Dr. Sylvester for analysis. One sample revealed several peptides from 70 different proteins as expected

Results and Discussion

from the physiological liquid but, unfortunately, no trace of IL-1 β fragments could be detected. This could be due to the very low amount of this fragment as well as the lack of tryptic degradation, which enables the statistical threshold to be lowered. The second sample, unexpectedly, did not demonstrate anything other than the fibrinogen alpha chain.

A custom synthesis of the 25 amino acid peptide, the cleavage fragment of IL-1 β induced by MMP-2, was ordered from Proteogenix Inc. Upon testing in β -arrestin assay no agonistic activity at MRGPRX4 of this peptide could be detected even in concentrations up to 100 μ M. The screening of the same peptide at MRGPRX1 and MRGPRX2 did not show any activity either (neither agonism nor antagonism). A second custom peptide was ordered according to the sequencing results of untrypsinated IL-1 β . This sequence (APVRSLNCTLRD) was N-terminal as well as shown in table 24. The second peptide was also inactive at MRGPRX4 and other MRGPRX receptors as well.

These negative results led to the search for other degradosome products as potential ligands for MRGPRX4 receptor. MMP-3 seemed to be the most suitable protease candidate owing to the observation that MMP-3 can degrade IL-1 β completely into small fragments.¹⁷⁰ In the first experiment both MMP-3 and IL-1 β were from InvitrogenTM and had 85% purity. In this experiment 5 μ g of IL-1 β were dissolved in water and then fractionated as usual into a fraction of less than 3 kDa and another of more than 3 kDa. The inactive fraction (more than 3 kDa) was incubated with MMP-3 for 2 h at 37 °C in a final volume of 500 μ l. As a control, 5 μ g MMP-3 from the same lot was dissolved in 500 μ l (30 μ l PBS and 470 μ l water) and incubated for 2 h at 37 °C. Both the digested inactive fraction and the control MMP-3 were fractionated via an Amicon[®] Ultra. The fraction of less than 3 kDa was lyophilized and then dissolved in 30 μ l PBS and tested in β -arrestin assays. The digestion was immediately stopped after 2 h through freezing of the sample in liquid N₂. Since it was not possible to determine the concentration of the resultant digestion products, the concentration in β -arrestin assays will be given as μ l of test solution in 100 μ l (the total volume of one well) as shown in figure 36.

Results and Discussion

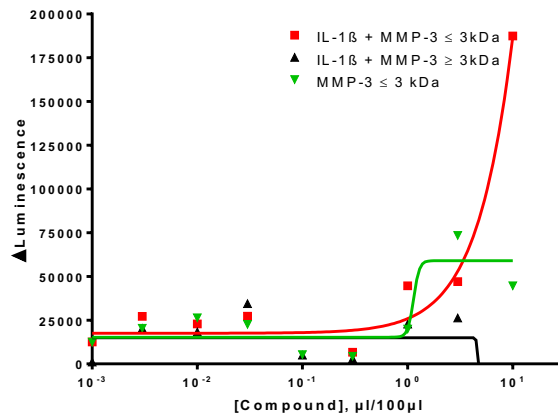


Figure 36: The resultant curves of one β -arrestin assay after incubation of the inactive fraction of IL-1 β with MMP-3 and subsequent fractionation into more and less than 3 kDa fractions. The curve of MMP-3 alone was also plotted as a control.

The previous results may suggest that the inactive fraction of IL-1 β was digested by MMP-3 to an active species at MRGPRX4 receptor. The experiment was repeated twice, once with the same, less pure IL-1 β (InvitrogenTM) and another time with highly pure IL-1 β (R&D systems). In both cases the same MMP-3 (Sigma Aldrich) was used. In one experiment, the less pure IL-1 β was treated in exactly the same way as in the previous experiment with the exception of incubating for 4 h. In this experiment the digested fraction of >3 kDa was again tested. The results are given in figure 37A. In a second experiment, the highly pure proteins were used. In this case, 4 μ g of the IL-1 β was incubated with 5 μ g of MMP-3 (total volume of 500 μ l). After the incubation, the solution was fractionated and both fractions >3 kDa and <3 kDa were lyophilized, dissolved in 30 μ l PBS and tested in β -arrestin assays as shown in figure 37B.

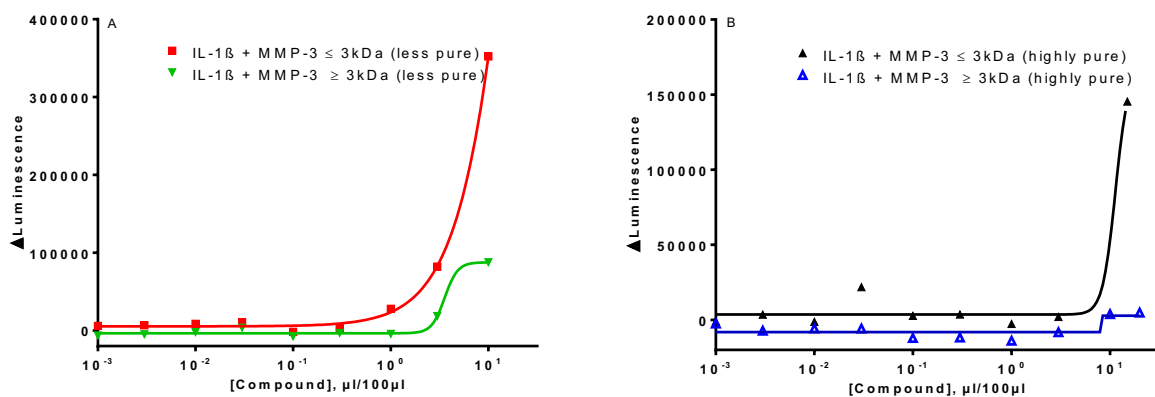


Figure 37: The resultant curves of two β -arrestin assays after incubation of the inactive fraction of IL-1 β with MMP-3 and subsequent fractionation into more and less than 3 kDa fractions. The experiment A was done using a less pure IL-1 β (85%), whereas experiment B was done using a pure IL-1 β (95%).

Results and Discussion

In principle, the results consolidate the findings of the first experiment. These digestion experiments have limitations (see chapter 2.4.6) but they indicate the ability of MMP-3 to produce an active moiety at MRGPRX4 receptor. Unfortunately, efforts to identify and isolate this potential agonist remained elusive. Despite that fact that 5 µg of the highly pure IL-1β were digested with 5 µg MMP-3 and the fraction of less than 3 kDa was sent to Dr. Sylvester for analysis, the data he provided did not show any trace of MMP-3 or IL-1β in this fraction. This result could not be easily explained. Hereafter, it was not possible to continue our search for an active peptide because of the bound risk; in addition a breakthrough had meanwhile taken place during parallel screening efforts for agonists (see chapter 2.4.7).

2.4.6 Discussion I

The investigation of MRGPRX4 began with a hypothesis, based on sequence identity, that this receptor could be the human receptor for the nucleobase adenine. Screening adenine in functional assays (β-arrestin and calcium mobilization assay) did not show any activity in spite of the fact that very high concentrations were employed. Capitalizing on the availability of [³H]adenine in our lab competition binding studies have also been attempted to investigate any binding of adenine (role as a modulator or an antagonist). These also have proven that adenine does not bind to MRGPRX4. These data are sufficient to refute the hypothesis of MRGPRX4 as the human adenine receptor. Adenine has previously been investigated at other MRGPRX subfamily members and has shown no activity (data from Bernt Alsdorf). The search for a potential human adenine receptor has not been fruitful yet.

The following efforts were to find an agonist for MRGPRX4 via screening several compound libraries. Unfortunately, no agonist could be identified in this search, which left the possibility for identifying a ligand for MRGPRX4 very dim. The inability to find an agonist through screening of small molecule libraries might have been due to the possibility of a native peptidergic agonist requiring interaction of several amino acids in an extended area of the binding pocket of the receptor for inducing a

Results and Discussion

conformational change. Therefore, a small molecule could not easily imitate a sizable peptide. This assumption is substantiated by BAM22 and CST-14 being the cognate ligands at the related MRGPRX1 and MRGPRX2, respectively. In order to break this impasse, a second deorphanization approach was put to test. Taking advantage of the restricted expression pattern of MRGPRX4 in the DRG and the fact that DRGs are surrounded by CSF, a search for an assumed peptide in the CSF was initiated. Such an approach is an imitation of earlier successful efforts, which led to the identification of several neuropeptides (orphanin FQ at Opioid receptor-like 1^{142,143}, orexin A and B at orexin receptors¹⁴⁴, prolactin-releasing peptide and ghrelin at their receptors).^{146,148} Our simplified approach was based on analyzing a physiological fluid and not an organ extract, especially because in the case of MRGPRX4 human tissues would be required. CSF was concentrated 10-fold via lyophilization and tested in β -arrestin assays. It was possible for the first time to induce a robust signal, which seemed to be sample-dependent. These interindividual differences could be due to different levels of the agonist in CSF samples corresponding to the nociceptive input. Further fractionation of the samples revealed that the active moiety is less than 3 kDa in molecular weight. Further efforts to digest the peptides using trypsin led to cell toxicity and death of the cells. In an attempt to avoid cell toxicity, a soybean trypsin inhibitor (STI) was added that caused an unspecific increase in signal, which confounded the signal induced by CSF. In principle, this approach is an interesting one but the search did not show a clear results and no peptide has been found so far. The search for neuropeptides combines, as from the above mentioned publications, a tissue extract and then extensive analytical work to separate and fractionate this extract. Such an approach requires a hypothesis of the nature of the ligand (peptide, fatty acid etc.) in order to use the suitable extraction solvent and then the application of several chromatographic methods (RP-HPLC, size exclusion chromatography, ion exchange and desalting methods) followed by LC-MS/MS detection (NMR could also be beneficial for clarifying the structure). The yield is usually very limited; for instance 16 μ g of ghrelin were extracted from 40 g of rat stomach tissue and merely 200 pmol of orphanin FQ were isolated of 4.5 kg of porcine hypothalamus.^{143,148} This means that a relatively very large amount of CSF, much more than

Results and Discussion

we had at hand would be required to apply the same procedure, since the concentration in CSF could be considered a dilution of the actual concentration in the DRG.

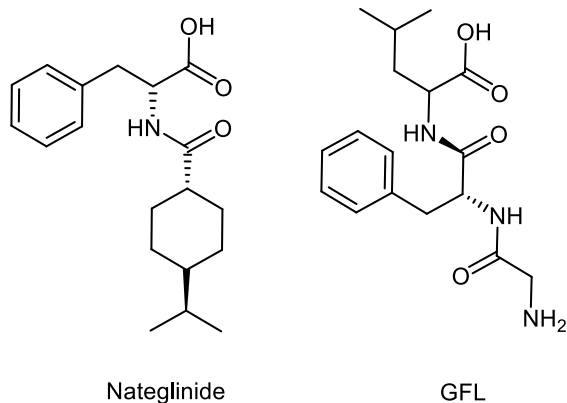
The search for an agonist took a new turn by investigating IL-1 β . Upon investigating this cytokine, more than one important player in neuropathic pain came into play, namely, the cross-talk between cytokines, opioid and MRGPRX receptors, in addition to the role of proteases, especially MMPs, in neuropathic pain and in modifying chemokine signaling. Our results after investigating IL-1 β showed that the observed activity of an IL-1 β preparation at MRGPRX4 did not result from the mature IL-1 β but from an entity, which is less than 3 kDa and may be an impurity or another constituent of the tested solution. This impurity could be due to proteolysis of IL-1 β during extraction or it could be from the host in which IL-1 β is produced (*E.Coli* in this case). The degradome of IL-1 β is not well-understood but it seems that MMP-2, MMP-3 and MMP-9 play a role in it. Since MMP-3 was suggested to be the most effective degrader of IL-1 β , the degradome of IL-1 β was tested at MRGPRX4. The results seem to indicate an activation of MRGPRX4 via the degradome but no clear sequence has been found. Our search and hypothesis could have a sound theoretical grounding; the up-regulation of IL-1 β and its role in neuropathic pain has already been discussed. The role of MMPs in neuropathic pain, inflammation, immunity and cancer has been reviewed and their complex relationships with cytokines have been established.¹⁷²⁻¹⁷⁴ The role of MMP-9 in activating the central and peripheral glia has been described.¹⁷⁵ In neuropathic DRG, MMP-9 has been up-regulated in the early phase and was involved in the activation of IL-1 β , whereas MMP-2 showed an increase in the late phase (from day 7) of neuropathic pain and was implicated in the maintenance of neuropathic pain and astroglial activation.¹⁷⁶ In rat models of paclitaxel-induced neuropathy, MMP-3 has been demonstrated to be up-regulated.¹⁷⁷ Moreover, a cross-talk between MRGPRX1 and chemokine receptor 2 has been described. BAM8-22, the selective MRGPRX1 agonist, could up-regulate chemokine receptor 2 expression, which has been linked to neuropathic pain, in both HEK and a rat dorsal root ganglia cell line. BAM8-22 was investigated at LAD-2 mast cells and it could, interestingly, induce the release of the chemokine CCL2, the native agonist at chemokine receptor 2.⁶⁸ Acute

Results and Discussion

morphine administration (a potent μ receptor agonist and a weak MRGPRX2 receptor agonist) could activate glial cells in the DRG and cause an up-regulation of MMP-9, which causes an enhanced release of IL-1 β and result in an analgesic effect.^{178,179} Moreover, the role of MMPs in proteolytic processes of chemokines has been studied extensively. MMP-2 seems to play the most important role in trimming the N-termini of chemokines and thus regulating their activities. This could lead to inactivation and transforming agonists into antagonists (CCL2, CCL4, CCL7, CCL8, CCL11, etc) or to activating other chemoattractants (CCL16 and CCL23).¹⁸⁰⁻¹⁸² In fact, it is now established that all 54 human chemokines are modified regarding to their biological activity via MMP members.¹⁸³ In order to highlight the pervasiveness of proteolytic processing in general, the origin of the N-terminal modification in the human proteome has been studied computationally on a global scale and the findings indicate that approximately 24,000 N-termini in the human proteome differ from canonical encoded or methionine processed N-termini.¹⁸⁴ The N-terminomics and C-terminomics (degradomics in general) have been reviewed and special mass spectrometrical techniques have been developed to study them.^{185,186} A recent publication showed that not only MMPs but also cathepsins could modify chemokines.¹⁸⁷ In another important paper, a new concept of protease activated 7TMR was put forward, in which a protease cleaves the N-terminus of a 7TMR and thus induces conformational changes that causes downstream signaling without any tethered or diffusible ligand. It was suggested that cathepsin S could cleave the N-terminus and activate mouse MRGPC11 receptor with an EC₅₀ value of 140 nM. It was also reported that cathepsin S could activate MRGPRX2 and papain could activate MRGPRX1 but no EC₅₀ values were given.¹⁸⁸ All the interesting previous findings investigated the proteolytic process and the resultant truncated protein but any potential activity of the cleaved fragments was not followed. Our initial results indicate that a fragment of IL-1 β (degradation vs. proteolytic processing) could be the native ligand of MRGPRX4, which could be the first example of a degradation product as a means of cross-talk between IL-1 β (and its toll-like receptor) and MRGPRX4 (7TMR) via a protease (MMP-3). Nonetheless some caveats should be mentioned. The digestion of IL-1 β with MMP-3 was based on the experiments in references^{170,171}, in which identical amounts of

Results and Discussion

MMP-3 and IL-1 β were incubated. These high concentrations of proteases represent extreme conditions, which are usually not met physiologically.¹⁸³ A further limitation was the lack of conducting SDS-PAGE gels in order to confirm the extent of IL-1 β digestion as a function of time or MMP-3 concentration. In the digestion experiments the resultant curves did not reach a plateau (see figure 35 and figure 36). This could indicate an artifact if the plateau is still not reached even at very high concentrations (see figure 32). In the case of degraded IL-1 β the concentration remains low even if there were no loss during the filtration via Amicon® Ultra and the plateau could possibly be reached if higher concentrations were tested. In more details, the concentration of IL-1 β in synovial fluid is reported to be 100 pg/ml¹⁸⁹ and in the CSF to be 50 pg/ml¹⁹⁰ but we should keep in mind that the concentration at inflammatory sites is probably considerably higher. Moreover, IL-1 β has a very high potency at its receptors in the lower nanomolar range and not in the picomolar range. According to literature the K_D value is in the range between 1-3 nM.^{191,192} It is plausible to expect such a value for a cleavage product at MRGPRX4 receptor as well. Our experiments do not allow the calculation of a molar concentration because no estimate of the amount of the active moiety could easily be made. Another aspect is often the lower sensitivity of the β -arrestin assay due to the lacking of the phenomenon of a “receptor reserve”. It should be mentioned that an IL-1 β preparation was further tested in calcium assays and in a native cell line expressing MRGPRX4. The result was always positive, which indicates the existence of a real agonist and not an artifact. The search for a peptidergic ligand is tedious and frustrating but the finding that nateglinide, a phenylalanine derivative, is an agonist at MRGPRX4 is an indication that this receptor might be activated by an endogenous peptide. Nateglinide shows some similarity to the tripeptide GFL. GFL should be a not-investigated endogenous peptide resulting from the subtraction of BAM22 from peptide E (see figure 5).



In conclusion, the hypothesis of the degradome of IL-1 β containing an agonist at MRGPRX4 could not yet be proven and the active entity remains elusive.

2.4.7 Screening further compound libraries: a breakthrough

Due to the lacking success with the hypothesis-driven deorphanization approaches, further compound libraries (not available at the first screening in 2012) were screened; these were compound library 2, 7, 8, 10 and 11 (see chapter 4.10). All screenings were performed at a final concentration of 10 μ M unless the solubility of the compound did not allow the screening at that concentration.

In the compound library 11 lithocholic acid induced a signal but that was probably an artifact since no plateau could be reached even up to a concentration of 100 μ M (data not shown). The lipophilic nature of this agonist could be responsible for inducing this non-specific signal. In the natural compounds library, Δ^9 -tetrahydrocannabinol (Δ^9 -THC) was active at MRGPRX4. The calculated EC_{50} value was 9.63 ± 0.72 μ M as demonstrated in figure 38. Since the increase in signal is very steep as seen in figure 38, and Δ^9 -THC is previously reported to activate cannabinoid receptors and GPR55 in addition to several ion channels¹⁹³⁻¹⁹⁵, the signal was deemed unspecific. In the compound library 8 one hit could be identified, Gü-1924, which induced an S/N ratio of 2 at 100 μ M but it was too weak to plot a complete concentration-response curve (data not shown).

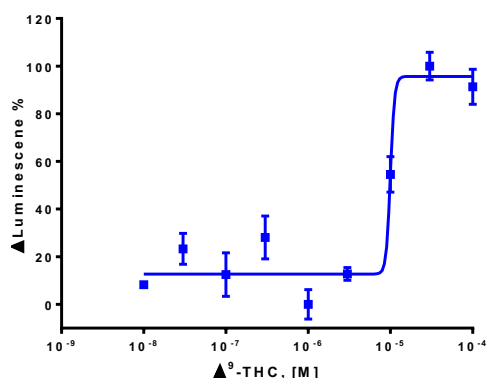


Figure 38: The mean curve of three independent β -arrestin assays of Δ^9 -THC at MRGPRX4.

The real breakthrough was the identification of the phosphoric acid ester derivative MSX-3 as a hit while screening the compound library 2.

2.4.8 MSX-3 and its related compounds as agonists at MRGPRX4

MSX-3 induced a robust and reproducible signal upon screening at MRGPRX4. MSX-3 is a prodrug of MSX-2, a potent and selective A_{2A} adenosine receptor antagonist. This compound is vulnerable to light-induced E/Z- isomerization.^{196,197} Due to this instability, a new stock solution of MSX-3 was prepared and a concentration-response curve was plotted as demonstrated in figure 39. The determined EC_{50} value was 175 ± 28 nM. This represented a breakthrough as a first agonist and a relatively potent one as well.

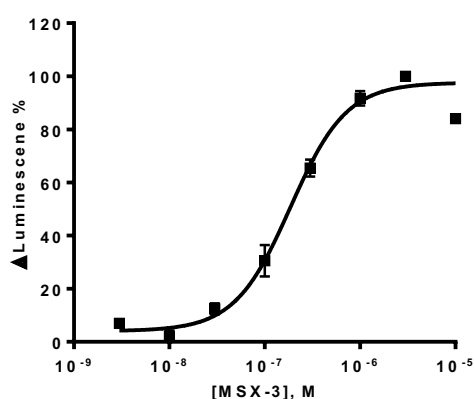


Figure 39: The mean curve of three independent β -arrestin assays of MSX-3 at MRGPRX4 receptor. The EC_{50} value was 175 ± 28 nM.

MSX-3 was counter-screened at MRGPRX1, MRGPRX2, GPR18, GPR55 and GPR143 that are expressed in the same CHO β -arrestin system and there was no activity at all these targets. In addition, MSX-3

Results and Discussion

did not show any inhibition of human NTPDase 1, NTPDase 2, NTPDase 3, NTPDase 8. Thus, selectivity was ensured.

Interestingly, MSX-3 is prodrug of an A_{2A} adenosine receptor antagonist and at MRGPRX4 it is a potent agonist. This led us to investigating the actual drug MSX-2 and other related compounds like MSX-4, another prodrug of MSX-2 coupled to valine, and Istradefylline, which shares the 8-styrylxanthine structure with MSX-2¹⁹⁸, as well as preladenant as shown in figure 40. All of these compounds were not active at all. Therefore, MSX-3 represents an active entity at MRGPRX4 and the phosphate is essential for the agonistic activity and cannot be replaced e.g. by valine. In order to further our SAR understanding, related 8-ethynylxanthine derivatives like NT 021071, NT 021033, NT 02109, NT 020052¹⁹⁹ (figure 40) were screened and all were inactive. The NT compounds show some differences to MSX-3. They possess a triple bond in their linker and they have a di-methoxy substituent; only NT 021071 has a phosphorylated substitution at N3 of its xanthine moiety. The inactivity could be due to the additional methoxy group or the triple bond. JH 14021 was an interesting compound since its only difference to MSX-3 is the triple bond in its linker. Thus, it has no light sensitivity problem. This compound was considerably less potent than MSX-3 with an EC₅₀ value of more than 10 μM, and its efficacy was also lower than that of MSX-3. This demonstrated the importance of the double bond being superior to the triple bond. The decrease in activity could be explained by the rigidity of the triple bond in comparison to the double bond, which can form *cis*- and *trans*-isomers and fit better into the binding pocket of the receptor. Hence, so far the agonism requires a phosphate group and a linker with a double bond. In addition, two methoxy groups at the phenyl ring seem to be intolerable.

Results and Discussion

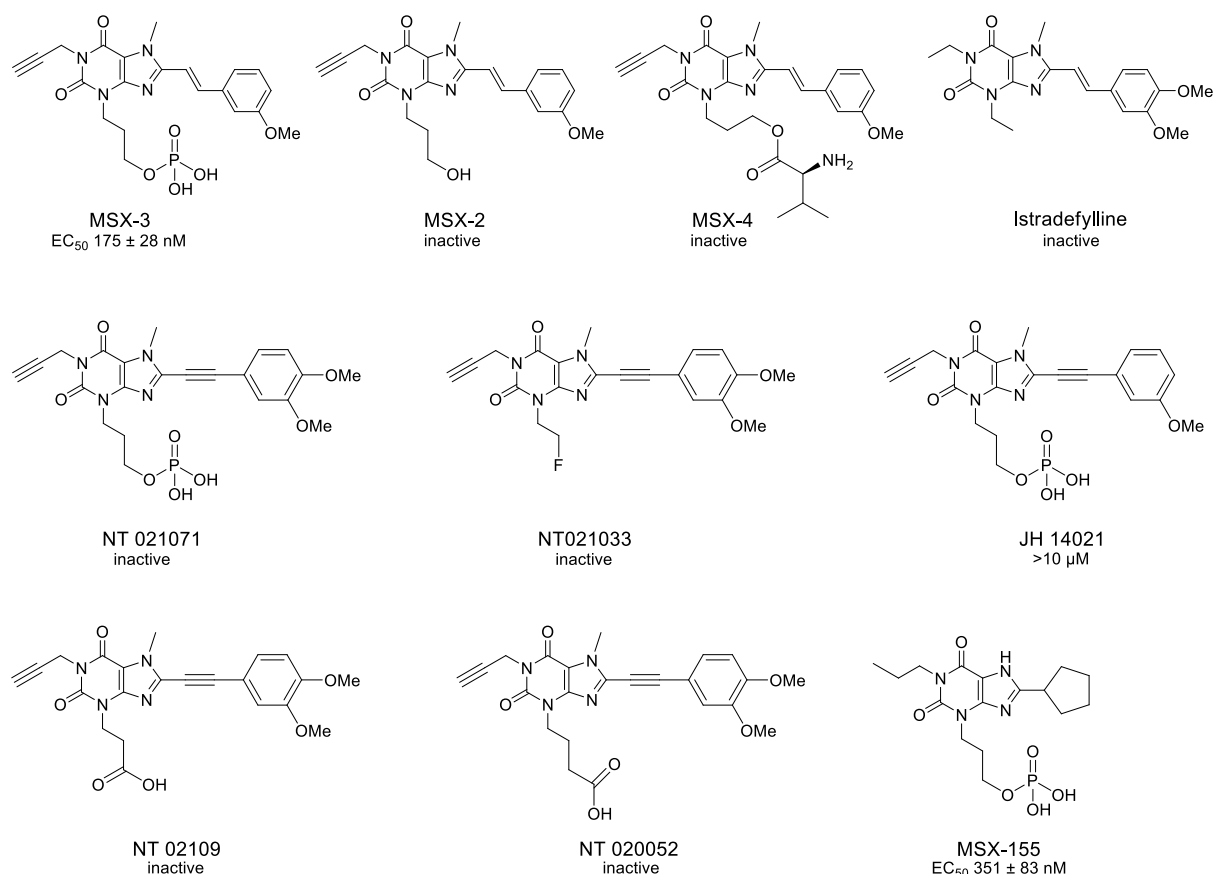


Figure 40: Structures and potencies of MSX-3-related compounds at MRGPRX4 in β-arrestin assay

MSX-155 is another important compound in the quest to understand the SARs of this scaffold.²⁰⁰

MSX-155 is a phosphate prodrug of DPCPX, a potent and selective A₁ adenosine receptor antagonist.

This compound has a xanthine core and a phosphate group but has no propargyl but, propyl group at N1, no methyl at the N7 position and linked aromatic group but only a direct cyclopentyl substitution at C8 of the xanthine core. At first glance this compound is considerably different. However, it was potent at the MRGPRX4 receptor with an EC₅₀ value of 351 ± 83 nM as shown in figure 41. It seems that the linker could be spared altogether. This is especially important since the double bond is vulnerable to light-induced E/Z-isomerization. It should be mentioned that despite the importance of these novel ligands, it was difficult to obtain reproducible results the whole time. This concerns both the potency and the efficacy of these compounds. This hampered using these ligands for antagonist screening. This hard reproducibility could be attributed to the enzymatic instability of these phosphoric acid esters, which can be cleaved by phosphatases expressed on the cell membrane.

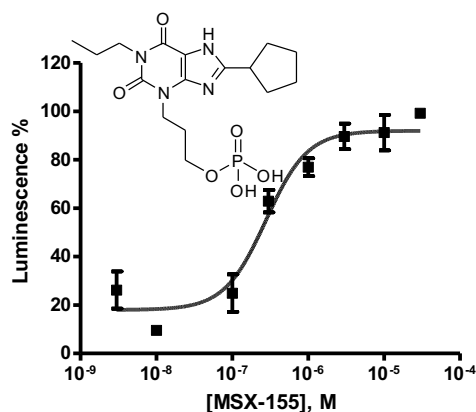


Figure 41: The mean curve of three independent β -arrestin assays of MSX-155 at MRGPRX4 receptor. The EC_{50} value was 351 ± 83 nM.

Since the β -arrestin assay requires a relatively long incubation time (90 min), substantial hydrolysis may take place. Therefore, it was decided to inhibit ecto-5'-nucleotidase and to compare the S/N ratio and the EC_{50} value. In order to do that the assay should be slightly modified. Therefore, Optimem medium was discarded, immediately before pipetting the agonists, and substituted by PBS containing the stable ADP analog, AMP-CP²⁰¹, at a final concentration of 40 μ M. The results showed an increase in S/N ratios both for MSX-3 (from 1.3 to 1.7) and MSX-155 (from 1.3 to 1.5) and the EC_{50} values were improved (for MSX-3 up to 67 nM and for MSX-155 up to 266 nM) but there were still variations in the determined EC_{50} values, which could be due to other phosphatases.

These results indicate the importance of developing more stable compounds as agonists at MRGPRX4 receptor. Phosphonates instead of phosphates seemed to be the most reasonable solution. Yet it was not easy to synthesize suitable derivatives. The first synthesized phosphonate, JH 14102, demonstrated encouraging results with an EC_{50} value of 17.4 ± 5.6 nM and an S/N ratio of 2.2 as shown in figure 42, which makes it one of the most potent agonist so far. JH 14102 is a phosphonate analog of MSX-3 but without the methyl group at the N7 position. A direct phosphonate analog has not yet been synthesized, but is in preparation.

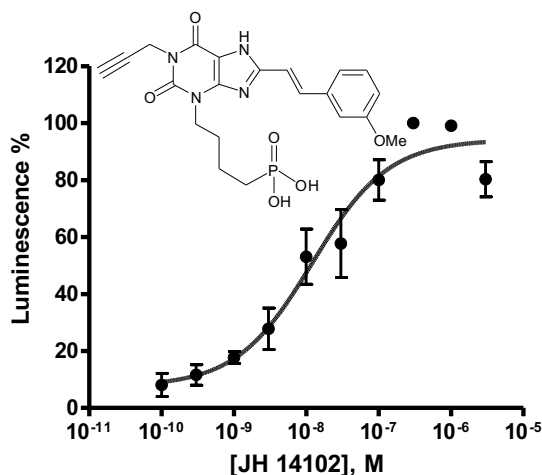


Figure 42: The mean curve of three independent β -arrestin assays of JH 14102 at MRGPRX4. The EC_{50} value was 17.4 ± 5.6 nM

2.4.9 Determination of the G-protein coupling of MRGPRX4 receptor

The G protein coupling of MRGPRX4 was predicted to be a sole G_q coupling via a proliferation assay²³ but since no agonist had been described previously, our next step was to determine this coupling using our novel pharmacological tools.

It was not possible to conduct calcium mobilization assay using the β -arrestin cell line in the attached cells format but it was only possible as a suspension, which is more tedious and needs 10 times more cells to be seeded. Nevertheless, it was possible to confirm MSX-3 as a potent agonist with an EC_{50} value of 47.8 ± 12.5 nM as shown in figure 43. It was also possible to demonstrate that JH 14021 is considerably less potent with an EC_{50} value of ca. 10 μ M, which is in harmony with the SAR obtained from β -arrestin assays. Therefore, the G_q coupling was confirmed. The fraction of IL-1 β less than 3 kDa induced a robust calcium signal as well (data not shown).

Utilizing JH 14102, it was decided to investigate the G_s and G_i coupling via cAMP assays. JH 14102 could not induce any cAMP accumulation at 1 μ M final concentration, which means that MRGPRX4 is not G_s coupled (data not shown). The screening for G_i coupling was done twice at 1 μ M final concentration and no inhibition of 10 μ M forskolin-induced cAMP accumulation was detected (data not shown).

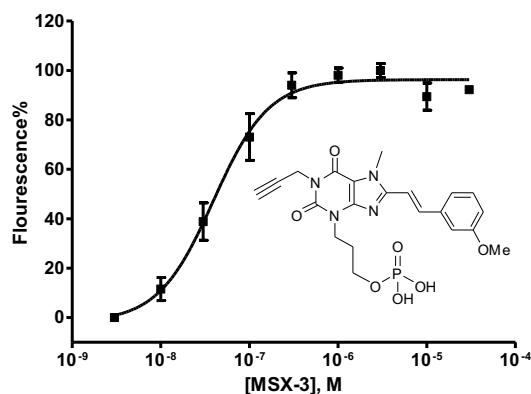


Figure 43: The normalized curve of three independent calcium mobilization assays of MSX-3 at MRGPRX4 receptor. The EC₅₀ value was 47.8 ± 12.5 nM

Herewith it was possible to confirm the findings of Burstein et al.²³ for a sole G_q coupling using a potent, selective pharmacological tool for the first time. While conducting these experiments, Kroeze et al. published nateglinide as an agonist at MRGPRX4 receptor.¹¹² Like our approach a β-arrestin assay was employed to detect the agonist and a HEK cell line overexpressing MRGPRX4 revealed a sole G_q coupling of this receptor in harmony with our findings. It is noteworthy to keep in mind that the calcium assay is not easy to conduct using the CHO β-arrestin cell line due to the modest increase in signal, which could be inherent to CHO cell lines, which appears to express only a small level of G_q-proteins (unpublished data). Therefore, β-arrestin assays were further employed for investigating SAR of MRGPRX4 agonists.

2.4.10 Structure-activity relationships of MRGPRX4 receptor agonists

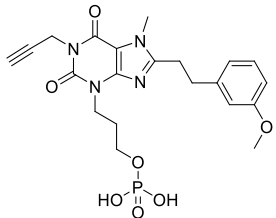
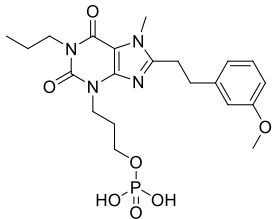
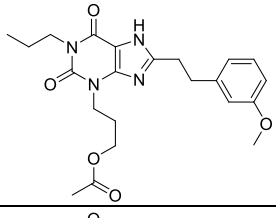
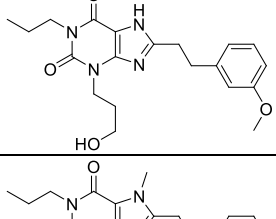
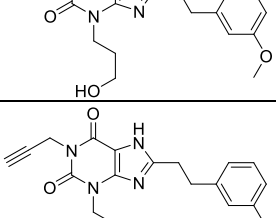
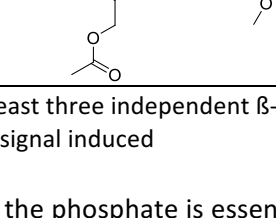
More than one series of compounds have been synthesized as agonists at MRGPRX4 receptor. It should also be noted that in all assays from now on a modified protocol for the β-arrestin assay has been used. This change resulted in a slight increase in the EC₅₀ value but the S/N ratio stayed the same. For example the phosphonate JH 14102 showed an increase in EC₅₀ value from 17.4 ± 5.6 nM with the old buffer to 76.1 ± 12.5 nM with the new one.

Since dividing the compounds should have a reference point, it was decided to divide them according to the linker between the xanthine moiety and the aromatic ring. Accordingly, four categories of ligands have been synthesized; 1) compounds that have an ethylene linker, 2) compounds that have

Results and Discussion

an ethenyl linker, 3) compounds with methylene as a linker, 4) compounds with no linker. The results are shown in the following tables (see tables 26 to 29).

Table 26: The structures, the EC₅₀ values and S/N ratios (efficacy) of the synthesized compounds with an ethylene linker

Compounds that have an ethylene linker			
Compound	Structure	EC ₅₀ value ± SEM (μM)*	S/N ratio**
Yazh 473		0.160 ± 0.048	4
Yazh 479		0.674 ± 0.050	3
Yazh 438		>>10	2
Yazh 449		>>10	
Yazh 474		>>10	
Yazh 599		27.1 ± 13	1.4

*: Results are mean ± SEM of at least three independent β-arrestin experiments

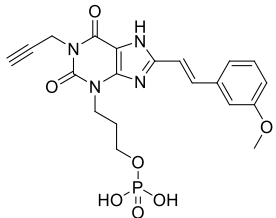
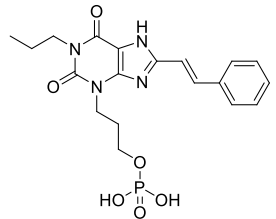
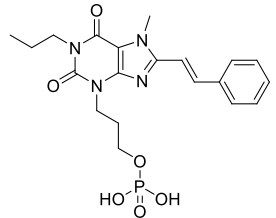
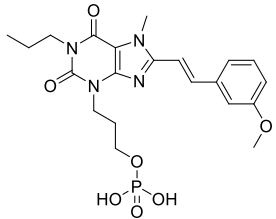
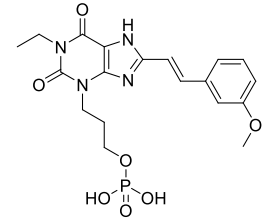
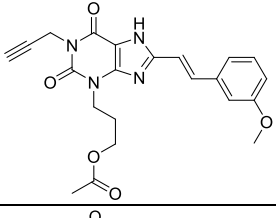
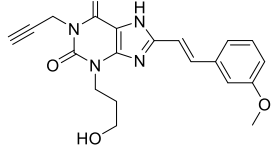
** : S/N ratio not given means no signal induced

The results showed again that the phosphate is essential since all the compounds without phosphate were inactive or weakly active. Yet the most important conclusion from these compounds is the importance of an ethylene linker. Yazh 473 and Yazh 479 with an S/N ratio of 4 and 3, respectively, showed the best efficacy so far. Yazh 473 is more potent than MSX-3 as well. This means the simple

Results and Discussion

bond derivatives are more potent and stable than double bond ones. The second conclusion is the superiority of propargyl to propyl as shown in the higher potency of Yazh 473 compared to Yazh 479.

Table 27: The structures, the EC₅₀ values and S/N ratios (efficacy) of the synthesized compounds with an ethenyl linker

Compounds that have an ethenyl linker			
Compound	Structure	EC ₅₀ value ± SEM (μM)*	S/N ratio
Yazh 556		4.34 ± 0.99	2
Yazh 517A		>100	2.5
Yazh 529		>100	1.6
Yazh 466		>10	
Yazh 562		67.3 ± 47.5	2
Yazh 436		>10	
Yazh 552		>100	

Results and Discussion

Yazh 509		>10	2
Yazh 516		>>10	3
Yazh 519		>100	2
Yazh 525		>100	
Yazh 559		8.79 ± 3.57	1.8
Yazh 560		>100	
Yazh 561		>100	
Yazh 562		>100	

*: Results are mean ± SEM of at least three independent β -arrestin experiments

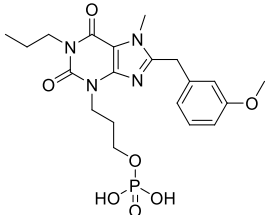
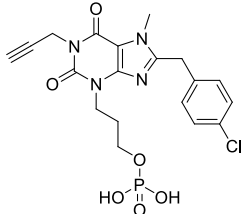
** : S/N ratio not given means no signal induced

Keeping in mind that MSX-3 and JH 14102 belong to this category as well, it is clear again that propargyl is better than propyl (MSX-3 vs. Yazh 466). A methyl at N7 seems to be better than H, since MSX-3 is more active than Yazh 556. The exact EC_{50} value of Yazh 562 was determined since it is the first derivative with an ethyl at N1. The ethyl does not seem to be beneficial but there is no direct

Results and Discussion

comparison since other compounds with propargyl or propyl have a methyl at N7. Intriguingly, Yazh 559 with no phosphate but acetyl residue showed a moderate potency but it should be noted that many compounds have demonstrated variation in results, which necessitated up to seven assays sometimes to get these EC₅₀ values and this fact is reflected in the high SEM.

Table 28: The structures, the EC₅₀ values and S/N ratios (efficacy) of the synthesized compounds with a methylene linker

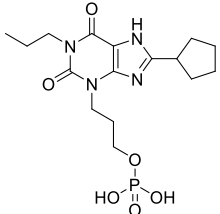
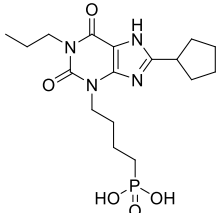
Compounds that have a methylene linker (8-benzyl derivatives)			
Compound	Structure	EC ₅₀ value ± SEM (μM)*	S/N ratio
Yazh 555		>100	
Yazh 564		14.8 ± 3.4	1.8

*: Results are mean ± SEM of at least three independent β-arrestin experiments

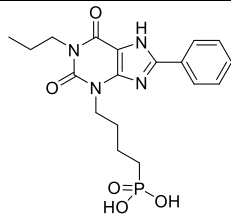
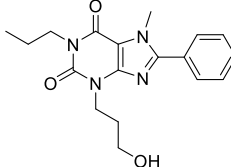
** : S/N ratio not given means no signal induced

Only two 8-benzyl derivatives have been synthesized. Hence, no SAR could be obtained from these derivatives.

Table 29: The structures, the EC₅₀ values and S/N ratios (efficacy) of the synthesized compounds with no linker

Compounds that have no linker			
Compound	Structure	EC ₅₀ value ± SEM (μM)*	S/N ratio
MSX-155		0.351 ± 0.083	1.7
Yazh 499		10.6 ± 1.6	3.5

Results and Discussion

Yazh 496		11.9 ± 2.2	2.5
Yazh 527		Very weak antagonist! Maximal inhibition of 12% at 100 μ M	

*: Results are mean \pm SEM of at least three independent β -arrestin experiments

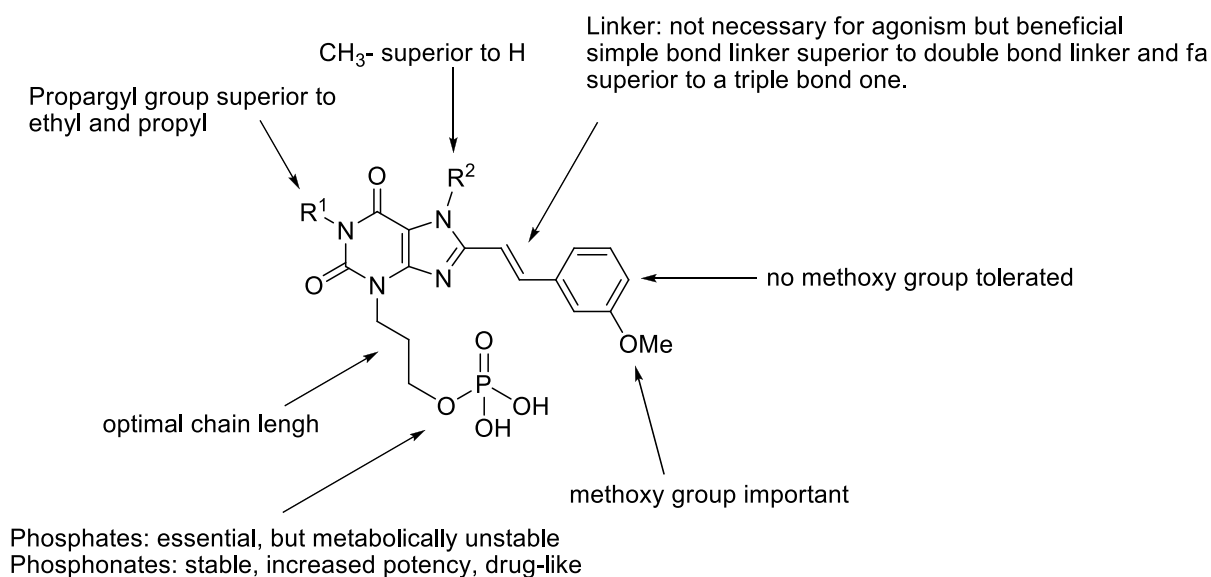
** : S/N ratio not given means no signal induced

Both Yazh 449 and Yazh 496 are phosphonates and they indicate that a cyclopentyl is equally well tolerated as an aryl group if the linker is omitted. Interestingly, Yazh 449 showed a considerably weaker potency than MSX-155; its phosphate analog. This means that the phosphate is necessary for the compounds without a linker whereas phosphonates showed better potency and efficacy when there was linker with a double bond (MSX-3 vs. JH 14102). This could implicate that omitting the linker changes the mode of binding of the ligands to MRGPRX4. This hypothesis and its interesting consequence were confirmed later when conducting calcium mobilization assays in LN229 cell line (see chapter 2.4.12).

In summary, several ligands have been synthesized, but only Yazh 473 and Yazh 479 were significantly potent and efficacious. The elucidated SARs thus far are summarized in figure 44.

SAR of MRGPRX4 agonists

A



B

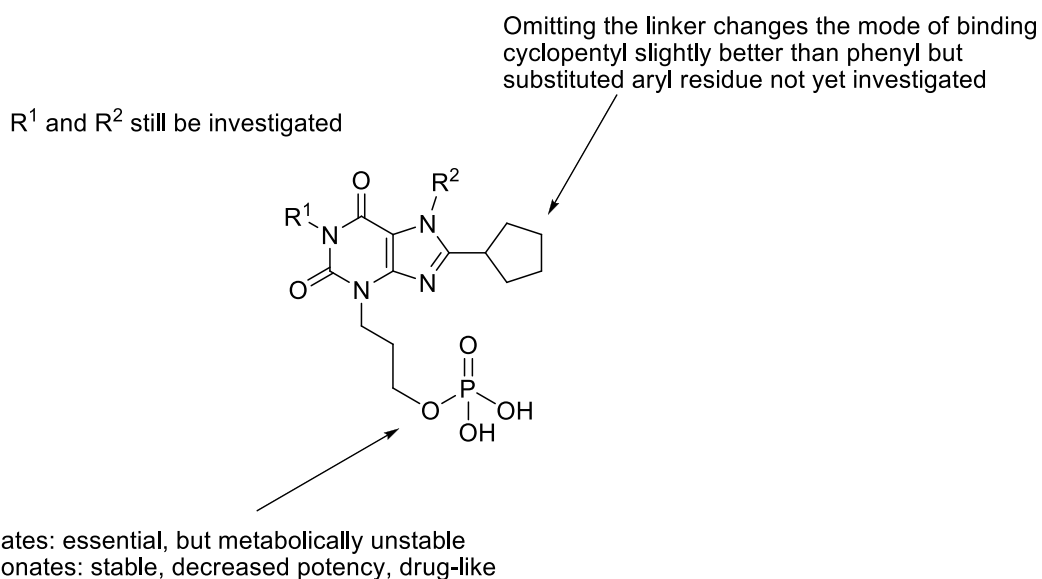


Figure 44: The determined SARs from the available ligands synthesized so far. (A) The structure-activity relationships of the synthesized compounds with a linker (B) The structure-activity relationships of the synthesized compounds without a linker

2.4.11 Adenosine monophosphate: final deorphanization approach

The final deorphanization attempt arose out of the structural properties of the synthetic agonists of MRGPRX4, MSX-3 and MSX-155, discovered by screening. Both of them were designed as selective and potent water-soluble prodrugs at adenosine A_{2A} and adenosine A₁ receptors, respectively. Both

Results and Discussion

of them activated MRGPRX4 receptor with a comparable potency. The negatively charged phosphate appears to be essential for the activity. Both compounds are prodrugs and after hydrolysis they interact with adenosine receptor. Addition of a phosphate to these competitive adenosine receptors ligands produced potent MRGPRX4 ligands. So what would happen if adenosine was phosphorylated? This approach results in AMP. Therefore, AMP was screened at MRGPRX4 initially in the suspension format of the calcium assay at 1 mM. AMP indeed induced a reproducible and selective signal at MRGPRX4 but not at MRGPRX1, MRGPRX2, MRGPRX3 or β -arrestin empty cells (data not shown). AMP is a physiological metabolite that can be degraded by several ectonucleotidases and phosphatases (see chapter 2.4.14). Moreover, calcium mobilization assays are difficult to conduct using CHO cells. Nevertheless, AMP considerably and reproducibly induced a signal at 1 mM, and it was possible to obtain a complete concentration-response curve as shown in figure 45. The determined EC_{50} value was $61.7 \pm 22.7 \mu\text{M}$.

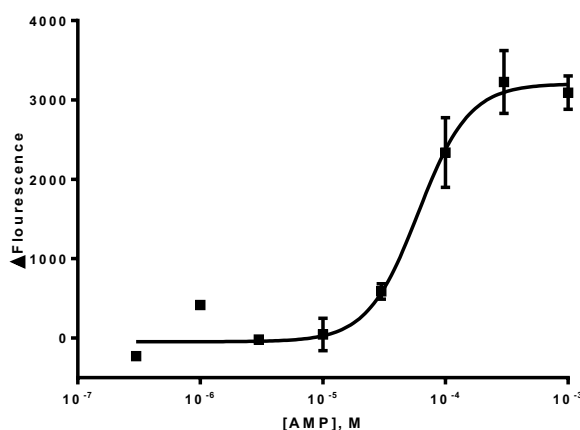


Figure 45: The mean curve of three independent calcium mobilization assays of AMP at MRGPRX4 receptor. The EC_{50} value was $61.7 \pm 22.7 \mu\text{M}$

Testing of AMP using the β -arrestin assay was subsequently attempted. Screening conducted at 1 mM showed, like in the calcium assay, a clear signal (data not shown) but plotting dose-response curves in the β -arrestin assay showed high variability as expected due to the long incubation time of 90 min, which may result in (partial) hydrolysis. The first assays were done using the commercial lysis buffer. The determined EC_{50} value was $19.4 \pm 4.8 \mu\text{M}$ as demonstrated in figure 46.

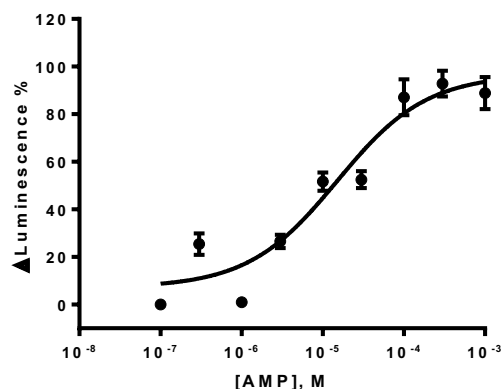


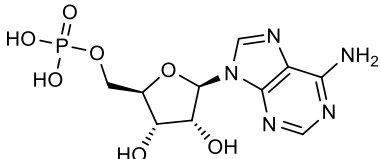
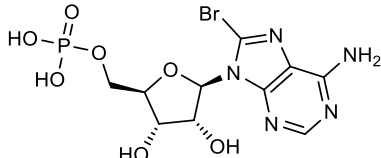
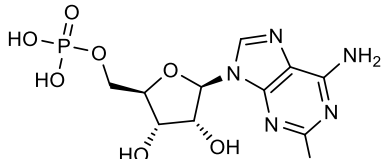
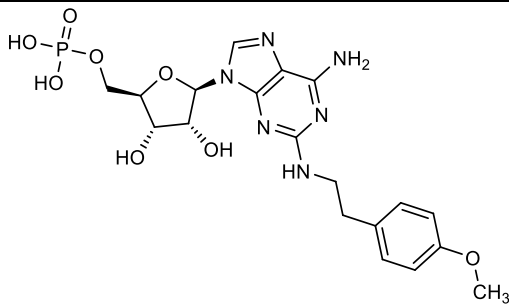
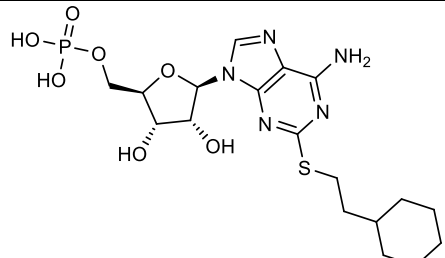
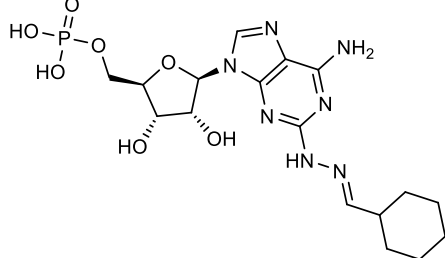
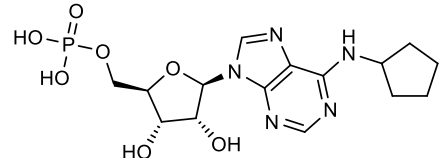
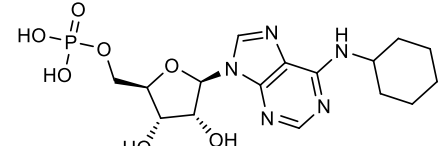
Figure 46: The mean normalized curve of three independent β -arrestin assays of AMP at MRGPRX4. The EC_{50} value was $19.4 \pm 4.8 \mu\text{M}$

It should be noted that incubation in the presence of AMP-CP, ecto-5'-nucleotidase inhibitor, did not have any effect on the results (data not shown). The results indicate a lower EC_{50} value in the β -arrestin assay than in the calcium assay. This is unexpected because the incubation time in the β -arrestin assay is longer. This could indicate that an optimization of calcium assay conditions should be done. The β -arrestin assays were later switched to another protocol, in which the EC_{50} value of AMP was $214 \mu\text{M}$ (see table 30), which is considerably higher. Radioligand binding experiments using [^3H]AMP were tried but were not successful probably due to the low affinity of the radioligand. Moreover, an unspecific binding of [^3H]AMP to the GFB filters was observed (data not shown).

Next we investigated other nucleotides and related compounds. ATP, ADP, cAMP, cGMP, UMP, dAMP and AMP α S were also screened at 1 mM but were not active. GMP showed an increase in signal at 1 mM but a complete curve could not be plotted. Several AMP derivatives were available for screening at MRGPRX4 receptor. All of these derivatives were inactive (no complete curve without extrapolation). However, the induced S/N ratio of 9 at maximal concentration for Ali 909 was exceptionally high (see table 30). This could mean that MRGPRX4 could theoretically be activated to such a high S/N ratio. All these assays were done using the new lysis buffer.

Results and Discussion

Table 30: Structure and EC₅₀ value of some AMP derivatives, which were tested at MRGPRX4 receptor using β-arrestin assay

Compound	Structure	EC ₅₀ value (μM)	S/N ratio at 2mM
AMP		214	1.8
8-Br-AMP		40.9 ± 11.3	2
Ali 901A		> 2 mM	3
Ali 909		> 2 mM	9
CHETP		> 2 mM	2
Ali 900D		> 2 mM	2
Ali 913		> 2 mM	2.5
Ali 916		> 2 mM	2.5

Results and Discussion

The results showed that only 8-Br-AMP (figure 47) is more active than AMP as shown but no SAR analysis can be proposed at present because no systematic ligand synthesis of AMP-derivatives have been conducted yet.

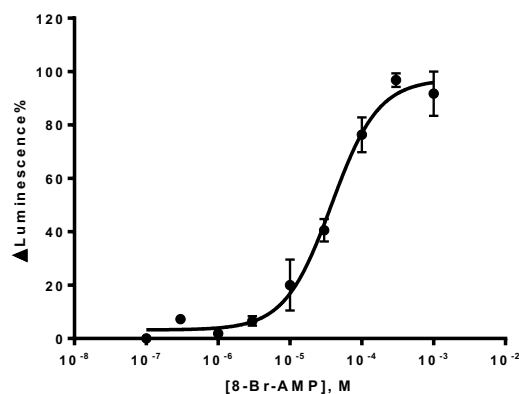


Figure 47: The mean normalized curve of three independent β -arrestin experiments of 8-Br-AMP at MRGPRX4. The EC_{50} value was $40.9 \pm 11.3 \mu\text{M}$

2.4.12 A search for a native cell line expressing MRGPRX4 receptor

The search for a cell line that natively expresses MRGPRX4 went into three directions according to the information found in the literature about MRGPRX4. Sensory neurons, CD8+ lymphocytes and tumor cell lines were investigated

2.4.12.1 Differentiation of stem cells to DRG-like sensory neurons

The expression of all MRGPRX receptors in the sensory neurons was described from the very beginning.^{17,18} In order to investigate this, further collaboration with Prof. Brüstle was initiated. The aim was to differentiate fibroblasts into DRG-like sensory neurons, which express MRGPRX4 on the protein level. This kind of differentiation is not well investigated in the literature, in which only three relevant publications are found.²⁰²⁻²⁰⁴ The protocol of Young et al.²⁰⁴ was mainly adopted in the attempted differentiation. Two different variations were tried, in which all MRGPRX subtypes have been detected on the mRNA level. The first protocol seemed to be more efficient than the second one because the DNA bands are clearer at the same number of qPCR cycles as demonstrated in figure 48. It seems that the expression is restricted in time since the fixation at day 35 did show mRNA of MRGPRX receptors but the fixation at day 46 did not demonstrate an expression of

Results and Discussion

MRGPRX receptors. These initial results are encouraging but further confirmation is required and detection on the protein level should be carried out. It should be noted that these experiments were done by Svetlana Ritzenhofen from the group of Prof. Brüstle.

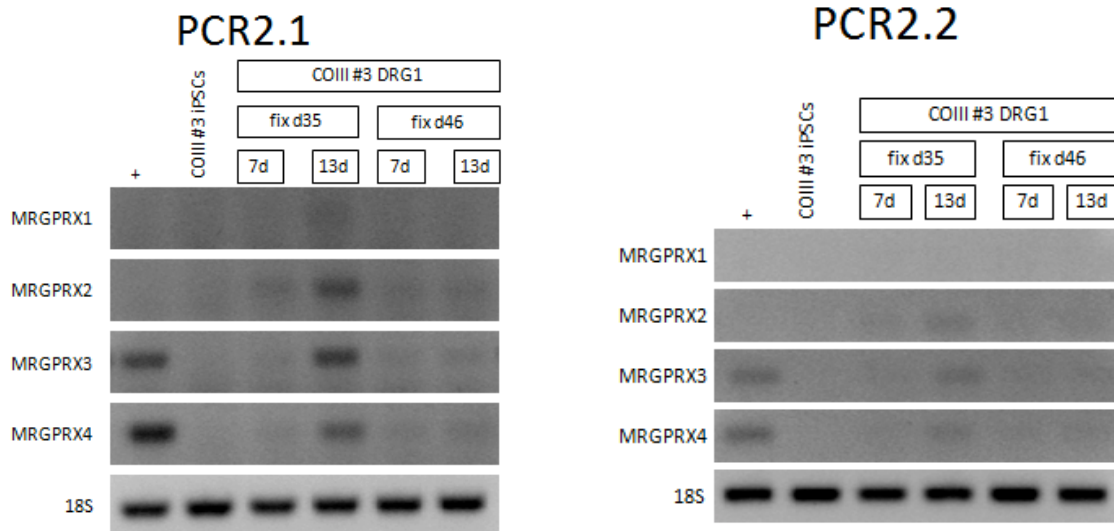


Figure 48: The results of qPCR experiments from two different differentiation protocols with two fixations at day 35 and day 46. The first protocol seems to be more efficient. The qPCR data were thankfully provided by Svetlana Ritzenhofen.

2.4.12.2 Investigating different lymphocytes subpopulations

The second direction was focused on investigating MRGPRX4 in the immune system, especially in CD8+ lymphocytes.¹¹⁴ In order to do this, collaboration with Prof. Nattermann was started. The first step was to confirm the finding that MRGPRX4 is expressed in lymphocytes. This was suggested to be performed by fluorescence-activated cell sorting (FACS), in which a limited number of cells will suffice. FACS is advantageous because these lymphocytes are native cells isolated from blood and Western blotting (WB) would be more material consuming. The problem was the inavailability of a commercial FACS-validated antibody (Ab). Therefore, an immunofluorescence (IF) Ab was employed in the FACS experiments (see chapter 4.6). The initial results using 3 $\mu\text{g}/\text{ml}$ from the Ab showed a small shift (expression) in T-cells (blue), NK cells (green) and B-cells (orange). The expression was in the following order as demonstrated in figure 48: T-cells > NK cells > B-cells. These data in figure 49 are from one patient with hepatitis C virus (HCV) infection.

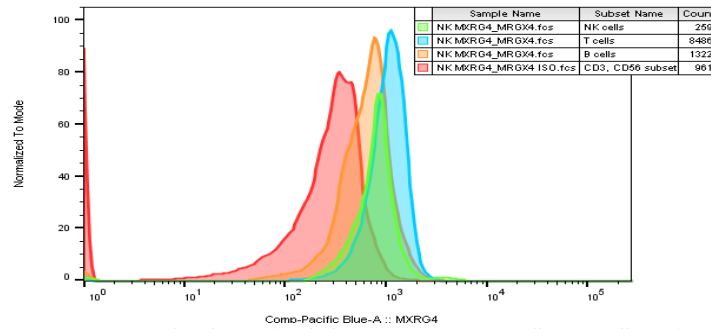


Figure 49: FACS results showed a slight expression in T-cells, NK cells and B-cells

In order to confirm the initial data the peripheral blood mononuclear cells (PBMC) from 8 healthy subjects were investigated via FACS and the results showed that CD56Bright NK cells have the highest expression whereas other lymphocytes subsets (NK, CD4, CD8 and CD 56Dim NK cells) have less expression as demonstrated in figure 50.

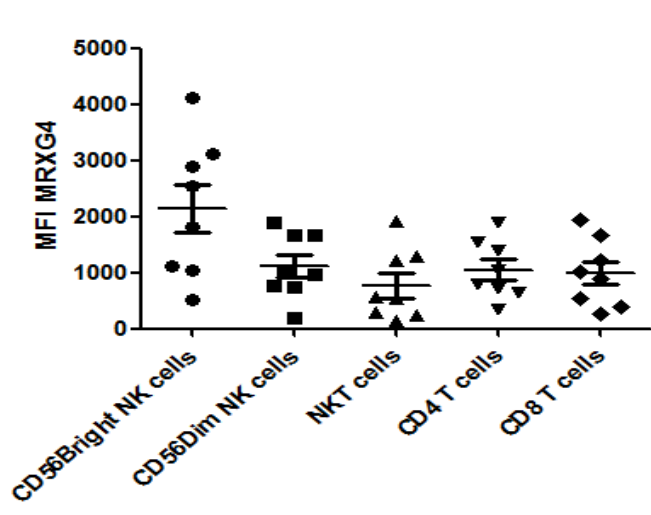


Figure 50: The mean expression of MRGPRX4 receptor in five different subsets of lymphocytes from 8 healthy subjects. The results show an increased expression of MRGPRX4 in CD 56Bright NK cells compared to other subsets of lymphocytes.

These data are highly interesting because they prove that MRGPRX4 may play a role in the immune system and is not exclusively expressed in the DRG as reported in literature. This could lead to the identification of novel roles of this receptor in the immune system. The different expression pattern between the HCV patient and the healthy subjects could also be important but more data should be collected before reaching any conclusion.

2.4.12.3 Investigating different tumor cell lines

The third area of our search was focused on cancer cell lines. The suggestion that MRGPRX4 receptor could function as an oncogene in colorectal cancers¹¹³ was the rationale behind this search. There are many commercially available colorectal cancer cell lines but we have been interested in cancers that are difficult to treat. Several mRNA samples of glioblastoma cell lines were obtained from Prof. Scheffler, Life & Brain (Bonn), and it was decided to investigate the expression of MRGPRX receptors in these cell lines. The Cq values are given in the following table (results in table 31 are from Katharina Sylvester).

Table 31: The results of qPCR experiments performed as n=1 in duplicates. The expression of the 4 MRGPRX members and ecto-5'-nucleotidase

Cell line	MRGPRX1	MRGPRX2	MRGPRX3	MRGPRX4	hNT5E	hGAPDH*	hβ-actin*
LN229	>35	>35	32.19	29.57	27.0	21.19	19.35
T98G	>35	>35	>35	>35	31.6	19.14	18.52
U138	>35	>35	>35	>35	28.65	20.80	17.49
106Z	>35	>35	>35	32.67	28.06	19.56	18.14
46Z	>35	>35	>35	34.68	25.04	19.56	17.36
78Z	>35	>35	34.39	>35	25.04	18.31	17.26

*: hGAPDH and hβ-actin were the positive control

The results show that the LN229 cell line is the most suitable one. However, the expression is pretty low on the mRNA level. It is also notable that this cell line also expresses mrgprX3 at a very low level but not mrgprX1 or mrgprX2.

Fortunately, the group of Prof. Scheffler provided us with an aliquot of the LN229 cell line. This enabled the investigation of MRGPRX4 on the protein level. The previously mentioned Ab against the C-terminus was used. Immunofluorescence experiments in an overexpressing cell line (β-arrestin) and the native LN229 glioma cell line were conducted. The results from the overexpressing cell line indicate that this Ab is able to detect the receptor in a very effective manner. The experiment in the LN229 cell line proved the expression of MRGPRX4 on the protein level and demonstrated a low expression of the receptor in harmony with the mRNA data as shown in figure 51.

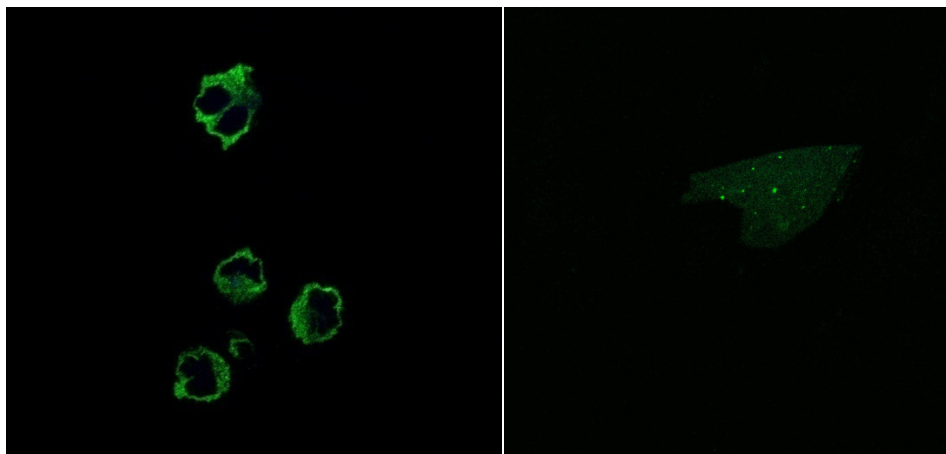


Figure 51: Left, the expression of MRGPRX4 receptor in the β -arrestin cell line. The expression is very high in the cell membrane as expected. Right, the expression of MRGPRX4 in LN229 cell line is low as predicted from the mRNA data.

This finding is important because it represents the identification of an immortalized human cell line with a native expression of MRGPRX4, which can easily be propagated in culture. This is a decisive difference compared to neurons and native lymphocytes.

After proving that LN229 cells are expressing MRGPRX4 natively, it was decided to establish calcium mobilization assay using this cell line. The calcium assay was chosen because the overexpressing cell line showed G_q coupling (see chapter 4.2.9). By the same token, it was decided to begin with the suspension cell protocol because the adherent cell protocol had not shown positive results in the β -arrestin cell line. Yazh 473 (see table 25) was initially used because it had been the agonist with the best efficacy in the β -arrestin assay with an S/N ratio of 4.

The first experiments were conducted with a measurement time of 60 seconds per well. Yazh 473 induced a weak calcium signal but the increase in signal was slow and not always reproducible. Therefore, it was decided to increase the measurement time to 120 seconds per well. In this case the signal of Yazh 473 was still weak but reproducible, whereas PBS as a negative control did not induce any signal. The EC_{50} value was 621 ± 143 nM as shown in figure 52A. In the suspension cell format, AMP and ATP did not show any increase in signal at 1 mM and MSX-3 showed only a minimal increase at 100 μ M and it was not possible to plot a curve.

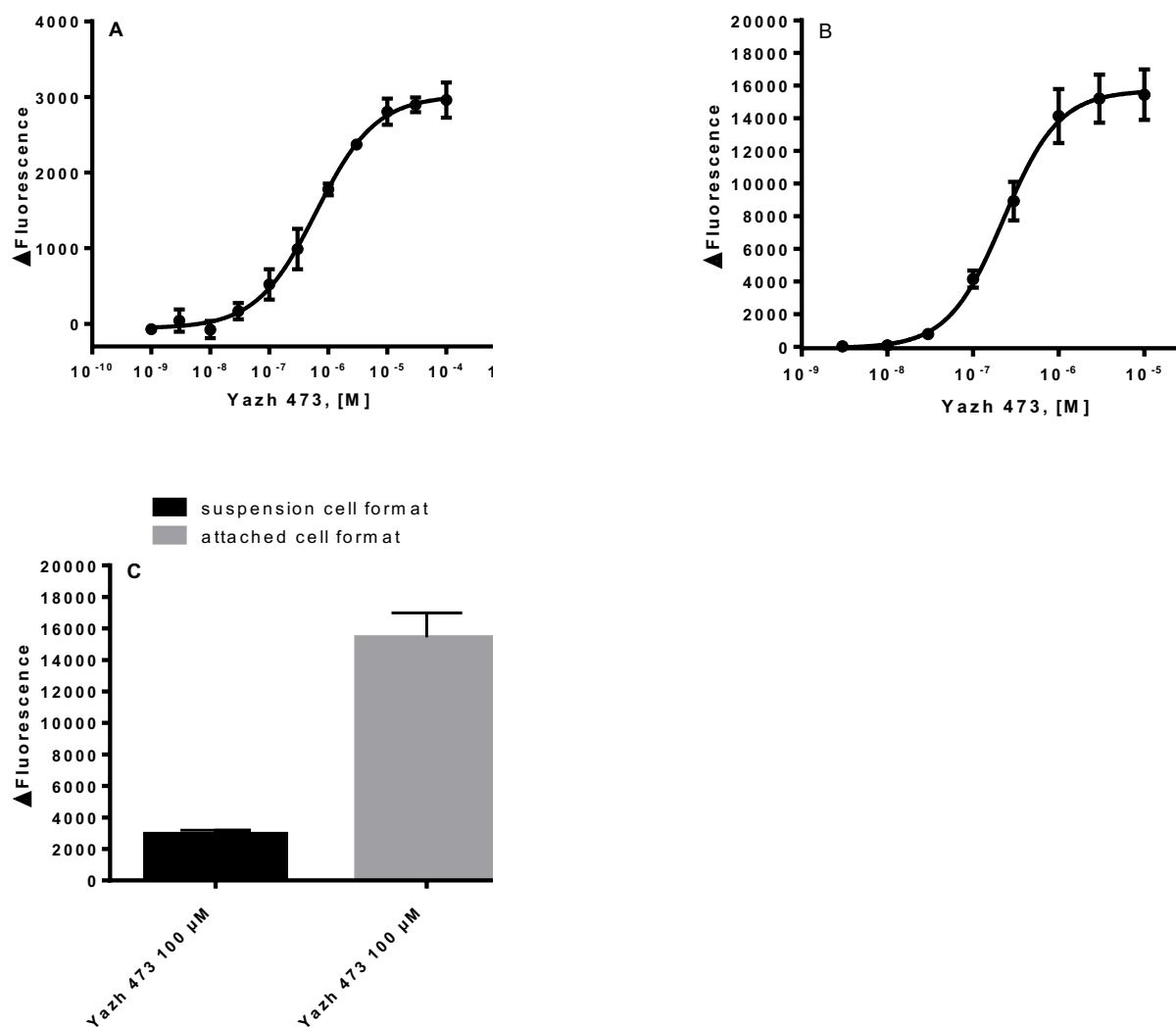


Figure 52: (A) Mean dose-response curve of three calcium assays of Yzh 473 in LN229 cell line using the suspension cell format. The determined EC₅₀ value was 621 ± 143 nM. (B) Mean dose-response curve of three calcium assays of Yzh 473 in LN229 cell line using the attached cell format. The determined EC₅₀ value was 234 ± 13 nM. (C) A comparison of the induced signal of Yzh 473 at 100 μM in both the suspension and attached cell format of the calcium mobilization assay.

The concentration-response curve reflects an MRGPRX4-dependent signaling. However, the ability to conduct a curve only with the most efficacious compound is a big limitation. Therefore, the attached cells protocol was performed in both 60 seconds and 120 seconds formats. Interestingly, there was a robust increase in signal up to 19,000 units, which is comparable or even better than that in the overexpressing cell lines. The 120 seconds per well was initially adopted since the increase in signal continued for more than 60 seconds. Yzh 473 demonstrated more potency and the assay had a better reproducibility in this protocol with an EC₅₀ value of 234 ± 13 nM as shown in figure 52B.

Results and Discussion

It should be noted that some other modification has been adopted to get an optimal signal like the increase in fluo-4 concentration (an aliquot of fluo-4 used for 2 assays only instead of 3 assays) and as a rule of thumb: a confluent 175 cm² flask is enough for 1.5 96-well plates. The time of measurement was later reduced to 80 seconds per well.

After reaching suitable conditions, several compounds were investigated using this new cell line. These compounds have already been characterized via β -arrestin assay and have been shown to be active, including 8-Br-AMP, MSX-3 and MSX-155, but also newly suggested P2X receptor agonist (a locked AMP analog) MRS2339 was also tested.²⁰⁵ All of these compounds were active as shown in figure 53. The EC₅₀ values for MSX-3, MRS2339 and 8-Br-AMP were 460 \pm 13 nM, 257 \pm 28 and 152 \pm 23 μ M, respectively.

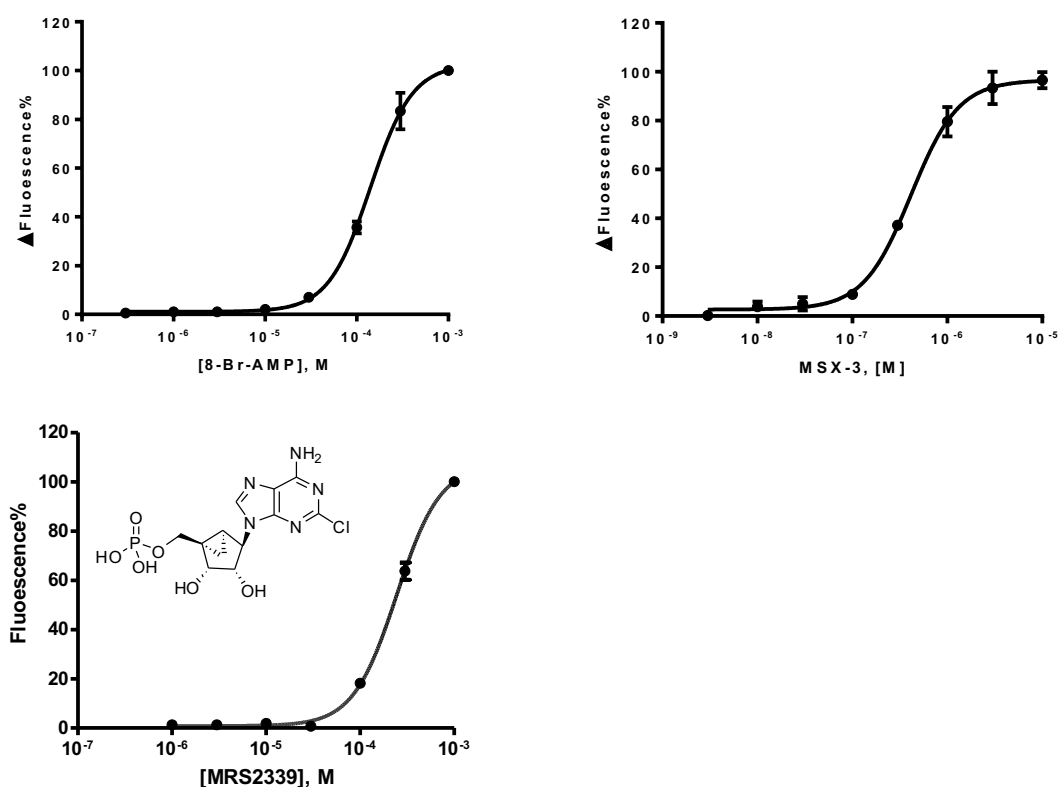


Figure 53: Mean dose-response curves of three calcium assays of 8-Br-AMP, MSX-3 and MRS2339 in LN229 cell line using the attached cell format. The determined EC₅₀ values for 8-Br-AMP, MSX-3 and MRS2339 were 152 \pm 23 μ M, 460 \pm 13 nM, and 257 \pm 28 μ M, respectively.

These results show the same rank order of potency as in β -arrestin assay. The EC₅₀ values are higher than in the β -arrestin assay due to the lower expression levels. In accordance with the β -arrestin

Results and Discussion

results, UMP, GMP, cAMP, cGMP, AMP α S, dAMP and AMP-CP were all inactive at 1 mM (data not shown).

The phosphonate compound JH 14102 showed an unexpectedly high potency and efficacy with an EC₅₀ value of 11.6 \pm 1.3 nM as demonstrated in figure 54. Intriguingly, this value is higher than the potency determined in the overexpressing β -arrestin cell line.

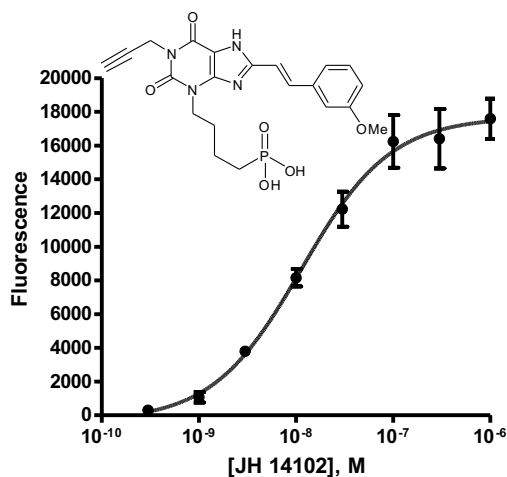


Figure 54: Mean dose-response curves of three calcium assays of JH 14102 in LN229 cell line using the attached cell format. The determined EC₅₀ value was 11.6 \pm 1.3 nM.

The most interesting finding might well be the result of MSX-155 (figure 40), which had an EC₅₀ value of 351 nM in β -arrestin assay. Surprisingly, this compound did not induce any signal in the calcium mobilization assay in three independent experiments and in concentrations up to 100 μ M (see figure 57). The stability of MSX-155 was confirmed and the activity in β -arrestin assay was reproduced (data not shown). This could only be explained by MSX-155 being a biased agonist capable of activating the β -arrestin signaling pathway but not the G_q pathway due to a distinct binding mode to MRGPRX4. The distinct binding mode could be explained by the considerable differences regarding the chemical structure compared to MSX-3. In addition, this explains the previous finding that Yazh 499 (see table 28), the phosphonate analog of MSX-155, is much weaker at MRGPRX4 than MSX-155, whereas the phosphonate analog of MSX-3 (like JH14102) is considerably more potent. The binding mode of MSX-155 requires the oxygen of the phosphate for interacting with the receptor and replacing this oxygen with methine (CH) results in a much weaker interaction (probably loss of an H-bond). Moreover, the MSX-155-induced conformation of the receptor appears not to allow the engagement of the G_q

Results and Discussion

signaling pathway. To the contrary, in the distinct binding mode of MSX-3 the oxygen of the phosphate is apparently not involved in an important interaction with the receptor and replacing it with a carbon (like in JH 14102) results in a more potent compound (may be due to a hydrophobic interaction). The conformational change induced by MSX-3 and JH 14102 leads to the activation of both β -arrestin and G_q signaling pathways.

AMP was also investigated using the LN229 cell line. AMP induced a robust signal at 1 mM but then the signal considerably decreased at 300 μ M and disappeared at further dilutions. Therefore, it was not feasible to plot a concentration-response curve and determine an EC_{50} value for AMP. This could be due to ectonucleotidase/phosphatase activities in this cell line. Ecto-5'-nucleotidase is more highly expressed on the mRNA level in this cell line than MRGPRX4 as shown in table 30. It was tried to use HBSS buffer with 50 μ M final concentration of the Ecto-5'-nucleotidase inhibitor AMP-CP in the assay but this did not have an effect on the signal of AMP in the calcium mobilization assay (data not shown). The active fraction of IL-1 β induced a robust signal at a concentration of 10 μ l/100 μ l. This indicates clearly that the active moiety in the IL-1 β is not the nucleotide, AMP, due to the low concentration in this fraction. ATP (1 mM) induced a signal, whereas adenosine (1 mM) and the non-selective adenosine receptor agonist NECA (100 μ M) did not induce any signal (data not shown). Keeping in mind that native adenosine A_{2B} receptor induce a delayed calcium signal in Jurkat cells²⁰⁶, the lack of adenosine receptor agonism is important because it demonstrates that the observed slow increase in the calcium signal in LN229 cell line could not be an indication that the phosphates were hydrolyzed and the adenosine ligands induced the observed signal (see figure 57). It should also be mentioned that no binding of Yazh 473 was found in radioligand binding experiments at all four subtypes of human adenosine receptors (data not shown). This confirms that the detected signals in LN229 cell experiments are MRGPRX4-dependent.

The susceptibility of MRGPRX1 and MRGPRX2 receptors to sensitization and endocytosis has proven controversial, with some groups suggesting no sensitization^{54,101} and other groups suggesting the opposite.^{55,94} Since these findings have been reported using cell lines with overexpression, we

Results and Discussion

intended to investigate this point using natively expressed MRGPRX4 receptor in LN229 cell line. The cells were preincubated with 200 nM of Yazh 473 for 20, 25 and 30 min and then challenged with 1 μ M Yazh 473 (EC_{80} value). The change in the signal was compared to the signal induced by cell preincubated with PBS. Our results show a time-dependent decrease in signal (sensitization) of MRGPRX4 receptor as shown in figure 55.

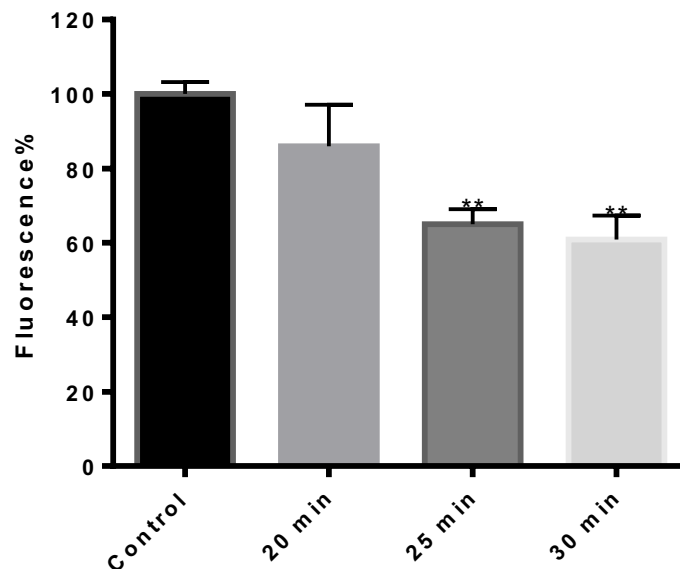


Figure 55: The results of unpaired t-test of the induced calcium assay signals after preincubation with PBS (control) or with 200 nM of Yazh 473 and then challenged with 1 μ M of Yazh 473 after 20, 25, 30 min.

The results showed no significant decrease in signal after 20 min of preincubation but the decrease was significant after 25 and 30 min of preincubation. Thus our data suggest that MRGPRX4 receptor is susceptible to endocytosis and sensitization, and this process is slow.

Another aspect which was observed during calcium mobilization assays was the ability of Yazh 473 to induce a prolonged increase in the signal as shown in figure 56. The signal of Yazh 473 tended to decrease with considerably more delay compared to other agonists at MRGPRX4 receptor like MSX-3. This prolonged duration of signal and the higher efficacy (also in the case of β -arrestin signal) could be an indication that Yazh 473 has a longer residence time at MRGPRX4 receptor than MSX-3.²⁰⁷

Results and Discussion

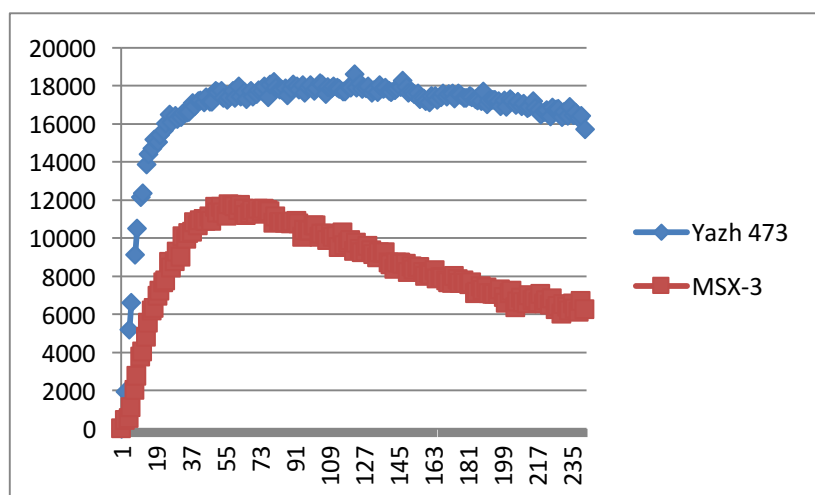


Figure 56: The profiles of real-time changes in the calcium mobilization signal induced by 10 μ M Yazh 473, a derivative with an ethylene linker, and 10 μ M MSX-3, a derivative with ethenyl linker. Yazh 473 showed an EC_{50} value of 234 ± 13 nM, while MSX-3 showed an EC_{50} value of 460 ± 13 nM. The duration of measurement was two minutes and the maximal signal was reached after 10 seconds.

This observation led us to shorten the measurement time to 80 sec per well as mentioned above.

Figure 57 shows the fluorescence tracks of the most important agonists at MRGPRX4 in calcium assays using the LN229 cell line.

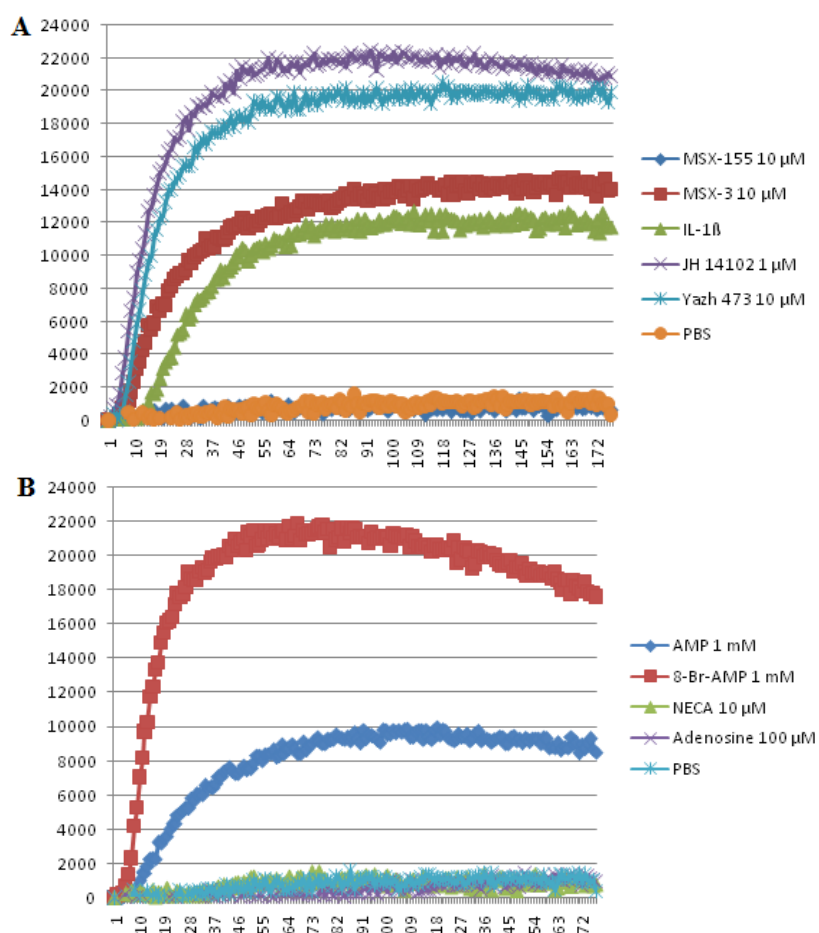


Figure 57: The fluorescence tracks of the most important agonists at MRGPRX4. (A) The most important synthetic agonists (B) AMP, 8-Br-AMP, adenosine and NECA as a potent non-selective AR agonist.

All in all, these results show the importance of the LN229 cell line as a tool to investigate MRGPRX4 in a native setting.

2.4.13 Screening of compound libraries in search for antagonists at MRGPRX4 receptor

The next step in investigating MRGPRX4 was to screen compound libraries with the goal to identify an antagonist. The compound libraries 1, 2, 7 and 12 were screened using β -arrestin assay. Interestingly, several hits have been identified in our search, which indicates that finding an antagonist will be easier than finding an agonist. In the compound library 7 the non-steroidal anti-inflammatory drug oxyphenbutazone was identified^{208,209}; in the compound library 2 KD162 and KD165 were identified; in the compound library 1, the serotonin receptor antagonist and β_3 -adrenoceptor partial agonist (*S*)-(-)-Pindolol^{210,211}, the β_3 -adrenoceptor partial agonist BRL 37344²¹², the NMDA receptor antagonist SDZ 220-040²¹³, the competitive c-Jun kinase inhibitor BI 78D3²¹⁴ and the protein kinase C suppressor Oncrasin 1²¹⁵ were identified (for structures see figure 58).

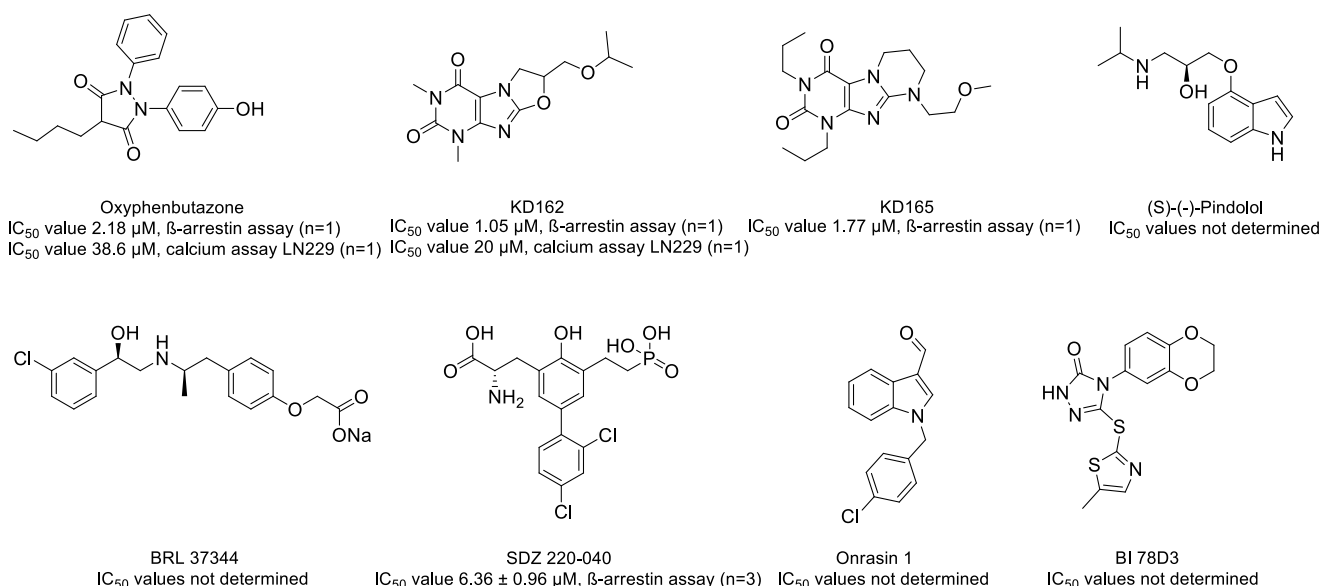


Figure 58: Chemical structure of the antagonistic hits at MRGPRX4 receptor identified using β -arrestin assay

Results and Discussion

Some of these antagonists were further investigated. Oxyphenbutazone showed an IC_{50} value of 2.18 μ M in β -arrestin assays; KD162 and KD165 demonstrated IC_{50} values of 1.05 and 1.77 μ M, respectively (all IC_{50} values, $n=1$).

Utilizing the LN229 cell line, it was possible to confirm the antagonistic activity of oxyphenbutazone, KD165, (*S*)-(-)-Pindolol and SDZ 220-040 in calcium mobilization assay. Oxyphenbutazone showed an IC_{50} value of 38.6 μ M, KD165 demonstrated an IC_{50} value of 20 μ M. SDZ 220-040 was the best investigated antagonist at MRGPRX4 receptor in calcium mobilization assay with an IC_{50} value of 6.36 ± 0.96 μ M as shown in figure 59.

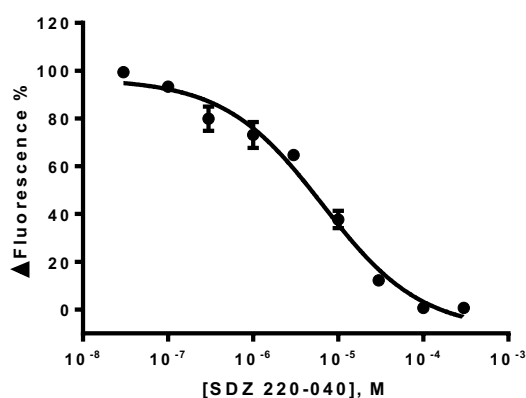


Figure 59: Mean dose-response curve of three calcium mobilization assays of SDZ 220-040 in the LN229 cell line

Although these results are encouraging, it should be stressed that those are preliminary results and should be further investigated and confirmed. Pindolol for instance seems to be active but there was no opportunity to further investigate this drug. These antagonists seem to be selective because they have already been screened at the related MRGPRX1 and MRGPRX2 and showed no activity (see above). In addition, screening at GPR143 in the same testing system showed also no antagonistic activity (data not shown).

2.4.14 Discussion II

After the different unsuccessful deorphanization and screening attempts, a second screening approach led to the identification MSX-3 as an agonist at MRGPRX4. This prodrug at the A_{2A} adenosine receptor¹⁹⁷ is a relatively potent MRGPRX4 agonist with an EC_{50} of 175 nM. This enabled

Results and Discussion

us to test related compounds to investigate the activation of the MRGPRX4 receptor. The most important finding was that a phosphate or phosphonate is essential for potency. Investigating the linker of MSX-3 revealed that the higher the rigidity of the linker, the lower were both potency and efficacy. Thus the 8-ethinylxanthine derivative JH 14021 was virtually inactive and the 8-styrylxanthine derivative MSX-3 was considerably more potent. Moreover, the 8-phenethylxanthine derivative Yazh 473 was the most potent and efficacious phosphate derivative so far. These observations are tempting to suggest that Yazh 473, due to the linker with an ethylene bond, can rotate freely and bind with the highest affinity in the binding pocket of the receptor. MSX-3 can only form E/Z isomers and this limited flexibility is responsible for the lower potency and efficacy compared to Yazh 473. JH 14021 with the rigid triple bond has the least ability to fit into the binding pocket of MRGPRX4 and consequently the lowest potency and efficacy. This SAR is particularly important because it distinguishes MRGPRX4 receptor from the A_{2A} receptor, for which both the double and triple bond seem to have comparably high potency.^{198,199} MSX-155 was also identified as an agonist with an EC₅₀ value of 351 nM. This was highly unexpected based on the SARs of other agonists since the linker is omitted and the aryl at position 8 is substituted by a cyclopentyl ring. MSX-155 provides a clue that activating MRGPRX4 is feasible without a linker and an indication of possibly distinct interactions with the amino acids of the receptors. In fact, MSX-155 is a prodrug of DPCPX, a potent A₁ adenosine receptor antagonist. DPCPX can also bind to A_{2A} adenosine receptor but with much lower affinity.^{200,216} The ability of these prodrugs to bind to MRGPRX4 could be of interest for a future mutagenesis experiments for defining the binding pocket of this receptor. Phylogenetically MRGPRX4 is more related to the P2Y₁₂ receptor since both are in the δ group of the *Rhodopsin* receptor family of the 7TMR tree^{2,4} but for identifying the binding pocket not only the P2Y₁₂ X-ray structure but also those of adenosine A_{2A} and possibly the A₁ receptor could be used as a template despite a lower relatedness. The rationale is the ability of MSX-2 and DPCPX to bind to A_{2A} and not P2Y₁₂ receptor. Several crystal structures of both, P2Y₁₂ and A_{2A} adenosine receptors have been previously published.²¹⁷⁻²²¹

Results and Discussion

However, the identified phosphoric acid esters may show enzymatic instability. Phosphonates seem to represent a stable alternative to the phosphates. Thus far only few phosphonates have been synthesized due to the challenging synthesis and purification. The phosphonate JH 14102 exhibited the best potency at MRGPRX4 in both β -arrestin and calcium assay thus far. It represents a valuable tool in investigating this orphan receptor. A future phosphonate analog of Yazh 473 would be very interesting. Unfortunately, such an analog could not be synthesized within the timeframe of this thesis. Taking the determined SAR so far into consideration, it would be appealing to assume that such a ligand could be a radioligand candidate. Since establishing a radioligand is a future aim, some points should be kept in mind. The increase of EC_{50} value of JH 14102 in β -arrestin assay from 17.4 to 76.1 nM upon changing the lysis buffer demonstrates the difficulty in deciding which value is a more accurate estimation of a K_i value. In addition, synthesis of more derivatives could also be a way to find more potent compounds as radioligand candidates. For example the substitution of the aryl at position 8 of the xanthine ring was not investigated thoroughly. An allyl group instead of a propargyl residue at N1 could also be an option.

The agonists were utilized to reveal the G protein coupling of MRGPRX4, which turned out to be sole coupling to G_q . The ligands neither induced nor inhibited cAMP accumulation. It should be noted that the effect of pertussis toxin on the calcium signal has not been tested, which could be a further confirmation of the sole G_q coupling. Further optimization of the calcium mobilization assay is urgently needed in the future. The overexpressing CHO β -arrestin cell line was not an optimal cell line for conducting calcium assays because the induced signal was weak and not easily reproducible. Therefore, generating a new cell line, e.g HEK cells overexpressing MRGPRX4, could result in more reproducible and robust calcium mobilization assay signals.

Since the only DRG neuronal immortalized cell line is from the rat²²², our aim to identify a cell line natively expressing MRGPRX4 led us to three approaches. The first one was to differentiate iPSC (induced pluripotent stem cells) into DRG-like sensory neurons. The results in this phase show that two differentiation protocols were able to induce the expression of the four MRGPRX receptors on

Results and Discussion

the mRNA level. The findings are encouraging but further investigations are necessary to detect the MRGPRX receptors on the protein level. This could be done using Ab for an IF or WB approach. Further steps could be investigating the functionality of the receptors using a neuron calcium imaging method.²²³ Further more complicated steps could be fusing the DRG-like neurons with neuroblastoma cells in order to establish an immortalized cell line in a similar way to establishing the F11 cell line from rat DRG neurons.²²⁴ This would enable even more sophisticated procedures like a co-culture for investigating communication between different kind of cells like those of the immune system and neurons. Such an approach has already been described for rat DRG neurons and human keratinocytes.²²⁵

The second search for a native expression of MRGPRX4 was carried out in the immune system, more precisely in the different lymphocyte subpopulations. The search was based on FACS (i.e on protein level) via a new Ab against the C-terminus of MRGPRX4 receptor. Initially, it was expected to detect an expression in CD8+ lymphocytes as described previously.¹¹⁴ Our preliminary data suggest that MRGPRX4 is represented in all different lymphocytes subpopulations with a higher expression in CD56Bright NK cells. The reason behind the expanded expression detected in our approach could be due to the use of an affinity based method for detection of 7TMRs. This is more sensitive than the mass spectrometry method used in by Kim et al.¹¹⁴ because 7TMRs possess a poor solubility and are difficult to detect in mass spectrometry.²²⁶ NK cells represent ca. 10% of blood lymphocytes. These cells could be subdivided into two subpopulations based on the density of CD56 marker (bright vs. dim) and presence or absence of CD16.²²⁷ CD56Bright NK cells are a minority of NK cells in blood (10%) but a majority in secondary lymphoid tissues. CD56Bright NK cells are abundant cytokine producers but exhibit a weak cytotoxicity.²²⁸ The wide expression could be a manifestation of unknown roles of the MRGPRX4 in the immune system, which have yet to be characterized. Our novel pharmacological tools would enable future investigation of possible roles of MRGPRX4 in the different cell types. The expression in other immune cells like macrophages, mast cells and dendritic cells could be interrogated in the future as well. In general, cytokine production and activation

Results and Discussion

markers should be investigated before being able to put forward any hypothesis regarding a role of MRGPRX4 in the immune system. Another perspective for a potential physiological role could be a change in the expression pattern of MRGPRX4 in immune cells in health and disease (e.g. HIV or HCV).

Tumor cell lines were our last area for searching a cell line with native expression. The motive behind this search was the finding that MRGPRX4 was proposed as a candidate oncogene in colorectal cancer.¹¹³ This is apparently a vast area for searching since more than 35 human colorectal tumor cell lines are commercially available according to the ATCC® database. In addition, the search could theoretically include all human tumor cell lines. That could be very time-consuming and expensive. Luckily, the glioblastoma cell line LN229 was already available and upon investigation it showed positive results both on mRNA and protein level. The LN229 cell line is usually used to study apoptosis.²²⁹

The most interesting aspect in this cell line was the excellent calcium mobilization assay signal regarding reproducibility and amplitude. The reason behind this exceptional signal despite the low expression (see figure 50) was not clear but could be due to an efficient coupling to G protein²³⁰ in this cell line or because of a higher expression of G_q protein and a better signal amplification. The implication is that LN229 is a novel tool for MRGPRX4 investigation. Capitalizing on this new cell line it was possible to demonstrate clearly that MRGPRX4 is subject to sensitization and endocytosis. But here it should be noted that showing the endocytosis using an Ab would be a good confirmation as well. It was also feasible to show that MSX-155 is a biased agonist towards β -arrestin signaling and completely lacks G_q protein signaling. The lack of G protein coupling implicates a distinct binding mode to MRGPRX4 as well as a different induced conformation of the receptor compared to the conformation induced by MSX-3 and related compounds. The different binding mode can, in turn, shed light on SAR and explain the decreased potency of the phosphonate analog of MSX-155 (Yazh 499) despite the increased potency of the phosphonate analog of MSX-3 (JH 14102). All these insights provide an evidence of the importance of the LN229 cell line. In the future a further

Results and Discussion

confirmation using ERK1/2 phosphorylation assays could provide more insights into the downstream signaling of these ligands. MSX-155 should actually function as an antagonist in calcium mobilization assays since it does not cause a calcium signal but evidently binds to the receptor because of the β -arrestin signal. The signal bias could have important implications like eliminating a side-effect. Activating the β -arrestin signal of the opioid receptors for instance results in respiratory depression. Hence, a biased opioid agonist towards the G protein signaling could be advantageous.^{231,232} On the other hand, the biased angiotensin ligand TRV 120027 blocks G protein coupling but activates β -arrestin pathway-bound benefits like the increase in cardiac performance.²³³⁻²³⁵ A further possibility is to investigate if MRGPRX4 is a real oncogene as suggested by Gylfe et al. and to investigate possible mutations like the proposed Ser114Arg and Ala115Thr¹¹³ mutations (both at the end of TM3 according to uniprot.org) and a potential role of such mutations in increasing their signaling that would explain the exceptionally efficient G_q coupling observed in the calcium mobilization assay. Proliferation assays could be a good starting point.

Taken together, all three approaches to identify a native cell line expressing MRGPRX4 are promising and have led to positive results, but more efforts are still needed and many questions are yet to be answered.

The search for antagonists was initiated and some preliminary results have been obtained. It was interesting to find several hits, although not all available compound libraries have been screened yet. This is an advantage because several scaffolds could be obtained and more room for chemical synthesis would be available. These antagonists should be investigated by plotting concentration-response curves in both β -arrestin and calcium mobilization assay. MSX-155 should be investigated as an antagonist in calcium assay only, as mentioned previously. The most interesting antagonists for now are oxyphenbutazone, KD165, (S)-(-)-Pindolol and SDZ 220-040. According to Gaucher et al.²⁰⁹ oxyphenbutazone reaches as high as 0.75 $\mu\text{g/ml}$ in CSF i.e 2.31 μM , which is higher than the EC_{50} value in the overexpressing β -arrestin cell line of 2.18 μM but considerably lower than 38.6 μM , the EC_{50} value of calcium assay in LN229 cell line. These findings are interesting because

Results and Discussion

oxyphenbutazone is an analgesic and anti-inflammatory drug. However, this high concentration in CSF should be critically judged. All in all, it is tempting to suggest that finding and optimizing an antagonist is possible but more efforts should be done in this direction in the future.

The SAR of our new agonists led us to a fourth and last deorphanization attempt of the MRGPRX4 receptor. The suggested physiological ligand is adenosine monophosphate (AMP) because it represents all characteristics necessary to activate MRGPRX4 (adenosine plus phosphate) as discussed previously (see chapter 4.2.11). The nature of the agonist as a nucleotide is distant from the originally assumed peptide as in the second and third deorphanization approaches and closer to the first deorphanization attempt with adenine. That means MRGPRX1 and MRGPRX2 have evolved to be peptide receptors while MRGPRX4 evolved to bind a nucleotide. An explanation could be the pronounced positive selection in the extracellular loops of MRGPRX receptors that has been previously reported.²¹ In fact, members of MRGPR receptor family have been described as sequence related 7TMR with structurally dissimilar ligands.¹²² Nevertheless, proving AMP as a physiological ligand is a very formidable task for several reasons. AMP has already been screened at MRGPRX4 receptor by DiscoverX® in their deorphanization campaign and failed to be identified as a hit.⁹⁵ No precise concentration, at which AMP was screened, has been given but the inability to detect AMP as an agonist could have been due to the low concentration used (usually 1 or 10 μM), which results in an S/N ratio below 1.4 (to be considered as a hit). To make matters worse, there have been two previous deorphanizations in the literature proposing AMP as a physiological ligand. GPR99 was suggested to be a novel nucleotide receptor, suggested to be renamed to P2Y₁₅, which could be activated by both, adenosine and AMP. [³²P]AMP was shown to bind GPR99 with a K_d value of 18.8 μM .²³⁶ This deorphanization was discredited and α -ketoglutarate was subsequently shown to be the native ligand.²³⁷⁻²³⁹ In 2012 AMP was suggested to activate A₁ adenosine receptors.²⁴⁰ This deorphanization has not been discounted in a publication but results from our lab indicate no binding of AMP to A₁ adenosine receptor (data not shown). Although AMP was reported to have physiological effects,²⁴¹⁻²⁴⁴ it is mainly through its degradation to adenosine or to its conversion to

Results and Discussion

ADP or ATP, all of which have their defined 7TMRs.^{245,246} The metabolism of extracellular AMP to adenosine is physiologically regulated by different ecto-phosphohydrolases like ecto-5'-nucleotidase (NT5E), prostatic acid phosphatases and more than one type of alkaline phosphatases.^{247,248} The pattern of expression of these enzymes in different tissues and cells represents a further complexity for determining a role for AMP. Among the AMP-degrading phosphatases, NT5E is the best investigated one and the rate-limiting enzyme in generating extracellular adenosine. NT5E has a K_m value in the lower micromolar range.²⁴⁷ NT5E is upregulated by IL-1 β , TNF- α and downregulated by INF- γ and IL-4.^{249,250} Therefore, it would be useful to look at its expression in the DRG, immune system and tumor cells (the three areas natively expressing MRGPRX4 that were found in this thesis). In the DRG it was found that the small diameter neurons (peptidergic and non-peptidergic) express NT5E and that this enzyme is responsible for regulating AMP in nociceptive circuits and thus inhibiting pain by producing adenosine.^{251,252} In the immune system, NT5E is a known maturation marker of T and B cells and has also been found in many other immune cells.^{114,247,253} Interestingly, the expression of this enzyme in CD56bright NK cells has recently been described. The role of CD56bright cells as cytokine releasers has already been reported but there are indications that these cells play a regulatory role in the immune system. Morandi et al. proposed this regulatory role (inducing proliferation of CD4+ T-cells) to be mediated via adenosine receptors. To address this hypothesis, the expression of NT5E and its ability to efficiently degrade AMP to adenosine was demonstrated in these cells in contrary to CD56dim cells. Moreover, patients with juvenile idiopathic arthritis showed CD56bright NK cells with a reduced NT5E activity and adenosine production in the synovial fluid.²⁵⁴ Chatterjee et al. proposed that the percentage of NT5E-expressing NK cells is low (ca. 1%) but upon contact with mesenchymal stem cells the NT5E-expressing NK cells increased to 10% and the ability to degrade AMP increased as well. Therefore, a subpopulation of NK cells acquire NT5E and the ability to convert AMP to adenosine upon contact with mesenchymal stem cells. Characterization of this subpopulation (bright or dim) has not been performed.²⁵⁵

Results and Discussion

Tumor cells and their expression of NT5E were thoroughly investigated. NT5E demonstrated an overexpression in bladder cancer,²⁵⁶ leukemia,²⁵⁷ melanoma,²⁵⁸ ovarian cancer,²⁵⁹ thyroid cancer,²⁶⁰ esophageal cancer,²⁶¹ prostate and breast cancer²⁶² and glioblastoma (LN229 for instance) cancer.²⁶³ NT5E is associated with poor prognosis for ovarian and glioma cancers.^{264,265} The catabolism of AMP in glioma cell lines showed a pronounced efficiency via NT5E.²⁶⁶ All these findings indicate that MRGPRX4 is probably co-expressed with NT5E. Our results as well showed higher expression of NT5E in LN229 cell line than MRGPRX4 receptor on the mRNA level (see table 30). Our data together with the published data prove on one side that MRGPRX4 is expressed at the same sites where AMP and NT5E are available and on the other side this co-expression may explain the weak signal of AMP in the LN229 cell line. Nevertheless, the co-expression and the reported AMP degradation could be an indication of preferred adenosine signaling and not MRGPRX4 signaling on these cancer cells. In this regard it is interesting to further investigate MRGPRX4 in NK cells since these cells seem not to have a basal expression of NT5E, which could mean that under some conditions AMP could accumulate and activate MRGPRX4 and upon inducing NT5E MRGPRX4 signaling would dwindle.

The International Union of Basic and Clinical Pharmacology (IUPHAR) published recently recommendations for deorphanizing a 7TMR. The deorphanization should ideally include a radioligand binding assay plus functional assays, both *in vitro* and in native tissues. The putative ligand should be present in the tissues in appropriate concentration. Further evidence could be from anatomical level, and plausible mechanisms for ligand to reach physiological concentrations in the tissues. Deleting the gene encoding the receptor in mice, exploiting a naturally occurring deletion in human tissues, or RNA silencing should abolish receptor characteristics, such as radioligand binding or physiologic and/or pharmacological actions of the endogenous ligand in functional assays. Conversely, receptor overexpression may be expected to potentiate these actions.²⁶⁷ Since AMP as a radioligand did not work due to its too low affinity (see chapter 2.4.11), it is possible to show binding using another potent ligand. We have performed two functional assays in an artificial system that showed the activity of AMP. The determined EC₅₀ value was in the micromolar range. The actual

Results and Discussion

concentration of AMP in the DRG, the microenvironment of tumor or on the surface of NK cells in secondary lymphoid tissues is difficult to measure. In the literature, AMP in the plasma was reported to be between 1.3 to 0.6 μM .^{268,269} The concentration of AMP in the CSF according to Eells et al. is < 0.2 μM .²⁷⁰ The CSF metabolome database (www.csfmetbolome.ca) provides useful information about metabolites in the CSF. In this database, more or less the same values for AMP in plasma and CSF are reported.²⁷¹ Rodríguez-Núñez et al. estimated the AMP concentration to be as high as 1.86 ± 1.11 mM in CSF of children suffering from sepsis. This value seems to be too high.²⁷² Most reported concentrations are lower than our determined EC_{50} values but they do not represent the local AMP concentration at the site of action. Another point is the inability to perform calcium mobilization assays using AMP in the native LN229 cell line because the signal was detected only at 1 mM. These are formidable barriers for a deorphanization proposing AMP as a cognate ligand. Nevertheless, our deorphanization proposal could be substantiated. The first step is to develop a radioligand and to demonstrate a specific binding of AMP at MRGPRX4 receptors. The phosphonate analog of Yasz 473 could be a suitable candidate. The second step is to synthesize a non-hydrolysable phosphonate analog of AMP, for which the EC_{50} should be determinable. Such a compound can be a plausible argument. For now 8-Br-AMP seems to be the most potent AMP-derivative. It would be plausible to systematically synthesize such derivatives with small modifications of AMP, in a similar way to the adenine derivatives,²⁷³ because they would probably not be degraded as efficiently as the physiological AMP. The third step is to find a physiological function for native MRGPRX4 which could be induced by AMP or a very similar derivative of AMP and then to demonstrate that this function could be abolished via a selective antagonist (unfortunately till now we do not have one) or via siRNA. Lymphocytes could be candidates for a physiological function like increasing the release of cytokines, and LN229 cells could also be candidates for proliferation assays or inducing apoptosis. DRG-like neurons would probably be more difficult to handle. Moreover, generating an MRGPRX4 overexpressing cell line for calcium mobilization assays should be carried out in order to get a better reproducibility, and HEK cells could be a suitable G_q -expressing cell line.

3. Summary and Outlook

The human MRGPRX receptors belong to the orphan 7TMRs within the *Rhodopsin* family of 7TMRs. The MRGPRX receptor subfamily is exclusively expressed in primates, which represents a hurdle for elucidating the (patho)physiological roles of these receptors. In this PhD thesis the four human MRGPRX receptors were pharmacologically investigated. The primary assay employed in this study was the β -arrestin assay using β -galactosidase complementation due to its high specificity for the expressed receptor. Additional assays like calcium mobilization and cAMP accumulation were also employed.

MRGPRX1 is the best investigated member of the MRGPRX subfamily of 7TMRs. Our efforts were focused on screening several compound libraries in order to identify new antagonists for this receptor subtype. Only one compound, MIRA-1, was found to have an antagonistic activity at MRGPRX1 in the performed β -arrestin assays. However, the chemical structure (unstable ester) and the steep concentration-response curve made us refrain from further investigation of this hit compound. Screening of further compound libraries should be performed in the future to identify ligands that are more suitable for drug development.

MRGPRX2 was paired to the peptide agonist CST-14, but several other agonists have been described in the literature. However, no antagonists have been described so far. In our screening approach for antagonists using the β -arrestin assay several hits were identified, e.g. vitamin K₃ (menadione) from compound library 7. One hit from compound library 3, designated CB8, with a tricyclic benzimidazole scaffold showed an IC₅₀ value of 2.42 μ M. It was decided to develop this hit further. Our efforts led to an establishment of SARs and to successive optimization of the parent compound. The best antagonist so far (CD63) exhibited an IC₅₀ value of 6.38 nM as shown in figure 60. The mode of action of these antagonists was determined to be competitive versus CST-14. In addition, initial pharmacokinetic data of the best three antagonists were determined. Lastly, the recently proposed functional ortholog of MRGPRX2 receptor, the mouse MRGPRB2 receptor, was cloned and a β -

Summary and Outlook

arrestin cell line was established. The aim was to test our novel antagonists at the mouse receptor as well. This could not be carried out so far due to the low potency of the agonist CST-14 at the mouse receptor in the β -arrestin assay.

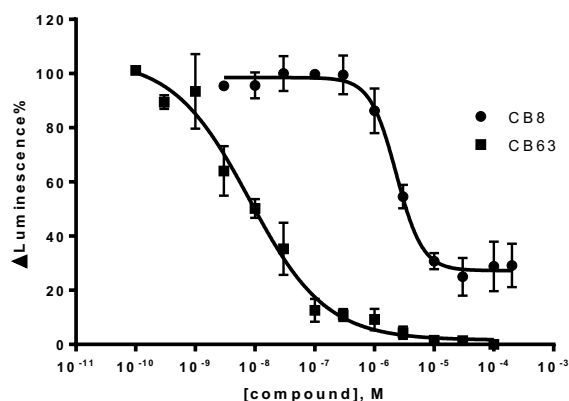


Figure 60: The curve of CB8, the first hit found at MRGPRX2 receptor, with an IC_{50} value of 2.42 μ M and CB6, the most potent antagonist so far, with an IC_{50} value of 6.38 nM. Both curves are from three independent β -arrestin assays

Our results provide valuable tools for investigating the MRGPRX2 receptor. CB63 is a good candidate for developing a radioligand or obtaining a co-crystal structure of MRGPRX2 due to its high potency. Given the newly elucidated role of this receptor in chronic urticaria and pseudoallergic reactions, our antagonists may contribute as tool compounds to expand the research and deepen the understanding of this receptor and its functions. These antagonists could be of crucial importance for animal experiments if they keep their affinity for the murine MRGPRB2 receptor. In the future, further improvement could result in compounds with improved properties. Some issues like low water solubility, and metabolic instability have to be addressed. Developing a radioligand should not be far from reach. Most importantly establishing a suitable MRGPRB2 cell line for calcium mobilization assays could be of significance for testing our novel antagonists. A HEK cell line may be used for expression due to high G_q -protein content.

The MRGPRX3 receptor is an orphan receptor with no reported pharmacological tool for now. This receptor was cloned and a β -arrestin cell line with high expression was established. Screening all available compound libraries during the time of this thesis resulted in no hit. The MRGPRX3 receptor remains an enigmatic receptor. Taking into account that an MRGPRX3 cell line is not available from

Summary and Outlook

DiscoverX® for undisclosed reasons and that the MRGPRX3 receptor is probably G_q-coupled, it is advisable to adopt calcium mobilization assays for new compound library screening in the future.

MRGPRX4 is an orphan receptor. The drug nateglinide was reported at the final stage of this thesis to act as a weak, non-selective agonist. Several screening and deorphanization approaches in the course of this thesis resulted in no progress until MSX-3 was identified as an artificial agonist. Related compounds subsequently were tested and initial SARs were established. Our efforts led to the optimization of both, efficacy and potency of the agonists. The best stable phosphonate agonist, JH 14102, shows EC₅₀ values in the nanomolar range in both, β-arrestin and calcium mobilization assays. Using these agonists we demonstrated only G_q coupling for this 7TMR. Further synthesis resulted in the phosphate derivative Yazh 473, which demonstrated the best signal-to-noise ratio in the β-arrestin assay so far indicating high efficacy of the compound. For a deeper understanding of this receptor a search for a native cell line led us to stem cells differentiated to DRG-like neurons, detection of MRGPRX4 in several lymphocyte subpopulations and to a tumor cell line, LN229, which expresses the receptor natively. The obtained information proved the expression and consequently a potential physiological role of MRGPRX4 in the immune system. This could be of high significance for a better understanding of the (patho)physiological role of this receptor. The tumor cell line, LN229, is an evidently invaluable tool for investigating MRGPRX4, which enabled us to demonstrate the susceptibility of this 7TMR to agonist-induced desensitization and endocytosis. Moreover, calcium mobilization assays showed a high signal with efficient G_q coupling. These natively expressing cell lines are important for elucidating the role of MRGPRX4. Screening for antagonists has also been carried out and several hits with different scaffolds have been identified. This opens up the door for the development of more potent and selective antagonists. Lastly, a pairing proposal of MRGPRX4 to AMP as its physiological agonist based on the structure of our novel agonists has shown promising results. AMP exhibited the activation of both, β-arrestin and G_q pathways. Figure 61 shows the most important agonists discovered and developed within this study.

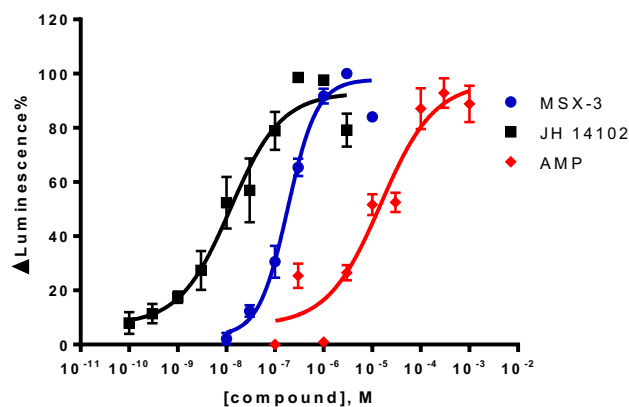


Figure 61: The curves of MSX-3, the first identified hit at MRGPRX4 receptor, with an EC₅₀ value of 175 nM and JH 14102 as the most potent agonist so far with an EC₅₀ value of 17.4 nM. Based on the similarity in structure, AMP was proposed as a physiological ligand and showed an EC₅₀ value of 19.4 μM. Each curve is the mean curve of three independent β-arrestin assays

Further steps are needed to support our proposal. Open questions remain due to inherent instability of AMP and regarding physiological and pathophysiological concentration of this nucleotide. In addition, improving the potency of our agonists with the goal to prepare a radioligand should be pursued.

All in all, the results of this thesis enrich our understanding of the so far not-well characterized MRGPRX receptor subfamily and provide important tools for further investigations.

4. Experimental part

4.1 General

4.1.1 Chemicals

2-Propanol, technical	ZVE Bonn-Endenich
2'-desoxy-AMP disodium salt	Sigma-Aldrich, D6375
8-Br-AMP disodium salt	Sigma-Aldrich, B3131
Adenine	Sigma-Aldrich, A8626
Adenosine	Sigma-Aldrich, A9251
ADP disodium salt	Sigma-Aldrich, A2754
Agarose	Roth, 2267
Ali 901A, Ali 909, Ali 900D, Ali 913, Ali 916	Synthetic compound from lab of Prof Christa Müller
AMP disodium salt	Sigma-Aldrich, 01930
AMP-CP	Sigma-Aldrich, M3763
Ampicilline sodium salt	Roth, K029
APVRSLNCTLRDSQQKSLVMSGPYE (synthetic peptide)	ProteoGenix SAS
APVRSLNCTLRD (synthetic peptide)	Genosphere Biotechnologies
ATP disodium salt	Sigma-Aldrich, A26209
BAM-22	Genscript, RP10424
BI03	Synthetic compounds from lab of Prof Christa Müller
BMS 191011	TOCRIS Bioscience, 2665
Calcium chloride dihydrat	Fluka, 21097; Sigma, C3306
cAMP	Enzo Life Science, 80-0056
Cantharidin	TOCRIS Bioscience, 1548
CB compounds	Synthetic compounds from lab of Steven De Jonghe
Chloroquine diphosphate	Sigma-Aldrich, C6628
Ciprofloxacin	Sigma-Aldrich, 17850
Cortistatin-14	Genscript, RP10972

Experimental part

D-(+)-Glucose	Sigma-Aldrich, G-7021
DMSO	Roth, 4720
DMSO, steril	AppliChem, A3672
EDTA, disodium dihydrate	Roth, X986.1
Ethanol, p.A.	Merck, 1.00983
Fetal calf serum	Sigma-Aldrich, F-0804
Fluo-4-AM	Lifetechnologies, F-14201
Forskolin	Enzo Life Sciences, BML-CN100
G418	AppliChem, A2167
GelRed™	Biotrend, 41002
Glycerol	Acros, 158920010
GMP disodium salt	Sigma-Aldrich, G8377
Hepes	Sigma-Aldrich, H3375
Hydrochloric acid 37%	Sigma-Aldrich, 30721
Hygromycine B	InvivoGen, ant-hm-5
Interleukin 1 beta (IL-1 β)	R&D Systems, 201-LB-005/CF Lifetechnologies, 10139-HNAE-5
Istradefylline	Synthetic compounds from lab of Prof Christa Müller
JH 14102, JH 14021	Synthetic compounds from lab of Prof Christa Müller
KD162, KD165	Synthetic compounds from lab of Prof Kiec-Kononowicz
Magnesium chloride	Fluka, 63068
Magnesium sulfate	Sigma-Aldrich, M2643
Matrix metalloproteinase 3 (MMP3)	Lifetechnologies, 10467-HNAE-25 Sigma-Aldrich, SRP7783
MIRA-1	TOCRIS Bioscience, 3362
Morphine, hydrochloride	Sigma-Aldrich, Y000451
MSX-2, MSX-3, MSX-4, MSX-155	Synthetic compounds from lab of Prof Christa Müller
NECA	Sigma-Aldrich, E2387
NT 021071, NT 021033, NT 02109, NT 02005	Synthetic compounds from lab of Prof Christa Müller

Experimental part

Oregon Green® 488 BAPTA-1 AM	Molecular Probes, O6807
Penicilline/Streptomycin solution	Cambrex, DE17-602E
Pluronic® F-127	Sigma-Aldrich, P2443
Polyclonal MRGPRX4 antibody	Aviva Systems Biology, OAAF04989
Potassium chloride	Fluka, 60128
Potassium dihydrogenphosphate	Sigma-Aldrich, P9791
Prin01	Princeton BioMolecular Research, OSSL_790375
Ro20-1724	Hoffmann la Roche
Saponin	Fluka, 84510
SDZ-220-040	TOCRIS Bioscience, 1251
Sodium carbonate	AppliChem, A1881
Sodium chloride	Roth, 3957.1
Sodium hydrogencarbonate	Sigma-Aldrich, S5761
Sodium hydroxid	Merck, 109959
Soybean trypsin inhibitor (STI)	Sigma-Aldrich, T9003 and T9767
Triton™ X-100	Sigma-Aldrich, X-100
UMP disodium salt	Sigma-Aldrich, U6375
Yazh compounds	Synthetic compounds from lab of Prof Christa Müller
ZM39923	TOCRIS Bioscience, 1367

4.1.2 Instruments and Software

Autoclave	VX-95, Systec 3850 ELV, Systec
Balance, precision	SBC 42, SCALTEC 440-47N, KERN
Benches	NUNC® Safe flow 1.2 NUNC® MICROFLOW
Cell culture flasks	25 cm ² , 75 cm ² , 175 cm ² steril, Sarstedt
Cell scraper	Josef Peske GmbH und Co.
Centrifugal filters	Amicon® Ultra, Merck Millipore
Centrifuges	Mikro 200, Hettich Allegra™ 21 R, Beckman Coulter

Experimental part

	Avanti™ J-201, Beckman Rotofix 32, Hettich
Cryovials steril	Starsedt
Dismozon® pur	Bode Chemie
Drying cabinet	Heraeus Instruments
Glass-fiber filters	Whatman®, Schleicher und Schüll (GF/B)
Filters (sterile)	Filtropur 0,22 µm, Sarstedt
Fluorimeter	NOVOstar®, bmg Labtech Mithras Research II LB 940, Berthold Technologies
Harvester	Brandel M24 Gaithersburg, MD, USA Brandel M48 Gaithersburg, MD, USA
Incubator	Jouan IG 650 Heraeus HERAccl® 240 Inc 240, Memmert
Incubator shaker	Innova 4200 Incubator shaker, New Brunswick Scientific
Liquid scintillation analyzer	Tri-Carb 2810 TR, Perkin-Elmer Topcount NXT™, Packard
Liquid scintillation	cocktail LumaSafe®, Perkin-Elmer
Microscope	Wilovert, Hund Wetzlar Axiovert 25, Zeiss
Microscope for fluorescence images	Leica, DM IL LED Fluo
Microwave	Microwave 800, Severin
Neubauer cell chamber	Marienfeld, Germany
pH meter	691 pH Meter, Metrohm Seven Easy, Mettler Toledo
Pipettes	Eppendorf Research
Pipette tips	Greiner Plastibrand®, Brand; Sarstedt
Pipette tips (electronical pipets)	Ritips® professional, Ritter
Photometer	DU-530, Beckman
Serological pipets	Starsedt
Software	BLAST® Protein Alignment GraphPad Prism®, Version 6.0 und 5.0

Experimental part

	ChemBiodraw Ultra 11.0 Microsoft Excel und Microsoft Word 2007 Clone Manager, Version 9 DNA Translator 2.0, Dr. Anke Schiedel/ J. Bosmann Chromas Version 1.45, Conor McCarthy OligoAnalyser 3.1, IDT, Scitools ClustalW2, European Bioinformatics Institute
Thermal block	Thermomixer comfort, Eppendorf
Thermocycler	Px2 Thermal Cycler, Thermo Scientific Biometra
Ultraturrax	T25 basic, IKA Labor Technik
Vaccume pump	MD 4C Vario, Vaccubrand
Vortexer	MS 1 Minishaker, IKA Labor Technik
Water bath	GFL® 1083, Gesellschaft für Labor Technik GmbH WWB 14, Memmert
Well-plates (96)	Starsedt Nunc Greiner Corning 3340
Well-plates (24)	Starsedt

4.1.3 Buffers

PBS buffer

8.0 g NaCl (150 mM), 0.2 g KCl (2.5 mM), 1.3 g Na₂HPO₄ and 0.2 g KH₂PO₄ (1.5 mM) are dissolved in 1 l of deionized water. Buffer is then sterilized via autoclave and stored at RT.

0.05 % Trypsin / 0.6 mM EDTA solution

6 ml of a 0.1 M EDTA stock solution are added to 1 l PBS buffer and autoclaved subsequently. 20 ml of a sterile 2.5 % trypsin solution and 750 µl of a sterile 0.5 % phenol red solution are added under a laminar flow bench. The solution is stored at 4 °C in 100 ml aliquots.

HEPES buffer

Experimental part

2.38 g HEPES (10 mM), 4.68 g NaCl (80 mM), 0.27 g KCl (3.6 mM), 0.11 g MgCl₂ · 6 H₂O (0.53 mM) , 0.18 g CaCl₂ · 2 H₂O (1.2 mM) were added to deionized 1 l water, pH is adjusted to 7.4 at 4 °C with saturated NaOH solution. The buffer is stored at 4 °C.

HBSS buffer

8 g NaCl (13 mM), 4.77 g Hepes (20 mM), 1 g Glucose (5.5 mM), 0.1 g MgSO₄ (0.8 mM), 0.1 g MgCl₂ (1 mM), 0.185 g CaCl₂ (1.25 mM), 0.35 g NaHCO₃ (4.2 mM), 0.4 g KCl (5.4 mM), 0.06 g KH₂PO₄ (0.44 mM), 0.048 g Na₂HPO₄ (0.34 mM) were added to 1.0 l deionized, autoclaved water and the pH is adjusted to 7.3. The buffer is stored at 4 °C.

Lysis buffer for cAMP assay

1.48 g EDTA (4 mM) und 100 µl Triton (0.01 %) were dissolved in 1.0 l of deionized, autoclaved water. The pH is adjusted to 7.3.

5X Krebs-Hepes buffer (KHB)

16.85 g NaCl (118.6 mM), 0.875 g KCl (4.7 mM), 0.4 g KH₂PO₄ (1.2 mM), 0.875 g NaHCO₃ (4.2 mM), 5.25 g D-Glucose (11.7 mM) und 5.95 g HEPES (10 mM) were added to 500 ml deionized water and the pH is adjusted to 7.3. The buffer is stored at -20°C.

1X Krebs-Hepes buffer (KHB)

100 ml of 5X KHP buffer were added to 650 µl of 1 mM CaCl₂ solution (f.c 1.3 mM) and 600 µl of 1 M MgSO₄ solution (f.c 1.2 mM) and then completed with deionized water to 500 ml. The pH was again adjusted to 7.3 and aliquots of 25 ml were frozn in -20°C.

Oregon-Green Solution

50 µg of Oregon Green were dissolved in 39.7 µl DMSO (f.c 1 mM). The solution was divided to 3 µl aliquots and these aliquots were stored in -20°C. The preparation should be done under light protection since Oregon Green is light-sensitive.

Fluo-4 AM Solution

50 µg of Flou-4 AM were dissolved in 45 µl DMSO. The solution was divided to 15 µl aliquots and these aliquots were stored in -20°C.

Experimental part

Pluronic®-F127 solution

200 mg of Pluronic were dissolved in 800 µl DMSO. The solution was kept in room temperature and approximately 15 min prior to use the solution was heated to 37°C in a water bath.

50x TAE buffer for molecular biology

242 g TRIS (2 M), 14.61 g EDTA (50 mM) and 57.1 ml acetic acid (glacial) are added to deionized water yielding a total volume of 1 l. Buffer is sterilized via autoclave, stored at RT and is diluted appropriately prior to usage.

4 % Paraformaldehyd in PBS

1 g Paraformaldehyd is added to 20 ml of 80°C heated water. 1 N NaOH solution is added dropwise until the solution becomes clear. 2.5 ml 10X PBS are added to the solution and the volume is completed to 25 ml with deionized water. After cooling pH was adjusted to 7.4 and the solution was stored at -20°C.

1 % BSA in PBS

Dissolve 1 g of BSA in 100 ml PBS and store the 25 ml aliquots in -20°C.

4.2 Cell culture

4.2.1 Cells and Media

PathHunter® CHO-K1 β-Arrestin Parental Cell Line	DiscoverX, 93-0164
PathHunter® CHO-K1 MRGPRX1 β-Arrestin Cell Line	DiscoverX, 93-0919C2
PathHunter® CHO-K1 MRGPRX2 β-Arrestin Cell Line	DiscoverX, 93-0309C2
PathHunter® CHO-K1 MRGPRX3 β-Arrestin Cell Line	Cloned within this thesis
PathHunter® CHO-K1 MRGPRX4 β-Arrestin Cell Line	DiscoverX, 93-0541C2A
PathHunter® CHO-K1 MRGPRB2 β-Arrestin Cell Line	Cloned within this thesis

Experimental part

LN229 Glioblastoma Cell line	ATCC [®] CRL-2611 [™] Provided by AK Prof. Dr. Björn Scheffler
------------------------------	---

β-arrestin cell lines were cultured using the following media

Basal medium	Culture medium	Selection medium
DMEM-F12 (1:1)	DMEM-F12 (1:1)	DMEM-F12 (1:1)
FCS 10%	FCS 10%	FCS 10%
Penicillin 100 U/ml	Penicillin 100 U/ml	Penicillin 100 U/ml
Streptomycin 100 µg/ml	Streptomycin 100 µg/ml	Streptomycin 100 µg/ml
Hygromycin 300 µg/ml	Hygromycin 300 µg/ml	Hygromycin 300 µg/ml
	G418 200 µg/ml	G418 800 µg/ml

LN229 cell line was cultured using the following medium

Basal medium
DMEM-F12 (1:1)
FCS 10%
Penicillin 100 U/ml

Generally all cells are maintained in cell culture flasks at 37 °C in a humidified atmosphere of 90 % air and 10 % CO₂. Once adherent cells have grown into a monolayer of approx. 90 % confluence they are passed into new flasks. This is done by decanting the medium and rinsing the cells with PBS to remove residual medium. A 0.05 % trypsin / 0.6 mM EDTA solution is added and cells are incubated for 3-5 minutes at 37 °C. In order to adhere to surfaces cells require integrin structures. These structures are digested by trypsin which belongs to the family of serine proteases. In addition, the concentration of divalent cations which are crucial for integrin stability is reduced by EDTA. Once cells are detached they are suspended in basal medium and separated by passing the suspension through a sterile pipette several times. Depending on the required amount of cells, a certain volume of cell suspension is transferred to a new flask containing preheated medium.

Experimental part

It should be noted that prior to seeding cells for a β -arrestin assay the cell should not be dissociated via a detachment buffer without trypsin. Hence, PBS buffer containing 2 mM EDTA and 10 mM Glucose was used in this case.

4.2.2 Membrane preparation

Once cells have reached a confluence of ~90 % the content of one 175 cm² flask is passed into twenty sterile 150 mm dishes. After the cells have grown into a monolayer of ~90 % confluence again the medium is decanted and dishes are rinsed with 5 ml PBS. After freezing the dishes at -20 °C or -80 °C for at least 15 min, 1 ml of ice-cold 5 mM TRIS / 2 mM EDTA / pH 7.4 buffer are added and dishes are scraped with a cell scraper. This step is repeated to ensure that all cells are collected from each dish. Once the content of all dishes is unified in a beaker, the cell suspension is treated with an ultraturrax for 1 min at 24,000 / min and homogenized via a dounce homogenizer subsequently. To remove nuclei and other larger organelles and cell debris the homogenate is centrifuged at 1000 g for 10 min (4 °C). The supernatant is collected and centrifuged at 48,400 g for 1 h (4 °C). The resulting pellets are resuspended in 0.1 ml / Dish of 50 mM TRIS / pH 7.4 buffer and crude membrane solutions are stored at -80 °C. All steps should be carried out swiftly at a temperature of 4 °C to avoid receptor internalization.

4.2.3 Reagents for protein determination (Lowry)

Reagent A: 10 g of Na₂CO₃ are dissolved in 500 ml of 0.1 N sodium hydroxide solution.

Reagent B: 0.25 g CuSO₄ x 5H₂O are dissolved in 20 ml of deionized water. 0.5 g of disodium- tartrate are dissolved in another 20 ml. Solutions are unified and deionized water is added to a final volume of 50 ml.

Reagent C: Reagent C always needs to be prepared freshly prior to usage. It is prepared by mixing reagent A and B in a ratio of 50:1.

Reagent D: Deionized water is added to 18 ml of folin reagent to a final volume of 90 ml. Solution has to be stored protected from light.

Experimental part

1 mg/ml bovine serum albumin (BSA) solution is prepared and its OD is measured in a quartz cuvette at a wavelength of 280 nm. Since there is a linear correlation between the BSA concentration of a solution and its OD the actual BSA concentration can be calculated using the following formula:

$$\text{BSA (mg/ml)} = 1 \text{ (mg/ml)} * \text{measured OD/reference OD}$$

Reference OD equals 0.66

Dilutions from 50 to 500 µg/ml of the BSA solution are prepared. Protein concentrations have to be adjusted according to the calculated BSA concentration.

Two dilutions (1:10 and 1:20) of crude membrane samples are prepared with 50 mM TRIS / pH 7.4 buffer yielding a total volume of 200 µl. Blank value is determined as 200 µl of 50 mM TRIS / pH 7.4 buffer. 1 ml of reagent C is added to each sample and incubated for 20 min at room temperature (RT). Another period of 30 min incubation follows after addition of 100 µl of reagent D. All samples are subsequently transferred to semi micro cuvettes and ODs are measured at 550 nm. OD values of the BSA dilution are plotted against their concentration and a linear regression analysis is performed using Microsoft Excel 2007. Protein concentrations of crude membrane samples can be calculated according to the results of the aforementioned linear regression analysis.

4.3 Molecular biology

4.3.1 Kits, enzymes and reagents

6x Gel Loading Dye, blue	New England BioLabs, N3026S
ΦX174 DNA-HaeIII Digest	New England BioLabs, B7021S
NheI	New England BioLabs, R0131S
HindIII	New England BioLabs, R0104S
DNA Clean & Concentrator™-25 Kit	Zymo Research, D4033
Lambda DNA/EcoRI+HindIII marker	Fermentas, SM0191
Lipofectamine™ 2000 Transfection Reagent	Invitrogen, 11668019
PathHunter® Detection Kit	DiscoverX, 93-0001L
PureLink® HiPure Plasmid Filter Midiprep Kit	Life Technologies, K2100-15
Pyrobest polymerase	TaKaRa, R005

Experimental part

Zymoclean™ Gel DNA Recovery Kit	Zymo Research, D4002
Zyppy™ Plasmid Maxiprep Kit	Zymo Research, D4028
Zyppy™ Plasmid Miniprep Kit	Zymo Research, D4020

DNA midipreparation: Invitrogen™ PureLink™ HiPure Plasmid Filter Purification Kits. The components of the kit were resuspension buffer with RNase A, Lysis buffer, precipitation buffer, equilibration buffer, wash buffer, elution buffer, TE buffer and HiPure Filter Midi Columns. The midipreparations were performed according to the manufacturer instructions.

DNA minipreparation: ZYMO RESEARCH CORP. ZR Plasmid Miniprep™-Classic. The components of the kit were P1 buffer, P2 buffer, P3 buffer, Endo-Wash buffer, Plasmid Wash buffer, DNA elution buffer, RNase A, Zymo-Spin™ IIN columns and collection tubes. The DNA minipreparations were performed according to the manufacturer instructions.

Both mini- and midipreparations aim at extracting the plasmid DNA from the bacteria. The most utilized principle is the alkaline lysis of the bacterial cell wall.

DNA-Recovery: ZYMO RESEARCH CORP. Zymoclean™ Gel DNA Recovery Kit. This kit is used to extract the DNA from the agarose gel and it consists of the following components the ADB (Agarose Dissolving Buffer), DNA wash buffer, Zymo-Spin™ I columns and collection tubes. The DNA recovery was performed according to the manufacturer instructions.

DNA-Recovery: ZYMO RESEARCH CORP. DNA clean & concentrator™-5 Kit. This kit is used to extract the DNA from PCR digestion, cell lysate, etc and it consists of the following components DNA binding buffer, DNA wash buffer, Zymo-Spin™ columns and collection tubes. The DNA recovery was performed according to the manufacturer instructions.

4.3.2 PCR DNA amplification

4.3.2.1 human MRGPRX3 receptor

The following PCR program was adopted to amplify the cDNA of human MRGPRX3 from the vector pCMV6-Entry provided by OriGene Company US.

98 °C 10 s

Experimental part

98 °C 10 s*

67 °C 1 min*

72 °C 3 min*

72 °C 10 min

* = 30 cycles

1 µl template DNA (~ 20 ng)

2 µl f-primer (~ 10 pM)

2 µl r-primer (~ 10 pM)

5 µl 10X-pyrobest-buffer

4 µl dNTP

0.5 µl pyrobest-polymerase

35.5 µl PCR-H₂O

50 µl total volume

Table 32 The restriction enzymes (**bold**) and the primer sequences used to amplify hMRGPRX3

Primer	Sequence 5` - 3`
f-hMRGPRX3- NheI	GCATAATGCTAGCACCATGGATTCAACCATCCCAGTCTTG
r- hMRGPRX3- HindIII	TTCGAAGCTTGACTGCTCCAATCTGCTTCCCGAC

4.3.2.2 mouse MRGPRB2 receptor

The following PCR program was adopted to amplify the cDNA of murine MRGPRB2 from the vector pCMV6-Entry provided by OriGene Company US.

98 °C 10 s

98 °C 10 s*

Experimental part

62 °C 1 min*

72 °C 3 min*

72 °C 10 min

* = 30 cycles

1 µl template DNA (~ 20 ng)

2 µl f-primer (~ 10 pM)

2 µl r-primer (~ 10 pM)

5 µl 10X-pyrobest-buffer

4 µl dNTP

0.5 µl pyrobest-polymerase

35.5 µl PCR-H₂O

50 µl total volume

Table 33 The restriction enzymes (**bold**) and the primer sequences used to amplify mMRGPRB2

Primer	Sequence 5` - 3`
f-mMRGPRB2- NheI	GCAATGCTAGCACCAT GTAGTGGAGATTTCTAATCAAG
r- mMRGPRB2- HindIII	CTAAGCTT GAGCTGCAGCTCTGAACAGTTCC

4.3.3 β-arrestin vectors

pCMV-ProLink™1 vector	93-0167
pCMV-ProLink™2 vector	93-0171
pCMV-ARMS1-ProLink™2 vector	93-0489
pCMV-ARMS1-ProLink™2 vector	93-0490

ARMS means Arrestin Recruitment Modifying Sequence and it facilitates the G protein receptor kinase (GRK) recruitment.

4.3.4 Subcloning of the cDNA

In order to subclone the cDNA in the vectors of interest (in this case the four β -arrestin plasmids) the recognition sites of the restriction enzymes have to be introduced adjacent to the genes. This can be achieved by the specific design of the primers. Chapters 4.3.2.1 and 4.3.2.2 contain the names of the restriction enzymes (bold) used for each gene as well as the recognition sites of these enzymes (underlined). The pCMV-ProLink™ series are suitable for subcloning the 7TMR of interest and the resulting plasmid, when expressed in a mammalian cell, will have a ProLink tag on the C-terminus of the 7TMR. It is important to design the primer so that the stop codon of the 7TMR is omitted. Moreover, the 7TMR should be in frame with the ProLink tag.

The gene and the vector of interest were then digested with the restriction endonuclease enzymes. The total volume was 20 μ l and the reaction was performed according to the manufacturer (New England Biolabs) protocol for 1 hour in the room temperature. The digested genes were then subjected to the gel electrophoresis in order to separate them from the restriction enzymes and to estimate their amount. The agarose gel was then excised and the digested PCR products were extracted with the Zymoclean™ Gel DNA Recovery Kit.

4.3.5 Ligation

After the digestion of the vector and the PCR products, they were ligated using the enzyme T₄ DNA ligase. This reaction was performed at room temperature for 2 hours according to the following protocol

X μ l vector DNA (~50 ng)

Y μ l Insert DNA (~150 ng)

2 μ l 100nM ATP solution

2 μ l 10X T₄-DNA ligase Buffer

1 μ l T₄-DNA ligase

Z μ l PCR water

20 µl total volume

4.3.6 Agarose gel electrophoresis

Agarose is added to TAE buffer yielding a concentration of 1 % and suspension is heated until agarose is completely dissolved. In order to avoid thermal degradation GelRed™ nucleic acid stain from Biotium, Inc. is added as a final concentration of 1:10,000 after the solution has cooled down to ~50 °C. The solution is then transferred to a gel holder. After the gel has hardened the comb is removed and the gel is put into the electrophoresis chamber containing 1x TAE buffer. Samples mixed with 6x loading dye are loaded into the pockets and the gel is run at a 100 V. DNA bands are visualized by exposure to UV light using the Bio-Rad Gel doc system.

4.3.7 LB medium

25 g of LB medium are dissolved in 1 l deionized water according to manufacturer's protocol. Medium is sterilized subsequently and stored at 4 °C until further use. If the medium is used to cultivate bacteria transformed with the four β-arrestin vector constructs, kanamycin is added to give a final concentration of 100 µg /ml.

4.3.8 Preparation of competent bacteria

E.Coli genotype TOP10 was used, from which 50 µl of a glycerol culture were given into 4 ml LB medium (without antibiotics), which was incubated in the bacteria shaker at 37 °C, 220 rpm over night. The following day, 500 µl of this preculture were transferred into 40 ml LB medium (without antibiotics) and again incubated in the bacteria shaker (37 °C, 220 rpm). After approximately 45 min, the optical density of this suspension at 550 nm (OD550) was measured against a blank (LB medium without bacteria). If necessary the incubation time was extended until an OD550 of 0.5 was obtained. At this time, it can be assumed that bacterial reproduction is within the exponential phase of the bacteria growth curve. The suspension was centrifuged (1700 g, 4 °C, 20 min) and the resulting pellet resuspended in 20 ml cold CaCl₂ solution (0.1 M). After incubation on ice for 30 min, the suspension

Experimental part

again was centrifuged (1700 g, 4 °C, 20 min). The obtained pellet was resuspended in 2 ml cold CaCl₂ solution (0.1 M). After addition of 0.5 ml glycerol and quick homogenization, the suspension was aliquoted à 100 µl and stored at -80 °C.

4.3.9 Transformation of competent bacteria

100 µl of competent bacteria are kept on ice until thawed completely. The ligation mixture is added to the thawed bacteria and the resulting mixture is incubated on ice for 30 min. Bacteria are then subjected to heat shock treatment at 37 °C for 2 min and another 2 min of incubation on ice directly thereafter. 300 µl of LB medium are added and the suspension is incubated at 37 °C and 600 rpm for 2 h. Within this incubation period successfully transformed bacteria are able to express the proteins coded in the plasmids resistance gene. Bacteria are then transferred to a Kanamycin containing agar plate and distributed evenly using a Drigalski spatula. Plates are incubated upside down at 37 °C overnight.

4.3.10 Bacterial cultures

Depending on the required downstream application bacteria can be cultured in 4 ml or 100 ml of LB medium plus kanamycin 100 µg/ml. To obtain bacteria cultures, a small amount of bacteria is taken either from agar colonies or previous bacterial cultures and transferred to the desired amount of medium. Cultures are then incubated at 37 °C and 220 rpm overnight.

4.3.11 Sequencing

All sequencing analyses were performed by GATC Biotech AG, Germany. Samples were prepared according to the manufacture's specifications.

4.3.12 Glycerol Stocks

In order to preserve the bacterial clones carrying the desired gene in vector construct for long periods of time, they can be kept as glycerol stocks. These are prepared by adding 200 µl of sterile glycerol to 800 µl of bacterial suspension in LB medium. Stocks are stored at either -20 °C or -80 °C.

4.4 Cell counting

To determine the number of cells in a given solution, a Neubauer cell chamber was used. Therefore, a glass slide was put on the chamber and the cell suspension was pipeted between the slide and the chamber. Cells within a square of the dimension 1 x 1 mm were counted under the microscope. Since a square of these dimensions – due to a depth of 0.1 mm – contains 100 nl, the number of cells counted in this square multiplied by 10,000 corresponds to the number of cells per ml. To increase the accuracy of the determination, cells within two or more of these squares were counted and the mean was used for calculation of cells per ml.

4.5 Transfection

The term transfection refers to the introduction of nucleic acids into eukaryotic cells by non-viral methods. If, as a result thereof, the nucleic acid molecule is integrated into the host genome (stable transfection), the transfected nucleic acid will be replicated along with the host genome with each cell cycle and the gene product will be stably expressed. If the nucleic acid molecule is not integrated into the host genome (transient transfection), it will only temporarily remain within the cell and will get lost during mitosis or will be degraded by time. Several different transfection methods are known at present, which make use of various electrical, chemical or physical principles.

4.5.1 Lipofection

In general, lipofection with Lipofectamine™ 2000 was performed according to the manufacturer's protocol, as described in the following: one day before transfection, 1-2 10^6 cells were seeded in seeding medium using 25 cm² flask and cultivated over night (1). On the following day, the culture medium was exchanged against F12 plus FCS (no antibiotic) several hours before transfection (2). In a tube 600 μ l Lipofectamine™ 2000 was added to 25 μ l F12 without any supplements, mixed by inverting and incubated for 5 min (3). In the meanwhile, the DNA solution (containing 10 μ g DNA) was prepared by adding the required amount of DNA into F12 without any supplement in a second tube so that the final volume is 625 μ l (4). Subsequently, the Lipofectamine™ 2000 solution was given into the DNA solution, mixed by inverting and the mixture was incubated for 20 min at room

Experimental part

temperature. At the end of the incubation time, liposome-DNA complexes have formed, which were given drop-by-drop onto the cells. After incubation till next day the medium was exchanged against basic culture medium (5). One the following day the selection medium was used till a stable growth of cells (usually 14 days) is evident (6). Thereafter, the culture medium should be continually used.

4.6 Immunofluorescence experiments

On the day preceding the experiment, cells are seeded on coverclips in a 12 well-plate. On the day of experiments the following steps were done: (1) washing the cells 3X with PBS (2) removal of PBS and addition of 500 µl of 4% Paraformaldehyde in PBS for 15 min (3) removal of PBS and washing 3X with 25mM glycine (4) removal of glycine, washing with PBS and solubilizing the cells with 1% saponin in PBS solution for 10 min (5) removal of saponin solution, washing 3X with PBS and blocking with 1% BSA in PBS solution for 15 min (6) taking of coverclips and addition of primary Ab (30-40 µl) diluted in PBS according to instruction of the manufacturer (7) washing 2X with PBS and addition of secondary Ab for 20-50 minutes (8) washing 2X with PBS. The overclips are then ready to be investigated.

In the case of the primary Ab against C-terminus of MRGPRX4, the dilution was 1/250 in PBS.

4.7 Competition radioligand binding assays

In order to investigate the binding of adenine at MRGPRX4, [³H]adenine was used as a radioligand as shown in the protocol below.

50 mM TRIS / pH 7.4 buffer	190 µl
DMSO / Adenine	10 µl
[³ H]Adenine	100 µl
Membrane preparation	100 µl
Total volume	400 µl

DMSO 100% was used to determine the total binding; adenine in DMSO to final concentration of 100 µM was used to determine the unspecific binding. The incubation time was 60 minutes. The final concentration of the radioligand was 10 nM. The filtration took place under reduced pressure over GF/B filter directly after the incubation time has finished and was performed 3 times each with

Experimental part

approx. 3 ml 50 mM TRIS. This filtration aims at removing the unbound radioactivity after reaching the equilibrium; the filters were then punched out and put into mini scintillation vials and 2.5 ml of scintillation cocktail Lumasafe from PerkinElmer Inc. are added. The counting of the radioactivity takes place in a Tri-Carb liquid scintillation counter, after an initial waiting period of at least 6 hours.

The following formulas were applied to determine the concentration of the protein and the RL

$$\text{Protein [ml]} = \frac{(\text{Anzahl Vials} + 6) * c_{\text{solL}} \text{Protein [\mu g]}}{c_{\text{ist}} \text{Protein [\mu g/ml]}}$$

$$c_{\text{ist}} \text{Protein [\mu g/ml]}$$

$$\text{Puffer [ml]} = (\text{Anzahl Vials} + 6) * 0,1 \text{ ml} - \text{Protein [ml]}$$

$$\text{Ligand [\mu l]} = \frac{(\text{Anzahl Vials} + 6) * \text{spez. Aktivit\u00e4t [Ci/mmol]} * c_{\text{solL}} \text{Ligand [nM]} * \text{Gesamtvolumen [ml]}}{1000 * c_{\text{ist}} {}^3\text{H[Ci/L]}}$$

$$1000 * c_{\text{ist}} {}^3\text{H[Ci/L]}$$

$$\text{Puffer [ml]} = (\text{Anzahl Vials} + 6) * 0,1 \text{ ml}$$

4.8 Pharmacological assays

4.8.1 β -Arrestin assay

The β -arrestin recruitment assay is based on the detection of the interaction of a 7TMR with β -arrestin by β -galactosidase fragment complementation (β -arrestin Path Hunter assay, DiscoverX, Fremont, CA, U.S.A.). The 7TMR of interest is fused to the ProLink tag, the N-terminal part of β -galactosidase, and β -arrestin is fused to the enzyme acceptor, which is β -galactosidase lacking the first 41 amino acids. Upon receptor activation, β -arrestin is recruited to the receptor which leads to the complementation of both β -galactosidase fragments.²⁷⁴ The activity of the functional β -galactosidase is measured by chemiluminescence.

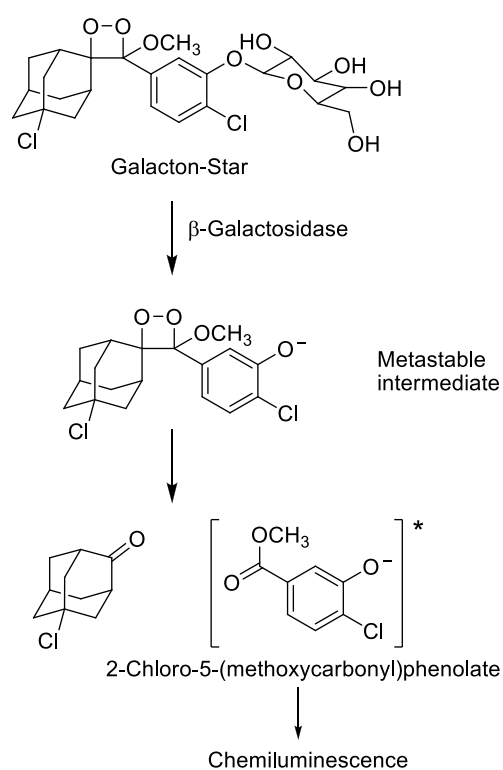
CHO cells stably expressing the respective receptor were seeded in a volume of 90 μ L into a 96-well plate and incubated at a density of 20,000 cells/well in Opti-MEMTM for 24 h at 37 $^{\circ}$ C.

After the incubation, test compounds were diluted in PBS buffer containing 10% DMSO and added to the cells in a volume of 10 μ L, followed by incubation for 90 min at 37 $^{\circ}$ C. For determination of baseline luminescence, PBS buffer (containing 10% DMSO) in the absence of test compound was

Experimental part

used. During the incubation period, the detection reagent was prepared. For determination of β -arrestin recruitment the detection reagent for the respective receptor was prepared (see below). After the addition of 50 μ L/well detection reagent to the cells, the plate was incubated for an additional 60 min at room temperature. Finally luminescence was determined in a luminometer (TopCount NXT, Packard/Perkin-Elmer).

For the determination of antagonistic properties of tested compounds the assay was performed as described for agonists except that the test compounds were added to the cells in a volume of 5 μ L/well 60 min prior to addition of the agonist (532 nM Yazh 473 final concentration, corresponding to EC_{80} , for MRGPRX4; 1000 nM CST-14 final concentration, corresponding to EC_{80} , for MRGPRX2 and 10 μ M BAM22 final concentration, corresponding to EC_{80} , for MRGPRX1). Data were obtained from three independent experiments performed in duplicate. Data were analyzed using Graph Pad Prism, version 6.02 (San Diego, CA, U.S.A.).



For human MRGPRX1-4 receptor and mouse MRGPRB2: The plating reagent was Opti-MEM™ and the commercial detection reagent kit was used.

4.8.2 cAMP assay

Cells were removed from a confluent 175-cm² flask, transferred into a 50-ml Falcon tube, and centrifuged at 200g, for 5 minutes. After removal of the supernatant, the cell pellet was resuspended in DMEM-F12 medium. The cell suspension (500 μ l, ~200,000 cells per well) was transferred to 24-well plates and incubated for 24 hours at 37°C. After removal of the culture medium, cells were washed HBSS buffer and then incubated with 230 μ l HBSS buffer for 2 h at 37°C. The phosphodiesterase inhibitor Ro20-1724 (final concentration 40 μ M) dissolved in 100% HBSS buffer was added to each well and incubated for 10 min. Thereafter, 25 μ l of the agonist was added and incubated for 20 min. After incubation with the agonist, the final DMSO concentration did not exceed 1.4%. For investigating the G_i coupling cAMP production was stimulated by addition of forskolin (final concentration 10 μ M) for 10 min. The reaction was stopped by removal of the reaction buffer followed by the addition of a hot lysis buffer (250 μ l; 90°C; 4 mM EDTA, 0.01% Triton X-100). The 24-well plates were kept at room temperature for 5 min and then kept at minus 20°C. For competition binding experiments, 50 μ l of the cell lysates were transferred into 2.5-ml tubes. [³H]cAMP (30 μ l) (3 nM final concentration) in lysis buffer and 40 μ l of cAMP-binding protein in the same buffer (75 μ g protein per vial) were added. Total binding was determined with 50 μ l of lysis buffer, 30 μ l of [³H]cAMP solution, and 40 μ l of cAMP-binding protein containing solution. Nonspecific filter binding was determined with 90 μ l of lysis buffer and 30 μ l of [³H]cAMP solution. For a cAMP standard curve, 50 μ l of known cAMP concentrations were used instead of 50 μ l of cell lysate. After an incubation time of 1 hour on ice, the assay mixture was filtered through GF/B glass fiber filters using a Brandel harvester. Filters were washed three times with ice-cold 50 mM Tris-HCl buffer, pH 7.4. Then filters were transferred into minivials, incubated for 9 h with 2.5 ml of scintillation cocktail and counted in a liquid scintillation counter.

4.8.3 Calcium mobilization assay

Calcium mobilization assays have been conducted only with MRGPRX4 receptor. Two cell lines have been used. The β -arrestin CHO and LN229 glioblastoma cell line. For the former cell line was the

suspension format suitable while for the latter the attached cell format was more appropriate. Novostar® microplate reader was used for the measurements.

4.8.3.1 The suspension cell format of calcium mobilization assay

Two confluent flasks of MRGPRX4 β -arrestin cells were harvested using 3 ml 0.05 % trypsin / 0.02 % EDTA and the volume was completed to 30 ml with culture medium. The cells were kept under 5 % CO₂ at 37°C for 45 min and then centrifuged at 200 x g for 5 min. The cells were resuspended in 994 μ l KHB (see chapter 4.1.3) and transferred to an Eppi. 3 μ l Oregon Green and 3 μ l 1 % Pluronic® F127 were added to the cells and rotated via a shaker for 1 h at room temperature under light protection. The cells were added to a V-shaped basin and 19 ml of KHB were added mixed thoroughly. 180 μ l of cell suspension were pipetted in each well of a 96-well plate (Greiner 655096) and left for 10 min in room temperature under light protection. In the mean time a dilution of the test compound was prepared. Fluorescence intensity was measured at 520 nm for 60 s at 0.4 s intervals. PBS was used as a negative control and ATP 100 μ M was used as a positive control. At least three independent experiments were performed in duplicates for each compound.

4.8.3.2 The attached cell format of calcium mobilization assay

The cells were harvested using 3 ml 0.05 % trypsin / 0.02 % EDTA. The volume was completed to 10 ml using the culture medium. The volume of cell suspension corresponding to 5 million cells was transferred into a sterile solution basin and sufficient nutrient medium added to give a final volume of 21 ml. Using an 8-channel pipette and sterile filtered tips, 200 μ l of cell suspension were pipetted into each well of a sterile 96-well corning 3340 microplate with clear bottom and incubated overnight (37 °C, 5 % CO₂, 96 % rel. humidity).

The cells at the bottom of the 96-well microplate were examined under a microscope. If they appeared viable, the experimental set-up was proceeded with by inverting the microplate on tissue paper to remove the nutrient medium. A solution containing 4970 μ l of HBSS buffer, 15 μ l of the detergent Pluronic® F-127 and 15 μ l of the fluorescent dye fluo-4 was prepared under reduced light conditions. With the aid of a stepper pipette, 40 μ l of this solution was placed into each well of the

Experimental part

microplate. The plate was incubated for 1 h at room temperature under light protection and with gentle shaking (200 rpm). Meanwhile, the test compounds were diluted in DMSO in a V-shaped 96-well microplate.

Following the removal of the dye solution by inversion over tissue paper, 178 μ l of HBSS buffer were transferred into each well using a multiple-channel pipette. Each well was subsequently loaded with 2 μ l of the antagonist dilution and the microplate incubated at room temperature under light exclusion. During this time, the reagent plate was prepared by pipetting 40 μ l of Yash 473 solution (5.32 μ M) or HBSS buffer into each well of a V-shaped 96-well microplate. For agonist assays, 180 μ l HBSS buffer were transferred into wells and the serial dilution of the agonist was prepared in a V-shaped 96-well plate. Following 10 min of incubation, the measurement and reagent plates were transferred into a fluorescence reader with pipettor function and the measurement initiated.

4.9 Digestion of IL-1 β

In order to get digest IL-1 β with MMP-3 the protocols in Schönbeck and Ito et al. were taken as an example.^{170,171} In the case of the less pure IL-1 β , the 5 μ g of IL-1 β were dissolved in water and subjected to filtration using a 3 kDa cutoff Amicon® Ultra according to the instructions of the manufacturer. The two fractions were then immediately freezed using liquid nitrogen and then lyophilized. The fraction of less than 3 kDa was active and could be directly dissolved and used in a functional assay.

The inactive fraction of more than 3 kDa of IL-1 β and MMP-3 were dissolved in 250 μ l H₂O each. Both solutions were combined and incubated at 37°C at least for 2 h (for more details for each experiment see chapter 2.4.5). The solution was then filtrated using a 3 kDa cutoff Amicon® Ultra. The two fractions were then immediately freezed using liquid nitrogen and then lyophilized. The lyophilized fractions were then dissolved in PBS and tested in a functional assay.

In the experiment with the highly pure IL-1 β and MMP-3 the first filtration step was not performed since the highly pure IL-1 β was not active. The subsequent steps were identical with the exception of incubating 4 μ g of IL-1 β and 5 μ g of MMP-3.

4.10 Compound libraries

Number	Name	Composition	Characteristics
1	TOCRIS	1120	small molecules with proven physiological activities
2	Xanthine	352	Drug-like xanthine derivatives
3	ChemBridge	689	Drug-like small molecules
4	ChemDiv	555	Drug-like small molecules
5	Herdewijn	354	Drug-like small molecules
6	Interbioscreen	346	Drug-like small molecules
7	Approved drugs	440	Commercially available approved drugs
8	Dipeptides	53	Nitrile amino acid derivatives
9	Briel and RaghuPrasad	38	Drug-like small molecules
10	Natural products	88	Natural products with reported physiological activity
11	Lipid	49	Lipids with reported physiological activity
12	Anthraquinones	222	Anthraquinones with physiological activity

5. Abbreviations

7-TMR	Seven transmembrane receptor
Ab	Antibody
ADP	Adenosine diphosphate
AMP	Adenosine monophosphate
ATP	Adenosine triphosphate
BAM	Bovine adrenal medulla
bp	Basenpaare
°C	Grad Celsius
cAMP	cyclic Adenosine monophosphate
cDNA	copy DNA
CFA	Complete Freund's adjuvant
CHAPS	3-[(3-Cholamidopropyl)dimethylammonio]-1-propanesulfonate hydrate
CHO	Chinese hamster ovary
CNS	Central nervous system
CSF	Cerebrospinal fluid
CST-14	Cortistatin-14
DAG	Diacylglycerine
dAMP	deoxyadenosine monophosphate
DMSO	dimethyl sulfoxide
DMEM	Dulbecco's modified Eagle Medium
DNA	deoxyribonucleic acid
DRG	Dorsal root ganglia
EC ₅₀	half maximal excitatory concentration
<i>E.coli</i>	<i>Escherichia coli</i>
EDTA	Ethylendiamintetraacetic acid
GABA	<i>gamma</i> -Aminobutyric acid
e.g.	<i>exempli gratia</i> (for example)
ERK	Extracellular-signal regulated kinase
et al.	<i>et alii</i> (and others)
IC ₅₀	half maximal inhibitory concentration
IF	Immunofluorescence

Abbreviations

IL-1 β	Interleukin-1 beta
f	forward
FCS	fetal calf serum
g	gram
G418	geneticin
GMP	Guanosine monophosphate
GPCR	G protein-coupled receptor
h	human or hour
hBD	human beta defensin
HBSS	Hancks' Buffered salt solution
HEK	Human Embryonic Kidney
HEPES	<i>N</i> -(2-hydroxyethyl)piperazine- <i>N'</i> -(2-ethanesulfonic acid)
HPLC	high performance liquid chromatography
K_D	equilibrium dissociation constant
K_i	equilibrium inhibition constant
KO	knockout
M	Molar
min	minute(s)
MMP	Matrix metalloproteinase
MRG	Mas-related gene
MRGPR	Mas-related gene protein receptor
mRNA	messenger RNA
MS	mass spectroscopy
NMR	nuclear magnetic resonance
NGF	Nerve growth factor
OD	Optical density
PAMP	Proadrenomedullin N-terminal peptide
PBS	phosphate buffered saline
PCR	polymerase chain reaction
PKA	Protein kinase A
PKC	Protein kinase C
POMS	proopiomelanocortin
PS	Penicilline-Streptomycin solution

Abbreviations

r	reverse
RNA	ribonucleic acid
rpm	rounds per minute
s	second(s)
s.c.	subcutaneous(ly)
SEM	standard error of the mean
SNSR	Sensory neuron specific receptor
SST	Somatostatin
TNF- α	Tumor necrosis factor α
TRPA1	Transient receptor potential A1
TRPV1	Transient receptor potential V1
TTX	Tetrodotoxin
UMP	Uridine monophosphate
WB	Western blotting
wt	wild-type

6. Literature

1. Nathans, J.; Hogness, D.S. Isolation, sequence analysis, and intron-exon arrangement of the gene encoding bovine rhodopsin. *Cell* **1983**, *34*, 807-14
2. Fredriksson, R.; Lagerström, M.C.; Lundin, L.G.; Schiöth, H.B. The G-protein-coupled receptors in the human genome form five main families. Phylogenetic analysis, paralogon groups, and fingerprints. *Mol. Pharmacol.* **2003**, *63*, 1256-72
3. Oldham, W.M.; Hamm, H.E. Heterotrimeric G protein activation by G-protein-coupled receptors. *Nat. Rev. Mol. Cell. Biol.* **2008**, *9*, 60-71
4. Lagerström, M.C.; Schiöth, H.B. Structural diversity of G protein-coupled receptors and significance for drug discovery. *Nat. Rev. Drug Discov.* **2008**, *7*, 339-57
5. Strotmann, R.; Schröck, K.; Bösel, I.; Stäubert, C.; Russ, A.; Schöneberg, T. Evolution of GPCR: change and continuity. *Mol. Cell. Endocrinol.* **2010**, *331*, 170-178
6. Katritch, V.; Cherezov, V.; Stevens, R.C. Diversity and modularity of G protein-coupled receptor structures. *Trends Pharmacol. Sci.* **2011**, *33*, 17-27
7. Overington, J.P.; Al-Lazikani, B.; Hopkins, A.L. How many drug targets are there? *Nat. Rev. Drug Discov.* **2006**, *5*, 993-6
8. Hopkins, A.L.; Groom, C.R. The druggable genome. *Nat. Rev. Drug Discov.* **2002**, *1*, 727-30
9. Garland, S.L. Are GPCRs still a source of new targets? *J. Biomol. Screen.* **2013**, *18*, 947-66
10. Adams, J.L.; Smothers, J.; Srinivasan, R.; Hoos, A. Big opportunities for small molecules in immuno-oncology. *Nat. Rev. Drug Discov.* **2015**, *14*, 603-22
11. van Hecke, O.; Austin, S.K.; Khan, R.A.; Smith, B.H.; Tórrance, N. Neuropathic pain in the general population: a systematic review of epidemiological studies. *Pain* **2014**, *155*, 654-62
12. Calvo, M.; Dawes, J.M.; Bennett, D.L. The role of the immune system in the generation of neuropathic pain. *Lancet Neurol.* **2012**, *11*, 629-42
13. Tórrance, N.; Smith, B.H.; Bennett, M.I.; Lee, A.J. The epidemiology of chronic pain of predominantly neuropathic origin. Results from a general population survey. *J. Pain* **2006**, *7*, 281-9
14. Sacerdote, P.; Franchi, S.; Moretti, S.; Castelli, M.; Proccacci, P.; Magnaghi, V.; Panerai, A.E. Cytokine modulation is necessary for efficacious treatment of experimental neuropathic pain. *J. Neuroimmune Pharmacol.* **2013**, *1*, 202-11
15. Ikoma, A.; Steinhoff, M.; Ständer, S.; Yosipovitch, G.; Schmelz, M. The neurobiology of itch. *Nat. Rev. Neurosci.* **2006**, *7*, 535-47
16. Xiao, B.; Patapoutian, A. Scratching the surface: a role of pain-sensing TRPA1 in itch. *Nat. Neurosci.* **2011**, *14*, 540-2
17. Dong, X.; Han, S.K.; Zylka, M.J.; Simon, M.I.; Anderson, D.J. A Diverse Family of GPCRs Expressed in Specific Subsets of Nociceptive Sensory Neurons. *Cell*, **2001**, *106*, 619-632
18. Lembo, P.M.; Grazzini, E.; Groblewski, T.; O'Donnell, D.; Roy, M.O.; Zhang, J.; Hoffert, C.; Cao, J.; Schmidt, R.; Pelletier, M.; Labarre, M.; Gosselin, M.; Fortin, Y.; Banville, D.; Shen, S.H.; Ström, P.; Payza, K.; Dray, A.; Walker, P.; Ahmad, S. Proenkephalin A gene products activate a new family of sensory neuron-specific GPCRs. *Nat. Neurosci.* **2002**, *3*, 201-9
19. Solinski, H.J.; Gudermann, T.; Breit, A. Pharmacology and signaling of MAS-related G protein-coupled receptors. *Pharmacol. Rev.* **2014**, *3*, 570-97
20. Bader, M.; Alenina, N.; Andrade-Navarro, M.A.; Santos, R.A. MAS and its related G protein-coupled receptors, Mrgprs. *Pharmacol. Rev.* **2014**, *66*, 1080-105
21. Choi, S.S.; Lahn, B.T. Adaptive Evolution of MRG, a Neuron-Specific Gene Family Implicated in Nociception. *Genome Res.* **2003**, *10*, 2252-9
22. Zhang, L.; Taylor, N.; Xie, Y.; Ford, R.; Johnson, J.; Paulsen, J.E.; Bates, B. Cloning and expression of MRG receptors in macaque, mouse, and human. *Mol. Brain Res.* **2005**, *2*, 187-97

23. Burstein, E.S.; Otto, T.R.; Feddock, M.; Ma, J.N.; Fuhs, S.; Wong, S.; Schiffer, H.H.; Braun, M.R.; Nash, N.R. Characterization of the Mas-related gene family: structural and functional conservation of the human and rhesus MrgX receptors. *Br. J. Pharmacol.* **2006**, *147*, 73-82
24. Zylka MJ, Dong X, Southwell AL, Anderson DJ. Atypical expansion in mice of the sensory neuron-specific Mrg G protein-coupled receptor family. *Proc. Natl. Acad. Sci.* **2003**, *100*, 10043-8
25. Molliver, D.C.; Wright, D.E.; Leitner, M.L.; Parsadanian, A.S.; Doster, K.; Wen, D.; Yan, Q.; Snider, W.D. IB4-binding DRG neurons switch from NGF to GDNF dependence in early postnatal life. *Neuron* **1997**, *4*, 849-61
26. Fang, X.; Djouhri, L.; McMullan, S.; Berry, C.; Waxman, S.G.; Okuse, K.; Lawson, S.N. Intense isolectin-B4 binding in rat dorsal root ganglion neurons distinguishes C-fiber nociceptors with broad action potentials and high Nav1.9 expression. *J. Neurosci.* **2006**, *27*, 7281-92
27. Hunt, S.P.; Mantyh, P.W. The molecular dynamics of pain control. *Nat. Rev. Neurosci.* **2001**, *2*, 83-91
28. Malmberg, A.B.; Chen, C.; Tonegawa, S.; Basbaum, A.I. Preserved acute pain and reduced neuropathic pain in mice lacking PKC γ . *Science* **1997**, *5336*, 279-83
29. Zylka, M.J.; Rice, F.L.; Anderson, D.J. Topographically distinct epidermal nociceptive circuits revealed by axonal tracers targeted to Mrgprd. *Neuron* **2005**, *45*, 17-25
30. Liu, Q.; Vrontou, S.; Rice, F.L.; Zylka, M.J.; Dong, X.; Anderson, D.J. Molecular genetic visualization of a rare subset of unmyelinated sensory neurons that may detect gentle touch. *Nat. Neurosci.* **2007**, *10*, 946-8
31. Liu, Y.; Yang, F.C.; Okuda, T.; Dong, X.; Zylka, M.J.; Chen, C.L.; Anderson, D.J.; Kuner, R.; Ma, Q. Mechanisms of compartmentalized expression of Mrg class G-protein-coupled sensory receptors. *J. Neurosci.* **2008**, *28*, 125-32
32. Liu, Q.; Tang, Z.; Surdenikova, L.; Kim, S.; Patel, K.N.; Kim, A.; Ru, F.; Guan, Y.; Weng, H.J.; Geng, Y.; Udem, B.J.; Kollarik, M.; Chen, Z.F.; Anderson, D.J.; Dong, X. Sensory neuron-specific GPCRs Mrgprs are itch receptors mediating chloroquine-induced pruritis. *Cell* **2009**, *7*, 1353-65
33. Wilson, S.R.; Gerhold, K.A.; Bifolck-Fisher, A.; Liu, Q.; Patel, K.N.; Dong, X.; Bautista, D.M. TRPA1 is required for histamine-independent, Mas-related G protein-coupled receptor-mediated itch. *Nat. Neurosci.* **2011**, *14*, 595-602
34. Han, L.; Ma, C.; Liu, Q.; Weng, H.J.; Cui, Y.; Tang, Z.; Kim, Y.; Nie, H.; Qu, L.; Patel, K.N.; Li, Z.; McNeil, B.; He, S.; Guan, Y.; Xiao, B.; Lamotte, R.H.; Dong, X. A subpopulation of nociceptors specifically linked to itch. *Nat. Neurosci.* **2013**, *16*, 174-82
35. LaMotte, R.H.; Dong, X.; Ringkamp, M. Sensory neurons and circuits mediating itch. *Nat. Rev. Neurosci.* **2014**, *15*, 19-31
36. Shinohara, T.; Harada, M.; Ogi, K.; Maruyama, M.; Fujii, R.; Tanaka, H.; Fukusumi, S.; Komatsu, H.; Hosoya, M.; Noguchi, Y.; Watanabe, T.; Moriya, T.; Itoh, Y.; Hinuma, S. Identification of a G protein-coupled receptor specifically responsive to beta-alanine. *J. Biol. Chem.* **2004**, *279*, 23559-64
37. Lautner, R.Q.; Villela, D.C.; Fraga-Silva, R.A.; Silva, N.; Verano-Braga, T.; Costa-Fraga, F.; Jankowski, J.; Jankowski, V.; Sousa, F.; Alzamora, A.; Soares, E.; Barbosa, C.; Kjeldsen, F.; Oliveira, A.; Braga, J.; Savergnini, S.; Maia, G.; Peluso, A.B.; Passos-Silva, D.; Ferreira, A.; Alves, F.; Martins, A.; Raizada, M.; Paula, R.; Motta-Santos, D.; Klempin, F.; Pimenta, A.; Alenina, N.; Sinisterra, R.; Bader, M.; Campagnole-Santos, M.J.; Santos, R.A. Discovery and characterization of alamandine: a novel component of the renin-angiotensin system. *Circ. Res.* **2013**, *112*, 1104-11
38. McNeil, B.; Dong, X. Mrgprs as Itch Receptors. *Itch: Mechanisms and Treatment*. CRC Press, **2014**, Chapter 12
39. Bender, E.; Buist, A.; Jurzak, M.; Langlois, X.; Baggerman, G.; Verhasselt, P.; Ercken, M.; Guo, H.Q.; Wintmolders, C.; Van den Wyngaert, I.; Van Oers, I.; Schoofs, L.; Luyten, W.

- Characterization of an orphan G protein-coupled receptor localized in the dorsal root ganglia reveals adenine as a signaling molecule. *Proc. Natl. Acad. Sci.* **2002**, *99*, 8573–8578
40. von Kügelgen, I.; Schiedel, A.C.; Hoffmann, K.; Alsdorf, B.B.; Abdelrahman, A.; Müller, C.E. Cloning and functional expression of a novel Gi protein-coupled receptor for adenine from mouse brain. *Mol. Pharmacol.* **2008**, *73*, 469-77
41. Thimm, D.; Knospe, M.; Abdelrahman, A.; Moutinho, M.; Alsdorf, B.B.; von Kügelgen, I.; Schiedel, A.C.; Müller, C.E. Characterization of new G protein-coupled adenine receptors in mouse and hamster. *Purinergic Signal.* **2013**, *9*, 415-26
42. Han, S.K.; Dong, X.; Hwang, J.I.; Zylka, M.J.; Anderson, D.J.; Simon, M.I. Orphan G protein-coupled receptors MrgA1 and MrgC11 are distinctively activated by RF-amide-related peptides through the Galpha q/11 pathway. *Proc. Natl. Acad. Sci.* **2002**, *99*, 14740-5
43. Grazzini, E.; Puma, C.; Roy, M.O.; Yu, X.H.; O'Donnell, D.; Schmidt, R.; Dautrey, S.; Ducharme, J.; Perkins, M.; Panetta, R.; Laird, J.M.; Ahmad, S.; Lembo, P.M. Sensory neuron-specific receptor activation elicits central and peripheral nociceptive effects in rats. *Proc. Natl. Acad. Sci.* **2004**, *101*, 7175-80
44. Lee, M.G.; Dong, X.; Liu, Q.; Patel, K.N.; Choi, O.H.; Vonakis, B.; Udem, B.J. Agonists of the MAS-related gene (Mrgs) orphan receptors as novel mediators of mast cell-sensory nerve interactions. *J. Immunol.* **2008**, *180*, 2251-5
45. Hin, N.; Alt, J.; Zimmermann, S.C.; Delahanty, G.; Ferraris, D.V.; Rojas, C.; Li, F.; Liu, Q.; Dong, X.; Slusher, B.S.; Tsukamoto, T. Peptidomimetics of Arg-Phe-NH₂ as small molecule agonists of Mas-related gene C (MrgC) receptors. *Bioorg. Med. Chem.* **2014**, *22*, 5831-7
46. Hook, V.; Funkelstein, L.; Lu, D.; Bark, S.; Wegrzyn, J.; Hwang, S.R. Proteases for processing proneuropeptides into peptide neurotransmitters and hormones. *Annu. Rev. Pharmacol. Toxicol.* **2008**, *48*, 393-423
47. Hook, V.; Bark, S.; Gupta, N.; Lortie, M.; Lu, W.D.; Bandeira, N.; Funkelstein, L.; Wegrzyn, J.; O'Connor, D.T.; Pevzner, P. Neuropeptidomic components generated by proteomic functions in secretory vesicles for cell-cell communication. *AAPS. J.* **2010**, *12*, 635-45
48. Höllt, V. Multiple endogenous peptides. *Trends Neurosci.* **1983**, *6*, 24-6
49. Mizuno, K.; Minamino, N.; Kangawa, K.; Matsuo, H. A new family of endogenous "big" Met-enkephalins from bovine adrenal medulla: purification and structure of docosa- (BAM-22P) and eicosapeptide (BAM-20P) with very potent opiate activity. *Biochem. Biophys. Res. Commun.* **1980**, *97*, 1283-90
50. Davis, T.P.; Hoyer, G.L.; Davis, P.; Burks, T.F. Proenkephalin A-derived peptide E and its fragments alter opioid contractility in the small intestine. *Eur. J. Pharmacol.* **1990**, *191*, 253-61
51. Goumon, Y.; Lugardon, K.; Gadroy, P.; Strub, J.M.; Welters, I.D.; Stefano, G.B.; Aunis, D.; Metz-Boutigue, M.H. Processing of proenkephalin-A in bovine chromaffin cells. Identification of natural derived fragments by N-terminal sequencing and matrix-assisted laser desorption ionization-time of flight mass spectrometry. *J. Biol. Chem.* **2000**, *275*, 38355-62
52. Goumon, Y.; Strub, J.M.; Moniatte, M.; Nullans, G.; Poteur, L.; Hubert, P.; Van Dorsselaer, A.; Aunis, D.; Metz-Boutigue, M.H. The C-terminal bisphosphorylated proenkephalin-A-(209-237)-peptide from adrenal medullary chromaffin granules possesses antibacterial activity. *Eur. J. Biochem.* **1996**, *235*, 516-25
53. Swain, M.G.; MacArthur, L.; Vergalla, J.; Jones, E.A. Adrenal secretion of BAM-22P, a potent opioid peptide, is enhanced in rats with acute cholestasis. *Am. J. Physiol.* **1994**, *266*, 201-5
54. Solinski, H.J.; Boekhoff, I.; Bouvier, M.; Gudermann, T.; Breit, A. Sensory neuron-specific Mas-related gene-X1 receptors resist agonist-promoted endocytosis. *Mol. Pharmacol.* **2010**, *2*, 249-59
55. Kunapuli, P.; Lee, S.; Zheng, W.; Alberts, M.; Kornienko, O.; Mull, R.; Kreamer, A.; Hwang, J.I.; Simon, M.I.; Strulovici, B. Identification of small molecule antagonists of the human mas-related gene-X1 receptor. *Anal. Biochem.* **2006**, *1*, 50-61

56. Liu, Q.; Wenig, H.J.; Patel, K.N.; Tang, Z.; Bai, H.; Steinhoff, M.; Dong, X. The distinct roles of two GPCRs, MrgprC11 and PAR2, in itch and hyperalgesia. *Sci. Signal.* **2011**, *4*, ra45
57. Zeng, X.; Huang, H.; Hong, Y. Effects of intrathecal BAM22 on noxious stimulus-evoked c-fos expression in the rat spinal dorsal horn. *Brain Res.* **2004**, *1028*, 170-9
58. Hong, Y.; Dai, P.; Jiang, J.; Zeng, X. Dual effects of intrathecal BAM22 on nociceptive responses in acute and persistent pain--potential function of a novel receptor. *Br. J. Pharmacol.* **2004**, *141*, 423-30
59. Cai, M.; Chen, T.; Quirion, R.; Hong, Y. The involvement of spinal bovine adrenal medulla 22-like peptide, the proenkephalin derivative, in modulation of nociceptive processing. *Eur. J. Neurosci.* **2007**, *26*, 1128-38
60. Cai, Q.; Jiang, J.; Chen, T.; Hong, Y. Sensory neuron-specific receptor agonist BAM8-22 inhibits the development and expression of tolerance to morphine in rats. *Behav. Brain Res.* **2007**, *178*, 154-9
61. Chen, T.; Hu, Z.; Quirion, R.; Hong, Y. Modulation of NMDA receptors by intrathecal administration of the sensory neuron-specific receptor agonist BAM8-22. *Neuropharmacology* **2008**, *54*, 796-803
62. Guan, Y.; Liu, Q.; Tang, Z.; Raja, S.N.; Anderson, D.J.; Dong, X. Mas-related G-protein-coupled receptors inhibit pathological pain in mice. *Proc. Natl. Acad. Sci.* **2010**, *107*, 15933-8
63. He, S.Q.; Li, Z.; Chu, Y.X.; Han, L.; Xu, Q.; Li, M.; Yang, F.; Liu, Q.; Tang, Z.; Wang, Y.; Hin, N.; Tsukamoto, T.; Slusher, B.; Tiwari, V.; Shechter, R.; Wei, F.; Raja, S.N.; Dong, X.; Guan, Y. MrgC agonism at central terminals of primary sensory neurons inhibits neuropathic pain. *Pain* **2014**, *155*, 534-44
64. Hager, U.A.; Hein, A.; Lennerz, J.K.; Zimmermann, K.; Neuhuber, W.L.; Reeh, P.W. Morphological characterization of rat Mas-related G-protein-coupled receptor C and functional analysis of agonists. *Neuroscience* **2008**, *151*, 242-54
65. Ndong, C.; Pradhan, A.; Puma, C.; Morello, J.P.; Hoffert, C.; Groblewski, T.; O'Donnell, D.; Laird, J.M. Role of rat sensory neuron-specific receptor (rSNSR1) in inflammatory pain: contribution of TRPV1 to SNSR signaling in the pain pathway. *Pain* **2009**, *143*, 130-7
66. Chen, H.; Ikeda, S.R. Modulation of ion channels and synaptic transmission by a human sensory neuron-specific G-protein-coupled receptor, SNSR4/mrgX1, heterologously expressed in cultured rat neurons. *J. Neurosci.* **2004**, *24*, 5044-53
67. Solinski, H.J.; Zierler, S.; Gudermann, T.; Breit, A. Human sensory neuron-specific Mas-related G protein-coupled receptors-X1 sensitize and directly activate transient receptor potential cation channel V1 via distinct signaling pathways. *J. Biol. Chem.* **2012**, *287*, 40956-71
68. Solinski, H.J.; Petermann, F.; Rothe, K.; Boekhoff, I.; Gudermann, T.; Breit, A. Human Mas-related G protein-coupled receptors-X1 induce chemokine receptor 2 expression in rat dorsal root ganglia neurons and release of chemokine ligand 2 from the human LAD-2 mast cell line. *PLoS One* **2013**, *8*, e58756
69. Sikand, P.; Dong, X.; LaMotte, R.H. BAM8-22 peptide produces itch and nociceptive sensations in humans independent of histamine release. *J. Neurosci.* **2011**, *31*, 7563-7
70. Wroblowski, B.; Wigglesworth, M.J.; Szekeres, P.G.; Smith, G.D.; Rahman, S.S.; Nicholson, N.H.; Muir, A.I.; Hall, A.; Heer, J.P.; Garland, S.L.; Coates, W.J. The discovery of a selective, small molecule agonist for the mas-related gene X1 receptor. *J. Med. Chem.* **2009**, *3*, 818-25
71. Malik, L.; Kelly, N.M.; Ma, J.N.; Currier, E.A.; Burstein, E.S.; Olsson, R. Discovery of non-peptidergic MrgX1 and MrgX2 receptor agonists and exploration of an initial SAR using solid-phase synthesis. *Bioorg. Med. Chem. Lett.* **2009**, *6*, 1729-32
72. Bayraktarian, M.; Butterworth, J.; Hu, Y.J.; Santhakumar, V.; Tomaszewski, M.J. Development of 2,4-diaminopyrimidine derivatives as novel SNSR4 antagonists. *Bioorg. Med. Chem. Lett.* **2011**, *21*, 2102-5
73. Wen, W.; Wang, Y.; Li, Z.; Tseng, P.Y.; McManus, O.B.; Wu, M.; Li, M.; Lindsley, C.W.; Dong, X.; Hopkins, C.R. Discovery and characterization of 2-(cyclopropanesulfonamido)-N-(2-

- ethoxyphenyl)benzamide, ML382: a potent and selective positive allosteric modulator of MrgX1. *Chem. Med. Chem.* **2015**, *10*, 57-61
74. Breit, A.; Gagnidze, K.; Devi, L.A.; Lagacé, M.; Bouvier, M. Simultaneous activation of the delta opioid receptor (deltaOR)/sensory neuron-specific receptor-4 (SNSR-4) hetero-oligomer by the mixed bivalent agonist bovine adrenal medulla peptide 22 activates SNSR-4 but inhibits deltaOR signaling. *Mol. Pharmacol.* **2006**, *70*, 686-96
75. Hindson, B.J.; Ness, K.D.; Masquelier, D.A.; Belgrader, P.; Heredia, N.J.; Makarewicz, A.J.; Bright, I.J.; Lucero, M.Y.; Hiddessen, A.L. High-throughput droplet digital PCR system for absolute quantitation of DNA copy number. *Anal. Chem.* **2011**, *83*, 8604-10
76. de Lecea, L.; Criado, J.R.; Prospero-Garcia, O.; Gautvik, K.M.; Schweitzer, P.; Danielson, P.E.; Dunlop, C.L.; Siggins, G.R.; Henriksen, S.J.; Sutcliffe, J.G. A cortical neuropeptide with neuronal depressant and sleep-modulating properties. *Nature* **1996**, *381*, 242-5
77. Tostivint, H.; Lihmann, I.; Bucharles, C.; Vieau, D.; Coulouarn, Y.; Fournier, A.; Conlon, J.M.; Vaudry, H. Occurrence of two somatostatin variants in the frog brain: characterization of the cDNAs, distribution of the mRNAs, and receptor-binding affinities of the peptides. *Proc. Natl. Acad. Sci.* **1996**, *22*, 12605-10
78. Fukusumi, S.; Kitada, C.; Takekawa, S.; Kizawa, H.; Sakamoto, J.; Miyamoto, M.; Hinuma, S.; Kitano, K.; Fujino, M. Identification and characterization of a novel human cortistatin-like peptide. *Biochem. Biophys. Res. Commun.* **1997**, *1*, 157-63
79. Méndez-Díaz, M.; Guevara-Martínez, M.; Alquicira, C.R.; Guzmán Vásquez, K.; Prospéro-García, O. Cortistatin, a modulatory peptide of sleep and memory, induces analgesia in rats. *Neurosci. Lett.* **2004**, *3*, 242-4
80. Muccioli, G.; Papotti, M.; Locatelli, V.; Ghigo, E.; Deghenghi, R. Binding of 125I-labeled ghrelin to membranes from human hypothalamus and pituitary gland. *J. Endocrinol. Invest.* **2001**, *3*, RC7-9
81. Robas, N.; Mead, E.; Fidock, M. MrgX2 is a high potency cortistatin receptor expressed in dorsal root ganglion. *J. Biol. Chem.* **2003**, *45*, 44400-4
82. Broglio, F.; Papotti, M.; Muccioli, G.; Ghigo, E. Brain-gut communication: cortistatin, somatostatin and ghrelin. *Trends Endocrinol. Metab.* **2007**, *6*, 246-51
83. Broglio, F.; Grottoli, S.; Arvat, E.; Ghigo, E. Endocrine actions of cortistatin: in vivo studies. *Mol. Cell. Endocrinol.* **2008**, *1-2*, 123-7
84. Siehler, S.; Nunn, C.; Hannon, J.; Feuerbach, D.; Hoyer, D. Pharmacological profile of somatostatin and cortistatin receptors. *Mol. Cell. Endocrinol.* **2008**, *1-2*, 26-34
85. Gahete, M.D.; Durán-Prado, M.; Luque, R.M.; Martínez-Fuentes, A.J.; Vázquez-Martínez, R.; Malagón, M.M.; Castaño, J.P. Are somatostatin and cortistatin two siblings in regulating endocrine secretions? In vitro work ahead. *Mol. Cell. Endocrinol.* **2008**, *1-2*, 128-34
86. Volante, M.; Rosas, R.; Allia, E.; Granata, R.; Baragli, A.; Muccioli, G.; Papotti, M. Somatostatin, cortistatin and their receptors in tumours. *Mol. Cell. Endocrinol.* **2008**, *1-2*, 219-29
87. Baranowska, B.; Bik, W.; Baranowska-Bik, A.; Wolinska-Witort, E.; Chmielowska, M.; Martynska, L. Cortistatin and pituitary hormone secretion in rat. *J. Physiol. Pharmacol.* **2009**, *1*, 151-6
88. van Hagen, P.M.; Dalm, V.A.; Staal, F.; Hofland, L.J. The role of cortistatin in the human immune system. *Mol. Cell. Endocrinol.* **2008**, *1-2*, 141-7
89. Capuano, A.; Currò, D.; Navarra, P.; Tringali, G. Cortistatin modulates calcitonin gene-related peptide release from neuronal tissues of rat. Comparison with somatostatin. *Peptides* **2011**, *1*, 138-43
90. Gonzalez-Rey, E.; Varela, N.; Sheibanie, A.F.; Chorny, A.; Ganea, D.; Delgado, M. Cortistatin, an antiinflammatory peptide with therapeutic action in inflammatory bowel disease. *Proc. Natl. Acad. Sci. U S A.* **2006**, *11*, 4228-33
91. Gonzalez-Rey, E.; Chorny, A.; Robledo, G.; Delgado, M. Cortistatin, a new antiinflammatory peptide with therapeutic effect on lethal endotoxemia. *J. Exp. Med.* **2006**, *3*, 563-71

92. Morell, M.; Camprubí-Robles, M.; Culler, MD.; de Lecea, L.; Delgado, M. Cortistatin attenuates inflammatory pain via spinal and peripheral actions. *Neurobiol. Dis.* **2014**, *63*, 141-54
93. Kamohara, M.; Matsuo, A.; Takasaki, J.; Kohda, M.; Matsumoto, M.; Matsumoto, S.; Soga, T.; Hiyama, H.; Kobori, M.; Katou, M. Identification of MrgX2 as a human G-protein-coupled receptor for proadrenomedullin N-terminal peptides. *Biochem. Biophys. Res. Commun.* **2005**, *4*, 1146-52
94. Akuzawa, N.; Obinata, H.; Izumi, T.; Takeda, S. Morphine is an exogenous ligand for MrgX2, a G protein-coupled receptor for cortistatin. *J. Cell Anim. Biol.* **2009**, *12*, 216-221
95. Southern, C.; Cook, J.M.; Neetoo-Isseljee, Z.; Taylor, D.L.; Kettleborough, C.A.; Merritt, A.; Bassoni, D.L.; Raab, W.J.; Quinn, E.; Wehrman, T.S.; Davenport, A.P.; Brown, A.J.; Green, A.; Wigglesworth, M.J.; Rees, S. Screening β -arrestin recruitment for the identification of natural ligands for orphan G-protein-coupled receptors. *J. Biomol. Screen.* **2013**, *18*, 599-609
96. Johnson, T.; Siegel, D. Complanadine A, a selective agonist for the Mas-related G protein-coupled receptor X2. *Bioorg. Med. Chem. Lett.* **2014**, *15*, 3512-5
97. Okayama, Y.; Saito, H.; Ra, C. Targeting human mast cells expressing g-protein-coupled receptors in allergic diseases. *Allergol. Int.* **2008**, *3*, 197-203
98. Tatemoto, K.; Nozaki, Y.; Tsuda, R.; Konno, S.; Tomura, K.; Furuno, M.; Ogasawara, H.; Edamura, K.; Takagi, H.; Iwamura, H.; Noguchi, M.; Naito, T. Immunoglobulin E-independent activation of mast cell is mediated by Mrg receptors. *Biochem. Biophys. Res. Commun.* **2006**, *4*, 1322-8
99. Subramanian, H.; Kashem, S.W.; Collington, S.J.; Qu, H.; Lambris, J.D.; Ali, H. PMX-53 as a dual CD88 antagonist and an agonist for Mas-related gene 2 (MrgX2) in human mast cells. *Mol. Pharmacol.* **2011**, *6*, 1005-13
100. Kashem, S.W.; Subramanian, H.; Collington, S.J.; Magotti, P.; Lambris, J.D.; Ali, H. G protein coupled receptor specificity for C3a and compound 48/80-induced degranulation in human mast cells: roles of Mas-related genes MrgX1 and MrgX2. *Eur. J. Pharmacol.* **2011**, *1-2*, 299-304
101. Subramanian, H.; Gupta, K.; Guo, Q.; Price, R.; Ali, H. Mas-related gene X2 (MrgX2) is a novel G protein-coupled receptor for the antimicrobial peptide LL-37 in human mast cells: resistance to receptor phosphorylation, desensitization, and internalization. *J. Biol. Chem.* **2011**, *52*, 44739-49
102. Tobin, A.B. G-protein-coupled receptor phosphorylation: where, when and by whom. *Br. J. Pharmacol.* **2008**, *153 Suppl 1*, 167-76
103. Subramanian, H.; Gupta, K.; Lee, D.; Bayir, A.K.; Ahn, H.; Ali, H. β -Defensins activate human mast cells via Mas-related gene X2. *J. Immunol.* **2013**, *1*, 345-52
104. Fujisawa, D.; Kashiwakura, J.; Kita, H.; Kikukawa, Y.; Fujitani, Y.; Sasaki-Sakamoto, T.; Kuroda, K.; Nunomura, S.; Hayama, K.; Terui, T.; Ra, C.; Okayama, Y. Expression of Mas-related gene X2 on mast cells is upregulated in the skin of patients with severe chronic urticaria. *J. Allergy. Clin. Immunol.* **2014**, *3*, 622-633
105. Nothacker, H.P.; Wang, Z.; Zeng, H.; Mahata, S.K.; O'Connor, D.T.; Civelli, O. Proadrenomedullin N-terminal peptide and cortistatin activation of MrgX2 receptor is based on a common structural motif. *Eur. J. Pharmacol.* **2005**, *1-2*, 191-3
106. McNeil, B.D.; Pundir, P.; Meeker, S.; Han, L.; Udem, B.J.; Kulka, M.; Dong, X. Identification of a mast-cell-specific receptor crucial for pseudo-allergic drug reactions. *Nature* **2015**, *519*, 237-41
107. Kaisho, Y.; Watanabe, T.; Nakata, M.; Yano, T.; Yasuhara, Y.; Shimakawa, K.; Mori, I.; Sakura, Y.; Terao, Y.; Matsui, H.; Taketomi, S. Transgenic rats overexpressing the human MrgX3 gene show cataracts and an abnormal skin phenotype. *Biochem. Biophys. Res. Commun.* **2005**, *330*, 653-7

108. Kwon, Y.J.; Choi, Y.; Eo, J.; Noh, Y.N.; Gim, J.A.; Jung, Y.D.; Lee, J.R.; Kim, H.S. Structure and Expression Analyses of SVA Elements in Relation to Functional Genes. *Genomics Inform.* **2013**, *11*, 142-8
109. Yoshihara, M.; Ohmiya, H.; Hara, S.; Kawasaki, S.; FANTOM consortium.; Hayashizaki, Y.; Itoh, M.; Kawaji, H.; Tsujikawa, M.; Nishida, K. Discovery of molecular markers to discriminate corneal endothelial cells in the human body. *PLoS One* **2015**, *10*, e0117581
110. Khulan, B.; Cooper, W.N.; Skinner, B.M.; Bauer, J.; Owens, S.; Prentice, A.M.; Belteki, G.; Constancia, M.; Dunger, D.; Affara, N.A. Periconceptional maternal micronutrient supplementation is associated with widespread gender related changes in the epigenome: a study of a unique resource in the Gambia. *Hum. Mol. Genet.* **2012**, *21*, 2086-101
111. Hsu, Y.H.; Liu, Y.; Hannan, M.T.; Maixner, W.; Smith, S.B.; Diatchenko, L.; Golightly, Y.M.; Menz, H.B.; Kraus, V.B.; Doherty, M.; Wilson, A.G.; Jordan, J.M. Genome-wide association meta-analyses to identify common genetic variants associated with hallux valgus in Caucasian and African Americans. *J. Med. Genet.* **2015**, doi: 10.1136/jmedgenet-2015-103142
112. Kroeze, W.K.; Sassano, M.F.; Huang, X.P.; Lansu, K.; McCorvy, J.D.; Giguère, P.M.; Sciaky, N.; Roth, B.L. PRESTO-Tango as an open-source resource for interrogation of the druggable human GPCRome. *Nat. Struct. Mol. Biol.* **2015**, *22*, 362-9
113. Gylfe, A.E.; Kondelin, J.; Turunen, M.; Ristolainen, H.; Katainen, R.; Pitkänen, E.; Kaasinen, E.; Rantanen, V.; Tanskanen, T.; Varjosalo, M.; Lehtonen, H.; Palin, K.; Taipale, M.; Taipale, J.; Renkonen-Sinisalo, L.; Järvinen, H.; Böhm, J.; Mecklin, J.P.; Ristimäki, A.; Kilpivaara, O.; Tuupainen, S.; Karhu, A.; Vahteristo, P.; Aaltonen, L.A. Identification of candidate oncogenes in human colorectal cancers with microsatellite instability. *Gastroenterology* **2013**, *145*, 540-3
114. Kim, M.S.; Pinto, S.M.; Getnet, D.; Nirujogi, R.S.; Manda, S.S.; Chaerkady, R.; Madugundu, A.K.; Kelkar, D.S.; Pandey, A. A draft map of the human proteome. *Nature* **2014**, *509*, 575-81
115. Wilhelm, M.; Schlegl, J.; Hahne, H.; Moghaddas-Gholami, A.; Lieberenz, M.; Savitski, M.M.; Ziegler, E.; Butzmann, L.; Gessulat, S.; Marx, H.; Mathieson, T.; Lemeer, S.; Schnatbaum, K.; Reimer, U.; Wenschuh, H.; Mollenhauer, M.; Slotta-Huspenina, J.; Boese, J.H.; Bantscheff, M.; Gerstmair, A.; Faerber, F.; Kuster, B. Mass-spectrometry-based draft of the human proteome. *Nature* **2014**, *509*, 582-7
116. Shemesh, R.; Toporik, A.; Levine, Z.; Hecht, I.; Rotman, G.; Wool, A.; Dahary, D.; Gofer, E.; Kliger, Y.; Soffer, M.A.; Rosenberg, A.; Eshel, D.; Cohen, Y. Discovery and validation of novel peptide agonists for G-protein-coupled receptors. *J. Biol. Chem.* **2008**, *283*, 34643-9
117. Hong, Y.; Alan, C.; Wei, L.; Bin, W.; Fabiola, S.; Francella, O.; Deborah, N.; Jeremy, C.; Yu, A.C. Lipid G Protein-coupled Receptor Ligand Identification Using β -Arrestin PathHunter™ Assay. *J. Biol. Chem.* **2009**, *284*, 12328–12338
118. Bykov, V.J.; Issaeva, N.; Zache, N.; Shilov, A.; Hultcrantz, M.; Bergman, J.; Selivanova, G.; Wiman, K.G. Reactivation of mutant p53 and induction of apoptosis in human tumor cells by maleimide analogs. *J. Biol. Chem.* **2005**, *280*, 30384-91
119. Honkanen, R.E. Cantharidin, another natural toxin that inhibits the activity of serine/threonine protein phosphatases types 1 and 2A. *FEBS Lett.* **1993**, *330*, 283-6
120. Brown, G.R.; Bamford, A.M.; Bowyer, J.; James, D.S.; Rankine, N.; Tang, E.; Torr, V.; Culbert, E.J. Naphthyl ketones: a new class of Janus kinase 3 inhibitors. *Bioorg. Med. Chem. Lett.* **2000**, *10*, 575-9
121. Bourne, H.; Horuk, R.; Kuhnke, J.; Michel, H. GPCRs: from deorphanization to lead structure identification, **2006**, Springer Verlag
122. Civelli, O.; Reinscheid, R.K.; Zhang, Y.; Wang, Z.; Fredriksson, R.; Schiöth, H.B.G protein-coupled receptor deorphanizations. *Annu. Rev. Pharmacol. Toxicol.* **2013**, *53*, 127-46
123. Romine, J.L.; Martin, S.W.; Meanwell, N.A.; Gribkoff, V.K.; Boissard, C.G.; Dworetzky, S.I.; Natale, J.; Moon, S.; Ortiz, A.; Yeleswaram, S.; Pajor, L.; Gao, Q.; Starrett, J.E. 3-[(5-

- Chloro-2-hydroxyphenyl)methyl]-5-[4-(trifluoromethyl)phenyl]-1,3,4-oxadiazol-2(3H)-one, BMS-191011: opener of large-conductance Ca(2+)-activated potassium (maxi-K) channels, identification, solubility, and SAR. *J. Med. Chem.* **2007**, *50*, 528-42
124. Möller, K.; Wienhöfer, G.; Westerhaus, F.; Junge, K.; Beller, M. Oxidation of 1,2,4-trimethylbenzene (TMB), 2,3,6-trimethylphenol (TMP) and 2-methylnaphthalene to 2,3,5-trimethylbenzoquinone (TMBQ) and menadione (vitamin K₃). *Catal. Today.* **2011**, *173*, 68-75
125. Loor, G.; Kondapalli, J.; Schriewer, J. M.; Chander, N. S.; Hoek, T. L. V.; Schumacker, P. T. Menadione triggers cell death through ROS-dependent mechanisms involving PARP activation without requiring apoptosis. *Free Radic. Biol. Med.* **2010**, *49*, 1925-1936.
126. Lee, J.; Lee, M.; Chung, S.; Chung, J. Menadione-Induced Vascular Endothelial Dysfunction and Its Possible Significance. *Toxicol. Appl. Pharmacol.* **1999**, *161*, 140-145.
127. McAmis, W.; Schaeffer Jr, R. C.; Baynes, J. W.; Wolf, M. B. Menadione causes endothelial barrier failure by a direct effect on intracellular thiols, independent of reactive oxidant production. *Biochim. Biophys. Acta.* **2003**, *1641*, 43-53.
128. Cerqueira, E. C.; Netz, P. A.; Diniz, C.; Canto, V. P.; Follmer, C.; Molecular insights into human monoamine oxidase (MAO) inhibition by 1,4-naphthoquinone: Evidences for menadione (vitamin K₃) acting as a competitive and reversible inhibitor of MAO. *Bioorg. Med. Chem.* **2011**, *19*, 7416-7424.
129. Vita, M. F.; Nagachar, N.; Avramidis, D.; Delwar, Z. M.; Cruz, M. H.; Siden, Å.; Paulsson, K. M.; Yakisich, J. S. Pankiller effect of prolonged exposure to menadione on glioma cells: potentiation by vitamin C. *Invest. New Drugs.* **2011**, *29*, 1314-1320.
130. Adnan, H.; Antenos, M.; Kirby G. M. The effect of menadione on glutathione S-transferase A1 (GSTA1): c-Jun N-terminal kinase (JNK) complex dissociation in human colonic adenocarcinoma Caco-2 cells. *Toxicol. Lett.* **2012**, *214*, 53-62.
131. Katzung, B. G; Masters, S. B.; Trevor, A. J. Vitamin K. *Basic & Clinical Pharmacology*, 9th edition; McGraw Hill: **2004**, pp 778-782.
132. Kenakin, T.; Jenkinson, S.; Watson, C. Determining the potency and molecular mechanism of action of insurmountable antagonists. *J. Pharmacol. Exp. Ther.* **2006**, *319*, 710-23
133. Colquhoun, D. Why the Schild method is better than Schild realised. *Trends Pharmacol. Sci.* **2007**, *28*, 608-14
134. Conn, P.J.; Lindsley, C.W.; Meiler, J.; Niswender, C.M. Opportunities and challenges in the discovery of allosteric modulators of GPCRs for treating CNS disorders. *Nat. Rev. Drug Discov.* **2014**, *13*, 692-708
135. Kenakin, T.; Christopoulos, A. Signalling bias in new drug discovery: detection, quantification and therapeutic impact. *Nat. Rev. Drug Discov.* **2013**, *12*, 205-16
136. Yoshimi, Y.; Watanabe, S.; Shinomiya, T.; Makino, A.; Toyoda, M.; Ikekita, M. Nucleobase adenine as a trophic factor acting on Purkinje cells. *Brain Res.* **2003**, *991*, 113-22
137. Yoshikuni, M.; Ishikawa, K.; Isobe, M.; Goto, T.; Nagahama, Y. Characterization of 1-methyladenine binding in starfish oocyte cortices. *Proc. Natl. Acad. Sci. U S A.* **1988**, *85*, 1874-7
138. Matthews, E.A.; Dickenson, A.H. Effects of spinally administered adenine on dorsal horn neuronal responses in a rat model of inflammation. *Neurosci. Lett.* **2004**, *356*, 211-4
139. Wengert, M.; Adão-Novaes, J.; Assaife-Lopes, N.; Leão-Ferreira, L.R.; Caruso-Neves, C. Adenine-induced inhibition of Na(+)-ATPase activity: Evidence for involvement of the Gi protein-coupled receptor in the cAMP signaling pathway. *Arch. Biochem. Biophys.* **2007**, *467*, 261-7
140. Watanabe, S.; Ikekita, M.; Nakata, H. Identification of specific [3H]adenine-binding sites in rat brain membranes. *J. Biochem.* **2005**, *137*, 323-9
141. Gorzalka, S.; Vittori, S.; Volpini, R.; Cristalli, G.; von Kügelgen, I.; Müller, C.E. Evidence for the functional expression and pharmacological characterization of adenine receptors in native cells and tissues. *Mol. Pharmacol.* **2005**, *67*, 955-64

142. Meunier, J.C.; Mollereau, C.; Toll, L.; Suaudeau, C.; Moisand, C.; Alvinerie, P.; Butour, J.L.; Guillemot, J.C.; Ferrara, P.; Monsarrat, B. Isolation and structure of the endogenous agonist of opioid receptor-like ORL1 receptor. *Nature* **1995**, *377*, 532-5
143. Reinscheid, R.K.; Nothacker, H.P.; Bourson, A.; Ardati, A.; Henningsen, R.A.; Bunzow, J.R.; Grandy, D.K.; Langen, H.; Monsma, F.J.; Civelli, O. Orphanin FQ: a neuropeptide that activates an opioid like G protein-coupled receptor. *Science* **1995**, *270*, 792-4
144. Sakurai, T.; Amemiya, A.; Ishii, M.; Matsuzaki, I.; Chemelli, R.M.; Tanaka, H.; Williams, S.C.; Richardson, J.A.; Kozlowski, G.P.; Wilson, S.; Arch, J.R.; Buckingham, R.E.; Haynes, A.C.; Carr, S.A.; Annan, R.S.; McNulty, D.E.; Liu, W.S.; Terrett, J.A.; Elshourbagy, N.A.; Bergsma, D.J.; Yanagisawa, M. Orexins and orexin receptors: a family of hypothalamic neuropeptides and G protein-coupled receptors that regulate feeding behavior. *Cell* **1998**, *92*, 573-85
145. de Lecea, L.; Kilduff, T.S.; Peyron, C.; Gao, X.; Foye, P.E.; Danielson, P.E.; Fukuhara, C.; Battenberg, E.L.; Gautvik, V.T.; Bartlett, F.S.; Frankel, W.N.; van den Pol, A.N.; Bloom, F.E.; Gautvik, K.M.; Sutcliffe, J.G. The hypocretins: hypothalamus-specific peptides with neuroexcitatory activity. *Proc. Natl. Acad. Sci. U S A* **1998**, *95*, 322-7
146. Hinuma, S.; Habata, Y.; Fujii, R.; Kawamata, Y.; Hosoya, M.; Fukusumi, S.; Kitada, C.; Masuo, Y.; Asano, T.; Matsumoto, H.; Sekiguchi, M.; Kurokawa, T.; Nishimura, O.; Onda, H.; Fujino, M. A prolactin-releasing peptide in the brain. *Nature* **1998**, *393*, 272-6
147. Tatemoto, K.; Hosoya, M.; Habata, Y.; Fujii, R.; Kakegawa, T.; Zou, M.X.; Kawamata, Y.; Fukusumi, S.; Hinuma, S.; Kitada, C.; Kurokawa, T.; Onda, H.; Fujino, M. Isolation and characterization of a novel endogenous peptide ligand for the human APJ receptor. *Biochem. Biophys. Res. Commun.* **1998**, *251*, 471-6
148. Kojima, M.; Hosoda, H.; Date, Y.; Nakazato, M.; Matsuo, H.; Kangawa, K. Ghrelin is a growth-hormone-releasing acylated peptide from stomach. *Nature* **1999**, *402*, 656-60
149. Ramesh, G.; Didier, P.J.; England, J.D.; Santana-Gould, L.; Doyle-Meyers, L.A.; Martin, D.S.; Jacobs, M.B.; Philipp, M.T. Inflammation in the pathogenesis of lyme neuroborreliosis. *Am. J. Pathol.* **2015**, *185*, 1344-60
150. Sylantsev, S.; Jensen, T.P.; Ross, R.A.; Rusakov, D.A. Cannabinoid- and lysophosphatidylinositol-sensitive receptor GPR55 boosts neurotransmitter release at central synapses. *Proc. Natl. Acad. Sci. U S A* **2013**, *110*, 5193-8
151. Rodriguez, J.; Gupta, N.; Smith, R.D.; Pevzner, P.A. Does trypsin cut before proline? *J. Proteome Res.* **2008**, *1*, 300-5
152. Rawlings, N.D.; Barrett, A.J.; Bateman, A. MEROPS: the peptidase database. *Nucleic Acids Res.* **2010**, *38*, 227-33.
153. <http://merops.sanger.ac.uk/inhibitors/>
154. Renko, M.; Sabotič, J.; Turk, D. β -trefoil inhibitors-from the work of Kunitz onward. *Biol. Chem.* **2012**, *10*, 1043-54.
155. Ozawa, K.; Laskowski, M.Jr. The reactive site of trypsin inhibitors. *J. Biol. Chem.* **1966**, *17*, 3955-61
156. Steiner, R.F.; Frattali, V. Purification and properties of soybean protein inhibitors of proteolytic enzymes. *J. Agr. Food Chem.* **1969**, *3*, 315-18
157. Murzin, A.G.; Lesk, A.M.; Chothia, C. beta-Trefoil fold, Patterns of structure and sequence in the Kunitz inhibitors interleukins-1 beta and 1 alpha and fibroblast growth factors. *J. Mol. Biol.* **1992**, *2*, 531-43
158. McMahan, C.J.; Slack, J.L.; Mosley, B.; Cosman, D.; Lupton, S.D.; Brunton, L.L.; Grubin, C.E.; Wignall, J.M.; Jenkins, N.A.; Brannan, C.I. A novel IL-1 receptor, cloned from B cells by mammalian expression, is expressed in many cell types. *EMBO J.* **1991**, *10*, 2821-32
159. Sims, J.E.; Acres, R.B.; Grubin, C.E.; McMahan, C.J.; Wignall, J.M.; March, C.J.; Dower, S.K. Cloning the interleukin 1 receptor from human T cells. *Proc. Natl. Acad. Sci. U S A.* **1989**, *22*, 8946-50.

160. Huang, J.; Gao, X.; Li, S.; Cao, Z. Recruitment of IRAK to the interleukin 1 receptor complex requires interleukin 1 receptor accessory protein. *Proc. Natl. Acad. Sci. U S A.* **1997**, *24*, 12829-32.
161. Volpe, F.; Clatworthy, J.; Kaptein, A.; Maschera, B.; Griffin, AM.; Ray, K. The IL1 receptor accessory protein is responsible for the recruitment of the interleukin-1 receptor associated kinase to the IL1/IL1 receptor I complex. *FEBS Lett.* **1997**, *1*, 41-4.
162. Munts, A.G.; Zijlstra, F.J.; Nibbering, P.H.; Daha, M.R.; Marinus, J.; Dahan, A.; van Hilten, J.J. Analysis of cerebrospinal fluid inflammatory mediators in chronic complex regional pain syndrome related dystonia. *Clin. J. Pain.* **2008**, *1*, 30-4
163. Balosso, S.; Maroso, M.; Sanchez-Alavez, M.; Ravizza, T.; Frasca, A.; Bartfai, T.; Vezzani, A. A novel non-transcriptional pathway mediates the proconvulsive effects of interleukin-1beta. *Brain* **2008**, *131*, 3256-65
164. Yan, X.; Weng, H.R. Endogenous interleukin-1 β in neuropathic rats enhances glutamate release from the primary afferents in the spinal dorsal horn through coupling with presynaptic N-methyl-D-aspartic acid receptors. *J. Biol. Chem.* **2013**, *288*, 30544-57
165. Copray, J.C.; Mantingh, I.; Brouwer, N.; Biber, K.; Küst, B.M.; Liem, R.S.; Huitinga, I.; Tilders, F.J.; Van Dam, A.M. Boddeke, H.W. Expression of interleukin-1 beta in rat dorsal root ganglia. *J. Neuroimmunol.* **2001**, *118*, 203-11
166. Takeda, M.; Takahashi, M.; Matsumoto, S. Contribution of activated interleukin receptors in trigeminal ganglion neurons to hyperalgesia via satellite glial interleukin-1 beta paracrine mechanism. *Brain Behav. Immun.* **2008**, *22*, 1016-23
167. Binshtok, A.M.; Wang, H.; Zimmermann, K.; Amaya, F.; Vardeh, D.; Shi, L.; Brenner, G.J.; Ji, R.R.; Bean, B.P.; Woolf, C.J.; Samad, T.A. Nociceptors are interleukin-1beta sensors. *J. Neurosci.* **2008**, *28*, 14062-73
168. Basha, E.; Friedrich, K.L.; Vierling, E. The N-terminal arm of small heat shock proteins is important for both chaperone activity and substrate specificity. *J. Biol. Chem.* **2006**, *281*, 39943-52
169. Sahoo, S.K.; Shaikh, S.A.; Sopariwala, D.H.; Bal, N.C.; Bruhn, D.S.; Kopec, W.; Khandelia, H.; Periasamy, M. The N Terminus of Sarcolipin Plays an Important Role in Uncoupling Sarco-endoplasmic Reticulum Ca²⁺-ATPase (SERCA) ATP Hydrolysis from Ca²⁺ Transport. *J. Biol. Chem.* **2015**, *290*, 14057-67
170. Schönbeck, U.; Mach, F.; Libby, P. Generation of biologically active IL-1 beta by matrix metalloproteinases: a novel caspase-1-independent pathway of IL-1 beta processing. *J. Immunol.* **1998**, *161*, 3340-6
171. Ito, A.; Mukaiyama, A.; Itoh, Y.; Nagase, H.; Thogersen, I.B.; Enghild, J.J.; Sasaguri, Y.; Mori, Y. Degradation of interleukin 1beta by matrix metalloproteinases. *J. Biol. Chem.* **1996**, *25*, 14657-60.
172. Lakhan, S.E.; Avramut, M. Matrix metalloproteinases in neuropathic pain and migraine: friends, enemies, and therapeutic targets. *Pain Res. Treat.* **2012**, 2012:952906
173. Dufour, A.; Overall, C.M. Missing the target: matrix metalloproteinase antitargets in inflammation and cancer. *Trends Pharmacol. Sci.* **2013**, *34*, 233-42
174. Khokha, R.; Murthy, A.; Weiss, A. Metalloproteinases and their natural inhibitors in inflammation and immunity. *Nat. Rev. Immunol.* **2013**, *13*, 649-65
175. Chattopadhyay, S.; Myers, R.R.; Janes, J.; Shubayev, V. Cytokine regulation of MMP-9 in peripheral glia: implications for pathological processes and pain in injured nerve. *Brain Behav. Immun.* **2007**, *21*, 561-8
176. Kawasaki, Y.; Xu, Z.Z.; Wang, X.; Park, J.Y.; Zhuang, Z.Y.; Tan, P.H.; Gao, Y.J.; Roy, K.; Corfas, G.; Lo, E.H.; Ji, R.R. Distinct roles of matrix metalloproteases in the early- and late-phase development of neuropathic pain. *Nat. Med.* **2008**, *14*, 331-6
177. Nishida, K.; Kuchiwa, S.; Oiso, S.; Futagawa, T.; Masuda, S.; Takeda, Y.; Yamada, K. Up-regulation of matrix metalloproteinase-3 in the dorsal root ganglion of rats with paclitaxel-induced neuropathy. *Cancer Sci.* **2008**, *99*, 1618-25

178. Berta, T.; Liu, T.; Liu, Y.C.; Xu, Z.Z.; Ji, R.R. Acute morphine activates satellite glial cells and up-regulates IL-1 β in dorsal root ganglia in mice via matrix metalloproteinase-9. *Mol. Pain* **2012**, *22*, 8-18
179. Liu, Y.C.; Berta, T.; Liu, T.; Tan, P.H.; Ji, R.R. Acute morphine induces matrix metalloproteinase-9 up-regulation in primary sensory neurons to mask opioid-induced analgesia in mice. *Mol. Pain* **2012**, *25*, 8-19
180. McQuibban, G.A.; Gong, J.H.; Tam, E.M.; McCulloch, C.A.; Clark-Lewis, I.; Overall, C.M. Inflammation dampened by gelatinase A cleavage of monocyte chemoattractant protein-3. *Science* **2000**, *289*, 1202-6
181. McQuibban, G.A.; Gong, J.H.; Wong, J.P.; Wallace, J.L.; Clark-Lewis, I.; Overall, C.M. Matrix metalloproteinase processing of monocyte chemoattractant proteins generates CC chemokine receptor antagonists with anti-inflammatory properties in vivo. *Blood* **2002**, *100*, 1160-7
182. Starr, A.E.; Dufour, A.; Maier, J.; Overall, C.M. Biochemical analysis of matrix metalloproteinase activation of chemokines CCL15 and CCL23 and increased glycosaminoglycan binding of CCL16. *J. Biol. Chem.* **2012**, *287*, 5848-60
183. Cox, J. H.; Overall, C. M. Cytokine Substrates: MMP Regulation of Inflammatory Signaling Molecules, *The Cancer Degradome: Proteases and Cancer Biology*, **2008**, 517-538. Springer Verlag
184. Fortelny, N.; Pavlidis, P.; Overall, C.M. The path of no return--Truncated protein N-termini and current ignorance of their genesis. *Proteomics* **2015**, *15*, 2547-52
185. Tanco, S.; Gevaert, K.; Van Damme, P. C-terminomics: Targeted analysis of natural and posttranslationally modified protein and peptide C-termini. *Proteomics* **2015**, *15*, 903-14
186. Marino, G.; Eckhard, U.; Overall, C.M. Protein Termini and Their Modifications Revealed by Positional Proteomics. *ACS Chem. Biol.* **2015**, *10*, 1754-64
187. Repnik, U.; Starr, A.E.; Overall, C.M.; Turk, B. Cysteine Cathepsins Activate ELR Chemokines and Inactivate Non-ELR Chemokines. *J. Biol. Chem.* **2015**, *290*, 13800-11
188. Reddy, V.B.; Sun, S.; Azimi, E.; Elmariah, S.B.; Dong, X.; Lerner, E.A. Redefining the concept of protease-activated receptors: cathepsin S evokes itch via activation of Mrgprs. *Nat. Commun.* **2015**, doi: 10.1038/ncomms8864
189. Kay, J.; Calabrese, L. The role of interleukin-1 in the pathogenesis of rheumatoid arthritis. *Rheumatology* **2004**, *43*, Suppl 3:iii2-iii9
190. Roberts, D.J.; Jenne, C.N.; Léger, C.; Kramer, A.H.; Gallagher, C.N.; Todd, S.; Parney, I.F.; Doig, C.J.; Yong, V.W.; Kubes, P.; Zygum, D.A. Association between the cerebral inflammatory and matrix metalloproteinase responses after severe traumatic brain injury in humans. *J. Neurotrauma* **2013**, *30*, 1727-36
191. Symons, J.A.; Eastgate, J.A.; Duff, G.W. Purification and characterization of a novel soluble receptor for interleukin 1. *J. Exp. Med.* **1991**, *174*, 1251-4
192. Jobling, S.A.; Auron, P.E.; Gurka, G.; Webb, A.C.; McDonald, B.; Rosenwasser, L.J.; Gehrke, L. Biological activity and receptor binding of human prointerleukin-1 beta and subpeptides. *J. Biol. Chem.* **1988**, *263*, 16372-8
193. Pertwee, R.G.; Howlett, A.C.; Abood, M.E.; Alexander, S.P.; Di Marzo, V.; Elphick, M.R.; Greasley, P.J.; Hansen, H.S.; Kunos, G.; Mackie, K.; Mechoulam, R.; Ross R.A. International Union of Basic and Clinical Pharmacology. LXXIX. Cannabinoid receptors and their ligands: beyond CB₁ and CB₂. *Pharmacol. Rev.* **2010**, *62*, 588-631
194. Ross, R.A. The enigmatic pharmacology of GPR55. *Trends Pharmacol. Sci.* **2009**, *30*, 156-63
195. Lile, J.A.; Kelly, T.H.; Hays, L.R. Separate and combined effects of the GABAA positive allosteric modulator diazepam and Δ^9 -THC in humans discriminating Δ^9 -THC. *Drug Alcohol Depend.* **2014**, *143*, 141-8

196. Vollmann, K.; Qurishi, R.; Hockemeyer, J.; Müller, C.E. Synthesis and properties of a new water-soluble prodrug of the adenosine A2A receptor antagonist MSX-2. *Molecules* **2008**, *2*, 348-59
197. Müller, C.E.; Sauer, R.; Maurinsh, Y.; Huertas, R.; Fülle, F.; Klotz, K.N.; Nagel, J.; Hauber, W. A2A-selective adenosine receptor antagonists: development of water-soluble prodrugs and a new tritiated radioligand. *Drug Dev. Res.* **1998**, *45*, 190-7
198. Sauer, R.; Maurinsh, Y.; Reith, U.; Fülle, F.; Klotz, K.N.; Müller, C.E. Water soluble phosphate prodrug of 1-propargyl-8-Styrylxanthine derivatives, A(2A)-selective adenosine receptor antagonists. *J. Med. Chem.* **2000**, *43*, 440-8
199. 8-Ethynylxanthine derivatives as selective A2A receptor antagonists, Patent number: EP1939197 A1
200. Sassi, Y.; Ahles, A.; Truong, D.J.; Baqi, Y.; Lee, S.Y.; Husse, B.; Hulot, J.S.; Foinquinos, A.; Thum, T.; Müller, C.E.; Dendorfer, A.; Lagerbauer, B.; Engelhardt, S. Cardiac myocyte-secreted cAMP exerts paracrine action via adenosine receptor activation. *J. Clin. Invest.* **2014**, *124*, 5385-97
201. Ujházy, P.; Berleth, E.S.; Pietkiewicz, J.M.; Kitano, H.; Skaar, J.R.; Ehrke, M.J.; Mihich, E. Evidence for the involvement of ecto-5'-nucleotidase (CD73) in drug resistance. *Int. J. Cancer* **1996**, *68*, 493-500
202. Chambers, S.M.; Fasano, C.A.; Papapetrou, E.P.; Tomishima, M.; Sadelain, M.; Studer, L. Highly efficient neural conversion of human ES and iPS cells by dual inhibition of SMAD signaling. *Nat. Biotechnol.* **2009**, *27*, 275-80
203. Chambers, S.M.; Qi, Y.; Mica, Y.; Lee, G.; Zhang, X.J.; Niu, L.; Bilslund, J.; Cao, L.; Stevens, E.; Whiting, P.; Shi, S.H.; Studer, L. Combined small-molecule inhibition accelerates developmental timing and converts human pluripotent stem cells into nociceptors. *Nat. Biotechnol.* **2012**, *30*, 715-20
204. Young, G.T.; Gutteridge, A.; Fox, H.D.; Wilbrey, A.L.; Cao, L.; Cho, L.T.; Brown, A.R.; Benn, C.L.; Kammonen, L.R.; Friedman, J.H.; Bictash, M.; Whiting, P.; Bilslund, J.G.; Stevens, E.B. Characterizing human stem cell-derived sensory neurons at the single-cell level reveals their ion channel expression and utility in pain research. *Mol. Ther.* **2014**, *22*, 1530-43
205. Kumar, T.S.; Zhou, S.Y.; Joshi, B.V.; Balasubramanian, R.; Yang, T.; Liang, B.T.; Jacobson, K.A. Structure-activity relationship of (N)-Methanocarba phosphonate analogues of 5'-AMP as cardioprotective agents acting through a cardiac P2X receptor. *J. Med. Chem.* **2010**, *53*, 2562-76
206. Hinz, S.; Lacher, S.K.; Seibt, B.F.; Müller, C.E. BAY60-6583 acts as a partial agonist at adenosine A2B receptors. *J. Pharmacol. Exp. Ther.* **2014**, *349*, 427-36
207. Schrage, R.; De Min, A.; Hochheiser, K.; Kostenis, E.; Mohr, K. Superagonism at G protein-coupled receptors and beyond. *Br. J. Pharmacol.* **2015**, doi: 10.1111/bph.13278
208. Singh, N.,; Jabeen, T.; Somvanshi, R.K.; Sharma, S.; Dey, S.; Singh, T.P. Phospholipase A2 as a target protein for nonsteroidal anti-inflammatory drugs (NSAIDs): crystal structure of the complex formed between phospholipase A2 and oxyphenbutazone at 1.6 Å resolution. *Biochemistry* **2004**, *43*, 14577-83
209. Gaucher, A.; Netter, P.; Faure, G.; Schoeller, J.P.; Gerardin, A. Diffusion of oxyphenbutazone into synovial fluid, synovial tissue, joint cartilage and cerebrospinal fluid. *Eur. J. Clin. Pharmacol.* **1983**, *25*, 107-12
210. Walter, M.; Lemoine, H.; Kaumann, A.J. Stimulant and blocking effects of optical isomers of pindolol on the sinoatrial node and trachea of guinea pig. Role of beta-adrenoceptor subtypes in the dissociation between blockade and stimulation. *Naunyn Schmiedebergs Arch. Pharmacol.* **1984**, *327*, 159-75
211. Corradetti, R.; Laaris, N.; Hanoun, N.; Laporte, A.M.; Le Poul, E.; Hamon, M.; Lanfumey, L. Antagonist properties of (-)-pindolol and WAY 100635 at somatodendritic and postsynaptic 5-HT1A receptors in the rat brain. *Br. J. Pharmacol.* **1998**, *123*, 449-62

212. Oriowo, M.A.; Chapman, H.; Kirkham, D.M.; Sennitt, M.V.; Ruffolo, R.R.; Cawthorne, M.A. The selectivity in vitro of the stereoisomers of the beta-3 adrenoceptor agonist BRL 37344. *J. Pharmacol. Exp. Ther.* **1996**, *277*, 22-7
213. Urwyler, S.; Laurie, D.; Lowe, D.A.; Meier, C.L.; Müller, W. Biphenyl-derivatives of 2-amino-7-phosphonoheptanoic acid, a novel class of potent competitive N-methyl-D-aspartate receptor antagonist--I. Pharmacological characterization in vitro. *Neuropharmacology* **1996**, *35*, 643-54
214. Stebbins, J.L.; De, S.K.; Machleidt, T.; Becattini, B.; Vazquez, J.; Kuntzen, C.; Chen, L.H.; Cellitti, J.F.; Riel-Mehan, M.; Emdadi, A.; Solinas, G.; Karin, M.; Pellecchia, M. Identification of a new JNK inhibitor targeting the JNK-JIP interaction site. *Proc. Natl. Acad. Sci. U S A.* **2008**, *105*, 16809-13
215. Guo, W.; Wu, S.; Liu, J.; Fang, B. Identification of a small molecule with synthetic lethality for K-ras and protein kinase C iota. *Cancer Res.* **2008**, *68*, 7403-8
216. Alnouri, M.W.; Jepards, S.; Casari, A.; Schiedel, A.C.; Hinz, S.; Müller, C.E. Selectivity is species-dependent: Characterization of standard agonists and antagonists at human, rat, and mouse adenosine receptors. *Purinergic Signal.* **2015**, *11*, 389-407
217. Jaakola, V.P.; Griffith, M.T.; Hanson, M.A.; Cherezov, V.; Chien, E.Y.; Lane, J.R.; Ijzerman, A.P.; Stevens, R.C. The 2.6 angstrom crystal structure of a human A_{2A} adenosine receptor bound to an antagonist. *Science* **2008**, *5905*, 1211-7
218. Xu, F.; Wu, H.; Katritch, V.; Han, G.W.; Jacobson, K.A.; Gao Z.G.; Cherezov, V.; Stevens, R.C. Structure of an agonist-bound human A_{2A} adenosine receptor. *Science* **2011**, *6027*, 322-7
219. Doré, A.S.; Robertson, N.; Errey, J.C.; Ng, I.; Hollenstein, K.; Tehan, B.; Hurrell, E.; Bennett, K.; Congreve, M.; Magnani, F.; Tate, C.G.; Weir, M.; Marshall, F.H. Structure of the adenosine A(2A) receptor in complex with ZM241385 and the xanthines XAC and caffeine. *Structure* **2011**, *19*, 1283-93
220. Zhang, K.; Zhang, J.; Gao, Z.G.; Zhang, D.; Zhu, L.; Han, G.W.; Moss, S.M.; Paoletta, S.; Kiselev, E.; Lu, W.; Fenalti, G.; Zhang, W.; Müller, C.E.; Yang, H.; Jiang, H.; Cherezov, V.; Katritch, V.; Jacobson, K.A.; Stevens, R.C.; Wu, B.; Zhao, Q. Structure of the human P2Y₁₂ receptor in complex with an antithrombotic drug. *Nature* **2014**, *509*, 115-8
221. Zhang, K.; Zhang, J.; Gao, Z.G.; Paoletta, S.; Zhang, D.; Han, G.W.; Li, T.; Ma, L.; Zhang, W.; Müller, C.E.; Yang, H.; Jiang, H.; Cherezov, V.; Katritch, V.; Jacobson, K.A.; Stevens, R.C.; Wu, B.; Zhao, Q. Agonist-bound structure of the human P2Y₁₂ receptor. *Nature* **2014**, *509*, 119-22
222. Fan, S.F.; Shen, K.F.; Scheideler, M.A.; Crain, S.M. F11 neuroblastoma x DRG neuron hybrid cells express inhibitory mu- and delta-opioid receptors which increase voltage-dependent K⁺ currents upon activation. *Brain Res.* **1992**, *590*, 329-33
223. Grienberger, C.; Konnerth, A. Imaging calcium in neurons. *Neuron* **2012**, *73*, 862-85
224. Platika, D.; Boulos, M.H.; Baizer, L.; Fishman, M.C. Neuronal traits of clonal cell lines derived by fusion of dorsal root ganglia neurons with neuroblastoma cells. *Proc. Natl. Acad. Sci. U S A.* **1985**, *82*, 3499-503
225. Le Gall-Ianotto, C.; Andres, E.; Hurtado, S.P.; Pereira, U.; Misery, L. Characterization of the first coculture between human primary keratinocytes and the dorsal root ganglion-derived neuronal cell line F-11. *Neuroscience* **2012**, *210*, 47-57
226. Feng, Y.; De Franceschi, G.; Kahraman, A.; Soste, M.; Melnik, A.; Boersema, P.J.; de Laureto, P.P.; Nikolaev, Y.; Oliveira, A.P.; Picotti, P. Global analysis of protein structural changes in complex proteomes. *Nat. Biotechnol.* **2014**, *32*, 1036-44
227. Deshmukh, U.S.; Bagavant, H. When killers become helpers. *Sci. Transl. Med.* **2013**, *5*, 195fs29
228. Poli, A.; Michel, T.; Thérésine, M.; Andrès, E.; Hentges, F.; Zimmer, J. CD56bright natural killer (NK) cells: an important NK cell subset. *Immunology* **2009**, *126*, 458-65

229. Knizhnik, A.V.; Roos, W.P.; Nikolova, T.; Quiros, S.; Tomaszowski, K.H.; Christmann, M.; Kaina, B. Survival and death strategies in glioma cells: autophagy, senescence and apoptosis triggered by a single type of temozolomide-induced DNA damage. *PLoS One* **2013**, *8*, e55665
230. Kenakin, T. Efficacy at G-protein-coupled receptors. *Nat. Rev. Drug Discov.* **2002**, *1*, 103-10
231. Raehal, K.M.; Walker, J.K.; Bohn, L.M. Morphine side effects in beta-arrestin 2 knockout mice. *J. Pharmacol. Exp. Ther.* **2005**, *314*, 1195-201
232. Bohn, L.M.; Lefkowitz, R.J.; Gainetdinov, R.R.; Peppel, K.; Caron, M.G.; Lin, F.T. Enhanced morphine analgesia in mice lacking beta-arrestin 2. *Science* **1999**, *286*, 2495-8
233. Rajagopal, K.; Whalen, E.J.; Violin, J.D.; Stiber, J.A.; Rosenberg, P.B.; Premont, R.T.; Coffman, T.M.; Rockman, H.A.; Lefkowitz, R.J. Beta-arrestin2-mediated inotropic effects of the angiotensin II type 1A receptor in isolated cardiac myocytes. *Proc. Natl. Acad. Sci. U S A.* **2006**, *103*, 16284-9
234. Wei, H.; Ahn, S.; Shenoy, S.K.; Karnik, S.S.; Hunyady, L.; Luttrell, L.M.; Lefkowitz, R.J. Independent beta-arrestin 2 and G protein-mediated pathways for angiotensin II activation of extracellular signal-regulated kinases 1 and 2. *Proc. Natl. Acad. Sci. U S A.* **2003**, *100*, 10782-7
235. Boerrigter, G.; Lark, M.W.; Whalen, E.J.; Soergel, D.G.; Violin, J.D.; Burnett, J.C. Jr. Cardiorenal actions of TRV120027, a novel β -arrestin-biased ligand at the angiotensin II type I receptor, in healthy and heart failure canines: a novel therapeutic strategy for acute heart failure. *Circ. Heart Fail.* **2011**, *4*, 770-8
236. Inbe, H.; Watanabe, S.; Miyawaki, M.; Tanabe, E.; Encinas, J.A. Identification and characterization of a cell-surface receptor, P2Y₁₅, for AMP and adenosine. *J. Biol. Chem.* **2004**, *279*, 19790-9
237. Abbracchio, M.P.; Burnstock, G.; Boeynaems, J.M.; Barnard, E.A.; Boyer, J.L.; Kennedy, C.; Miras-Portugal, M.T.; King, B.F.; Gachet, C.; Jacobson, K.A.; Weisman, G.A. The recently deorphanized GPR80 (GPR99) proposed to be the P2Y₁₅ receptor is not a genuine P2Y receptor. *Trends Pharmacol. Sci.* **2005**, *26*, 8-9
238. Qi, A.D.; Harden, T.K.; Nicholas, R.A. GPR80/99, proposed to be the P2Y(15) receptor activated by adenosine and AMP, is not a P2Y receptor. *Purinergic Signal.* **2004**, *1*, 67-74
239. He, W.; Miao, F.J.; Lin, D.C.; Schwandner, R.T.; Wang, Z.; Gao, J.; Chen, J.L.; Tian, H.; Ling L. Citric acid cycle intermediates as ligands for orphan G-protein-coupled receptors. *Nature* **2004**, *429*, 188-93
240. Rittiner, J.E.; Korboukh, I.; Hull-Ryde, E.A.; Jin, J.; Janzen, W.P.; Frye, S.V.; Zylka, M.J. AMP is an adenosine A₁ receptor agonist. *J. Biol. Chem.* **2012**, *287*, 5301-9
241. Moody, C.J.; Meghji, P.; Burnstock, G. Stimulation of P₁-purinoceptors by ATP depends partly on its conversion to AMP and adenosine and partly on direct action. *Eur. J. Pharmacol.* **1984**, *97*, 47-54
242. Salter, M.W.; Henry, J.L. Effects of adenosine 5'-monophosphate and adenosine 5'-triphosphate on functionally identified units in the cat spinal dorsal horn. Evidence for a differential effect of adenosine 5'-triphosphate on nociceptive vs non-nociceptive units. *Neuroscience* **1985**, *15*, 815-25
243. Mazurek, S.; Michel, A.; Eigenbrodt, E. Effect of extracellular AMP on cell proliferation and metabolism of breast cancer cell lines with high and low glycolytic rates. *J. Biol. Chem.* **1997**, *272*, 4941-52
244. Ching, L.L.; Williams, A.J.; Sitsapesan, R. AMP is a partial agonist at the sheep cardiac ryanodine receptor. *Br. J. Pharmacol.* **1999**, *127*, 161-71
245. Mustafa, S.J.; Nadeem, A.; Fan, M.; Zhong, H.; Belardinelli, L.; Zeng, D. Effect of a specific and selective A_{2B} adenosine receptor antagonist on adenosine agonist AMP and allergen-induced airway responsiveness and cellular influx in a mouse model of asthma. *J. Pharmacol. Exp. Ther.* **2007**, *320*, 1246-51

246. Patterson, S.L.; Sluka, K.A.; Arnold, M.A. A novel transverse push-pull microprobe: in vitro characterization and in vivo demonstration of the enzymatic production of adenosine in the spinal cord dorsal horn. *J. Neurochem.* **2001**, *76*, 234-46
247. Zimmermann, H. Extracellular metabolism of ATP and other nucleotides. *Naunyn-Schmiedeberg's Arch. Pharmacol.* **2000**, *362*, 299-309
248. Latini, S.; Pedata, F. Adenosine in the central nervous system: release mechanisms and extracellular concentrations. *J. Neurochem.* **2001**, *79*, 463-84
249. Savic, V.; Stefanovic, V.; Ardaillou, N.; Ardaillou, R. Induction of ecto-5'-nucleotidase of rat cultured mesangial cells by interleukin-1 beta and tumour necrosis factor-alpha. *Immunology* **1990**, *70*, 321-6
250. Christensen, L.D.; Andersen, V.; Nygaard, P.; Bendtzen, K. Effects of immunomodulators on ecto-5'-nucleotidase activity on blood mononuclear cells in vitro. *Scand. J. Immunol.* **1992**, *35*, 407-13
251. Sowa, N.A.; Taylor-Blake, B.; Zylka, M.J. Ecto-5'-nucleotidase (CD73) inhibits nociception by hydrolyzing AMP to adenosine in nociceptive circuits. *J. Neurosci.* **2010**, *30*, 2235-44
252. Street, S.E.; Walsh, P.L.; Sowa, N.A.; Taylor-Blake, B.; Guillot, T.S.; Vihko, P.; Wightman, R.M.; Zylka, M.J. PAP and NT5E inhibit nociceptive neurotransmission by rapidly hydrolyzing nucleotides to adenosine. *Mol. Pain* **2011**, *7*:80
253. Saze, Z.; Schuler, P.J.; Hong, C.S.; Cheng, D.; Jackson, E.K.; Whiteside, T.L. Adenosine production by human B cells and B cell-mediated suppression of activated T cells. *Blood* **2013**, *122*, 9-18
254. Morandi, F.; Horenstein, A.L.; Chillemi, A.; Quarona, V.; Chiesa, S.; Imperatori, A.; Zanellato, S.; Mortara, L.; Gattorno, M.; Pistoia, V.; Malavasi, F. CD56brightCD16- NK Cells Produce Adenosine through a CD38-Mediated Pathway and Act as Regulatory Cells Inhibiting Autologous CD4+ T Cell Proliferation. *J. Immunol.* **2015**, *195*, 965-72.
255. Chatterjee, D.; Tufa, D.M.; Baehre, H.; Hass, R.; Schmidt, R.E.; Jacobs, R. Natural killer cells acquire CD73 expression upon exposure to mesenchymal stem cells. *Blood* **2014**, *123*, 594-5
256. Stella, J.; Bavaresco, L.; Braganhol, E.; Rockenbach, L.; Farias, P.F.; Wink, M.R.; Azambuja, A.A.; Barrios, C.H.; Morrone, F.B.; Oliveira Battastini, A.M. Differential ectonucleotidase expression in human bladder cancer cell lines. *Urol. Oncol.* **2010**, *28*, 260-7
257. Mikhailov, A.; Sokolovskaya, A.; Yegutkin, G.G.; Amdahl, H.; West, A.; Yagita, H.; Lahesmaa, R.; Thompson, L.F.; Jalkanen, S.; Blokhin, D.; Eriksson, J.E. CD73 participates in cellular multiresistance program and protects against TRAIL-induced apoptosis. *J. Immunol.* **2008**, *181*, 464-75
258. Sadej, R.; Spsychala, J.; Skladanowski, A.C. Expression of ecto-5'-nucleotidase (eN, CD73) in cell lines from various stages of human melanoma. *Melanoma Res.* **2006**, *16*, 213-22
259. Jin, D.; Fan, J.; Wang, L.; Thompson, L.F.; Liu, A.; Daniel, B.J.; Shin, T.; Curiel, T.J.; Zhang, B. CD73 on tumor cells impairs antitumor T-cell responses: a novel mechanism of tumor-induced immune suppression. *Cancer Res.* **2010**, *70*, 2245-55
260. Kondo, T.; Nakazawa, T.; Murata, S.I.; Katoh, R. Expression of CD73 and its ecto-5'-nucleotidase activity are elevated in papillary thyroid carcinomas. *Histopathology* **2006**, *48*, 612-4
261. Fukuda, K.; Sakakura, C.; Miyagawa, K.; Kuriu, Y.; Kin, S.; Nakase, Y.; Hagiwara, A.; Mitsufuji, S.; Okazaki, Y.; Hayashizaki, Y.; Yamagishi, H. Differential gene expression profiles of radioresistant oesophageal cancer cell lines established by continuous fractionated irradiation. *Br. J. Cancer* **2004**, *91*, 1543-50
262. Spsychala, J.; Kitajewski, J. Wnt and beta-catenin signaling target the expression of ecto-5'-nucleotidase and increase extracellular adenosine generation. *Exp. Cell Res.* **2004**, *296*, 99-108

263. Ludwig, H.C.; Rausch, S.; Schallock, K.; Markakis, E. Expression of CD 73 (ecto-5'-nucleotidase) in 165 glioblastomas by immunohistochemistry and electronmicroscopic histochemistry. *Anticancer Res.* **1999**, *19*, 1747-52
264. Turcotte, M.; Spring, K.; Pommey, S.; Chouinard, G.; Cousineau, I.; George, J.; Chen, G.M.; Gendoo, D.M.; Haibe-Kains, B.; Karn, T.; Rahimi, K.; Le Page, C.; Provencher, D.; Mes-Masson, A.M.; Stagg, J. CD73 is associated with poor prognosis in high-grade serous ovarian cancer. *Cancer Res.* **2015**, pii: canres.3569.2014
265. Wu, X.R.; He, X.S.; Chen, Y.F.; Yuan, R.X.; Zeng, Y.; Lian, L.; Zou, Y.F.; Lan, N.; Wu, X.J.; Lan, P. High expression of CD73 as a poor prognostic biomarker in human colorectal cancer. *J. Surg. Oncol.* **2012**, *106*, 130-7
266. Wink, M.R.; Lenz, G.; Braganhol, E.; Tamajusuku, A.S.; Schwartzmann, G.; Sarkis, J.J.; Battastini, A.M. Altered extracellular ATP, ADP and AMP catabolism in glioma cell lines. *Cancer Lett.* **2003**, *198*, 211-8
267. Davenport, A.P.; Alexander, S.P.; Sharman, J.L.; Pawson, A.J.; Benson, H.E.; Monaghan, A.E.; Liew, W.C.; Mpamhanga, C.P.; Bonner, T.I.; Neubig, R.R.; Pin, J.P.; Spedding, M.; Harmar, A.J. International Union of Basic and Clinical Pharmacology. LXXXVIII. G protein-coupled receptor list: recommendations for new pairings with cognate ligands. *Pharmacol. Rev.* **2013**, *65*, 967-86
268. Yegutkin, G.G.; Samburski, S.S.; Mortensen, S.P.; Jalkanen, S.; González-Alonso, J. Intravascular ADP and soluble nucleotidases contribute to acute prothrombotic state during vigorous exercise in humans. *J. Physiol.* **2007**, *579*, 553-64
269. Harkness, R.A.; Coade, S.B.; Webster, A.D., ATP, ADP and AMP in plasma from peripheral venous blood. *Clin. Chim. Acta.* **1984**, *143*, 91-8
270. Eells, J.T.; Spector, R. Purine and pyrimidine base and nucleoside concentrations in human cerebrospinal fluid and plasma. *Neurochem. Res.* **1983**, *11*, 1451-7
271. Wishart, D.S.; Lewis, M.J.; Morrissey, J.A.; Flegel, M.D.; Jeroncic, K.; Xiong, Y.; Cheng, D.; Eisner, R.; Gautam, B.; Tzur, D.; Sawhney, S.; Bamforth, F.; Greiner, R.; Li, L. The human cerebrospinal fluid metabolome. *J. Chromatogr. B Analyt. Technol. Biomed. Life Sci.* **2008**, *871*, 164-73
272. Rodríguez-Núñez, A.; Cid, E.; Rodríguez-García, J.; Camiña, F.; Rodríguez-Segade, S.; Castro-Gago, M. Concentrations of nucleotides, nucleosides, purine bases, oxypurines, uric acid, and neuron-specific enolase in the cerebrospinal fluid of children with sepsis. *J. Child Neurol.* **2001**, *9*, 704-6
273. Borrmann, T.; Abdelrahman, A.; Volpini, R.; Lambertucci, C.; Alksnis, E.; Gorzalka, S.; Knospe, M.; Schiedel, A.C.; Cristalli, G.; Müller, C.E. Structure-activity relationships of adenine and deazaadenine derivatives as ligands for adenine receptors, a new purinergic receptor family. *J. Med. Chem.* **2009**, *52*, 5974-89
274. Olson, K.R.; Eglén, R.M. Beta galactosidase complementation: a cell-based luminescent assay platform for drug discovery. *Assay Drug Dev. Technol.* **2007**, *5*, 137-44

Throughout the time of this thesis I was lucky to be surrounded by many people who greatly contributed to its final form and to whom I will stay deeply indebted.

Prof. Christa Müller was always supportive, encouraging and highly motivating. This thesis is as hers as mine since she chose the challenging projects, constantly provided insight, valuable advice and was willing to make every effort within her group as well as in collaboration with other scientific groups to bring the thesis to its current form.

I am also thankful to PD. Dr. Anke Schiedel for her help introducing the mas-related gene receptors to me and guiding my first steps in this thesis. Discussions and tips from Anke were very useful and illuminating. Lastly, Anke agreed to be the second supervisor of this thesis.

I am indebted to Dr. Sonja Hinz who has contributed via various discussions and ideas to planning and designing of some of the important experiments and was always ready to sacrifice some of her time for spontaneous questions and explanations.

During my work in the lab I had the opportunity to supervise some of the students who contributed to some of the most exciting findings. Hamid Shah from Pakistan conducted the antagonist screening at MRGPRX2 receptor and was able to identify the first hits at this receptor. Jose Bonet Giner from Spain conducted the antagonist screening at MRGPRX4 receptor and despite his short stay he was able to generate valuable data. Sara Caeiro from Portugal conducted initial screening at MRGPRX2 receptor. I would like to thank all these colleagues whole-heartedly and wish them all success in their future.

In the final stage of the thesis we collaborated with different groups to whom I am enormously grateful.

Professor Ullrich Wüllner from University clinic in Bonn provided us with different cerebrospinal fluid samples.

Professor Oliver Brüstle, Dr. Michael Peitz and Svetlana Ritzenhofen from the Institute of reconstructive neurobiology in Bonn have conducted the differentiation experiments of fibroblasts to neurons. The lab work was performed mainly by Svetlana, who was able to reach exciting results.

The native cell line LN229 cell line was kindly provided by Professor Björn Scheffler and Dr. Anja Wieland from Life and Brain center in Bonn. This cell line proved to be an interesting tool. For this and the proliferation assay I would like to express my gratitude to them.

The investigation of the mas-related gene X4 in the immune system was carried out in the group of Professor Jacob Nattermann. The FACS experiments were done by Dr. Benjamin Krämer. Benjamin was always friendly, collaborative and made every effort to find a native expression of the receptor.

I am deeply grateful to Dr. Marc Sylvester from the biochemical institute in Bonn who was constantly ready to answer my questions regarding mass spectrometry and introduced me in a course to the important techniques in his field.

During the first 21 months of my PhD I got a scholarship from the graduate school of chemical biology. I am grateful to all who supervised me during the time of this scholarship.

For all the important novel agonists and antagonists I owe a debt to several talented chemists.

In the group of professor Müller Dr. Thanigaimalai Pillaiyar synthesized most of the novel agonists at MRGPRX4 receptor that led to a better understanding of the structure activity relationship. Dr. Jörg

Hockenmeyer and Daniel Marx synthesized JH14102, the most potent agonist at MRGPRX4 in this work.

Dr. Younis Baqi has provided valuable suggestions and advice for elucidating the structure activity relationships. He synthesized MSX-3, MSX-155 as well as BI03. Dr. Enas Malik and Dr. Ali El-Tayeb have also provided me with compounds for screening.

Dr. Steven De Jonghe and Dr. Piotr Leonczak from the lab of professor Piet Herdewijn in Belgium synthesized the antagonists at MRGPRX2 receptor. I would like to thank them for their constant cooperation and helpful feedback during the work together.

The daily work in the lab was made easier and provided occasional fun due to the nice team in the lab to whom I would be always thankful.

During my PhD Dr. Sangyong Lee, Dr. Nader Boshta, Dr. Amelie Fiene and Dr. Mario Funke were my colleagues in the office. Their presence was a nice companion to me in the 4 years period and the friendly atmosphere they created in the office was of great value.

In the whole PhD period I supervised undergraduates in the seventh semester. During this time I came in contact with a dedicated team that I enjoyed working with. Dr. Ralf Mayer was our head of the lab who gave us a big space for ourselves to organize the practical sessions. Other PhD candidates who shared the supervision with me made this duty enjoyable. Here I would like to mention Dr. Dominik Thimm, Dr. Viktor Rempel, Dr. Wenjin Li, Dr. Sabrina Gollos, Marianne Freundlieb, Dr. Claudia Spanier, Dr. Daniel Stölting, The Hung Vu, Clara Schöder, Samer Alshaibani and Dr. Meryem Köse.

It was a pleasure to work with several colleagues like Azeem Danish, Muhammad Rafehi, Mahmoud Rashed and York Ammon. All these guys were ready to help privately as well as in the lab. I wish them all success.

Stephanie Weinhausen and Elisabetta De Philipo were always friendly and ready give every possible help in the lab and shared their knowledge.

Markus Kuschak joined our group recently and was ,as an IT expert and friendly person, always on my side.

The technicians were a great source for smooth work in the lab on daily basis. Here I thank Anika Püsche for her patience in my four and half years in the lab throughout my master and PhD. She and Angelika Fischer corrected my mistakes and hectic in a kind way for which I am thankful. Katharina Sylvester provided a great help during my work in the lab. To both Katharina and Marc, her husband, I would like express my gratitude. Christin Vielmuth was from the first day I her in the compound library a nice and dedicated colleague who tried to answer my questions as quickly and precisely as possible. Many thanks are due to Stefanie Weyer and Inge Renner for their contributions.

My ultimate thanks and infinite gratitude are due to those who were the source of limitless love and care not only during my PhD but since I knew them. To those people no words would be able to shed light on my abysmal indebtedness to them.

My father, a Greek among Romans, had given me an immense support, confidence and faith all along my way.

My mother was always my refuge in any case of difficulty or problem. She is always able to calm me and boost my confidence. For her priceless standby I would be in eternal debt.

To my brother and two sisters I owe a lot of support, nostalgic times and beautiful memories.

Nurcan, my wife, was the real motivator behind me during the downs and she was more relieved than me during the ups of this thesis. She was always ready to sacrifice time and take every step to enable me make this thesis possible. For her encouragement, intelligence, support and love I will be always thankful.